

<b>17. FAR DETECTOR ASSEMBLY.....</b>	<b>3</b>
17.1 INTRODUCTION.....	3
17.2 TECHNICAL DESIGN CRITERIA .....	5
17.3 OVERVIEW OF THE FAR DETECTOR ASSEMBLY PROCEDURE.....	5
17.4 STRUCTURAL ISSUES .....	8
17.4.1 Structural Design Strategy.....	8
17.4.2 PVC and Adhesive Stresses.....	9
17.4.3 Analysis of Individual Extrusions .....	12
17.4.4 Vertical Module Edge Stiffeners .....	13
17.5 ANALYSIS OF DETECTOR BLOCK STRUCTURE .....	15
17.5.1 Modeling of Adhesive Joints .....	15
17.5.2 Description of the FEA Model of Assembled Blocks.....	30
17.5.3 Analysis of a 31-Plane “A” Block .....	32
17.5.4 Analysis of a 31-Plane “B” Block .....	50
17.5.5 Long-term Stability of the Assembled Detector .....	53
17.5.6 Structural Considerations During Scintillator Filling.....	62
17.5.7 Adhesive Requirements .....	62
17.6 MECHANICAL PROTOTYPES.....	63
17.6.1 Four-Foot Extrusion Under Internal Pressure .....	63
17.6.2 Three-layer/Single-extrusion X-Y Prototype.....	68
17.6.3 Seven-layer Hydrostatic Stress Transmission Prototype .....	78
17.6.4 Eleven-layer/Single-extrusion X-Y Prototype .....	83
17.6.5 Four-layer IPND-Block Prototype.....	84
17.6.6 Eight-layer/Single-extrusion X-Y Prototype .....	93
17.6.7 Adhesive shear measurements with 3-layer prototype sections .....	96
17.7 FAR DETECTOR INFRASTRUCTURE .....	99
17.7.1 Environmental Control Systems.....	99
17.7.2 The South Bookend .....	101
17.7.3 The North Bookend .....	101
17.7.4 Cosmic-Ray Shield Wall .....	102
17.7.5 Access to the Installed Detector Blocks .....	104
17.7.6 Detector Control Room.....	106
17.8 LIQUID SCINTILLATOR DISTRIBUTION AND SUPPLY SYSTEM .....	108
17.8.1 Scintillator Distribution System.....	108
17.8.2 Distribution Control System .....	108
17.8.3 Distribution Plumbing .....	110
17.8.4 Scintillator Filling Machines .....	111
17.8.5 Vapor Recovery System .....	113
17.8.6 Scintillator Distribution System Installation.....	114
17.9 FAR DETECTOR ASSEMBLY EQUIPMENT .....	115
17.10 MODULE VACUUM LIFTER .....	118
17.11 THE ADHESIVE DISPENSER.....	119
17.12 BLOCK PIVOTER.....	121
17.12.1 Block Pivoter – General Configuration .....	121
17.12.2 Block Pivoter – Detector Assembly Table.....	122
17.12.3 Block Pivoter – Pivoting Hydraulics .....	125
17.12.4 Block Pivoter – Propulsion Drive.....	128
17.12.5 Block Pivoter – Block Base Pallet .....	129
17.12.6 Block Pivoter – Upper Table Support Weldment.....	131
17.12.7 Block Pivoter – Lower Table Support Weldment.....	132
17.12.8 Block Pivoter – Rear Table Support .....	134
17.12.9 Block Pivoter – Parameter Summary.....	135
17.13 DETECTOR ASSEMBLY SEQUENCE.....	135
17.13.1 Overview of the Detector Assembly Process.....	135
17.13.2 Quality Control and Assurance .....	137

17.13.3	<i>Detector Component Delivery and Storage</i> .....	138
17.13.4	<i>Block Assembly on the Block Pivoter</i> .....	138
17.13.5	<i>Raising and Securing a Block</i> .....	143
17.13.6	<i>Construction of a Superblock</i> .....	145
17.14	FILLING THE DETECTOR WITH LIQUID SCINTILLATOR .....	146
17.15	INSTALLATION OF ELECTRONICS .....	148
17.15.1	<i>Detector Readout Infrastructure</i> .....	149
17.15.2	<i>Detector Outfitting Integration</i> .....	151
17.16	ASSEMBLY CREW AND RATE OF DETECTOR ASSEMBLY.....	155
17.16.1	<i>Job Classifications</i> .....	155
17.16.2	<i>Crew Size, Shift Schedule and Training</i> .....	156
17.16.3	<i>Block Installation Schedule</i> .....	157
17.17	CHANGES IN THE FAR DETECTOR ASSEMBLY SINCE THE CDR .....	160
17.18	WORK REMAINING TO COMPLETE THE FAR DETECTOR ASSEMBLY DESIGN .....	161
CHAPTER 17 REFERENCES .....		161

# 17. Far Detector Assembly

## 17.1 Introduction

This Chapter describes the structural design of the NOvA far detector, the tooling and infrastructure required to assemble the detector at the Ash River site, and the detector assembly process itself. These tasks are the responsibility of WBS 2.9, which receives detector components from WBS 2.2 (liquid scintillator), 2.5 (PVC modules), 2.6 (electronics) and 2.7 (data acquisition) for assembly at the facility provided by WBS 2.1 (far detector site and buildings). The close coordination and integration of these Level 2 WBS activities is one of the most important detector assembly tasks. WBS 2.9 is responsible for designing and building several large semi-automatic machines, especially the adhesive dispenser and the block pivoter, used for assembling modules into blocks and installing blocks in the detector. The task includes the checkout and validation of completed sections of the detector and the transition to routine data acquisition operation. The detector installation requires the hiring and training of a crew of technicians that will perform the actual assembly work over a 2.5-year period, beginning with beneficial occupancy of the detector building and ending when the 18 kton detector is fully operational. WBS 2.9 is responsible for the design and operation of the liquid scintillator supply system, which receives scintillator from delivery tankers, subjects it to quality assurance testing and uses it to fill the detector modules. The overall structure of the far detector is shown schematically in Figure 17.1 and its design parameters are summarized in Table 17.1.

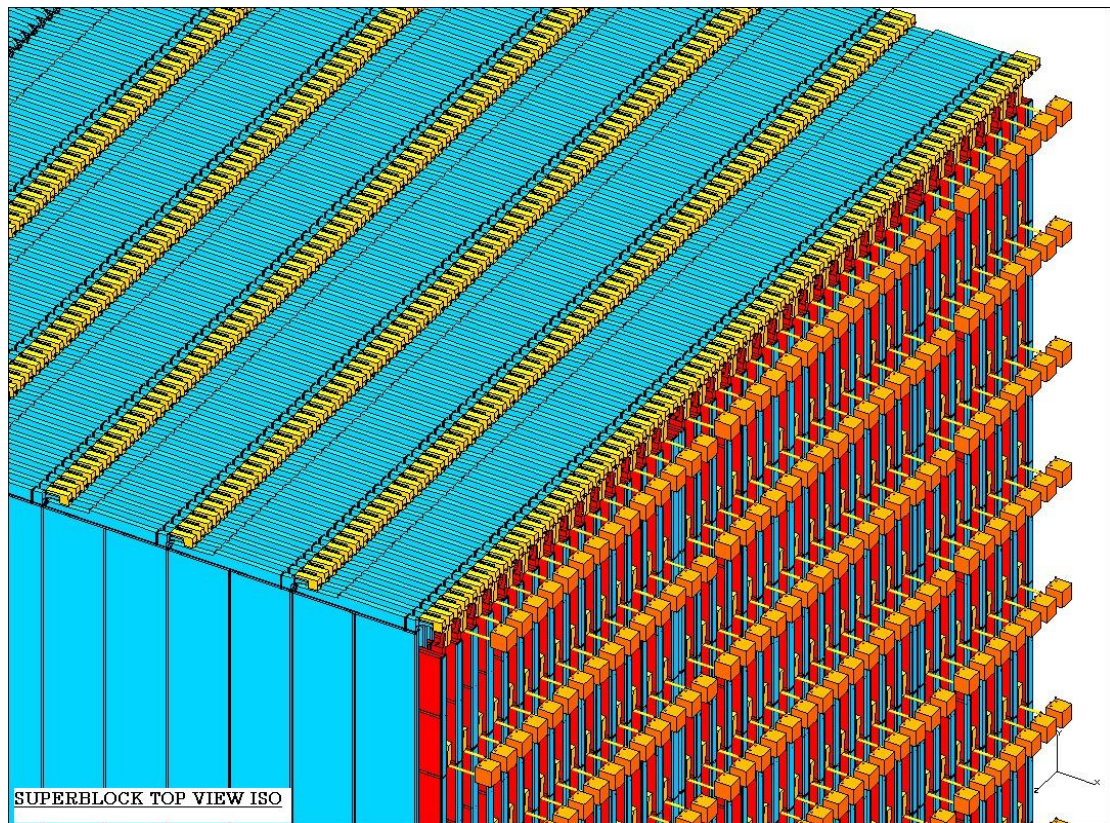


Fig. 17.1: Top quarter of one superblock of the NOvA far detector. Each superblock consists five 31-plane blocks. Blocks consist of alternating planes of twelve horizontal or twelve vertical modules. Superblocks begin and end with planes of vertical modules.

Total mass	17,350 metric tons (without manifolds and end seals)
Mass of rigid PVC extrusions	5,000 metric tons
Mass of liquid scintillator	12,200 metric tons
Liquid scintillator	Mineral oil base with 5.5% pseudocumene as the scintillant, PPO and bis-MSB waveshifters added.
Active mass fraction	69%
Active height × width	16.0 m × 15.7 m
Active length	78.2 m
Number of planes	1178 (593 vertical, 585 horizontal) 38 blocks (23 "A" and 15 "B") of 31 planes each
Radiation length per plane	~ 0.15
Mass of adhesive between planes	140 metric tons
Modules per plane	12
Module outer wall thickness	3.3 mm in horizontal cells, 4.8 mm in vertical cells
Module inner web thickness	2.3 mm in horizontal cells, 3.3 mm in vertical cells
Module width	1.3 m
Module length	15.7 m
Maximum pressure in vertical cells	19.2 psi
Cells per module	32
Cell interior width × depth, horizontal cells vertical cells	3.74 cm × 5.94 cm 3.64 cm × 5.64 cm
Total number of cells	452,352
Total number of modules	14,136
Wavelength-shifting fiber	0.7 mm diameter double clad fiber with 300 ppm K27 wave-shifting dye
Total WLS fiber length	14,930 km
Total WLS fiber mass	9.1 tons
Photodetector	Avalanche Photodiode

Table 17.1: Summary of far detector parameters.

## 17.2 Technical Design Criteria

The detector assembly R&D task, WBS 1.8, has provided a structural design for the far detector that meets physics performance criteria and is mechanically stable during all stages of the assembly process and throughout the operational lifetime of the detector. The primary task for WBS 2.9 is to provide equipment and procedures for assembling the detector in a safe and environmentally responsible manner, including quality assurance procedures to ensure that the structure meets all performance and mechanical stability requirements. The completed detector will be stable against the long-term effects of PVC creep and aging of materials for a minimum of 20 years. An important aspect of the assembly process is the safe transfer of liquid scintillator (69% of the detector mass) from delivery tanker trucks to the detector modules, including quality assurance tests to ensure that contaminated scintillator is never put into the detector and that the origin of the scintillator in every detector module can be traced. Liquid scintillator spills and vapors will be carefully controlled throughout the assembly process.

The mechanical assembly of each 31-plane detector block consists of applying adhesive to the lower surfaces of all 12 PVC extrusion modules in every plane except the first (bottom) one. The modules will be precisely located and held in position while the adhesive cures, in order to achieve the design geometry and the adhesive bond strength used in the structural stability analyses. Each of the 38 blocks will be raised into place against the previously installed block. Blocks are sequentially filled with liquid scintillator and then outfitted with photodetectors and readout electronics as assembly proceeds. External light that could affect the photodetectors is prevented from entering the detector by the thickness of the vertical extrusions, by the opaque module manifolds and by black paint on the exposed surfaces of the exposed surfaces of the thin-walled horizontal extrusions. After the final block is installed, the north bookend is erected, the last three blocks are filled and outfitted, and the cosmic ray shield wall is installed.

The NOvA far detector is unique in its composition and scale, and many of the assembly tasks are beyond our direct experience. Lack of relevant experience at this size and scale presents technical, cost and schedule risks that can only be mitigated by acquiring relevant experience. A number of the first 16-cell NOvA extrusions are being used to build and test small-scale (a few meters by a few layers) prototype structures to verify finite-element analysis (FEA) predictions. Many of the 16-cell extrusions are being cut to our full 15.7 m length and will be used for realistic time and motion studies. Full length extrusions will be used to benchmark our procedures for assembling extrusion modules into planes. We will also use full length extrusions to build a full-height, partial-width, 2-block prototype that will be raised to the vertical position. A full-height, full-width, multi-plane prototype will also be assembled (but not raised) to optimize block assembly procedures and to measure manpower and time requirements. These studies will help us to understand the structural and handling details with appropriately sized objects and allow us to verify requirements for the block pivoter.

## 17.3 Overview of the Far Detector Assembly Procedure

Completed and fully tested PVC modules from the extrusion module factories are delivered to the far detector hall where they are assembled into blocks of alternating horizontal and vertical planes. Each plane consists of 12 extrusion modules. Thirty-one planes of modules are glued together into a strong structure of alternating vertical and horizontal layers called a block. There are two types of blocks, each weighing 127 metric tons. An “A” block begins and ends with planes of vertical modules. A “B” block begins and ends with planes of horizontal modules. Three “A” blocks and two “B” blocks (A-B-A-B-A) form a superblock. There are no spaces between the extrusions in adjacent blocks. There is a 2-cm expansion gap between adjacent superblocks to prevent superblocks from touching after they filled with scintillator. The full detector consists of 38 blocks, arranged as seven 5-block superblocks and one 3-block mini-block (A-B-A).

The first block is erected and placed against the concrete bookend at the south end of the detector hall. Each subsequent block is placed against the previously erected block. The bookend structure is strong enough to resist any buckling deformation that could be exerted by the structural failure of blocks in the completed detector. The expansion gaps, which allow for swelling of the extrusions when they are filled with scintillator, are described in more detail below. Expansion gaps between superblocs are formed by gluing 2-cm-thick by 30-cm-high by 15.7-m-long PVC spacers between the top 30 cm of the blocks adjacent to the gap. Block spacer thicknesses are adjusted to maintain a vertical detector face as the assembly progresses. The deformations of empty blocks during raising, and of filled blocks in the completed detector, are limited by stiff steel base pallets that are built into each block as it is assembled.

The extrusion modules are handled using vacuum lifting fixtures attached to an overhead crane. Empty horizontal modules weigh 320 kg and vertical modules weigh 436 kg. Thirty-two beads of adhesive are applied to the top surface of each module using an automatic adhesive dispenser. A heavy roller presses each module accurately into position and spreads the glue out evenly. The requirements for the NOvA structural adhesive are described in NOVA-doc-145 and the requirements for the adhesive dispenser are described in NOVA-doc-144.

The planes are assembled horizontally on the same device that raises them to the vertical orientation and moves them against the previously erected block. The device is known as the “block pivoter” and looks like a giant fork-lift with a detachable steel block-base pallet instead of forks. The block pivoter is shown in the horizontal position in Figure 17.2 and in the vertical position in Figure 17.3

Cable trays, chilled water loops, power distribution boxes and other electronics infrastructure are installed on each set of two adjacent blocks after they are erected. This equipment does not interfere with the liquid scintillator filling process. Scintillator vapor vent lines and overflow tanks are also installed during this period.

The first block is filled with liquid scintillator as soon as the first two superblocs have been installed. The second superbloc serves as a temporary “bookend” to control any unexpected transient movements during the filling process. The filling process always lags at least one superbloc behind the block installation process. Figure 17.4 shows the front-end electronics boxes mounted to module manifolds on the top and side of a block. After filling, each block is outfitted with APDs, front-end electronics boxes, and all remaining infrastructure. After the last three blocks are erected, but before they are filled and outfitted, the north bookend is installed against the final block. This second bookend consists of the block pivoter, which is permanently installed with additional structures that strengthen it to resist the forces resulting from any unanticipated block-buckling structural failure.

The final step of the detector installation is the construction of a 1-m thick concrete-block cosmic-ray shield wall on the south end of the loading dock. This wall completes the cosmic-ray shielding of the detector, most of which is provided by the concrete roof, barite overburden and building walls that surround the rest of the detector hall. The shield wall consists of pre-cast concrete blocks that are stacked by the bridge crane up to its hook-height limit. The top part of the wall consists of smaller blocks that are hand stacked up to the ceiling.

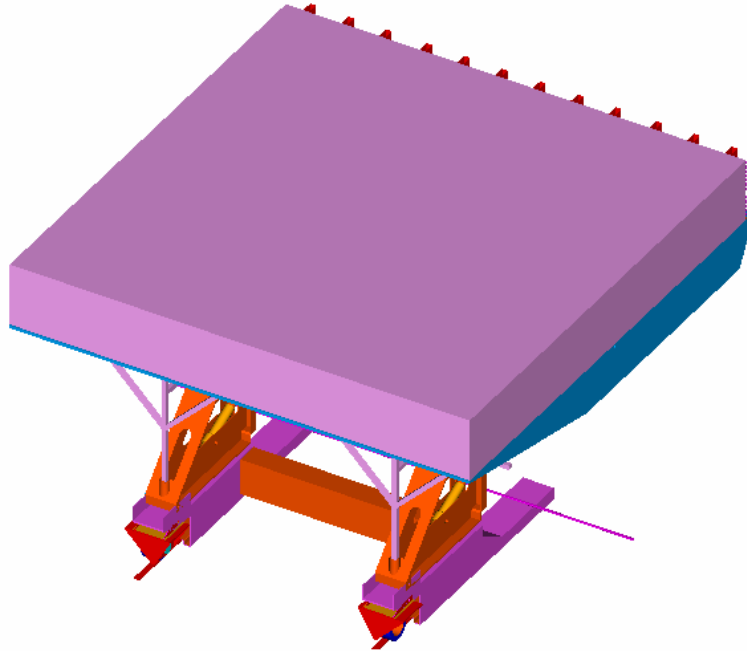


Fig. 17.2: The NOvA block pivoter in its horizontal position. The block pivoter is used in this position to assemble modules into alternating horizontal and vertical planes to form a 31-plane block. The edge of the block-base pallet is visible at the bottom edge of the block (top of figure).

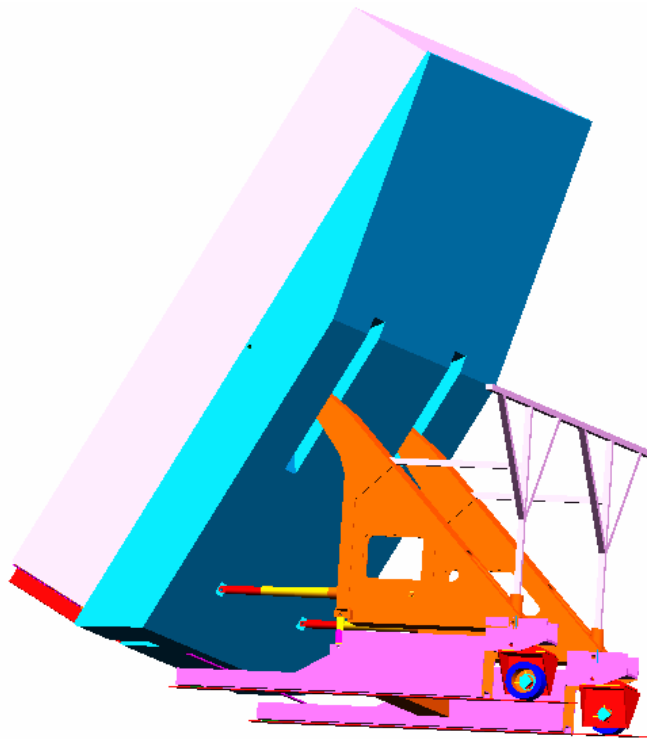


Fig. 17.3: The NOvA block pivoter in its vertical position. The steel block-base pallet on left side of the figure supports the block.

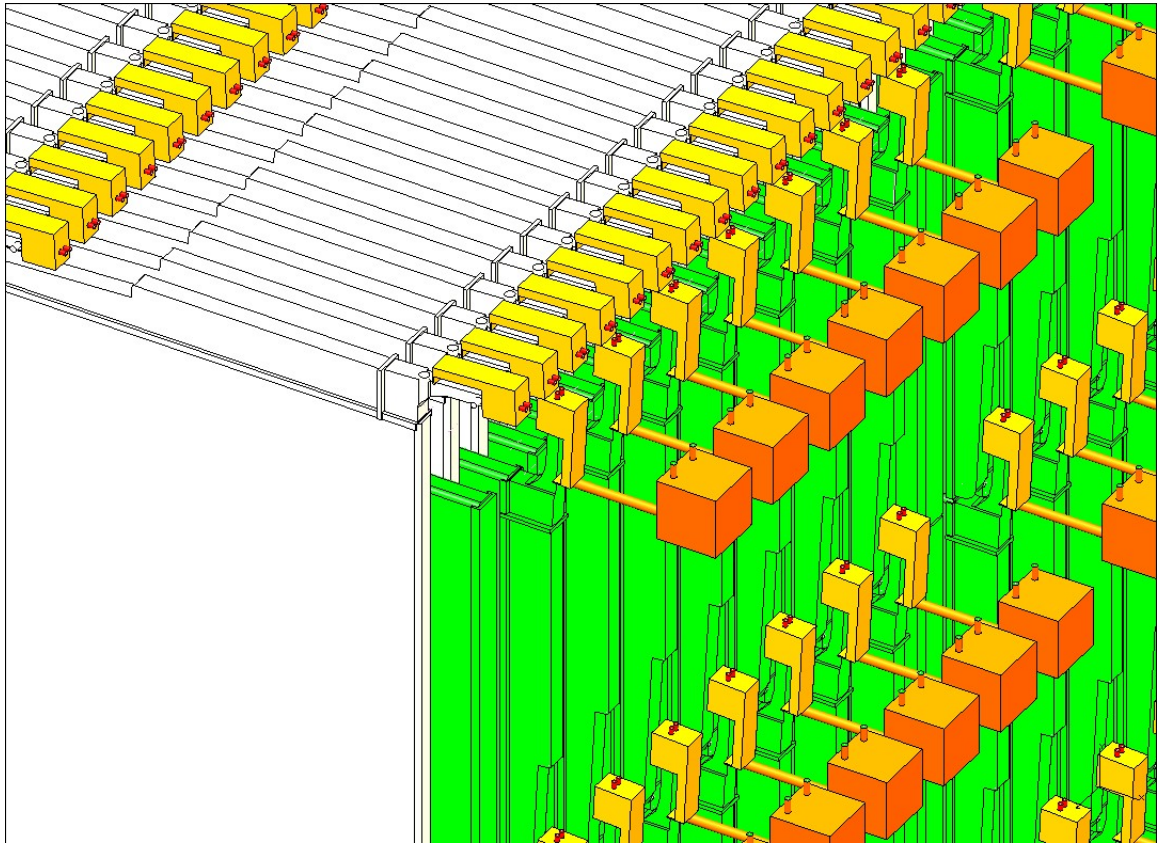


Fig. 17.4: Top corner of one block of a superblock, showing module manifolds and electronics boxes on alternating horizontal and vertical planes. The module readout manifolds of sequential horizontal planes alternate between the east and west sides of the detector. The cubical boxes on the right side of the drawing are the horizontal module overflow tanks.

## 17.4 Structural Issues

### 17.4.1 Structural Design Strategy

The NOvA detector is constructed from alternating layers (planes) of 15.7-m long vertical and horizontal PVC extrusion modules, connected together by adhesive bonds between layers. The basic structural unit of the detector is a subassembly of 31 planes of PVC extrusion modules called a block. The modules in each block are glued together in a horizontal orientation on the block pivoter. Each of the 38 blocks in the 18 kton detector is rotated to a vertical orientation after the adhesive has cured. The far detector is constructed from two types of blocks. “A” blocks have planes of vertical modules on both outside faces, while “B” blocks have planes of horizontal modules on both outside faces. Sets of five sequential blocks, called superblocks, are separated by 2-cm expansion gaps, to accommodate the swelling of the PVC extrusions under hydrostatic pressure. Every superblock begins and ends with an A block, but A and B blocks alternate within a superblock. Figure 17.1 shows one of seven 5-block superblocks. In addition to these superblocks, a single 3-block superblock is required to complete the 38-block detector.

The bottom of each vertical module is subjected to 19 psi hydrostatic pressure after it is filled with liquid scintillator. The horizontal modules are supported by the vertical modules through the adhesive bonds. There is a small gap between the horizontal extrusions within a

plane so there is no load transfer between them. The top of each horizontal module is at atmospheric pressure, so it needs to withstand only a small hydrostatic pressure plus the weight of its PVC and scintillator. The vertical extrusions have thicker walls than the horizontal extrusions in order to reduce stresses in the adhesive that connects them.

The use of plastic as a key structural element of such a large edifice presents a number of engineering challenges. The optimization of the far detector structural design, described in the remainder of this Section and in Section 17.5, is based on the following construction and stability conditions.

- During construction, the detector blocks are mechanically stable and act as independent, self-supporting structures.
- Individual blocks are filled with liquid scintillator as soon as possible, while installation of subsequent blocks is still in progress, in order to allow data taking to proceed.
- The expansion gaps between superblocks are large enough that the swelling of PVC extrusions under hydrostatic pressure is not transferred to adjacent superblocks.
- When the last block is in place, the second bookend is installed.
- The long-term stability of the detector against block buckling is achieved by limiting the amount of deformation any given block can have, by restraining the array of 38 blocks between the north and south bookends.
- Long-term deformations of the filled detector blocks could result from a decrease in PVC strength from plastic creep effects. If a block deforms or buckles to fill the neighboring expansion gaps, it is supported adequately to prevent any further deformation.

#### ***17.4.2 PVC and Adhesive Stresses***

The strengths of the adhesive bonds between extrusions are critical to the success of this design. The PVC is the main structural element of the detector and is also required to provide a high level of reflectivity to ensure sufficient light output from the detector. In parallel with the structural design studies described here, NOvA engineers were developing a special PVC formulation with high reflectivity. Samples of the final NOvA PVC formulation were not available for most of the experimental tests described in the following sections, although all types of PVC tested to date have very similar mechanical properties. NOvA R&D studies of long-term creep effects in PVC (Chapter 12) give quantitative predictions that are incorporated into the structural design of the detector. The prediction of creep weakening of the PVC modulus based on measurements of PET-B PVC is the one we believe best reflects the properties of NOvA PVC over time. A second, more pessimistic prediction was derived from measurements of another early PVC formulation, NOvA-2.

Figure 17.5 and Table 17.2 show the predictions of PVC modulus variation over time for both of these models. For the structural design we have attempted to bracket our analysis between these two predictions. We believe that this technique, coupled with a requirement of a stability safety factor of five for both PVC and adhesive stresses, ensures structural stability against time dependent effects. Also, we have set a target of 600 psi as a maximum von Mises stress in the PVC at any point in time. (Von Mises stress is a measure of the combined stress that is calculated from the stress components provided by the FEA analysis.) Based on the Engineered Materials Handbook [1] we believe that if the PVC stress is kept below this value, then the PVC will remain in the viscoelastic range where the value of the modulus is not stress dependent and a single value of the modulus can be used to model the structure.

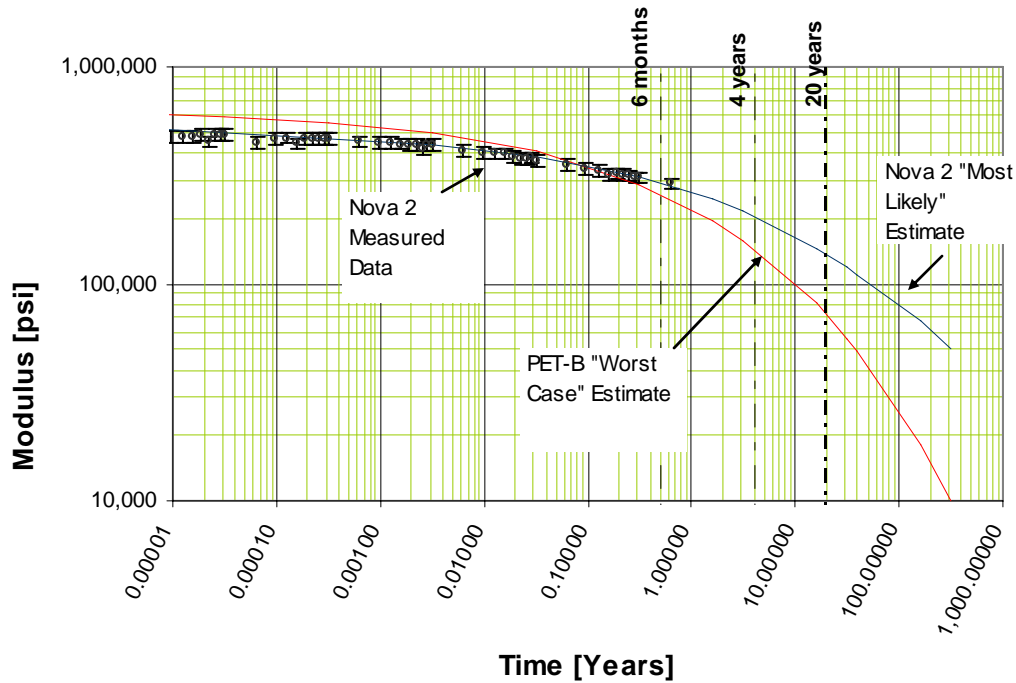


Fig. 17.5: Projected time variation of the PVC modulus caused by creep effects. “Most Likely Estimate” is the creep modulus in the middle of the range estimated by our consultant [2, 3]. Table 17.2 gives numerical values for the PVC modulus at important times on both curves. This figure is identical to Figure 12.X except that the time scale is changed from seconds to years.

The adhesive that is used between detector planes is also critical to the structural integrity of the structure. The adhesive will be applied over large surfaces, so ES&H concerns about vapor release and control have been important considerations in our selection of the plane adhesive. The adhesive must also have a work life of about 20 minutes to match the handling time estimates for PVC extrusion modules during far detector assembly. We have selected Devcon Plastic Welder 60, which is a special formulation of Devcon’s Plastic Welder II, as the baseline adhesive. Devcon developed this formulation specifically to satisfy NOvA requirements for high shear and peel strength (average shear strength of 1200 psi and peel strength of 115 lb/in) and a work life of 30 minutes. Devcon 60 is substantially stronger than our earlier choice of 3M 2216 epoxy, and superseded it as our baseline adhesive as soon as we were convinced that ES&H concerns about Devcon’s methyl methacrylate vapor control could be mitigated (Section 17.7.1).

Creep Condition	Year	Modulus (psi) for the “Worst Case Estimate” in Fig 17.5	Modulus (psi) for the “Most Likely Estimate” in Fig 17.5	Comments
Modulus at 6 Months	0.5	262,631	292,488	6 months in the maximum time over which creep can occur between the assembly of a superblock and completion of filling
Modulus at 2 years	2	183,244	235,341	2 years is the schedule for assembly of the detector
Modulus at 4 years	4	145,544	205,195	This TDR assumes the 140,000 psi value as a worst case where the assembly time might get extended to four years before the second bookend is in place.
Years between start of test station creep measurements and first assembly of Far Detector	Five	134,011	195,454	This means that we will know the first part of the creep curve for our specific PVC before construction begins. The error bars in Fig 17.5 indicate the two curves will be separated by about 2 standard deviations at that time.
Modulus at 20 years	20	72,046	136,965	This TDR assumes a 20 year “life” requirement for the detector and we use the lower “Worst Case” value of the modulus for structure performance at 20 years. This value translates into structural requirements for the bookends
Estimated year that the “Best Estimate” equals the “Most Conservative Prediction” 20 year value	120	n/a	n/a	If the “Most Likely Estimate” curve is correct, then our structure and bookend design may actually have a very long lifetime.

Table 17.2: Values extracted from Figure 17.5. This illustrates our conservative approach to the PVC structure design. One should not infer larger safety factors based on the ratio of “Best Estimate” to “Most Conservative Estimate” moduli since the modulus enters safety factor calculations in different ways depending on the failure mode analyzed.

Based on an evaluation of the published engineering literature on the design of plastic and adhesive structures, NOvA engineers have concluded that a safety factor of five is needed in a unique structure such as the NOvA far detector, which is constructed completely from PVC extrusion modules bonded together. Throughout the analysis, a safety factor of five for stress and buckling stability has been a design requirement.

Our analysis of the NOvA far detector structure is divided into four distinct stages:

- Analysis of individual extrusions determines the optimum extrusion profile.
- Analysis of 31-plane blocks and adhesive stresses ensures that individual blocks can be assembled and filled and will stand as independent structures during the detector assembly process. Separate analyses are performed for A-type and B-type blocks.
- Stability of independent 31-plane blocks is required during assembly and throughout the 20-year lifetime of the detector.
- Long-term stability of the entire structure is provided by expansion gaps between superblocks during assembly and filling, and by the second bookend that is installed at the end of the construction.

The following sections describe each of these stages of analysis.

### ***17.4.3 Analysis of Individual Extrusions***

The initial analysis examined individual PVC extrusions (Chapter 12), with the goal of optimizing the profile for extrudability, minimum PVC stress, and optimum reflectivity.

The pressure at the bottom of a vertical extrusion is 19 psi due to the 15.7-m head of the liquid scintillator. The horizontal extrusion modules are not subjected to this pressure because they are supported individually by adjacent vertical extrusions and there is no accumulation of weight from the extrusions above. Within the structure individual extrusions are adhered together and provide support to each other. The first stage of our analysis examines the properties of an individual vertical extrusion under internal hydrostatic pressure.



Fig. 17.6: Schematic representation of a PVC extrusion profile. The square box outlines the part of the extrusion used for the FEA calculations described in this section.

The geometry of the extrusions and cells was optimized to minimize the stress within an extrusion to approximately 600 psi when subjected to the maximum 19 psi hydrostatic pressure. The 600 psi stress was chosen based on initial understanding of the PVC creep as described above. The baseline extrusion geometry for horizontal modules has a 3.0-mm thick outer wall and a 2.0-mm thick inner web. Vertical module extrusions have 4.5-mm thick outer walls and 3.0-mm thick inner webs. The difference in wall thickness between vertical and horizontal extrusions minimizes adhesive stresses as described below. The internal radii reduce the stress concentrations in the corners of a cell. In addition, the outer scallops are required by the extruding process. The scallop geometry gives the same wall thickness all around the outer perimeter, which is important for uniform cooling in the final stages of the extrusion process. The ratio of the outer wall thickness to the inner web thickness was recommended by extruders as being optimal for reliable extruding. A PVC modulus used in this analysis,  $E = 150$  ksi, is the predicted value of the modulus at 20 years (or at 10 years for the pessimistic prediction). Figure 17.7 shows the stress distribution within the PVC extrusion under the 19 psi internal pressure and Figure 17.8 shows the corresponding deflections.

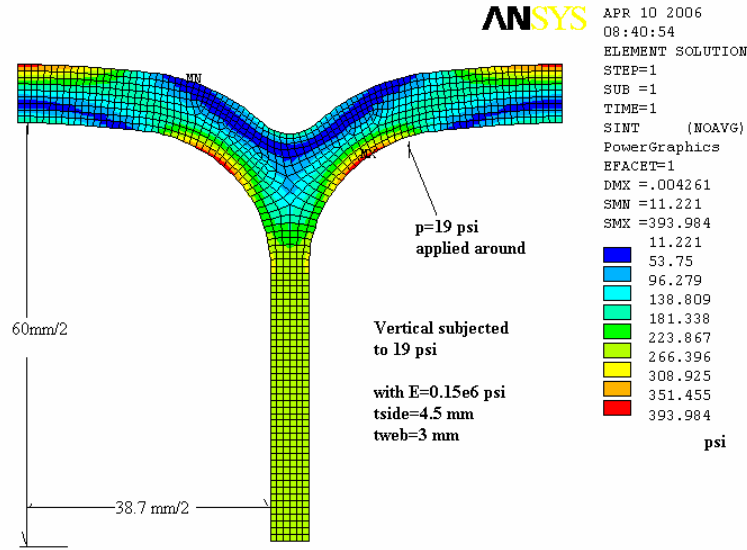


Fig. 17.7: Stress distribution for one vertical extrusion cell subjected to 19 psi with E = 150 ksi.

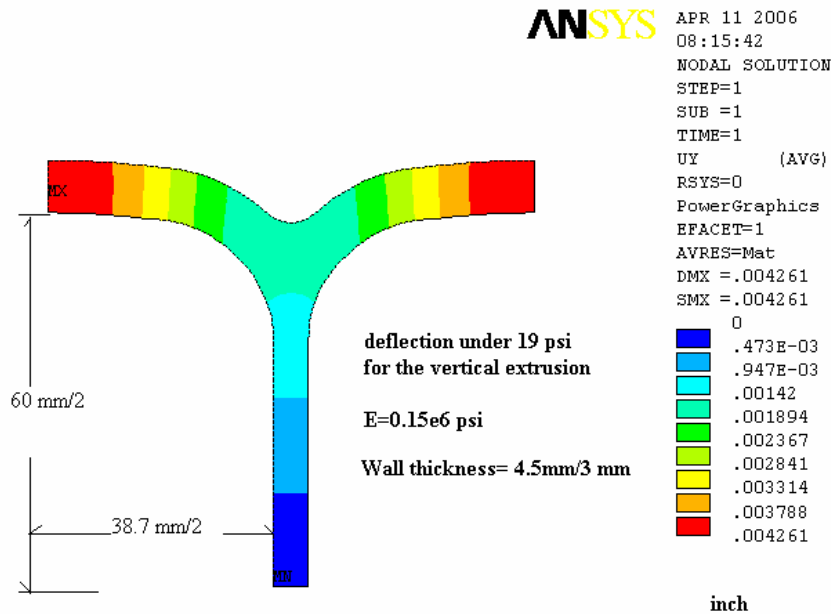


Fig. 17.8: Deflections in a single vertical extrusion cell subjected to 19 psi with E = 150 ksi.

#### 17.4.4 Vertical Module Edge Stiffeners

The edges of vertical modules within a block are in contact with each other and are not subject to hydrostatic pressure differentials. However, this is not the case for the edges of vertical module planes. The stress and deflections of the vertical edges of these outside modules are reduced by gluing 2-mm thick by 4-cm wide by 6-m high PVC edge stiffeners them, effectively increasing PVC thickness along these edges. NOVA-doc-1204 describes the design of the edge stiffeners in detail.

The end cell of PVC extrusion with a 3.88-cm x 6.0-cm cell size has a 6 cm span length, which is subjected to 19 psi hydrostatic load. With a 4.5 mm exterior wall, the maximum bending stress is around 1,200 psi. The 2-mm thick stiffener plate brings the stress down to ~ 700 psi,

similar to stresses in other parts of the structure. The peak shear stress at the corner for the adhesive layer is around 581 psi, which is substantially below the average shear strength of ~1000 psi. The adhesive peeling force at the corner is 3.7 lbf/in, which is also below to the peeling strength of 19 lbf/in. The 20-year PVC modulus of 75 ksi is used for the design calculation described in NOVA-doc-1204. The stiffener reduces the end-cell stress from 1300 psi to 719 psi and the end-cell deflection from 0.088 inches to 0.034 inches.

Figure 17.9 shows the calculated deflection of an end cell with a stiffener under 19 psi hydrostatic pressure. Figure 17.10 is a CAD drawing of the bottom of a vertical extrusion with an edge stiffener attached.

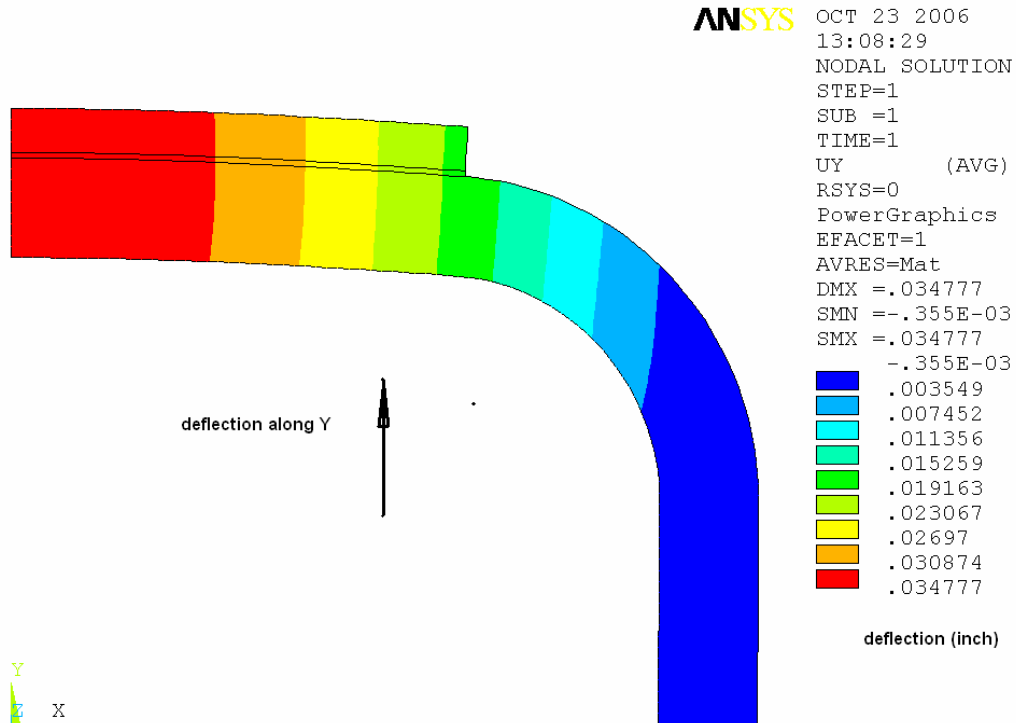


Fig. 17.9: Deflections in a outside vertical extrusion cell, with edge stiffener attached, subjected to 19 psi with a PVC modulus of  $E = 75$  ksi.

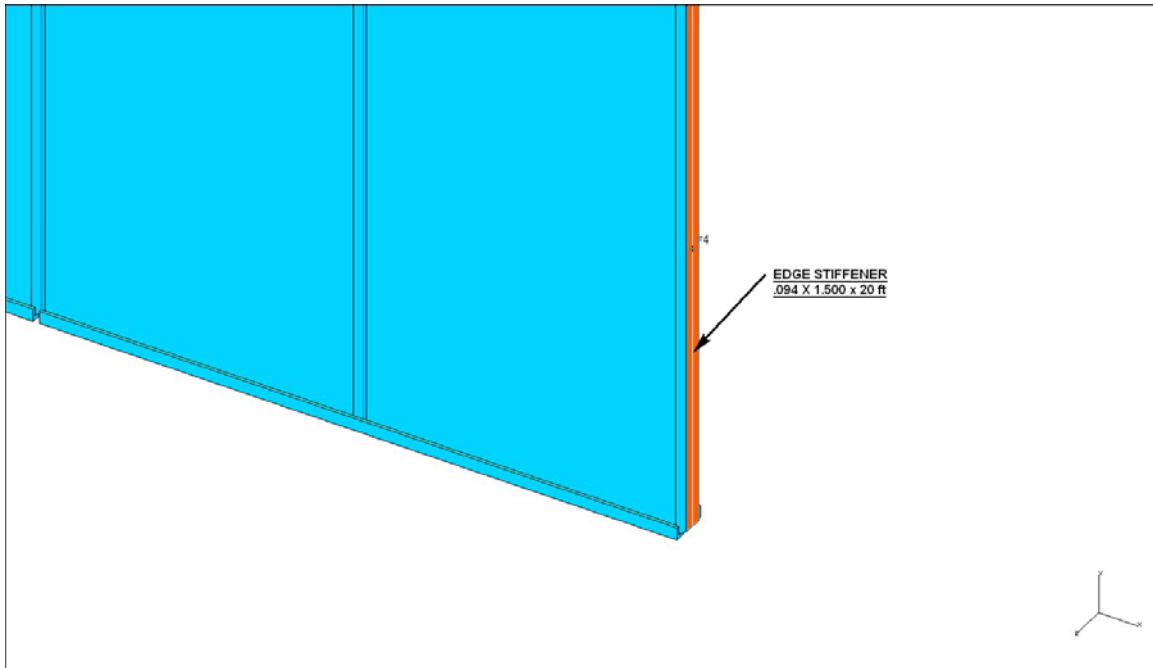


Fig. 17.10: CAD drawing of the bottom of an outside vertical module with edge stiffener attached.

## 17.5 Analysis of Detector Block Structure

Modeling a 31-plane block of PVC extrusion modules is challenging. In order to have accurate predictions of the structure's behavior from the FEA model, it is important to use a very high mesh density to get convergence of the solution. This requires state-of-the-art computer hardware and software because the number of degrees of freedom in the model is very large. The following sections describe the FEA models we have developed for the PVC extrusion modules and the adhesive bonds between them.

### 17.5.1 Modeling of Adhesive Joints

Optimizing the geometry of a single PVC extrusion to withstand the 19 psi hydrostatic pressure within the detector is a fairly straightforward analysis. However, once these extrusions are bonded together to form a monolithic structure, the structural analysis problem becomes much more complex. The buckling/stress/deflection analyses of the assembled detector that are described in the sections below depend on how the adhesive bond is modeled.

The analysis of an adhesive-bonded joint is considered to be a challenging FEA task. The difficulty arises from both the complex stress state within the adhesive and the constraints imposed by computational capacity on the modeling of a complicated geometry. Several methods including the average stress method, the maximum stress method and fracture mechanics method are discussed in detail in Reference [1]. However, application of this approach to our large structure, with a 3-D 0.25-mm adhesive bond, would result in an FEA model of formidable size.

As an alternative, two widely used approaches were considered in this study of the structure. One is to extract the nodal force by assuming the interface between the vertical and horizontal plane will move together with a connected node – merged node. The second approach is to model the adhesive layer as three spring elements, as suggested by Tahmasebi [4] and Zhu & Keyword [5]. Two springs account for the in-plane shear stiffness of adhesive and one models the normal stiffness of adhesive. This can be implemented by using a spring element (#14) in

ANSYS. Both of these methods were tried for NOvA adhesive bonds and yielded the same result. For the analysis presented below the spring element method was used.

Throughout the analysis the nodal forces are extracted and divided by its element area to calculate the average shear and normal stress around that location. By using a Mohr's circle, a maximum shear stress (principle shear stress) can be obtained as

$$\tau_{\max} = \sqrt{\left(\frac{\sigma_{\text{normal}}}{2}\right)^2 + \tau^2}$$

This maximum average shear stress over the area of the element is calculated and compared to the average shear stress for the adhesive measured in double-lap shear tests of NOvA adhesive bonds. The ratio of measured average shear stress at bond failure to the maximum average shear stress from the FEA model is taken as the safety factor (SF) on the adhesive strength. This approach is similar to that described in Reference [1].

The FEA model for a 31-plane NOvA block is very large and it is only possible to extract the average adhesive stresses from it due to the size of the elements used. However, we were concerned that stress concentrations along the edges of the bond areas that would cause progressive structural failure to occur. Following the methodology outlined in Reference [1], a highly detailed model of the bond joint in the structure was created in order to calculate potential stress concentrations in the adhesive. Next, we created a detailed FEA model of the standard ASTM tests used to measure the average strength of actual adhesive bonds. The peak stresses found in the model of the ASTM tests and in the detailed model of the detector bond joint were then compared when loaded to the average failure stress. We found that the ratio of the maximum stresses (safety factor) was similar to the ratio of the average stresses under this loading condition. We therefore believe that the safety factor (SF) calculated for average stresses will provide a SF that is similar to that for the peak stresses.

Instead of using a single element over the adhesive pad area, a refined mesh with more elements was used to obtain the stress variation over the bond area. A peak stress at the adhesive bond termination is used as the maximum calculated stress. A corresponding safety factor is calculated as:

$$SF = \text{Maximum measured (test) peak stress} / \text{maximum calculated stress.}$$

The difficulty here is the lack of actual "maximum measured peak stress" values. Conventional measurements and most available technical data sheets give only average stress data. These data are obtained by applying a force to the ASTM test piece up to its breaking point. The shear strength is calculated by dividing the force over the overlap area (F/A psi) or a width of the overlap to give a peeling strength (F/width lbf/in). There is no measured data related how this stress is distributed within the bond area and what the failure peak stresses are at the bond edge. A calculation of the safety factor is not valid without this information to account for peak stresses. To overcome this shortcoming, a maximum stress approach is proposed by Reference [1]. The idea is to produce a "quasi" stress distribution by modeling both the test specimen and the actual structure with FEAs using the same mesh size and element type. The stress distribution and its peak stress value at the bond termination is highly dependent upon of the element type and mesh size. This is because geometry in the model has a sudden change (sharp corner, no filler radius and so on) causing a stress singularity where dissimilar materials are joined together. As the mesh density increases, the peak stresses correspondingly increase. By applying a similar mesh density for both the test piece and the actual NOvA geometry, as suggested in Reference [1], a similar stress singularity state should be expected.

#### **17.5.1.1 Modeling the ASTM Tests**

Figures 17.11 to 17.13 show test geometries and the corresponding FEA models for three ASTM tests of NOvA bonds: the double-lap test for shear and the T-shape and cleavage tests for peel. The actual tests used 3M 2216 epoxy (before the change of baseline plane adhesive to

Devcon 60). The FEA model uses a 3-D element with a 20-node brick element (higher order). The mesh size is 0.0625 inches (1.57 mm). The tests measured the force at failure and a stress distribution/peak stress was calculated.

Next, we use the same element type (20-node brick) and a very similar mesh size for a mini 3-D model of the NOvA geometry, shown in Figure 17.14. The model represents a pair of vertical and horizontal cells joined by an adhesive layer. The mesh size of 0.064 inches (1.65 mm) resulted in 1,300 nodes for the adhesive area and 37,000 nodes for the whole model. A 19-psi pressure is applied to the vertical extrusion with a symmetry boundary over the sides. A “free to move” boundary condition is used for the horizontal side. Both shear and peeling forces are calculated.

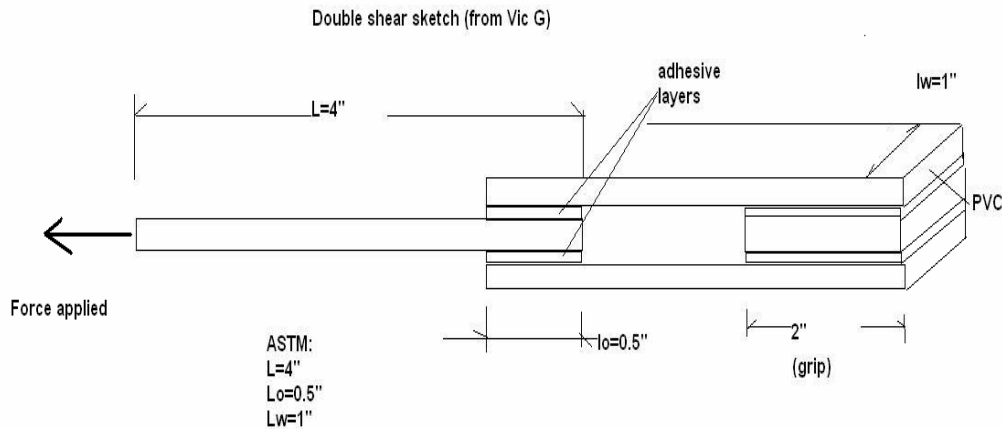


Fig. 17.11(a): Test specimen for double-lap test.

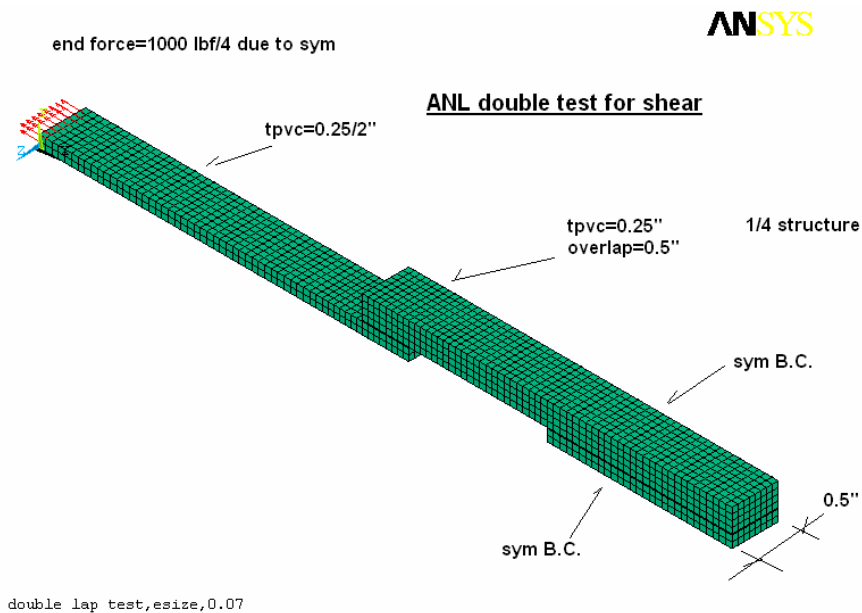


Fig. 17.11(b): FEA model for double-lap test.

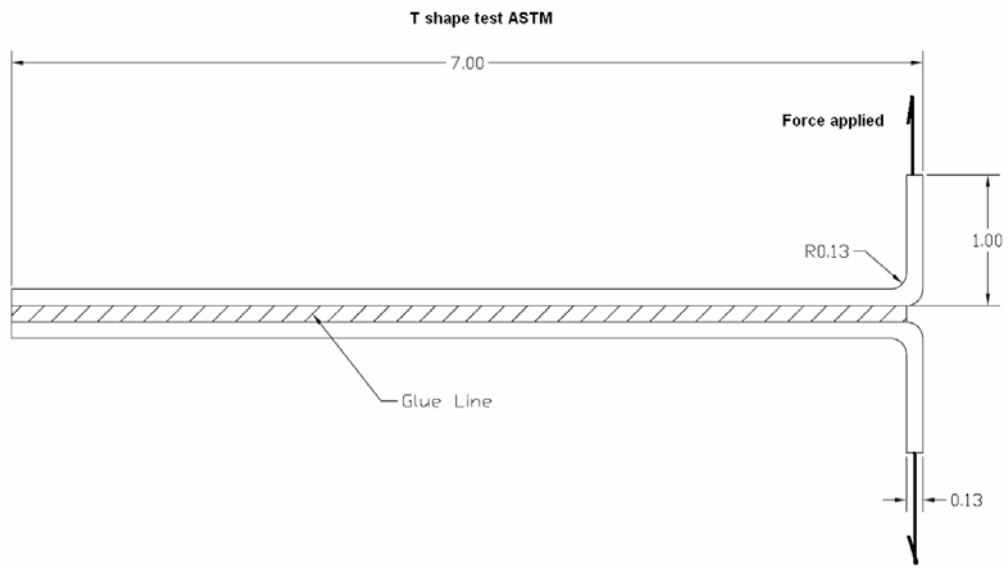


Fig. 17.12(a): T-shape test specimen.

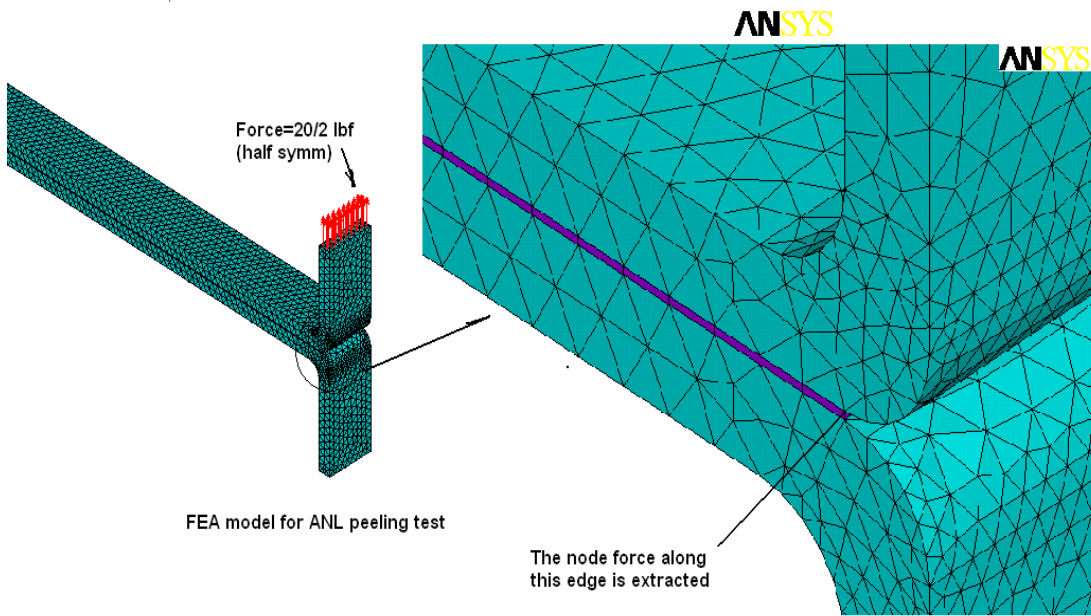


Fig. 17.12(b): FEA model for T-shape test.

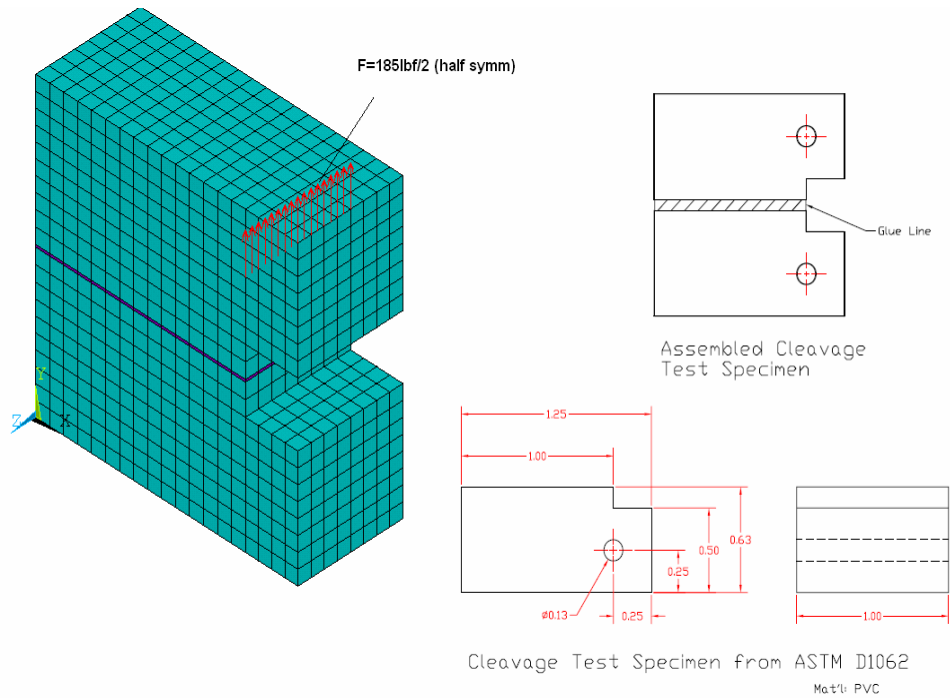


Fig. 17.13: The cleavage test specimen and FEA model.

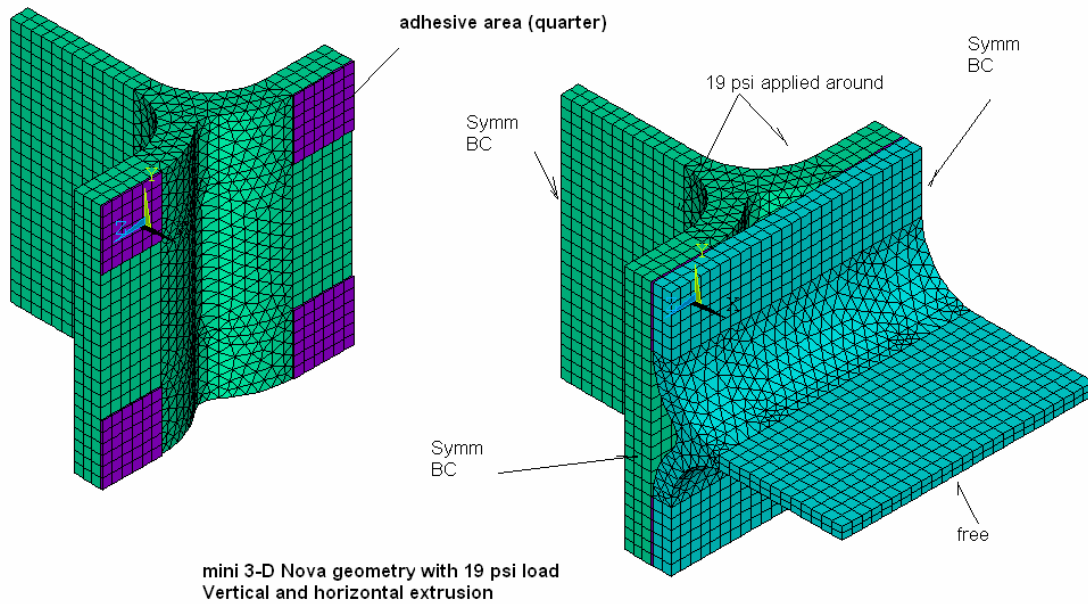


Fig. 17.14(a): Mini 3-D model for NOvA geometry.

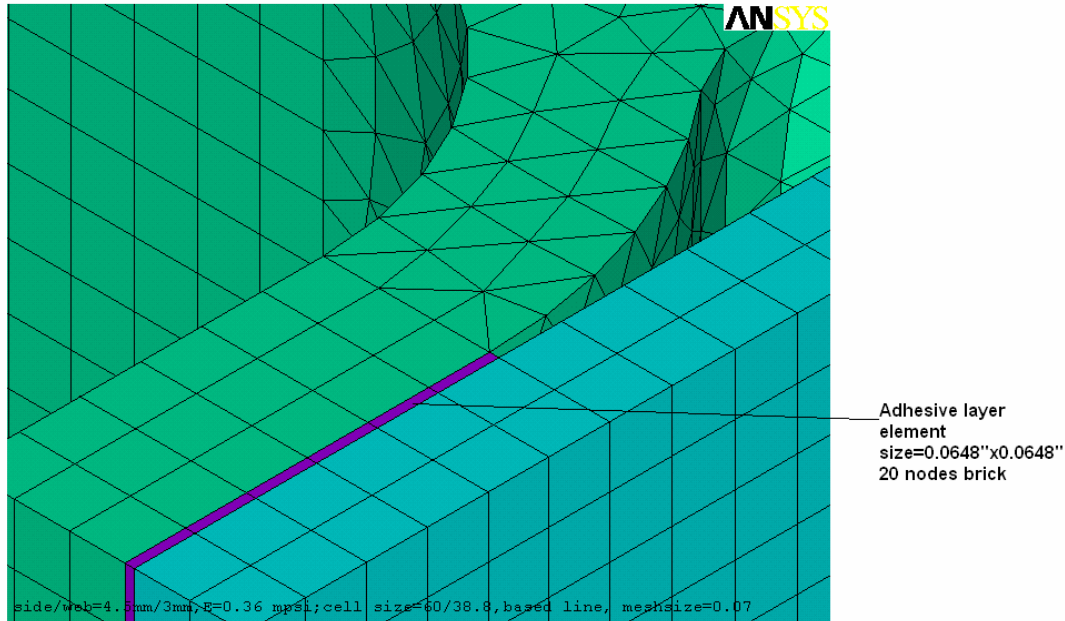
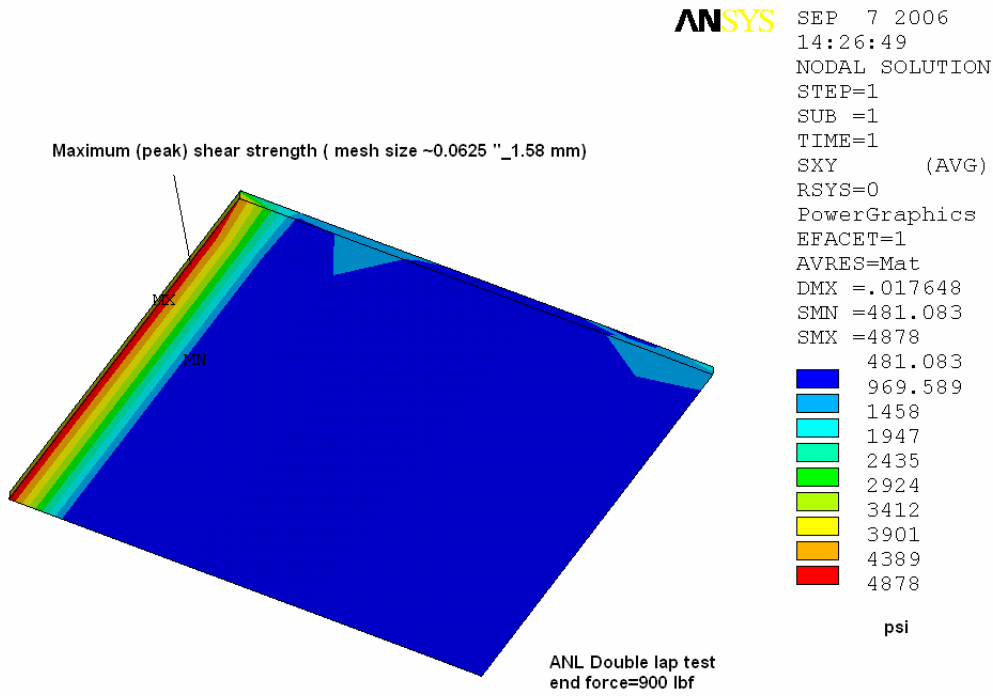


Fig. 17.14(b): The mesh over the adhesive layer in the NOvA mini 3-D model.

#### 17.5.1.2 Peak Stresses in NOvA Structure Bond with ASTM Tests: Shear stress

Double-shear measurements of test specimens found that a force of 900 lbf was required to cause failure of the adhesive. This can be compared to a calculated peak stress of 4878 psi, using a mesh size of 0.0625 inches, as shown in Figures 17.15 and 17.16. With a similar mesh size for the mini 3-D model with 19 psi loading, the maximum shear stress is around 1130 psi, yielding a safety factor  $SF = 4878/1130 = 4.3$ . A detailed examination of the stress pattern showed that the peak stress of the double lap is mostly concentrated along the edge and is uniformly distributed along its width. However, the mini 3-D model shows that the peak stress is at the corner where the model has a sudden geometry change and dissimilar materials. The model calculation is therefore considered to be more severe in terms of the stress singularity, so the  $SF = 4.3$  value calculated above is quite conservative.

Section 17.6.7 describes measurements of Devcon 60 shear strength in the actual detector geometry, using 3-layer assemblies of NOvA extrusions. The strengths found from standard ASTM tests closely match the strength measured in this test, indicating that these results are a good predictor of the strength that can be expected in the far detector geometry.



double lap test, esize, 0.07

Fig. 17.15: The maximum shear strength calculation, based on the double-lap shear test.

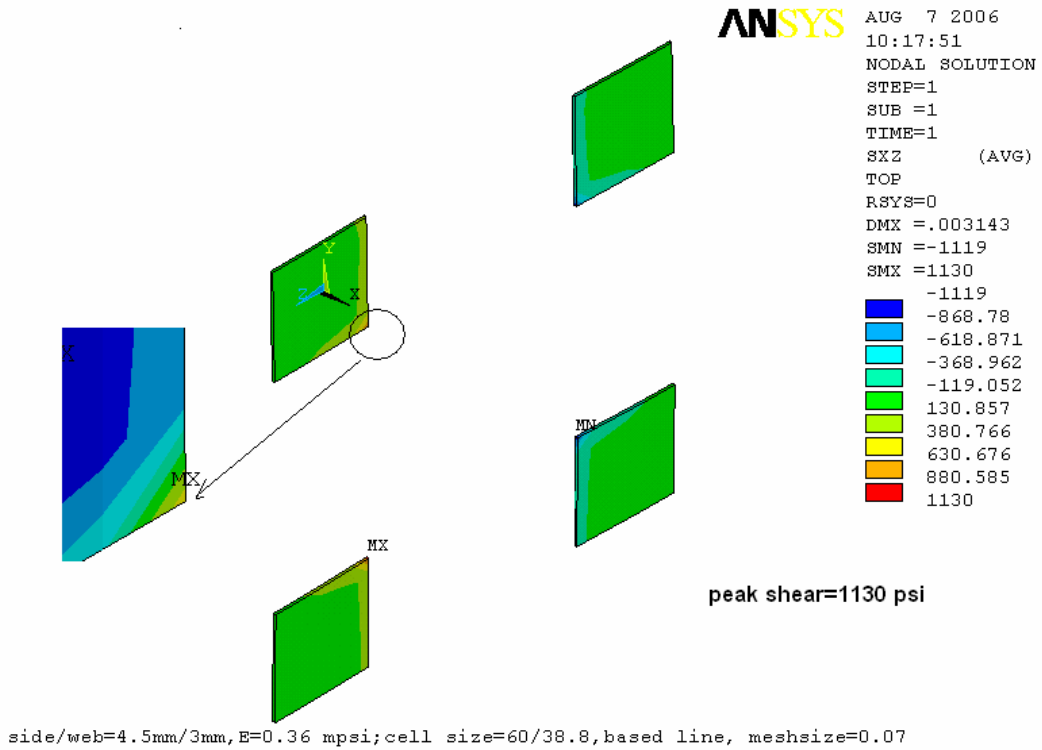


Fig. 17.16: The calculated maximum shear stress, based on mini 3-D model.

### 17.5.1.3 Peak Stresses in NOvA Structure Bond: Peeling Force and Normal Stress

Our calculation of peak peeling force and normal stress begins with the FEA model for the T-shape and cleavage peel tests. The comparisons to test measurements are made as follows:

#### a) The edge peeling force comparison

We use a 3-D 20-node brick to model the T-shape test, in which a 20 lbf force was applied as shown in Figure 17.17. The element edge force along the bond termination line is extracted as shown in Figure 17.18. The maximum edge force is found to be 20 lbf/in. With a similar mesh size, an element edge (peeling) force is also extracted from the NOvA mini 3-D model shown in Figure 17.19. This gives 4.98 lbf/in, yielding a safety factor  $SF = 20/5 = 4$ .

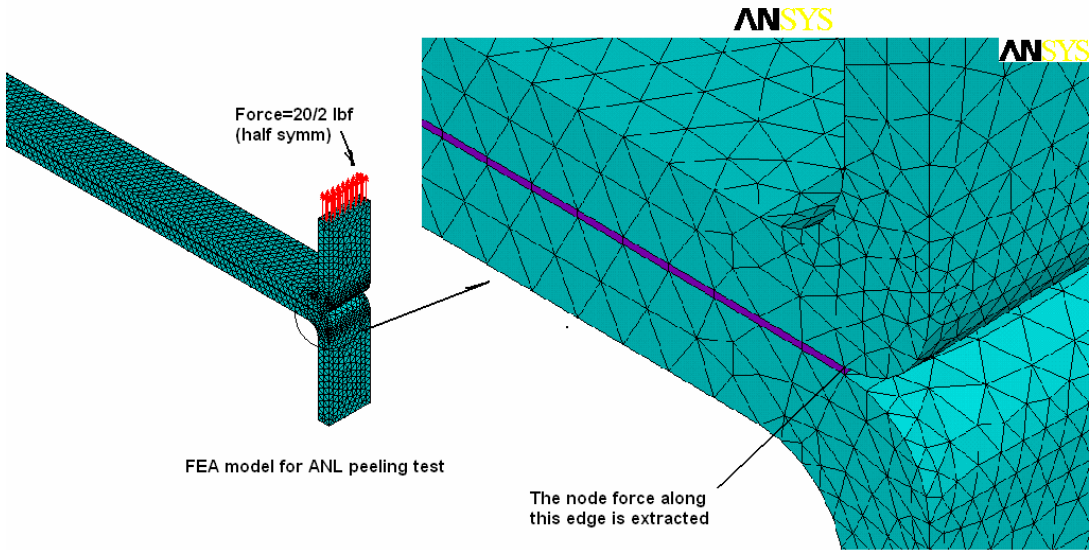


Fig. 17.17: The FEA model for peel test ( $F = 20/2$  lbf applied).

The edge force (peeling force) extraction from T-shape test done in ANL

$$\text{summation of the element edge force} = (1+0.139+0.145)/0.0625 \text{ (element length)} = 20 \text{ lb/in}$$

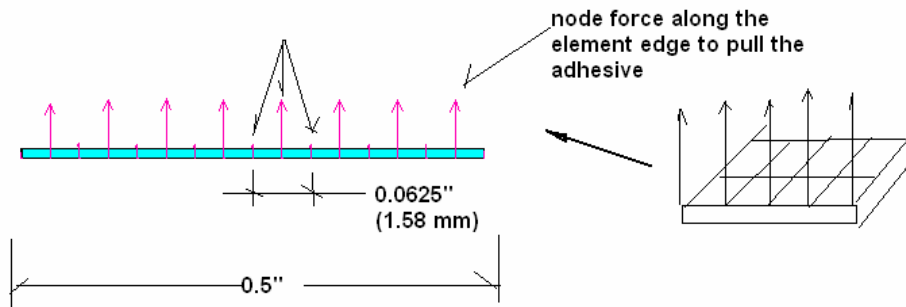


Fig. 17.18: The node force along the edge of the adhesive, extracted from T-shape test.

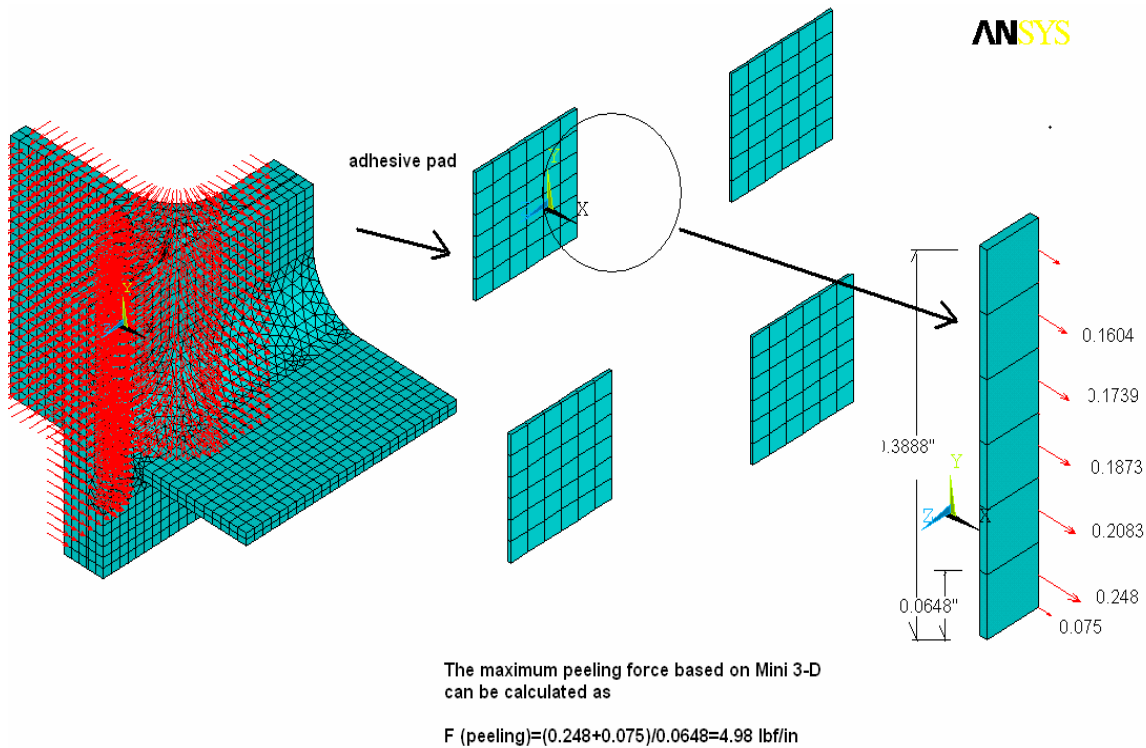


Fig. 17.19: The element edge force for the NOvA mini 3-D model.

### b) The normal stress comparison

The calculation of normal adhesive stress in the T-shape test, shown in Figure 17.20, yields a peak value of 1661 psi. The peak stress is concentrated along the adhesive edge line and is uniformly distributed along its width. However, the normal stress in the mini 3-D model has a maximum value of 1300 psi, shown in Figure 17.21. This is concentrated in the corner where the stress singularity is more severe than in the actual T-shape test specimen. There are two ways to handle this difficulty. The first is to use the stress calculated one or two elements away from the corner, as shown in Figure 17.22. This gives a stress of 516 psi and a  $SF = 1661/516 = 3.2$ . The second method is to slightly modify the geometry for both T-shape and cleavage tests to produce a similar stress singularity pattern. Figure 17.23 shows the modified geometry, obtained by simply deleting a set of elements along the edge (about 0.0625 inches) to create two sides of the “geometry sudden change” effect, as in the mini 3-D model. A similar stress singularity pattern is observed. The peak stress is concentrated in the corner, rather than uniformly along the width. Figure 17.23 shows a normal peak stress of 3600 psi and a  $SF = 3912/1300 = 2.76$ .

A similar result is obtained from the cleavage test as shown in Figure 17.24. The edge force comparison yields  $SF = 19.8/5 = 4$ . The normal stress comparison with a slightly modified geometry similar to the T-shape yields a  $SF = 3912/1300 = 3$ .

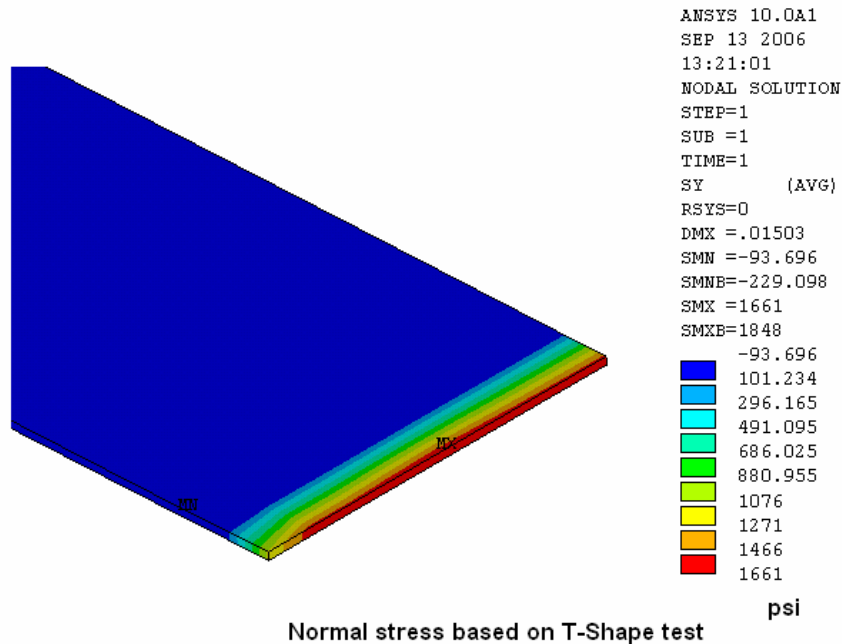


Fig. 17.20: Normal stress based on T-shape test.

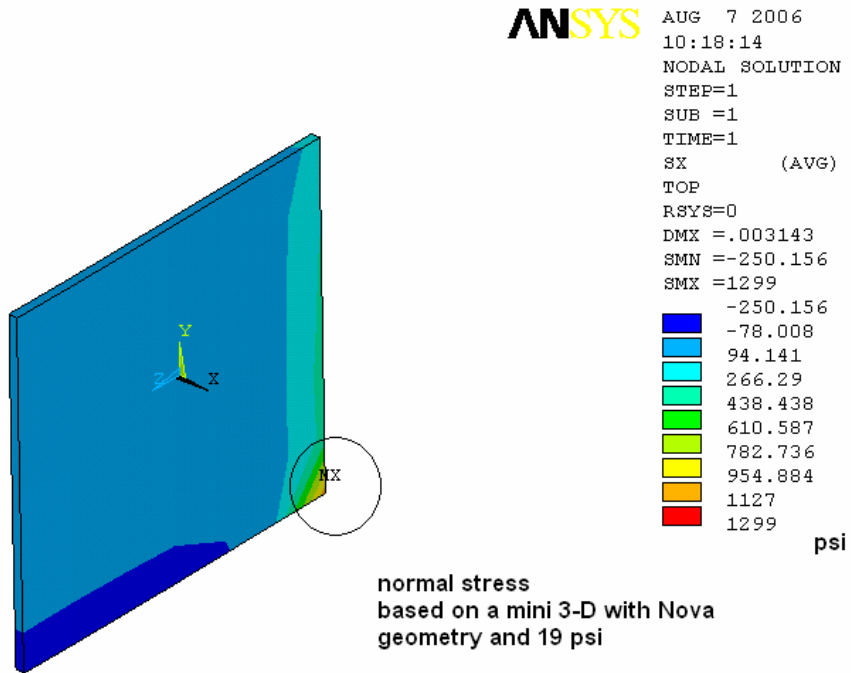


Fig. 17.21: Normal adhesive stress in the NOvA mini 3-D model with 19 psi.

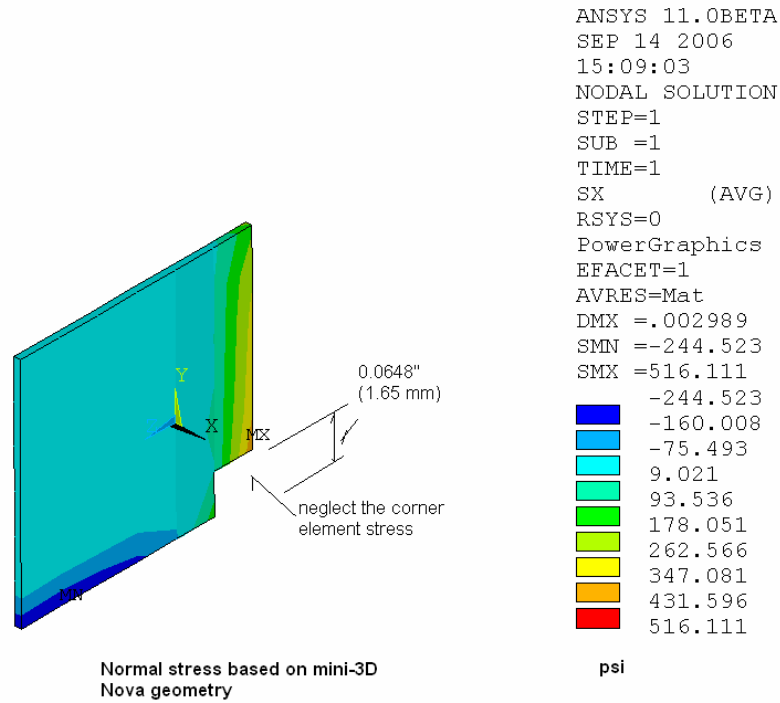


Fig. 17.22: Normal adhesive stress at 1.65 mm from the corner in the mini 3-D model with 19 psi.

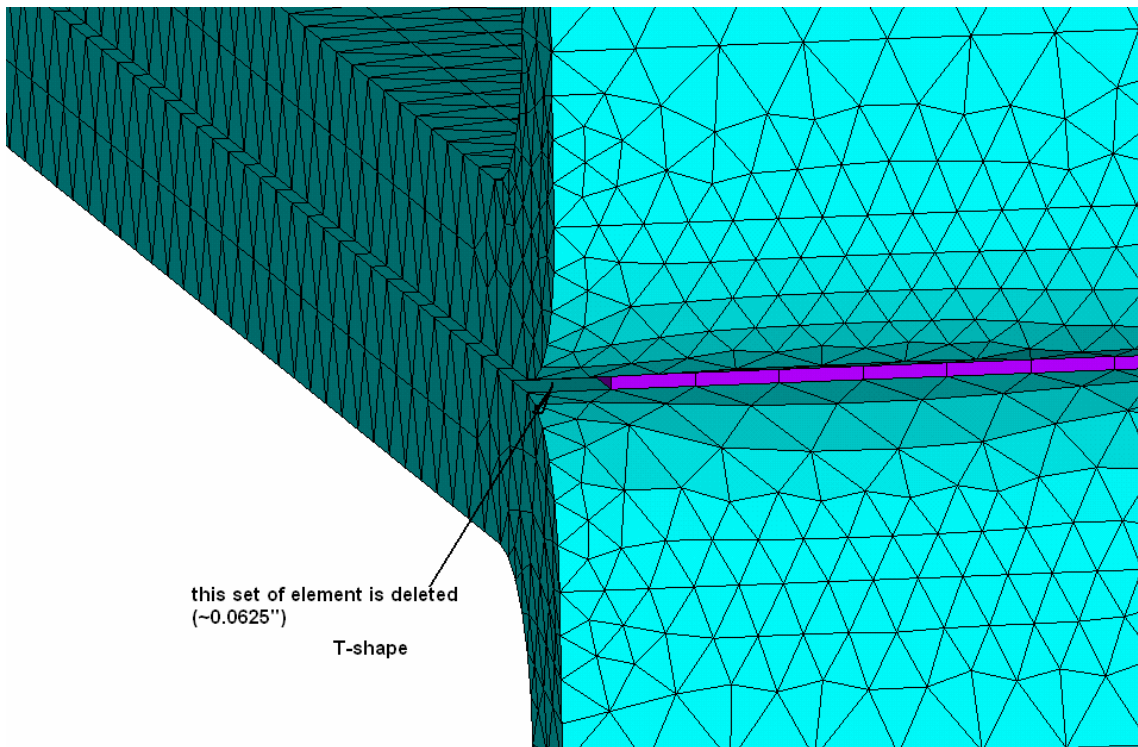


Fig. 17.23(a): The modified T-shape geometry.

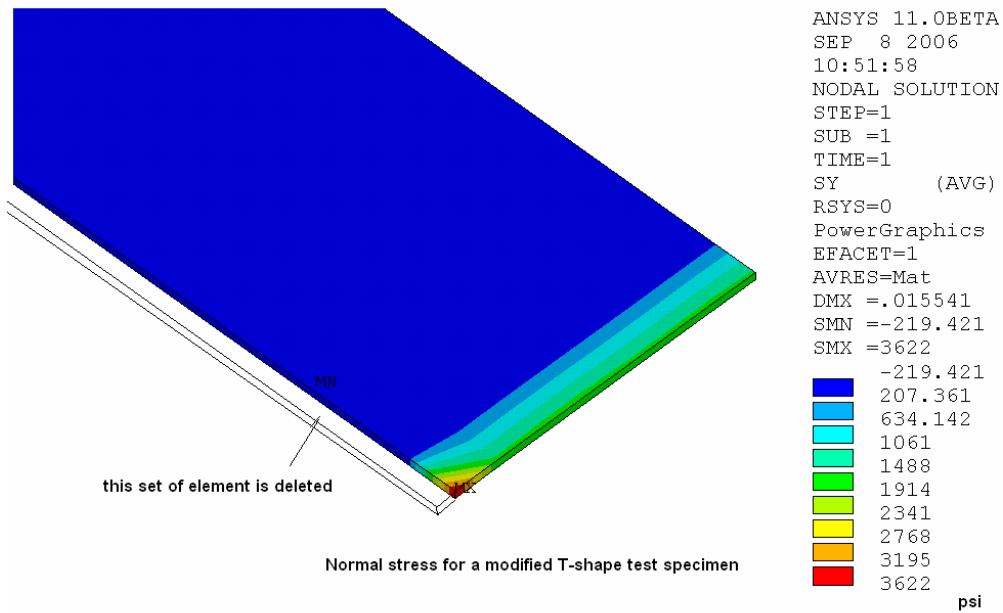


Fig. 17.23(b): Adhesive normal stress based on the slightly modified T-shape geometry.

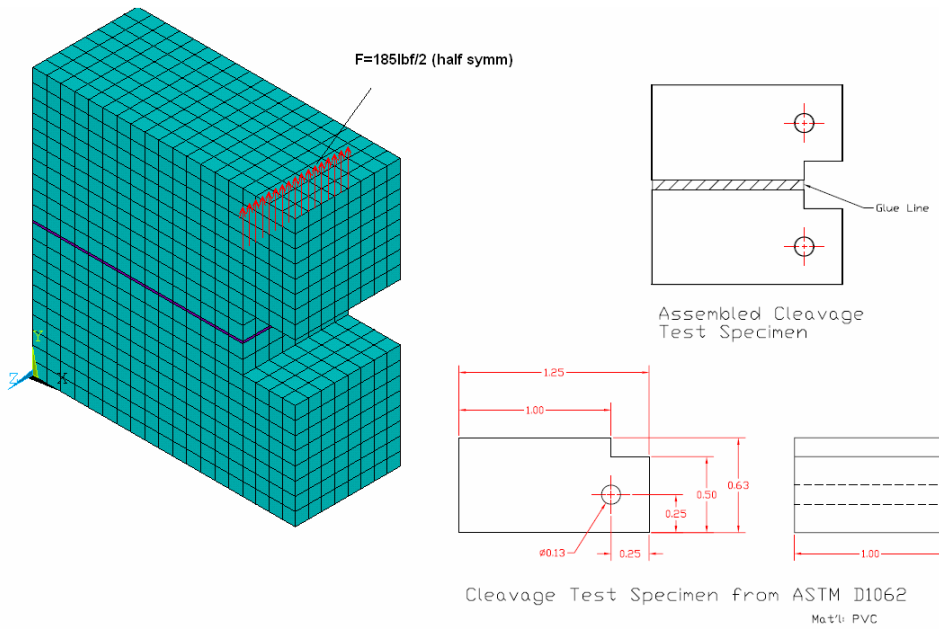
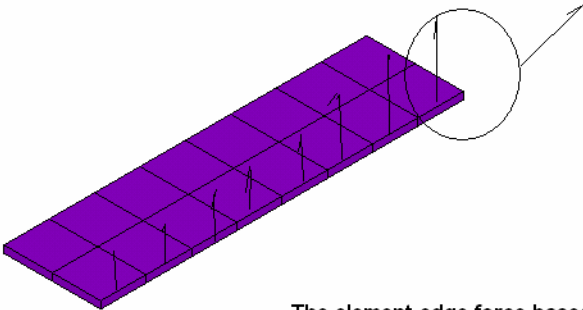


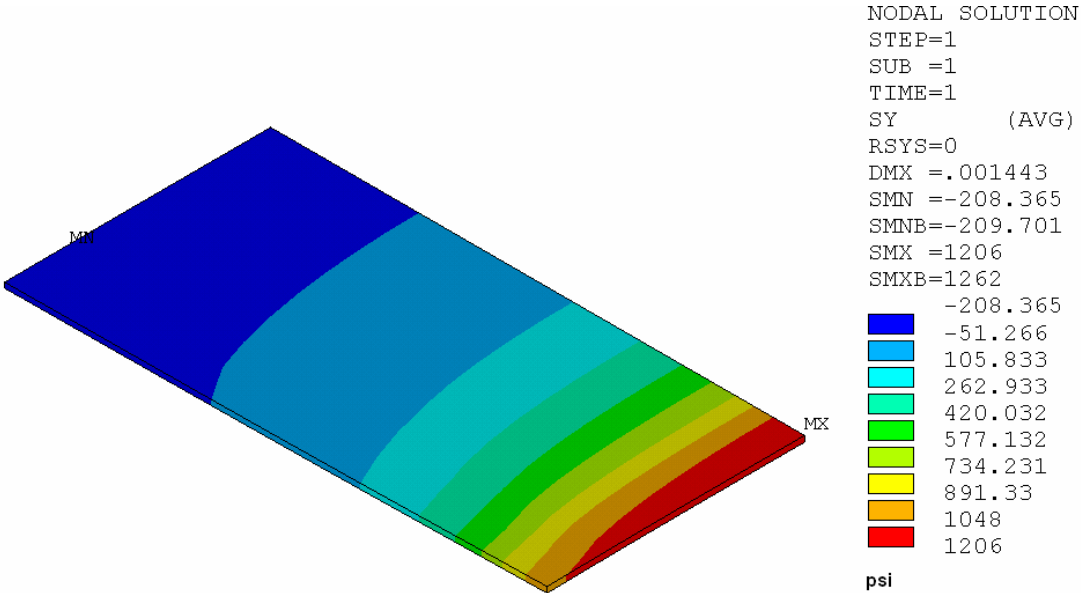
Fig. 17.24(a): The cleavage test geometry.

Edge peeling force  
 $= (1.588 - 0.3776) / 0.0625 = 19.36 \text{ lbf/in}$



The element edge force based on cleavage test

Fig. 17.24(b): The adhesive element edge force extraction from cleavage test.



Normal stress based on the ANL cleavage test

Fig. 17.24(c): Adhesive normal stress for cleavage test.

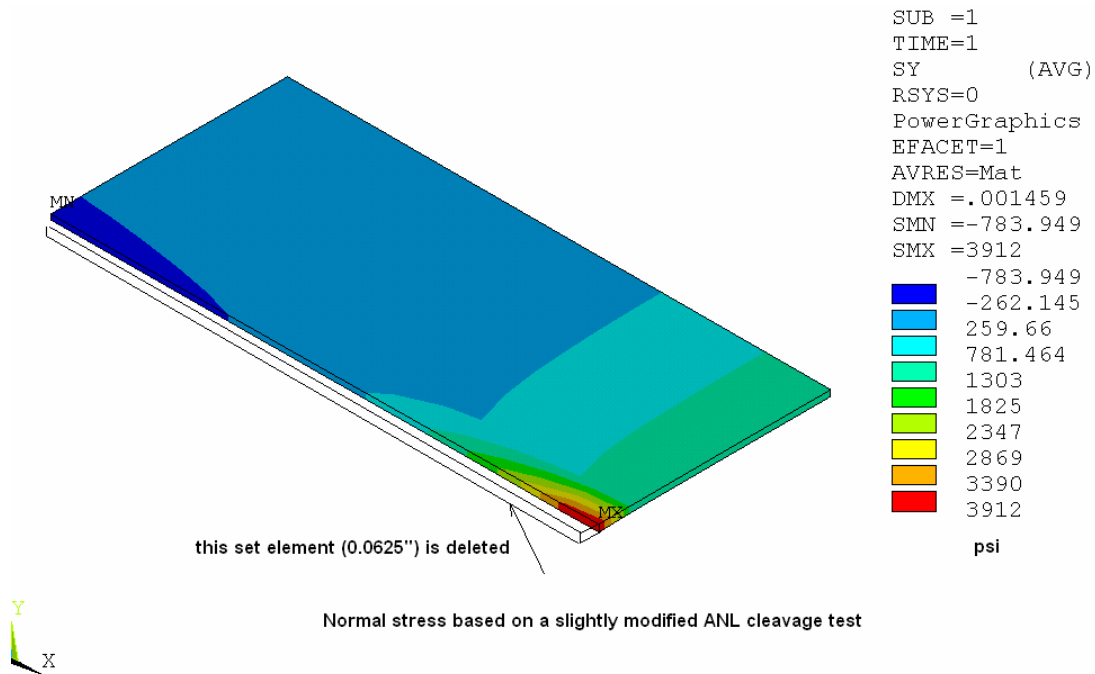


Fig. 17.24(d): Adhesive normal stress for slightly modified cleavage test.

#### 17.5.1.4 Summary of Adhesive Bond Modeling

Tables 17.3, 17.4 and 17.5 summarize the results of shear and peel tests with 3M 2216 epoxy and compare them with FEA calculations to obtain adhesive bond strength safety factors. The safety factors for the shear and peel stresses are around 4.6 and 3, respectively, based on this refined mesh study. Since the adhesive stress analysis is considered to be very complex due to the complicated geometry being modeled and inability of the method to quantize the stress singularity at the bond termination, the analysis results are mainly used to provide guidelines for design optimization.

	<b>Peak shear psi</b>	<b>Normal stress psi</b>	<b>Peeling force lbf/in</b>	<b>Von Mises stress psi</b>	<b>Mesh size 20 node brick</b>
<b>Mini 3-D (19 psi) Nova geometry</b>	<b>1130</b>	<b>1299 (or 500 psi, neglecting the corner)</b>	<b>4.98</b>	<b>2152</b>	<b>~0.0648 inch (~1.65 mm)</b>

Table 17.3: Summary of results for mini 3-D model of NOvA geometry (19 psi, one pair of cells).

	Peak shear psi	Normal stress psi	Peeling force lbf/in	Von Mises stress psi	Mesh size
Double lap test for shear	4878			9564	~0.0625"
T-shape test for peeling		1661	20		~0.0625
Cleavage test for peeling		1206	19.8		~0.0625
Slightly modified T- shape geometry		3662			~0.0625
Slightly modified cleavage geometry		3912			~0.0625

Table 17.4: Summary adhesive strength results from shear and peel tests with 3M 2216 epoxy.

	SF peak shear stress	SF normal stress	SF Peeling force	SF Von Mises stress
Double-lap shear test	SF = 4878/1130 = 4.31			SF = 9564/2152 = 4.4
T-shape peel test		SF=1611/1300 =1.23	SF = 20/5 = 4	
Peeling strength from cleavage peel test		SF=1206/1300 =0.93	SF = 19.8/5 = 4	
Slightly modified T-shape peel test		SF = 3622/1300 = 2.76		
Slightly modified cleavage geometry		SF = 3912/1300 = 3.0		

Table 17.5: Summary of safety factor calculations from shear and peel tests for 3M 2216 epoxy.

### ***17.5.2 Description of the FEA Model of Assembled Blocks***

NOvA engineers have developed several finite element models for the NOvA far detector structure. An initial 2-D FEA model was used to calculate the stress due to 19 psi hydrostatic pressure in the vertical extrusions. Subsequently, a more complex model was developed to understand the complete block structure in terms of its stresses and stability. The actual PVC structure has a 15.7 m × 15.7 m cross section with 1178 layers of alternating horizontal and vertical PVC extrusion modules. The most efficient way to model this structure is to use the shell element (STIF 63/STIF 181 in ANSYS). This has characteristics similar to those of a beam element. To limit the size of the problem and reduce computational time, only a slice in the middle of the structure was modeled. A symmetry boundary condition was imposed on both sides to reflect the rest of the structure. The mesh size of the shell element is 0.5 inches to 0.7 inches, in a structure whose full height is ~600 inches. The resulting model has approximately 260,000 nodes and 6 degrees of freedom (DOF) per node, giving a total of 1.5 million DOF for a 31-plane block, without counting the spring elements used for the adhesive layers. We used “top free” and “bottom fixed” boundary conditions as a worst case. The hydrostatic load of 19 psi was applied linearly along the vertical extrusion and zero pressure was used for the horizontal extrusion. The density of PVC was increased to account for the weight of the liquid. This baseline model and its boundary conditions were modified many times to study the structural characteristics under different scenarios, as described in detail in NOVA-doc-1147, 1151, 1172, 1297, 1298, 1351, 1490 and 1876. Figure 17.25 shows basic structure of the FEA model.

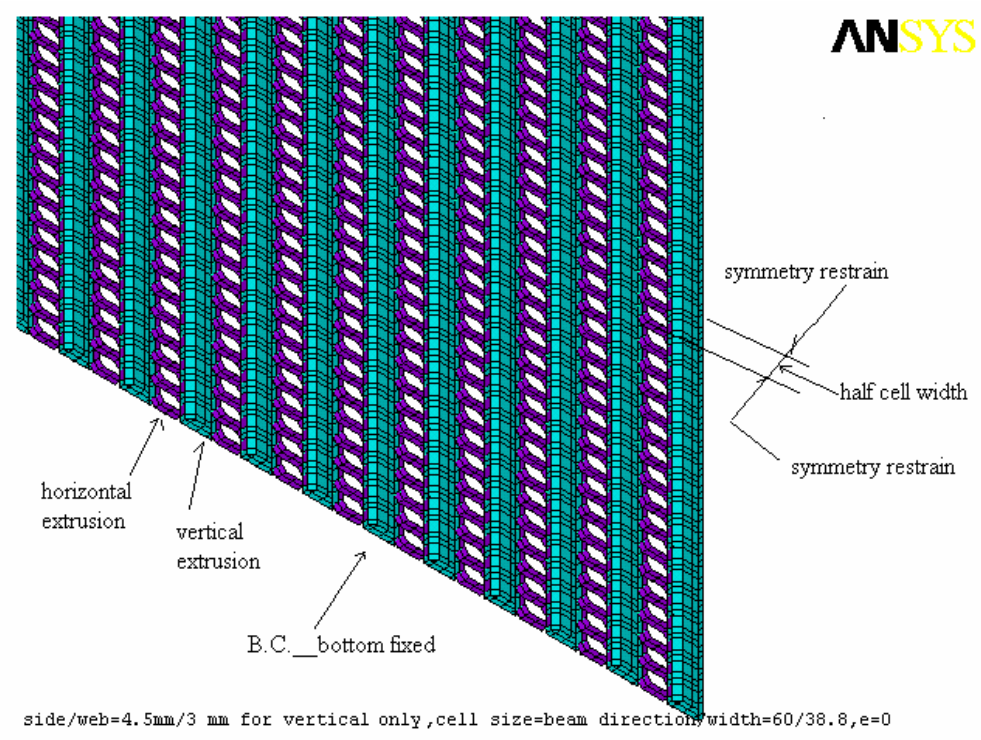
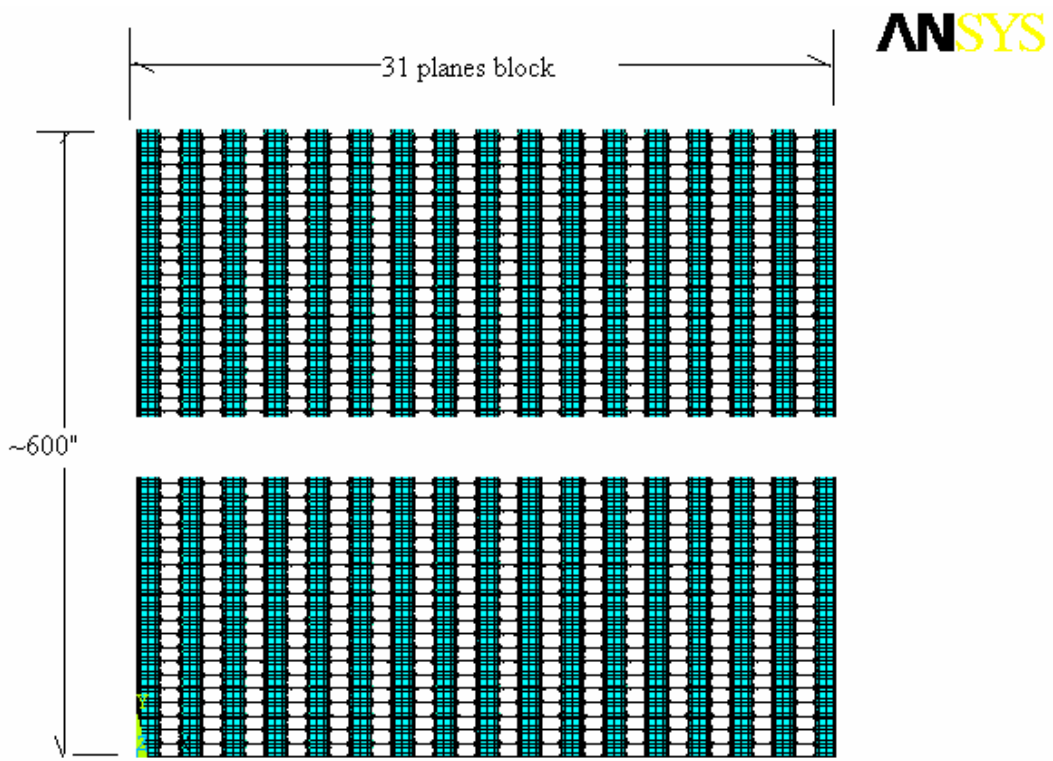


Fig.17.25: FEA model of the NOvA far detector with the shell element.

### ***17.5.3 Analysis of a 31-Plane “A” Block***

From a physics performance point of view, it is desirable to have as many planes of modules glued together into a block as possible. However, there are practical limits to how large a block can be, including the maximum physical size that can be constructed on the block pivoter, the allowable internal stresses within the block and the stability of the block.

We examined the stresses and deflections of the assembled planes, including stresses and deflections of the PVC and adhesive. This study used a PVC modulus for 4 years ( $E = 146$  ksi), which is the maximum time period of the assembly, and for 20 years, which is the nominal operating lifetime of the detector. The analysis of A-type blocks, with planes of vertical modules on the outside faces, is treated in this section. Section 17.5.4 describes the analysis of B-type blocks, with planes of horizontal modules on the outside faces.

This initial series of analyses shows that the cumulative swelling at the bottom of the detector, due to the hydrostatic pressure in the vertical extrusions, increases with the number of planes in a block. This in turn increases the stresses in the PVC and in the adhesive supporting the horizontal extrusions. In order to keep the stresses within an acceptable range for the creep-weakened PVC, the number of planes within a block was limited to 31. The stresses in the PVC could be lowered further by reducing the number of planes within a block, however, below 31 planes the block buckling stability falls below the target safety factor of 5.

A second series of FEA models used a PVC modulus of 75 ksi as the worst case prediction for the modulus at 20 years. The calculation was done for 31, 59, 123 and 187 layers in a single block.

The results for 4-year and 20-year PVC modulus values are summarized in Tables 17.6 and 17.7, and in Figures 17.26 through 17.34. For 31 planes per block, the stresses and deflections for both PVC and adhesive are acceptable. As the number of planes per block increases, both the deflections and stresses of the PVC extrusions rise. The peel stress in the adhesive become unacceptably high for a block with more than 123 planes per block.

Figures 17.26 through 17.34 show that the maximum PVC stress occurs at the very bottom of the vertical extrusions. However, the FEA model does not include the support of extrusions by the module end seals. Therefore, the maximum stresses predicted by this analysis would not occur because of the additional strength provided to the vertical extrusions by the end seals. The remaining PVC stresses appear to be at an acceptable level after 20 years of PVC creep. However, the adhesive stresses were still of concern for 3M 2216 epoxy. The current baseline adhesive, Devcon Plastic Welder 60, provides 1200 psi shear strength and 115 lbs/in of peel strength, giving a safety factor of 5 for adhesive peel failure with 31 planes per block.

E=0.146 mpsi (4y)							
Number of the layers in a block	31	59	123	187	251	315	371
Total swelling (inch)	0.11	0.218	0.408	0.598	0.776	0.944	1.084
Von Mises stress (peak, psi)	776	866	969	1029	1071	1105	1129
Von Mises stress(excluding peek, psi)	497	564	644	691	726	752	772
Von Mises strain(peak, %)	0.53	0.6	0.66	0.7	0.73	0.75	0.77
Von Mises strain(excluding peak,%)	0.34	0.39	0.44	0.47	0.49	0.51	0.53
Adhesive shear stress (psi)	159	190	216	232	238	247	252
Adhesive Peeling force (lbf/in)	4.27	5,64	9.59	11.83	13.26	14.31	15.01

Table 17.6: Block properties versus number of planes/block for a 4-year PVC modulus.

E=0.075 mpsi (20 y)				
Number of the layers in a block	31	59	123	187
Total swelling (inch)	0.2	0.38	0.78	1.16
Von Mises stress(peak, psi)	776	866	969	1029
Von Mises stress(excluding peek, psi)	497	564	644	691
Von Mises strain(peak, %)	1	1.1	1.2	1.37
Von Mises strain(excluding peak,%)	0.6	0.7	0.8	0.9
Adhesive shear stress (psi)	162	188	217	233
Adhesive Peeling force (lbf/in)	4.31	5.23	9.52381	11.84

Table 17.7: Block properties versus number of planes/block for a 20-year PVC modulus.

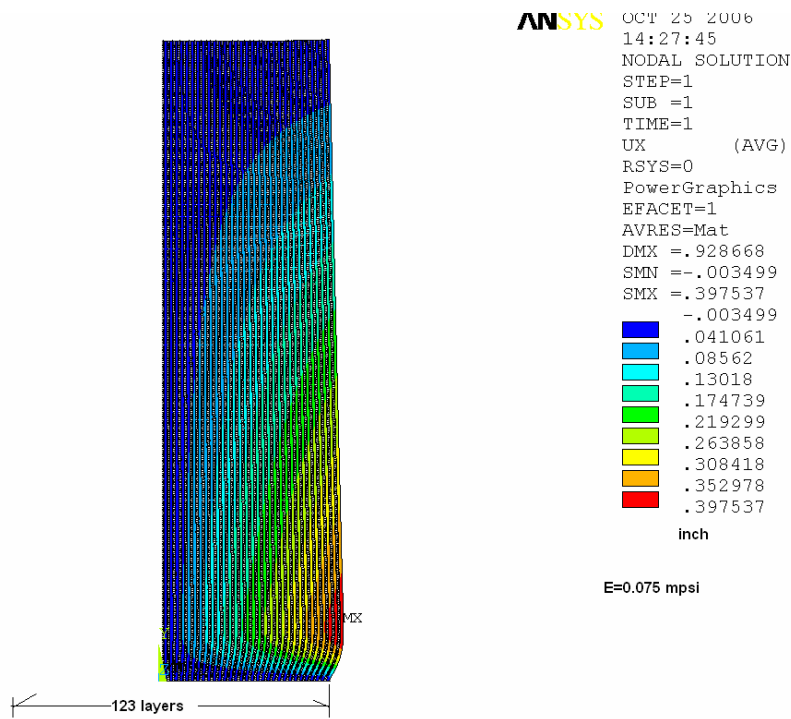


Fig. 17.26: The swelling shape for a NOvA A-type block at 20 years.

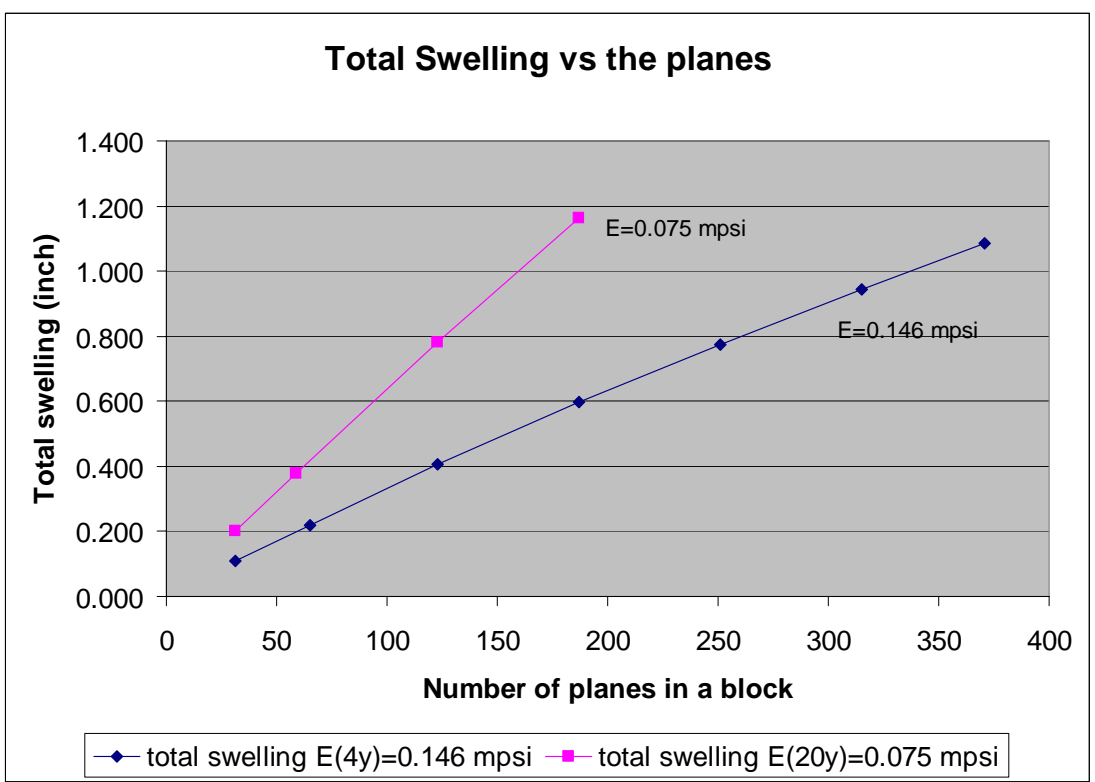


Fig. 17.27: Maximum swelling vs the number of planes per block.

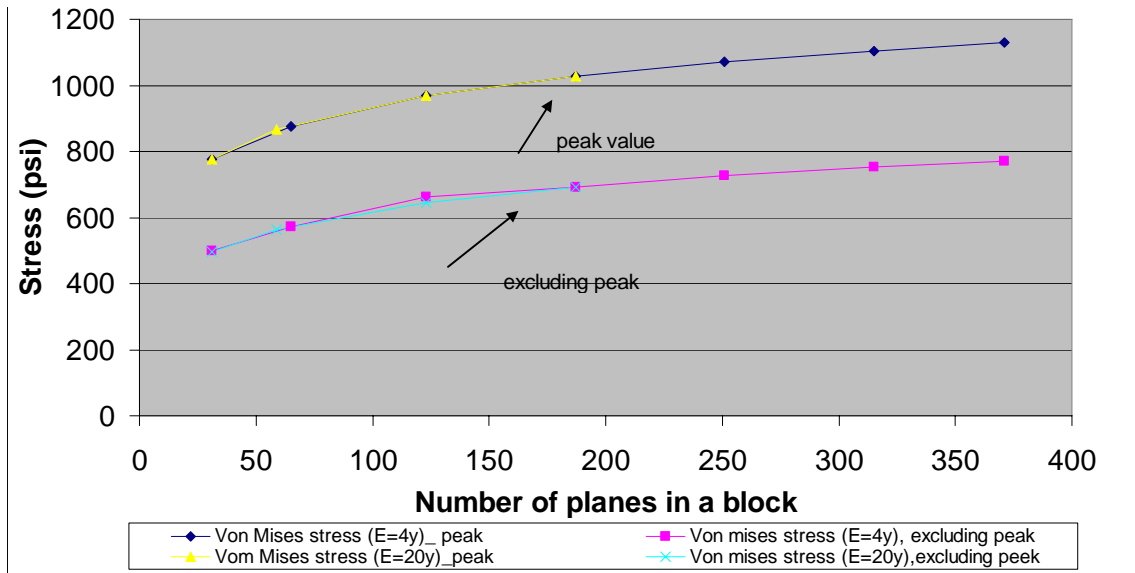


Fig. 17.28: Von Mises stress vs the number of planes per block at 4 years and 20 years.

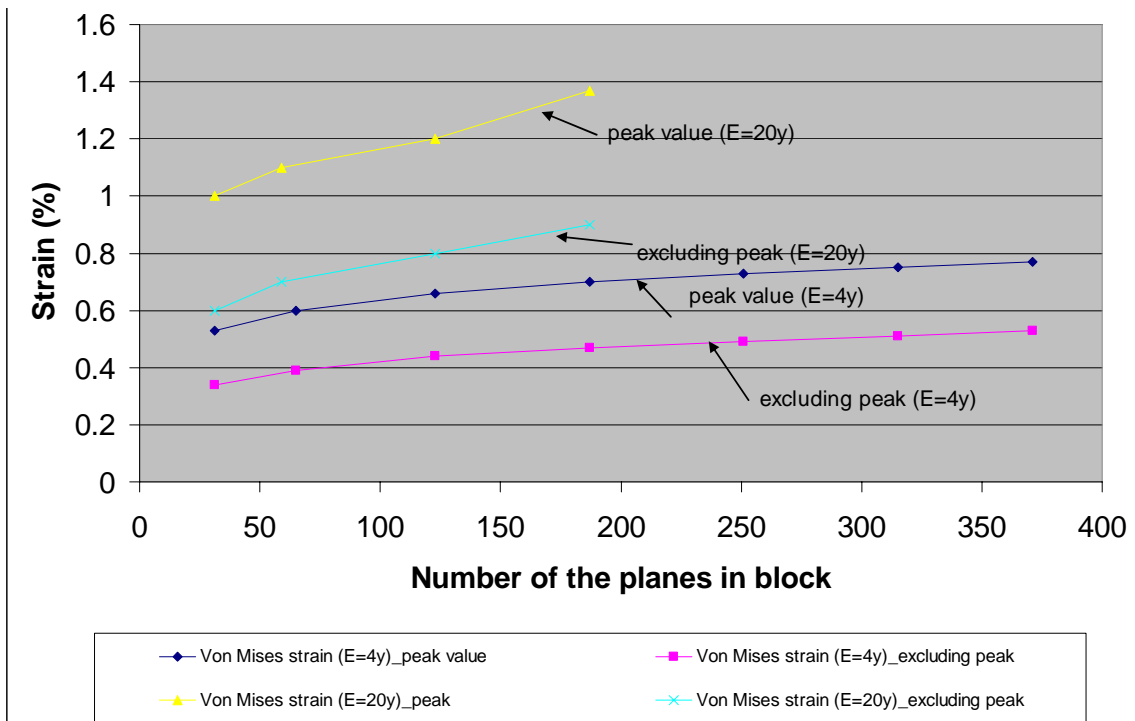


Fig. 17.29: Von Mises strain vs the number of planes per block at 4 years and 20 years.

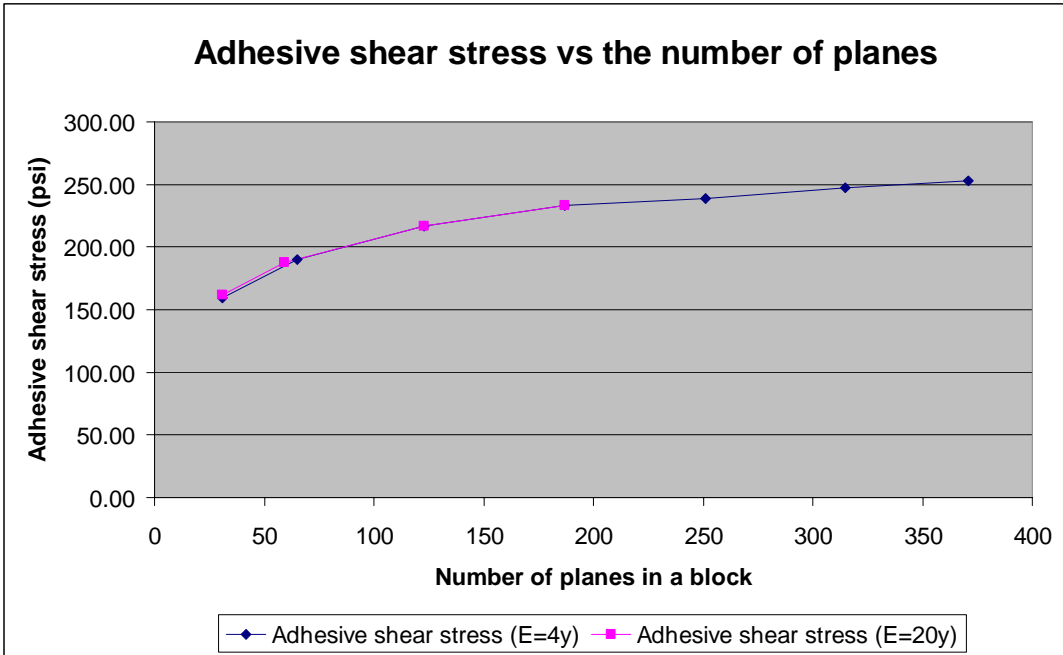


Fig. 17.30: Adhesive shear stress vs number of planes per block.

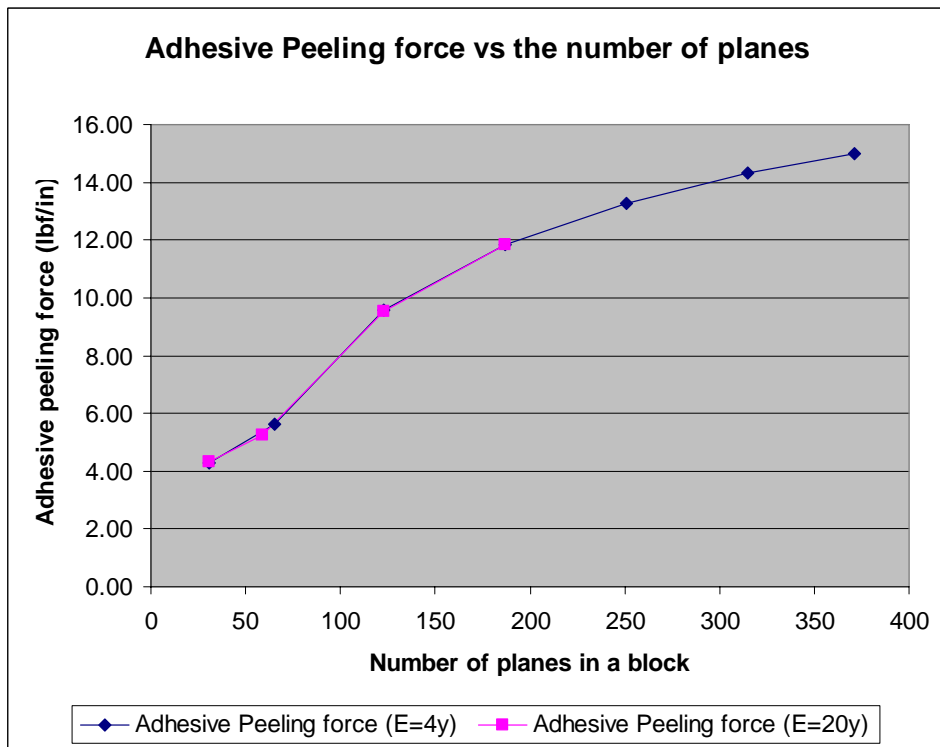


Fig. 17.31: Peeling force vs number of planes per block.

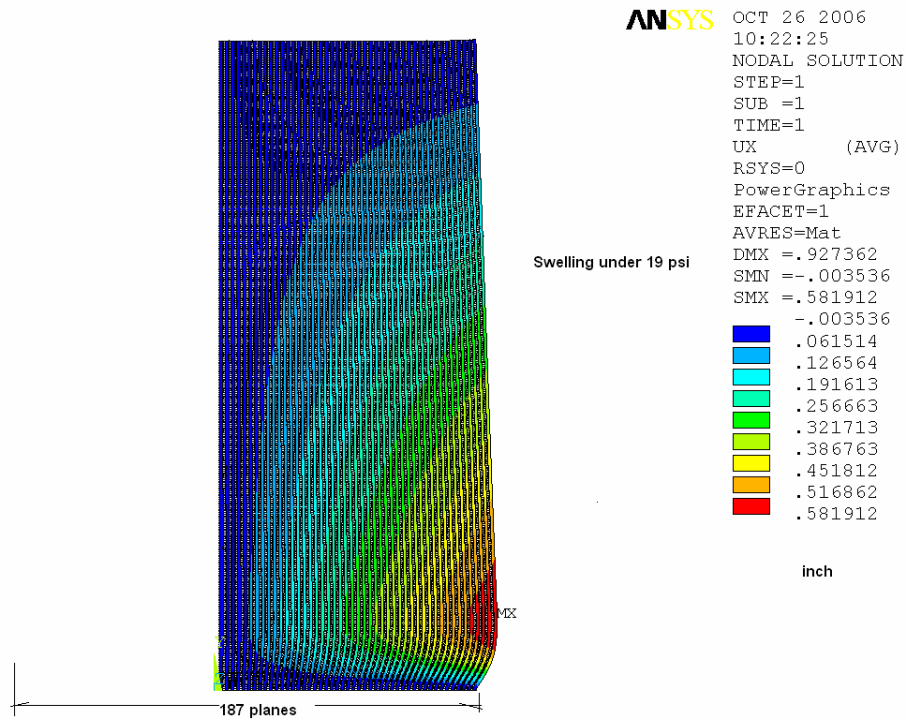


Fig. 17.32: Block swelling for 187 planes case at 20 years.

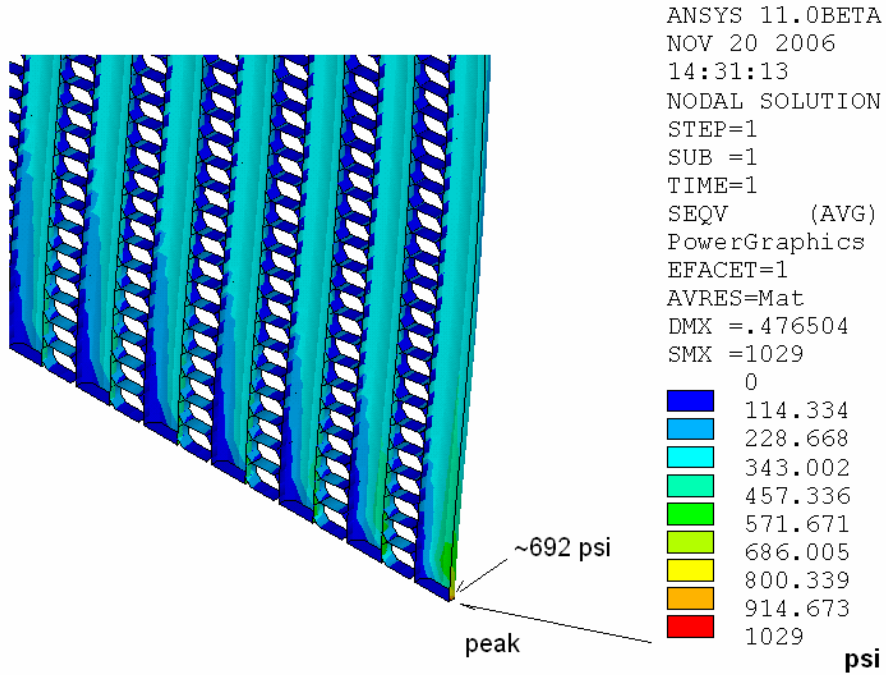


Fig. 17.33(a): Von Mises stress for a block with 187 planes at 4 years.

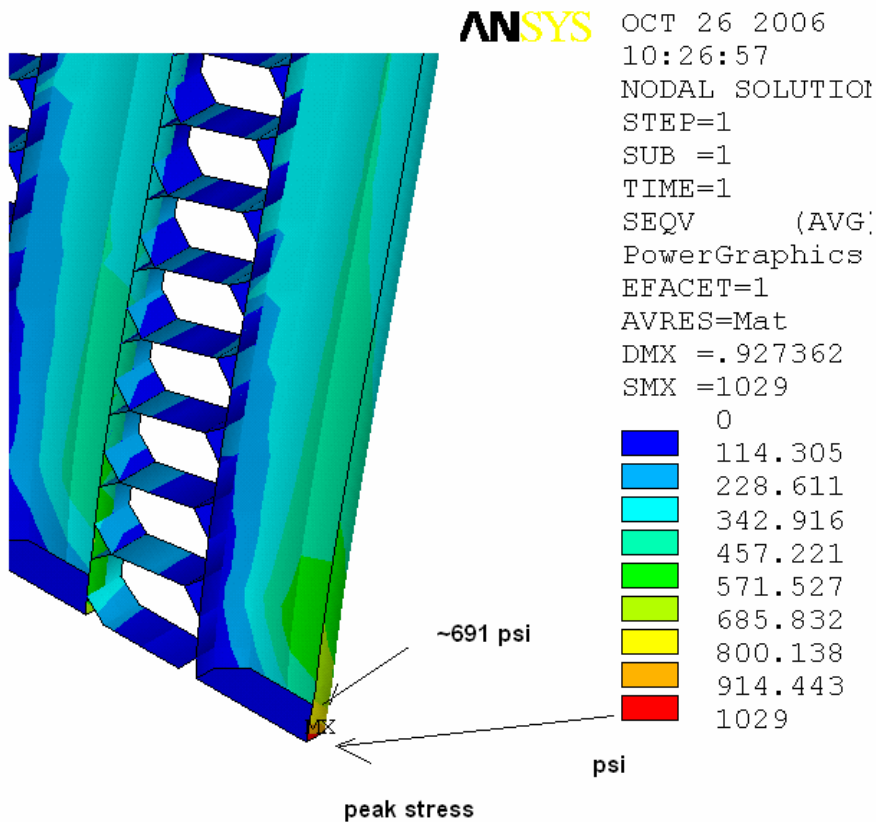


Fig. 17.33(b): Von Mises stress for a block with 187 planes at 20 years.

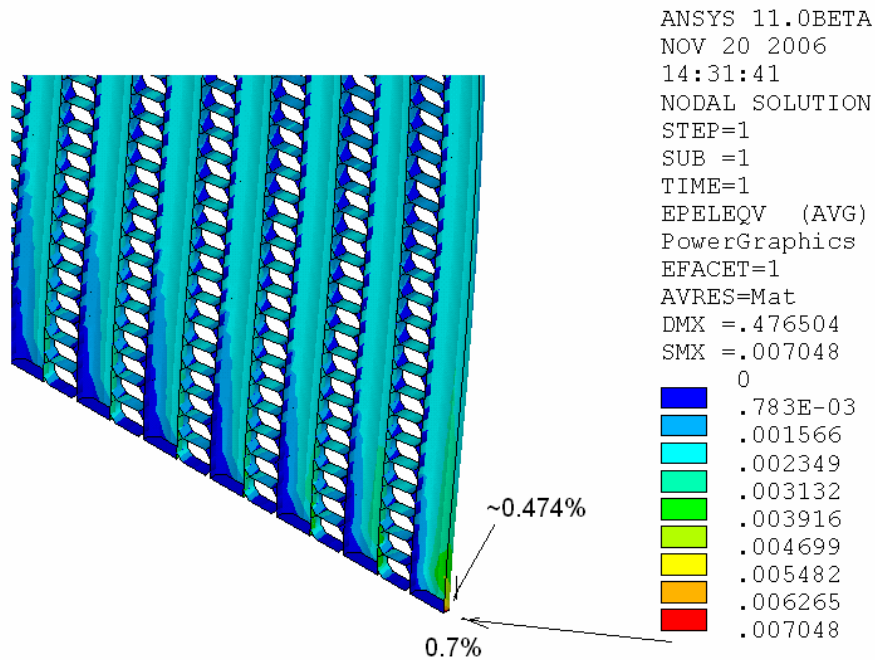


Fig. 17.34(a): Von Mises strain for a block with 187 planes at 4 years.

**ANSYS** OCT 26 2006  
 10:27:29  
 NODAL SOLUTION  
 STEP=1  
 SUB =1  
 TIME=1  
 EPELEQV (AVG)  
 PowerGraphics  
 EFACET=1  
 AVRES=Mat  
 DMX =.927362  
 SMX =.013717  
 0  
 .001524  
 .003048  
 .004572  
 .006096  
 .00762  
 .009144  
 .010669  
 .012193  
 .013717

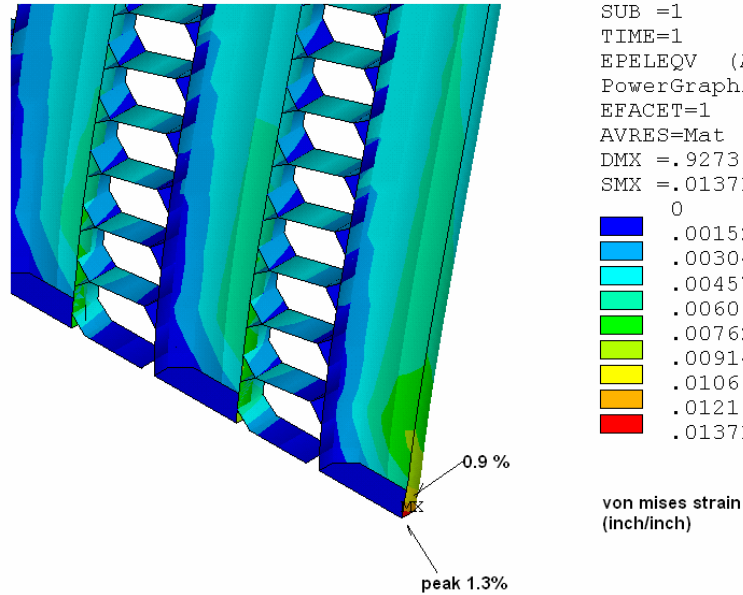


Fig. 17.34(b): Von Mises strain for a block with 187 planes at 20 years.

### 17.5.3.1 “A” Block Adhesive Strength Requirements

The model described in the previous sections was used to examine adhesive stresses in order to understand the strength requirements for the plane adhesive. The initial analysis examined 32 planes filled with scintillator. Figure 17.35 shows the distribution of the adhesive stresses from the bottom to the top of the detector and Figure 17.36 shows the location of the shear stresses in the FEA model. The maximum adhesive shear stresses occur at the bottom of the detector and are approximately 165 psi but are less than 140 psi throughout the remainder of the plane.

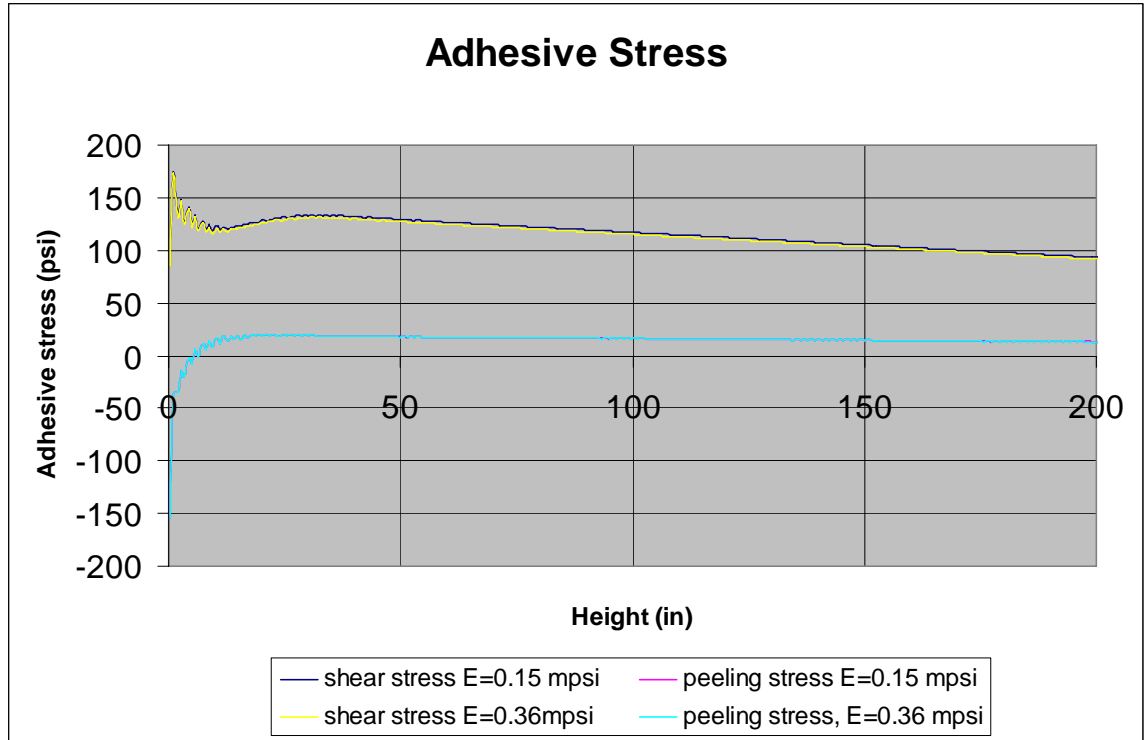


Fig. 17.35: Adhesive stress vs height.

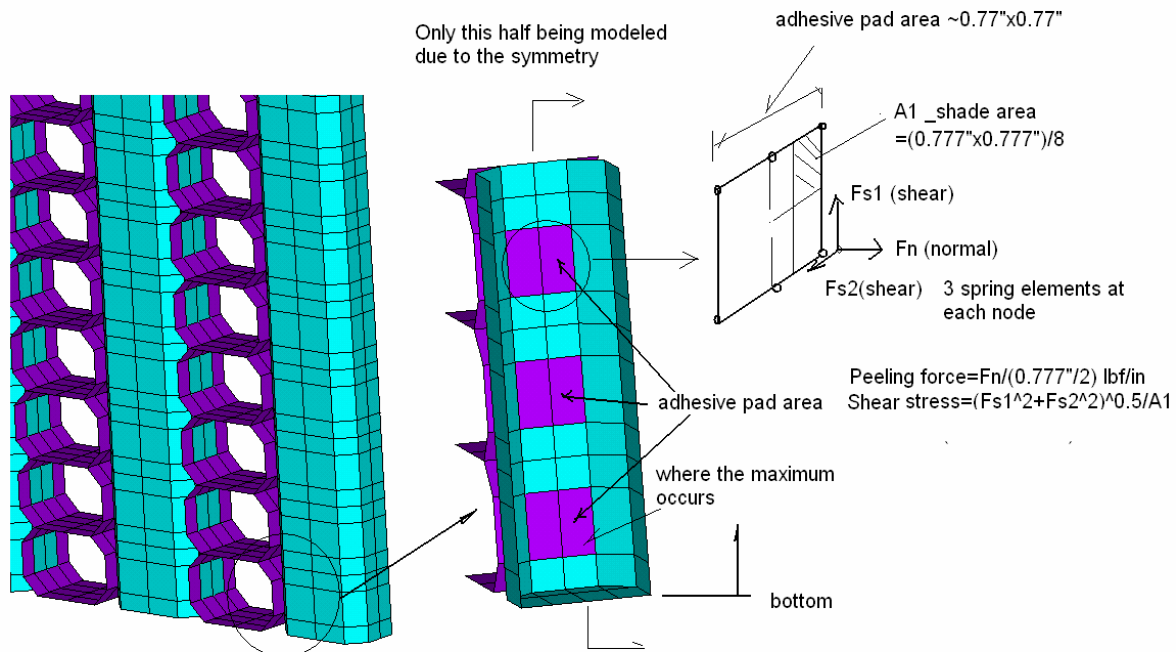


Fig. 17.36: Location of shear stresses in the FEA model.

Three components contribute to adhesive stresses. The (small) first component is due to the weight of the horizontal extrusions being transferred to the vertical extrusions. The second component is due to the stress from the PVC deformation under hydrostatic pressure. The third component is due to the differential strain between the vertical and horizontal extrusions from the weight of the extrusions and scintillator.

### 17.5.3.2 Buckling Analysis of a 31-Plane "A" Block

The stability of a 31-plane A-type block filled with liquid scintillator was examined in a number of different ways in order to gain confidence in the result. First, an eigenvalue analysis was done using the creep modulus at a particular time. Second, a static nonlinear analysis was performed. The modulus of the PVC at 20 years was used as input, an initial displacement was given to the block and the load was increased in steps until instability occurred. Finally, a time dependent nonlinear analysis was performed. The creep curve shown in Figure 17.5 above was input into the model, the block was given an initial deformation, and the deformation calculated as a function of time. These different analyses gave similar results for the time when block instability would occur.

#### 17.5.3.2.1 Eigenvalue buckling calculation

The first calculation is done by using an eigenvalue linear analysis with a modulus at 4 years and 20 years. Four years was used because this is the time assumed for assembly of the detector and the maximum period through which blocks will have to stand as independent structures. Twenty years is the required lifetime of the detector. The 4-year and 20-year safety factors for a 31-plane block, calculated by the eigenvalue analysis, are summarized in Table 17.8. The boundary condition used was "top free" and "top guided," as shown in Figure 17.37.

Year	E creep_1/D (mpsi)	SF_top guided	SF_top free
4	0.146	2.626	2.02
20	0.0725	1.173	0.926

Table 17.8: Results of eigenvalue buckling analysis of block stability.

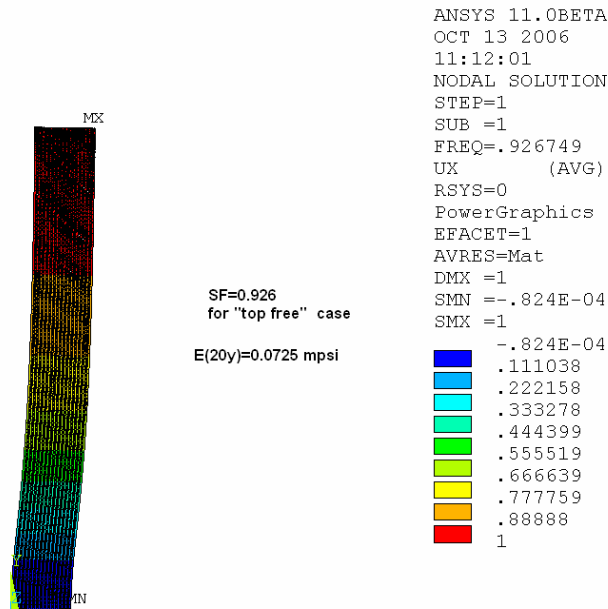


Fig. 17.37(a): Eigenvalue calculation for  $E(20y) = 0.0725$  mpsi (top free).

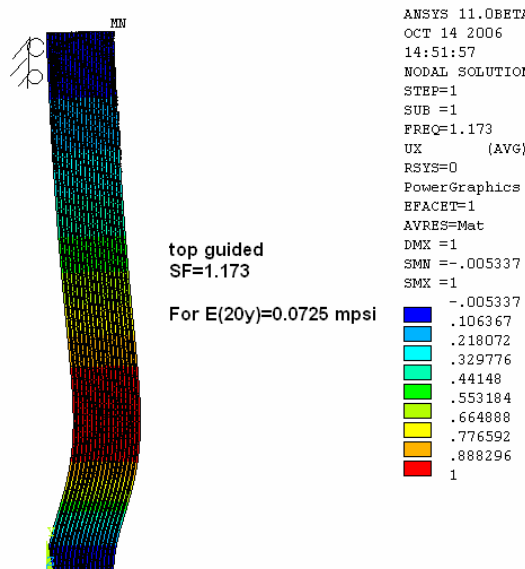


Fig. 17.37(b): Eigenvalue calculation for  $E(20y) = 0.0725$  mpsi (top guided).

### 17.5.3.2.2 Buckling calculation using a static nonlinear analysis

The second analysis uses a static nonlinear large-deflection approach, with  $E(20 \text{ year}) = 72.5$  ksi. We assume that the structure has an initial 1-inch offset at its top or middle portion to simulate a worst-case initial condition, as shown in Figure 17.38. The load is increased gradually

to find the value at which the structure becomes unstable. Figure 17.39 shows that the deflection of a block increases rapidly for loads greater than 0.8 G in the “top free” case, and for loads greater than 1.1 G in the “top guided” condition. The results are consistent with the eigenvalue approach, as shown in Table 17.9.

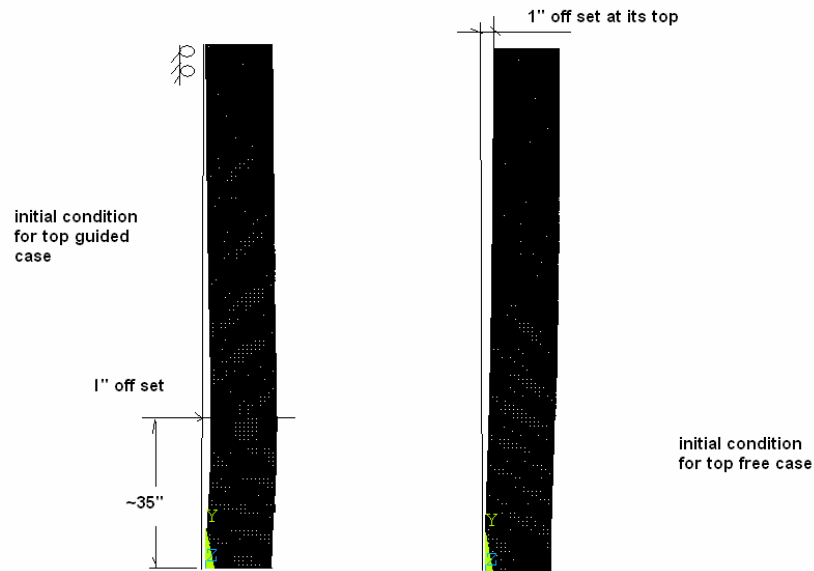


Fig. 17.38: FEA model for a top free and top guided case.

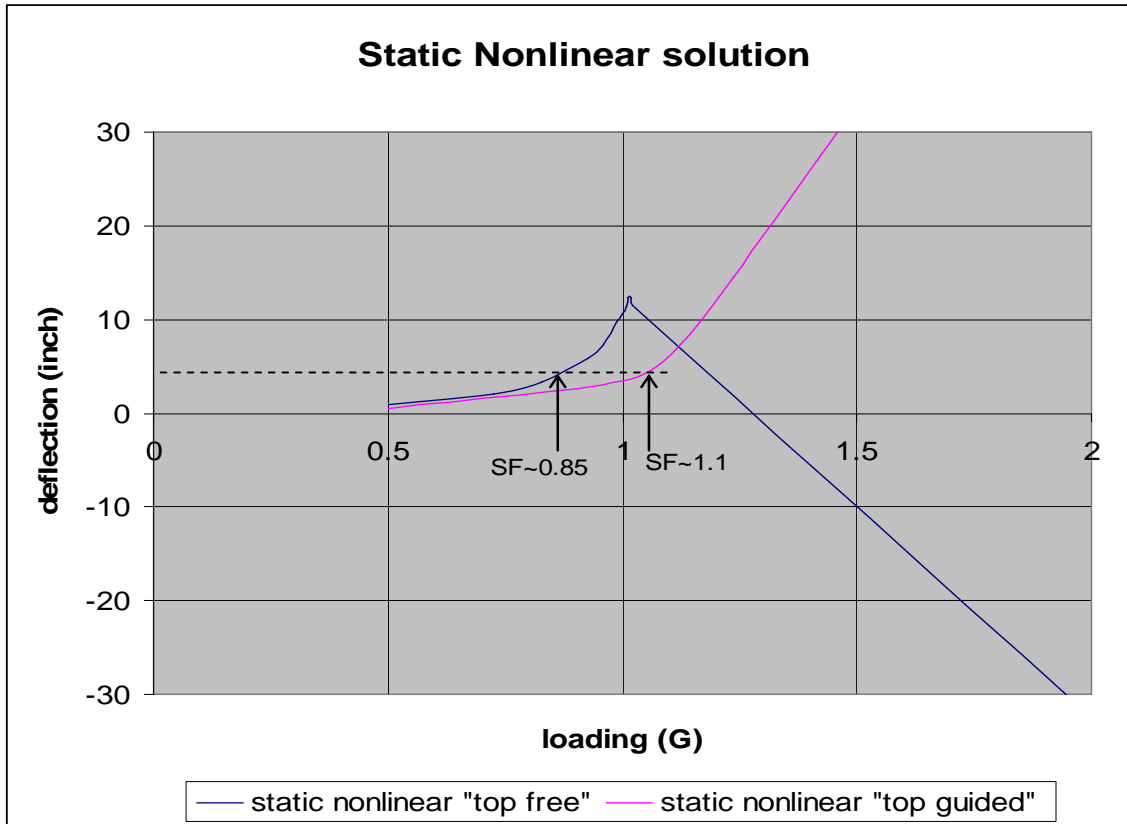


Fig. 17.39: Block deflection as a function of the G load.

<b>E(20y)=0.0725 msi</b>	<b>Eigenvalue (Euler)</b>	<b>Static nonlinear large deflection</b>
<b>SF _ top guided</b>	<b>1.173</b>	<b>~1.1</b>
<b>SF _ top free</b>	<b>0.926</b>	<b>~0.85</b>

Table 17.9: Comparison of eigenvalue and static nonlinear large deflection solutions with  $E(20y) = 72.5$  ksi.

### 17.5.3.2.3 Time dependent of nonlinear large deflection analysis.

The two approaches described in the previous sections give an estimate of the additional force ( $\Delta F$ ) the structure may be able to withstand before it becomes unstable. However, it does not address how much time is needed to develop this excessive structural deformation for the structure under a constant load.

The FEA model described in the previous sections with top-free and top-guided cases was used to perform a time dependent nonlinear large deflection analysis. The result is shown in Figure 17.40. For the top-free case, the structure is stable up to ~17 years and then its deflection starts to accelerate. This is in agreement with the first two analyses, which gave SF ~0.8 for  $E(20y) = 0.0725$  mpsi. For the top-guided case the critical time is around 22 years. Again, this is consistent with the predictions from first two approaches (SF~1.1).

Table 17.10 shows the PVC and adhesive stresses at 10 years since a single block is unstable at 20 years.

If PVC material is described by the pessimistic creep curve, the stability of individual blocks, constrained at the top, would limit their lifetime to less than 20 years. Section 17.5.5 describes how installation of the second bookend after four years guarantees that the 38-block detector is structurally stable for much longer than 20 years.

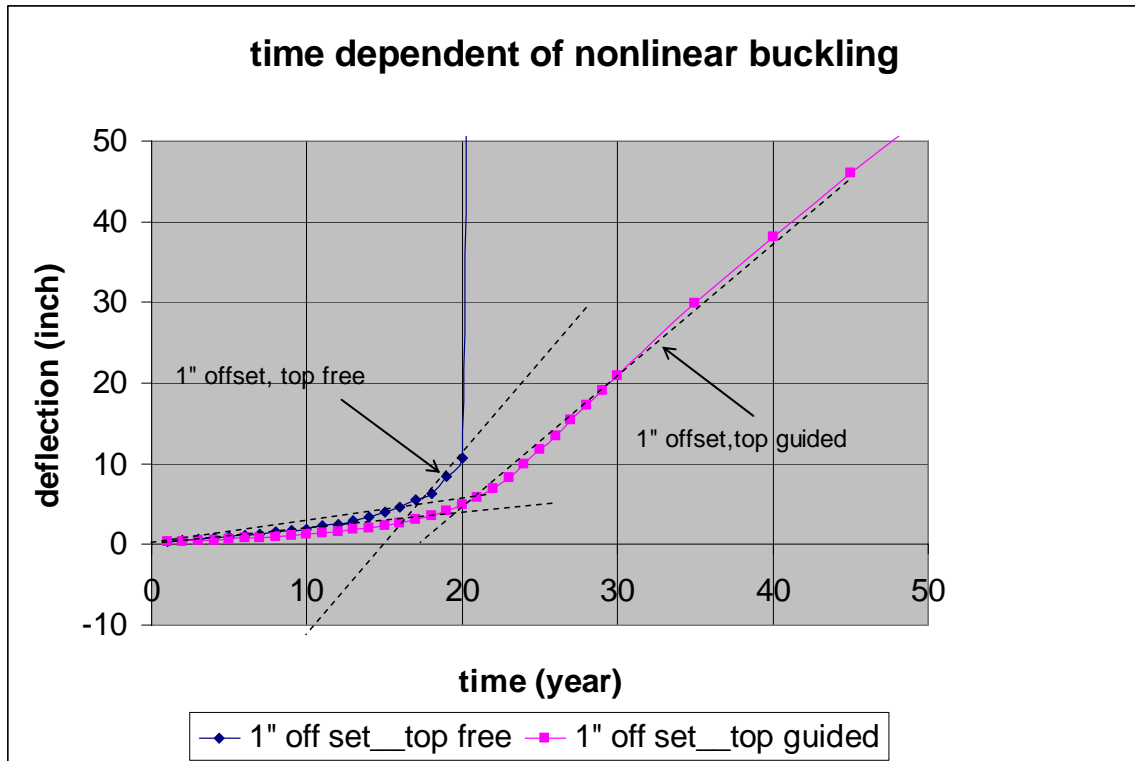


Fig. 17.40: Deflection as function of the time for first 50 years.

<b>Time (year) t=10 year</b>	<b>Deflection (inch)</b>	<b>*Maximum stress (psi)</b>	<b>*Maximum Strain (%)</b>	<b>*Maximum adhesive Shear (psi)</b>	<b>*Maximum Adhesive Peeling force</b>
<b>Top free</b>	<b>1.92 (top)</b>	<b>858/561</b>	<b>0.85/0.55</b>	<b>173</b>	<b>5.1 (lbf/in)</b>
<b>Top guided</b>	<b>1.7 (~35" from bottom)</b>	<b>896/598</b>	<b>0.88/0.59</b>	<b>178</b>	<b>8.8 (lbf/in)</b>

Table 17.10: The stress and deflection at t = 10 years from the time dependent nonlinear large-deflection analysis.

\* Note: The peak values listed in the stress and strain columns ignore the corner peak values, as illustrated in Figure 17.42 and 17.43. The shear stress is an average stress over the 1/8 of the adhesive pad area (0.777 inch x 0.777 inch).

The stresses and deflections of the block at 10 years are described in detail below to provide an example of the performance of a block.

Figures 17.41 and 17.42 show the regions of the maximum stress in the block for the top-free and top-guided cases, respectively. The maximum stress is approximately 858 psi and occurs at the bottom corner of the extrusions. The average stress in this region is much smaller and well within the limits of being considered viscoelastic which is important for insuring that creep is not a function of stress.

Figures 17.43 and 17.44 show the overall deformation of the block for both the top-free and top-guided cases, respectively. The deflections are less than 2 inches, which is insignificant compared to the size of the detector.

Figures 17.45 and 17.46 plot the height dependence of the adhesive peel and shear stresses within the detector, respectively. The maximum adhesive stresses occur at the bottom of the block in the outermost layers. The maximum peel stress is approximately 13 lbs/in, which is far below the adhesive peel strength of 115 lbs/in. The maximum shear stress is approximately 180 psi, which is also far below the 950 psi adhesive shear strength. The peel stresses shown in Figure 17.45 vary rapidly because the maximum peel force occurs at the edges of the contact pad between extrusions but is virtually zero in the center of the pad.

Finally, the top guided case is used to extract the edge-pulling force at t = 10 years. The result, shown in Figure 47, is a value of F (pulling) = 5514 lbf/total (or 18.48 lbf/in) at t = 10 years. With this pessimistic E(creep) curve, a block has no safety margin against the buckling for both top free and top guided cases after 20 years.

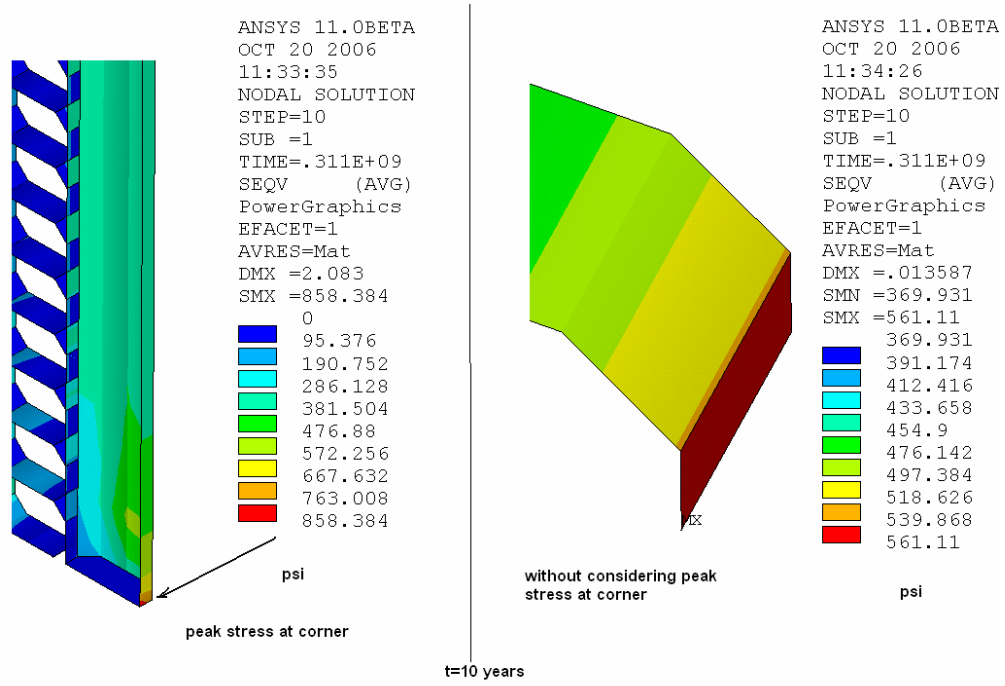


Fig. 17.41: Von Mises stress at t = 10 years for the top-free case.

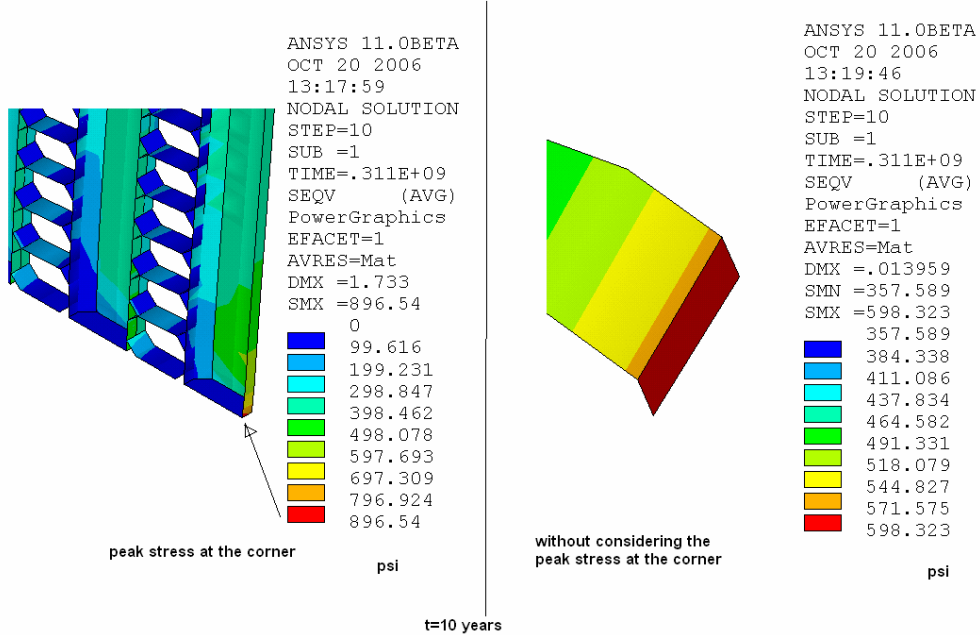


Fig. 17.42: Von Mises stress at t = 10 years for the top-guided case.

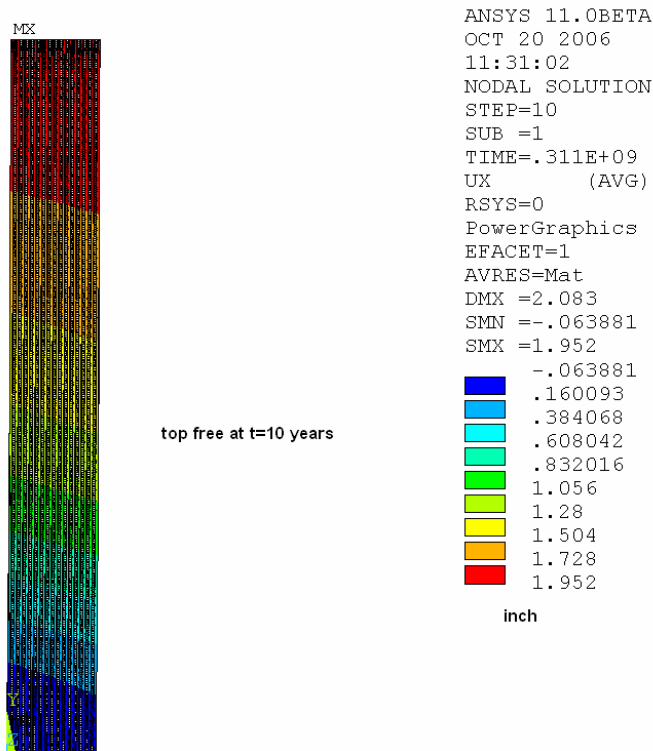


Fig. 17.43: Deflection at 10 years for top-free case.

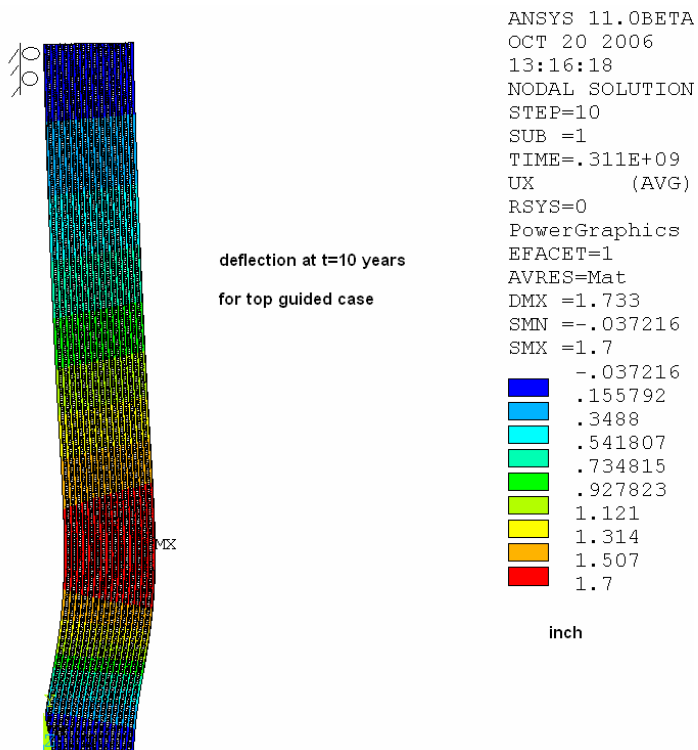


Fig. 17.44: Deflection at t = 10 years for top-guided case.

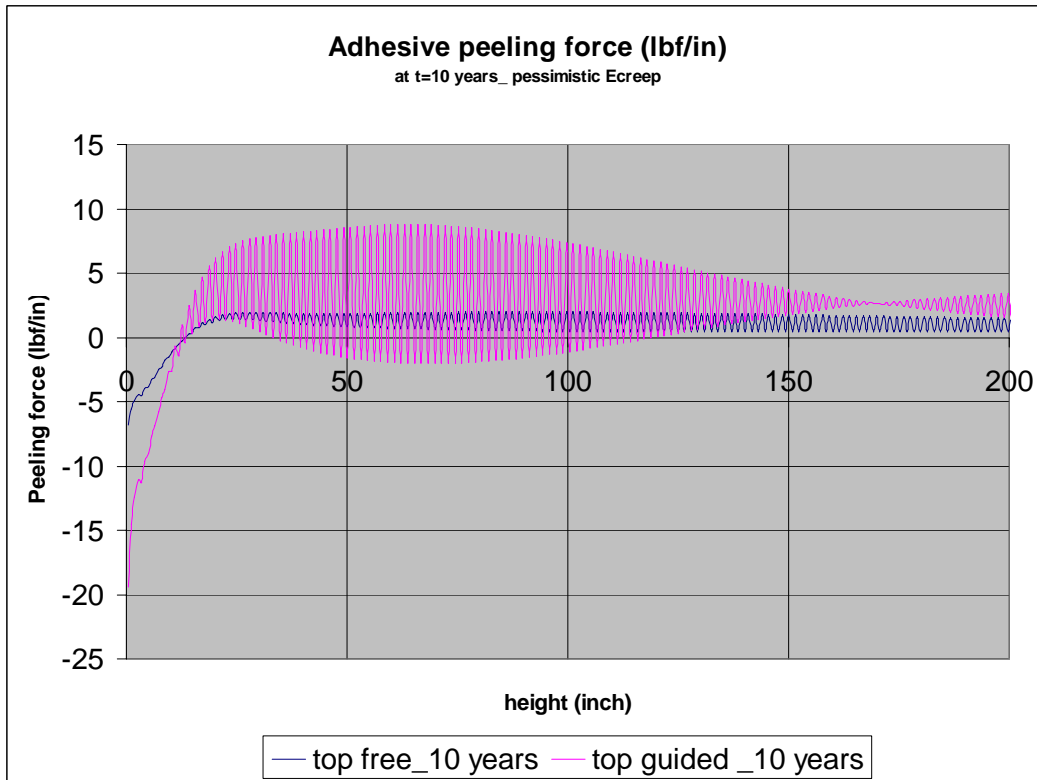


Fig. 17.45: Dependence of adhesive peel stress on height in the detector at t = 10 years.

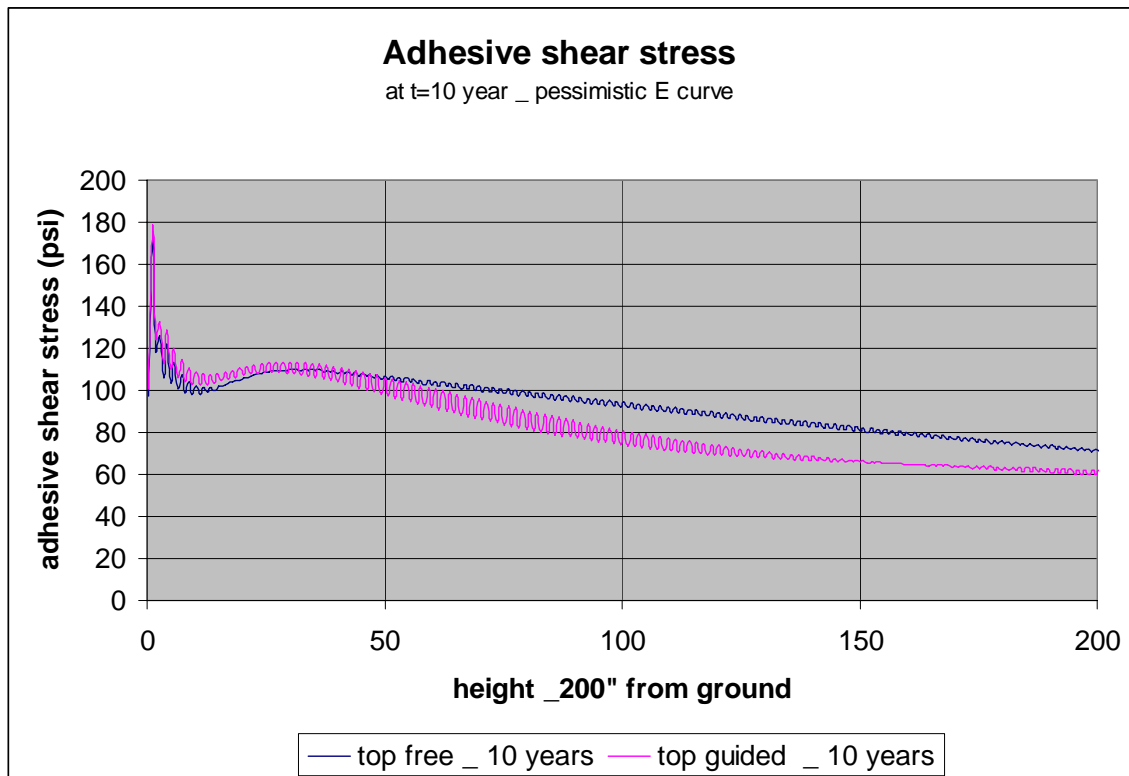


Fig. 17.46: Dependence of adhesive shear stress on height in the detector at t = 10 years.

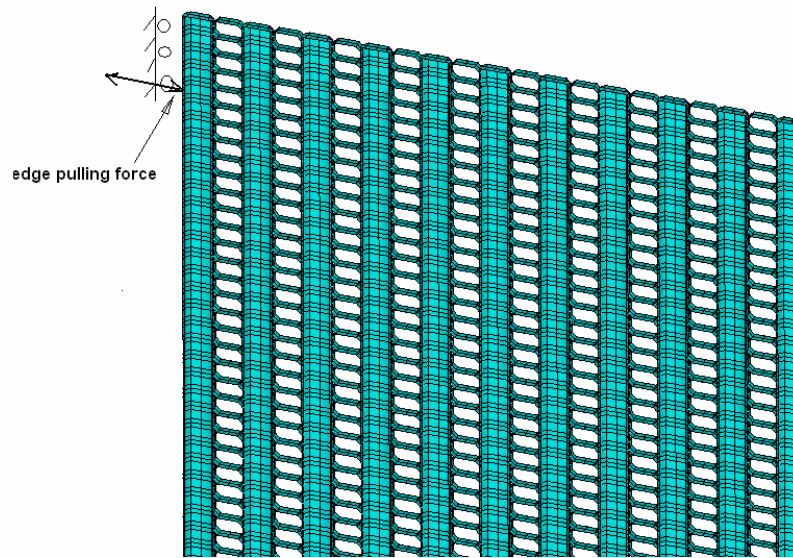


Fig. 17.47: Edge-pulling force extraction.

#### ***17.5.4 Analysis of a 31-Plane “B” Block***

The construction of a B block is similar to that of an A block except that B blocks have planes of horizontal extrusions on the outside surfaces where A blocks have vertical extrusions. The layout of a B block is shown in Figure 17.48. This difference has a small impact on the maximum stresses in both the PVC and adhesive, which occurs on the outside layers of the block. The buckling safety factors of A and B blocks are also different. The model of B blocks is very similar to that for A blocks. It was used to calculate the PVC and adhesive stress based on the both  $E = 145$  ksi (4-year worst case PET B) and  $E = 75$  ksi (20-year worst case PETB). The result is summarized in Table 17.11.

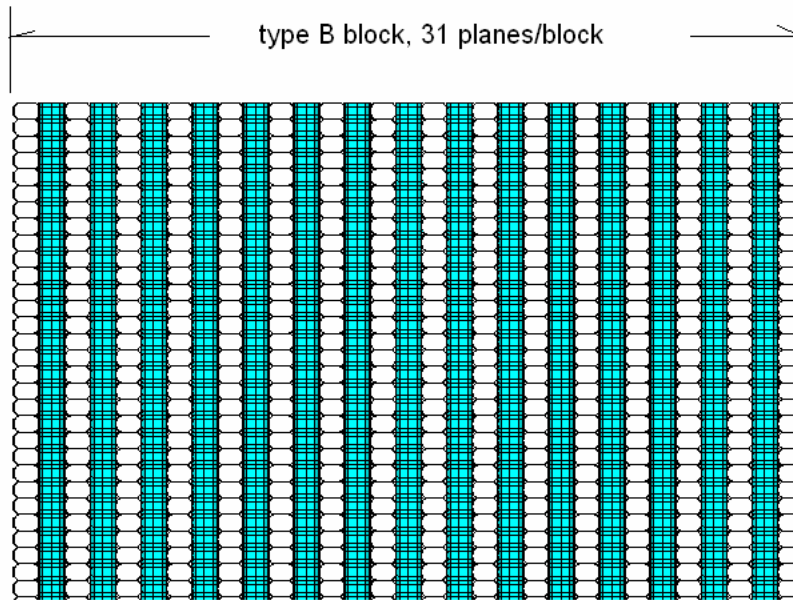


Fig. 17.48: Layout of a B block.

Number of planes In a block	31 planes _ B type	31 planes _ B type
Modulus E (ksi)	146	75
Total swelling (inch)	0.109	0.21
Stress peak (psi)	564	564
Excluding peak (psi)	533	533
Strain peak (%)	0.38	0.75
excluding peak (%)	0.36	0.71
Adhesive Peeling force (lbf/in)	4.78	4.83
Adhesive Shear stress (psi)	234	236

Table 17.11: Summary of FEA stress calculations for a B-type block.

#### 17.5.4.1 “B” Block Adhesive Strength Requirements

Table 17.11 lists the shear and peel stresses in the adhesive for different values of modulus of the PVC. The maximum adhesive stresses occur in the outermost layers of the B block and at the bottom of the layer. The maximum peel stress is only 4.8 lbs/in which is far below the 115 lbs/in peel strength of the adhesive. However, the shear stresses are higher than in the A blocks because the outside horizontal modules are essentially hanging from the vertical extrusions. The maximum shear strength of the adhesive is 950 psi, which gives a safety factor in shear of 4.0 compared to the design goal of SF = 5.0.

#### 17.5.4.2 Buckling Analysis of a 31-Plane “B” Block

The B-block buckling analysis is similar to the one for A blocks described in Section 17.5.3.2. In that section it was shown that the three approaches used to understand the buckling and long term stability of the blocks produced similar results. Table 17.12 shows the buckling

safety factor for the B blocks for the eigenvalue and nonlinear static approaches. B blocks have a slightly lower SF than A blocks. Figure 17.49 shows the deflection versus gravity load using the 20-year modulus. At the full gravity loading, the deflections increase dramatically, indicating that the structure is unstable. The long term stability of the detector is addressed in Section 17.5.5.

A time dependent nonlinear analysis was also done in which the actual pessimistic creep curve was used in the analysis and the deformation over time was calculated. Figure 17.50 below shows how the B block deformed over time. The free standing B block becomes unstable at approximately 15 years when the top is not guided and become unstable at approximately 18 years when the top is guided. The B blocks are therefore less stable than the A blocks, which become unstable at approximately 22 years. However, the long term stability of the detector is achieved by having adjacent block mutually support each other and being restrained between two bookend (Section 17.5.5).

E(20y) = 0.0725 mpsi	Eigenvalue (Euler)	Static nonlinear large deflection
SF_top guided	1.056	0.95
SF_top free	0.86	0.80

Table 17.12: Buckling safety factor (SF) for a B block with E(20y) = 72.5 ksi (pessimistic curve).

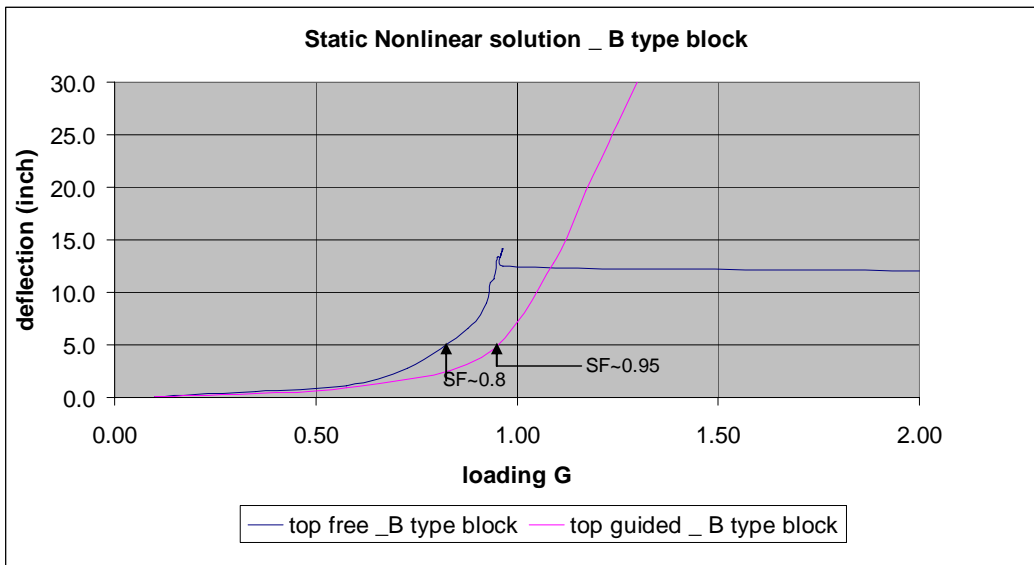


Fig. 17.49: B-type block deflection as a function of the G load for 75 ksi modulus (20 year).

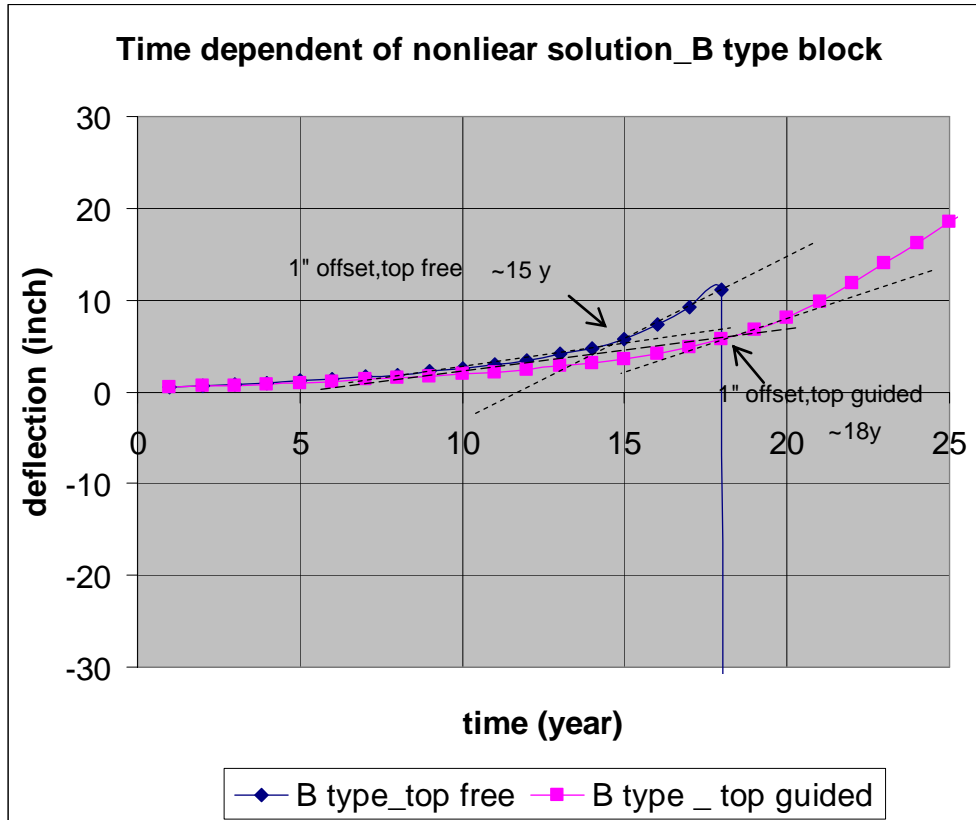


Fig. 17.50: B-type block deflection as a function of the time.

### 17.5.5 Long-term Stability of the Assembled Detector

The buckling analysis of structurally independent blocks in Sections 17.5.3 and 17.5.4 showed that at 20 years (using the most pessimistic prediction for the PVC modulus), there is no safety factor against buckling. It also showed that during the 4-year period of detector construction, there is a safety factor of ten for empty blocks and of nearly three for filled blocks, assuming that a support is provided at the top of each detector block.

Long term buckling stability is achieved by installing the second (north) bookend at the end of the construction period and restraining the movement of the blocks between the two bookends. Once the second bookend is in place, a block can deform until it makes contact with an adjacent block. The total deflection of the blocks is limited by the spacing between blocks and the constraint provided by the two bookends. The bookends are designed to withstand the forces from cumulative block deformation after 25 years of PVC creep.

Blocks are assembled together in groups of five to form a superblock. Within a superblock, the blocks are pushed as close together as possible but they are not glued to each other. The 2-cm (0.75-inch) expansion gap between superblocks allows superblocks to be filled while detector installation is still in progress, before the second bookend is installed. Gaps between blocks within a superblock are made as small as possible to minimize the amount of space that a block can deform into over time. However, gaps between superblocks ensure that the swelling of filled blocks does not grow progressively larger as it propagates down the length of the detector. As shown above, the swelling of the blocks increases the stresses in the PVC and adhesive. The swelling within a superblock is within acceptable limits for stresses in the adhesive and PVC. Figure 17.51 shows the spacing of blocks and superblocks within the detector. In the worst case,

all blocks will deform in the same direction and make contact with one of the bookends. The block adjacent to that bookend will deform the least and the deformation of each successive block will increase. The space available for the block furthest from the bookend will be equal to the sum of all of the gaps between the blocks. The detector is stable as long as the buildup of forces acting between blocks that have deformed against each other can be supported by the PVC extrusions. When the forces exceed the buckling strength of the weakest member, the webs in the horizontal extrusions, structural failure occurs. The force between blocks is dependent on spacing between blocks and superblocks.

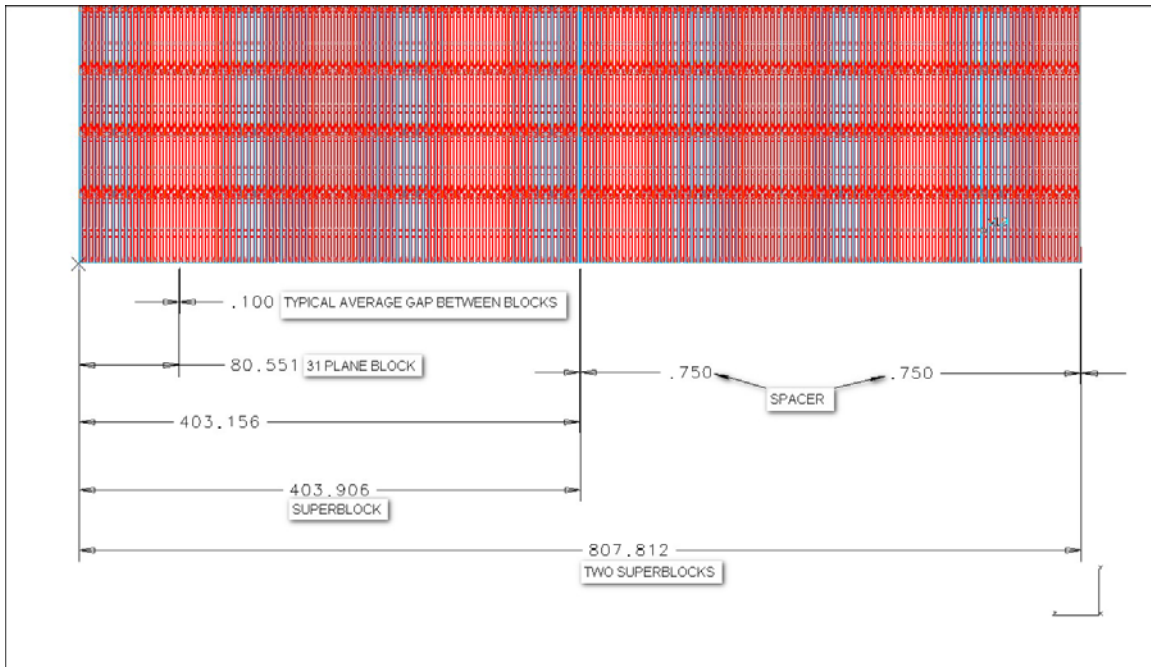


Fig. 17.51: Spacing of blocks and superblocks in the detector.

The analysis of the assembled detector is very computer intensive and requires several weeks to complete because it is an iterative process and because of the large model size. The initial analysis of the assembled detector was done using all A-type blocks in the detector. Several scenarios were examined in order to understand the forces between the blocks and on the bookends. Whereas the exact forces found in this analysis may not apply to the current arrangement of alternating B-A-B blocks, the dependency of the block forces on gap size is illustrative and therefore included in the Section 17.5.5.1 below. This section is followed by Section 17.5.5.2 which describes the forces acting on the blocks in the B-A-B super block arrangement. In this analysis only gap spacing of 0.1 inch between blocks within a super block and 0.75 inch between super blocks was examined because it was determined in Section 17.5.5.1 that this would result in the largest forces.

#### 17.5.5.1 Analysis of Assembled Detector with “A” Blocks Only

The initial analysis of the assembled detector was done with only “A” blocks in the detector. The blocks make contact at the top and are completely constrained at the top between the bookends. As the blocks deform over time, contact will be made in the lower half of the detector. The contact area between blocks occurs approximately between 170 inches to 195 inches above the bottom of the vertical extrusions.

Figures 17.52, 17.53 and 17.54 show the forces acting at the top and middle of the blocks as they deform and make contact with each other. Block 40 is against the bookend and block 1 is the furthest from the bookend. The analysis assumes that all of the blocks deform in the same direction and buckle towards one bookend.

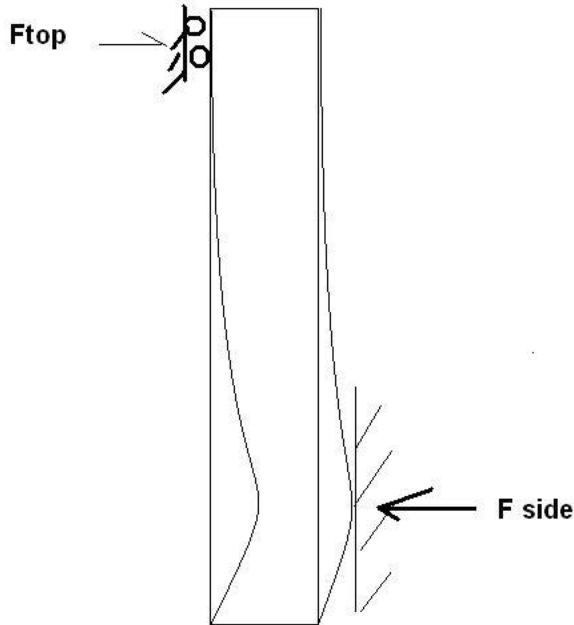


Fig. 17.52: Schematic of forces acting on a deformed block.

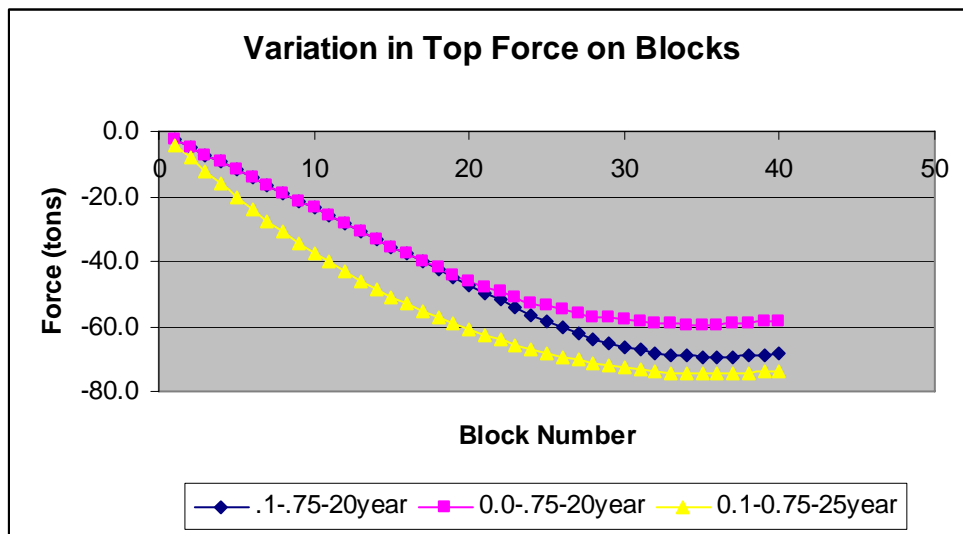


Fig. 17.53: Forces between the tops of blocks.

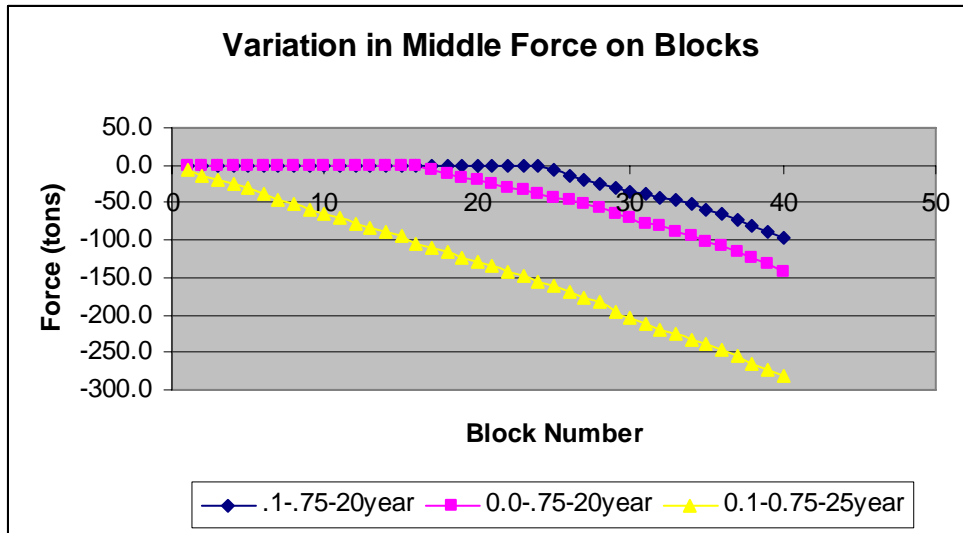


Fig. 17.54: Forces acting on block surface.

In Figures 17.53 and 17.54, the blue diamonds labeled “0.1-0.75-20year” show the analysis of the detector with a 0.1-inch gap between blocks within a superblock and a 0.75-inch gap between superblocks, using the PVC modulus at 20 years. The magenta squares labeled “0.0-0.75-20year” show the analysis when there is zero gap between blocks within a superblock and a 0.75-inch gap between superblocks, using the PVC modulus at 20 years. The yellow triangles labeled “0.1-0.75-25year” show the analysis of the detector with a 0.1-inch gap between blocks within a superblock, a 0.75-inch gap between superblocks, using the PVC modulus at 25 years from the pessimistic creep curve.

Figure 17.53 shows the forces acting at the tops of the blocks. The two curves with the same 20-year modulus follow each other until the point where blocks begin to make contact with each other. Blocks 1-23 do not make contact with each other and blocks 24-40 do contact each other, which is the point where these curves begin to diverge. In the block stability analysis discussed above, the blocks begin to become unstable after 20 years. This is reflected in the yellow curve which uses a modulus of 25 years. The deformation at 25 years becomes much larger and all of the blocks are now in contact.

In Figure 17.54, the force acting on the surface of the blocks is zero until contact is made at block 17 when there is a zero gap between blocks within a superblock, and at block number 24 when there is a 0.1-inch gap between blocks within a superblock. The force between blocks increases by nearly 50 tons when the gap between the blocks in each superblock is increased from zero to 0.1 inch. Figure 17.54 also shows that at 25 years the deformation of the blocks is unstable and all of the blocks are in contact. Use of the 25-year modulus increases the force between blocks dramatically, to a maximum of nearly 300 tons, which is three times the force at 20 years for the same gap between blocks. The bookends are designed to withstand the forces, shown in Figure 50, from cumulative block deformation after 25 years of PVC creep. The detector blocks will also withstand these forces at 25 years. Under the compressive forces shown in Figure 50, the 2-mm thick inner webs of the horizontal extrusions are the weakest detector component. NOVA-doc-1349 describes experimental measurements of the buckling strength of these webs and compares it to the FEA model of the test setup. The test and model results are in good agreement, giving confidence in the model predictions at 25 years with the lower PVC modulus.

Long term stability of the detector is ensured by restraining the blocks between two bookends. Each block is restrained at the top of the detector and the gaps between superblocks allow the detector to be filled while assembly is still in progress. During the years after the second

bookend is installed, the blocks will deform and fill these gaps, eventually making contact with adjacent blocks. These gaps between the lower surfaces of superblocks are small enough that the structure is stable, with an adequate safety factor, after 20 years of PVC creep. Although free-standing blocks are not stable at 20 years, the full detector structure is stable for much longer than 20 years because it is constrained between two bookends. The bookends limit the amount of deformation each block can undergo and therefore prevent the collapse of the detector or deformations that are large enough to cause excessively high stresses in the PVC or adhesive.

The PVC and adhesive stresses were examined within each block in the assembled detector at 20 years. Table 17.13 summarizes these stresses for the case of 0.1 inch between blocks and 0.75 inch between superblocks and a 75 ksi modulus at 20 years. The PVC and adhesive stresses are larger in the assembled detector that is making contact between blocks than it is for individual free standing blocks using the same modulus as shown in the sections above.

Block #	#16	#25	#26	#27	#28	#40
Max. deflection	4.507	3.013	3.013	3.013	3.013	0.8679
<b>Pvc stress</b>						
peak (psi)	996	924	925	925	925	803
excluding peak (psi)	684	622	623	624	624	521
<b>adhesive stress</b>						
Peeling (lbf/in)	14.30	11.16	11.21	11.26	11.26	6.31
shear (psi)	193.69	179.14	181.29	181.67	181.55	161.84

Table 17.13: Maximum PVC and adhesive deflections and stresses for different blocks in a 40-block detector at 20 years, with 0.75 inch expansion gaps between superblocks and 0.1 inch gaps between the blocks within a superblock.

#### 17.5.5.2 Analysis of the Assembled Detector with A-B-A-B-A Superblocks

An analysis of the assembled detector was performed using the A-B-A-B-A organization of a superblock and taking advantage of what was learned in the initial analysis described in the section above. In this analysis a gap of 0.1 inch was set between blocks within a superblock and a gap of 0.75 inch was set between superblocks. In this analysis blocks are given a 1 inch initial offset to begin deformation, for A blocks this results in a 5.03-inch deflection and 6.5 inch for B due to its slightly weaker structure. See Figures 17.55 and 17.56. For two blocks with B+A together, the expected deflection is somewhere between A and B. The result shows that the deflection is about 5.5 inches, see Figure 17.57. Each super block will have five single blocks in a pattern of A+B+A+B+A. This pattern suggests that the analysis can be accomplished by calculating A following by B+A. The gap size is assumed to be 0.1 inch between the blocks and 0.75 inch between super blocks. The modulus of  $E=0.075$  mpsi ( $t = 20$  years) is used based on the worst curve of PETB. An iterative process of calculating the force on the blocks and then transferring this force to the adjacent block can then be carried out in a manner similar to that described in Section 17.5.5.1 above.

The main conclusions of this analysis are:

- Blocks within the detector will not make contact with each other until #17 + #18 (B+A) where the available gap for the deformation is 5.5 inches.
- The force acting on the bookend/last extrusion is about 15% higher than all straight A case. Results are summarized on Table 17.14:  
 Total force = 172 tons  
 Total top force = 60 tons  
 Total side force = 111.16 ton (between 120 inches ~190 inches from ground)



	B+A	B+A
Block #	#14 (B) and 15 (A)	#39 (B) and 40 (A)
Max. deflection	5.625"	0.75"
PVC stress		
peak (psi)	1085	842
excluding peak 9psi)	759	552
Adhesive stress		
Peeling (lbf/in)	17.62	6.32
shear (psi)	312.50	243.72

Table 17.15: PVC and adhesive stresses. Note: (1) #14+#15 (B+A) is the B+A block whose available gap size = 6.5 inches ( no touching occurs on its side yet); (2) #39 and #40 is last B+A block in the detector.

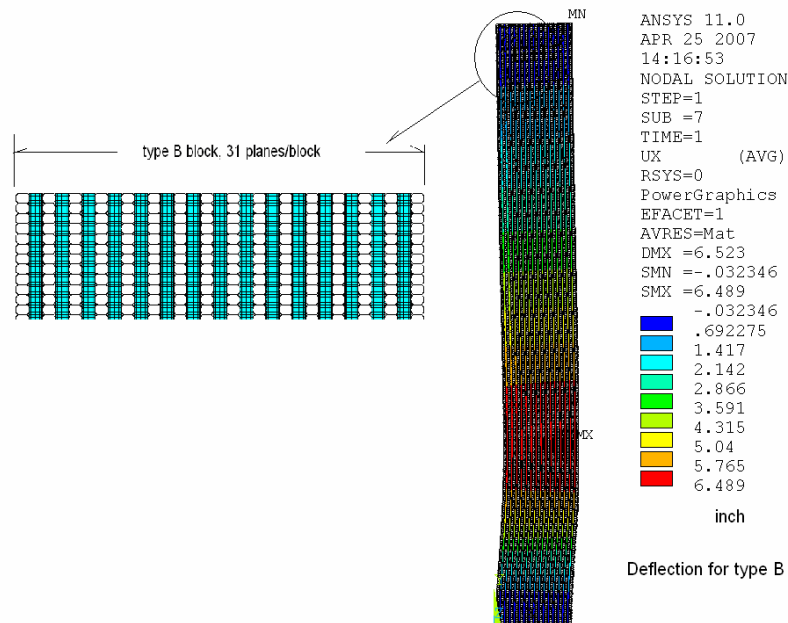


Fig. 17.55: Deflection of type B block with 31 planes.

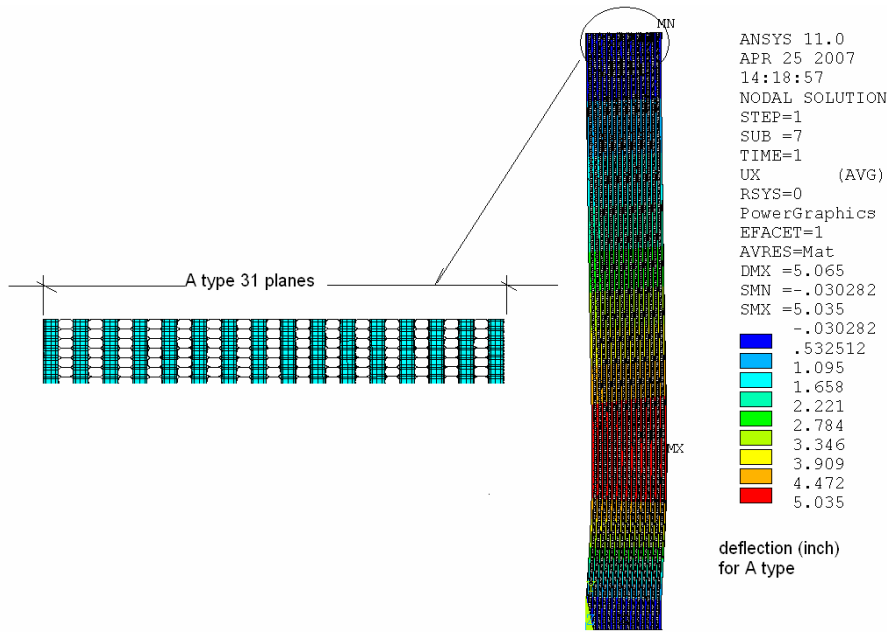


Fig. 17.56: Deflection of type A block with 31 planes.

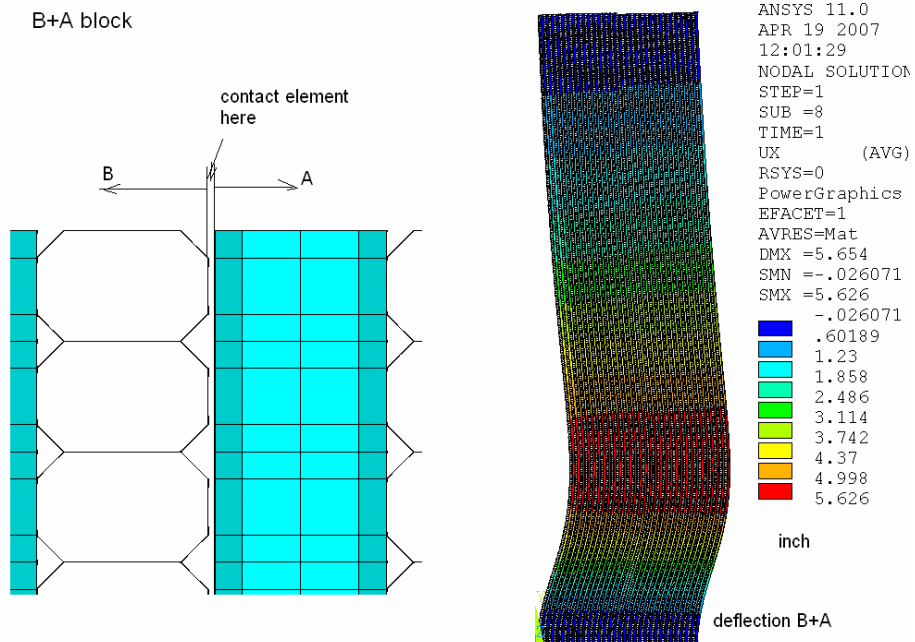


Fig. 17.57: Deflection of type B+A block with 31 planes.

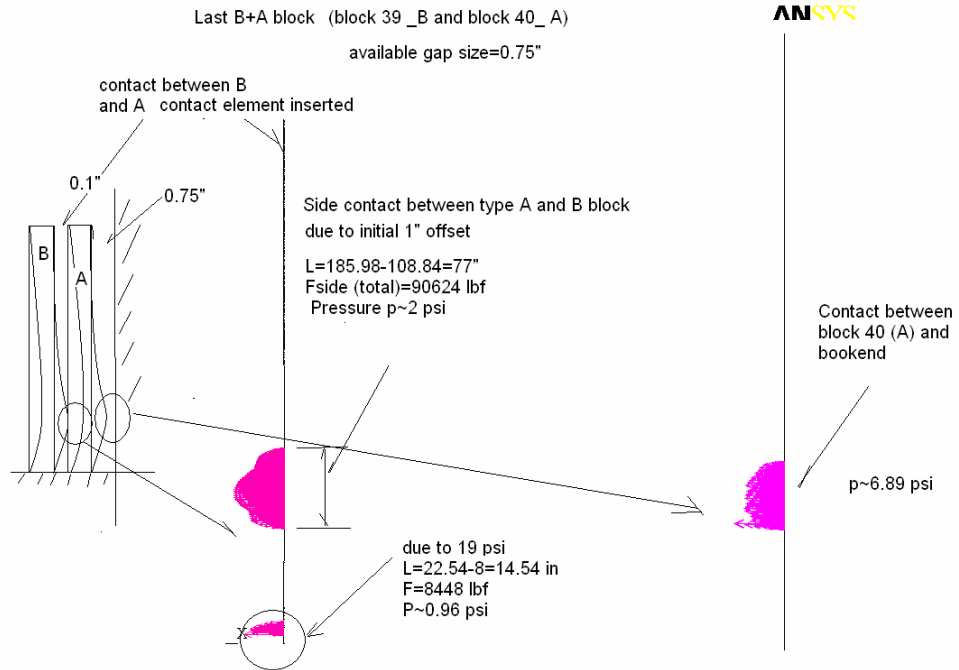


Fig. 17.58: Schematic representation of how contact occurs between blocks.

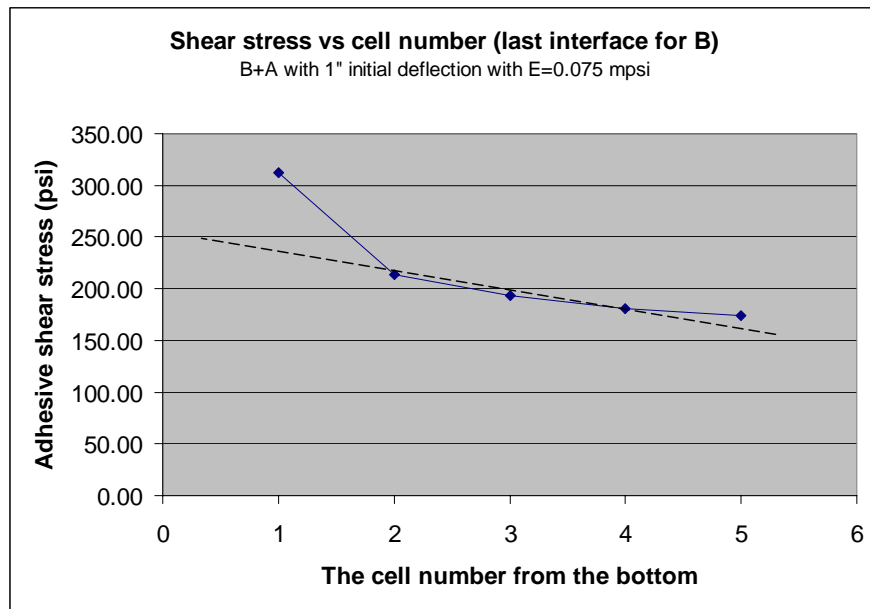


Fig. 17.59: Adhesive shear stress vs the cell number from the bottom.

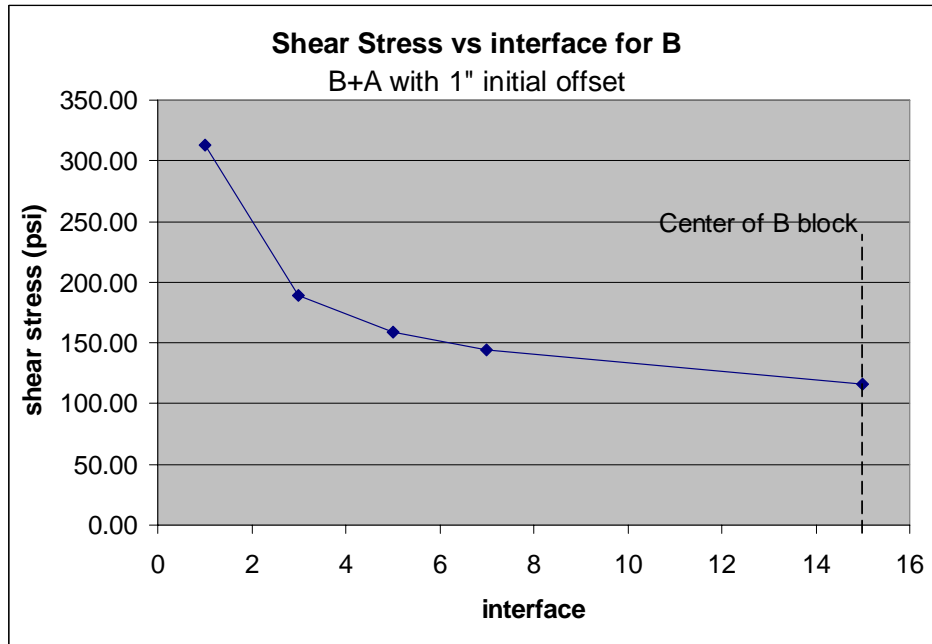


Fig. 17.60: Adhesive shear stress vs the plane interface.

### 17.5.6 Structural Considerations During Scintillator Filling

The far detector assembly plan calls for filling the modules in each superblock with liquid scintillator as soon as the last block in a superblock is installed. Blocks within a superblock are filled one at a time, beginning with the south-most block. Planes of horizontal modules within a block are completely filled before the filling of vertical modules begins (NOVA-doc-1298). During the full-rate installation period, a new superblock will be completed every three months, and filling will be finished around the time that the next superblock has been installed. Significant PVC creep weakening begins during the installation and filling process, as stress on the PVC increases. We assume conservatively that the PVC modulus has been weakened by six months of creep when a superblock is completely full (Table 17.2). At that time, the “top guided” constraint condition is provided by the presence of the next superblock. NOVA-doc-1490 indicates that, after 4 years of PVC creep, the buckling safety factor for a single empty A-type block will be about 16. As a worst case, a single filled B-type block has a safety factor of 3.6 against buckling after four years of creep. Safety factors for individual block stability at the time of filling can be obtained by scaling these results by the ratio of PVC modulus at 6 months to that at 4 years. This results in safety factors for individual blocks and for an assembled superblock well in excess of 5 after a newly installed superblock is filled with liquid scintillator. *[We need to have a NOVA note to show the safety factor calculation for a full superblock with the 6-month PVC modulus.]*

### 17.5.7 Adhesive Requirements

We have required a safety factor of 5.0 on the adhesive stresses throughout the design process. Sections 17.5.3.1, 17.5.4.1 and 17.5.5.2 describe the adhesive stresses in the detector under a range of loading conditions. We have calculated the maximum shear and peel stresses at 20 years in the assembled detector using the pessimistic creep prediction. Table 17.15 shows that the maximum peel force (17.6 lbf/in) and shear stress (312 psi) both occur in blocks #14-15. However, as explained in Section 17.5.5.2, the peak adhesive shear stress is very localized and the most adhesive shear stresses are below 200 psi. Our SF = 5.0 constraint requires an adhesive peel strength of 88 lbf/in and shear strength of 1000 psi for the average stress in the block.

Section 17.6.7 describes strength measurements of the Devcon 60 adhesive being used in this experiment and demonstrates that this adhesive meets these strength requirements.

## **17.6 Mechanical Prototypes**

It is very important to perform extensive mechanical prototype studies of the NOvA structure using actual extrusions. The production of the first prototype extrusions that were useful for such studies began in September 2006. The purposes of the mechanical prototypes described in this section are (1) to test the ability of the FEA modeling to predict the performance of the PVC extrusions and adhesive, (2) to evaluate the assumptions that have gone into the model, and (3) to have a realistic test of the adhesive bond using the actual geometry.

To date the following prototype structures have been built and tested:

- 4-ft extrusion under internal pressure
- 3-Layer/single-extrusion prototype under internal pressure (3M 2216 adhesive)
- 7-Layer hydrostatic stress transmission test (3M 2216 adhesive)
- 11-Layer/single-extrusion prototype under internal pressure (Devcon 60 adhesive)
- 4-Plane IPND block prototype (Devcon 60 adhesive)
- 8-plane IPND block prototype (Devcon 60 adhesive)
- 3-layer extrusion prototype measurements of Devcon 60 shear strength

In addition, the full height structural engineering prototype is planned for 2008.

The sections below describe the results of the prototyping that has been done to date.

### ***17.6.1 Four-Foot Extrusion Under Internal Pressure***

Extensive analysis has been done on the NOvA structure. These calculations have been difficult to verify experimentally because actual PVC extrusions of the correct geometry were not available until September 2006. Currently a die for 16 cell extrusions has been made and is being used to produce prototype extrusions. These extrusions are now being used to perform mechanical tests to confirm the structural analysis. The first test was simply to seal the ends of a 4-ft long extrusion and pressurize it to 19 psi (the operating hydraulic pressure at the bottom of the detector). Rosette strain gages have been placed on the surface of the extrusion to measure the stresses which are then compared to a FEA simulation. This prototype construction and test results are described in NOVA-doc-1120.

#### **17.6.1.1 Test description**

A 4-ft long extrusion had four rosette strain gages placed at the center of the length, at the locations shown in Figures 17.61 and 17.62. The rosettes are oriented as shown in Figure 17.63. The X direction is aligned with the direction of extrusion and the Y direction is aligned with the width of the extrusion. The pressure was applied using nitrogen from a tank. A pressure gage on the tank and on the extrusion confirmed the pressure within the extrusion. A barrier used by welders was placed around the extrusion as a precaution against failure of the extrusion or end seal. The extrusion was kept under pressure for five days and then released and allowed to relax for one day.

Future tests will use a temperature compensating gage to eliminate the effect of temperature on the measurements. A lack of data channels prevented the use of a temperature compensating gage on this test.

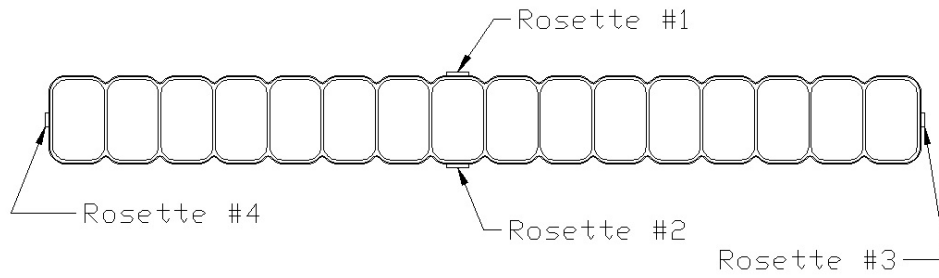


Fig. 17.61: Location of rosette strain gages on the 4-ft long extrusion.

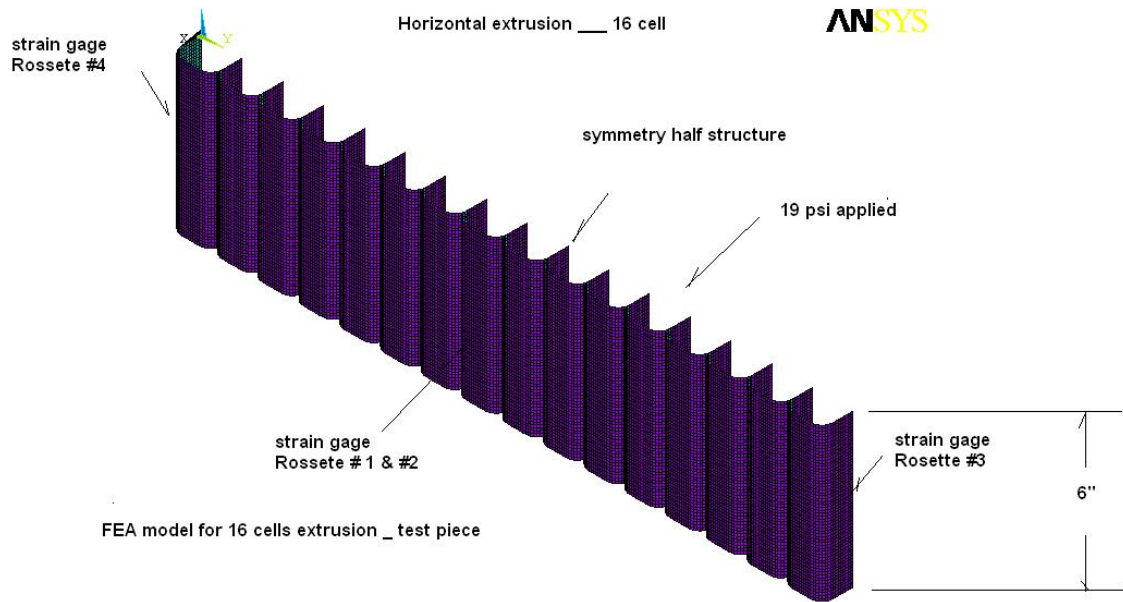


Fig. 17.62: Location of rosettes used for comparison to FEA model.

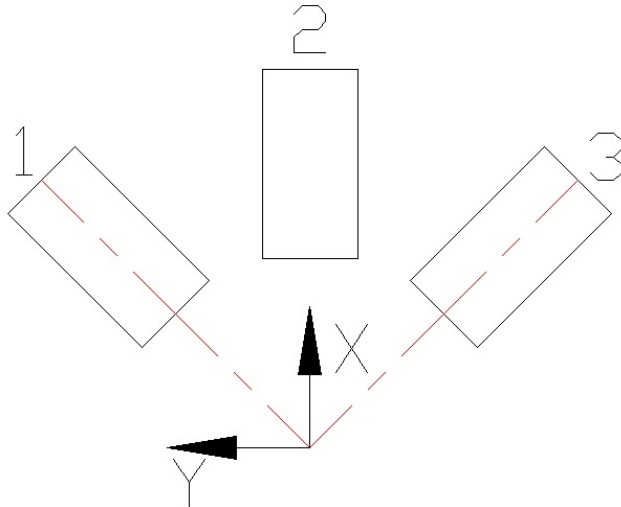


Fig. 17.63: Strain gage orientation and numbering within a rosette.

#### 17.6.1.2 Test results

The strain gages output strains in the direction of their axis. Through geometry the strains in any direction can then be found. The strains from the rosettes were converted to strains in the X and Y direction for comparison to the FEA model.

In order to make a valid comparison between the FEA model and the test measurements the thickness of the webs and sidewalls of the extrusion and the modulus of the material must be taken into account. Initial tests on the PVC show that in the short term modulus of the PVC is on the order of 500 ksi. Measurements on the PVC extrusion showed that the wall thickness averaged 1.5 mm for the web and 2.5 mm for the outside wall thickness. These values were used in the FEA model to compare to the experimental measurements.

NOVA-doc-1120 gives the detailed test results. Figure 17.64 shows the von Mises stress plotted versus time.

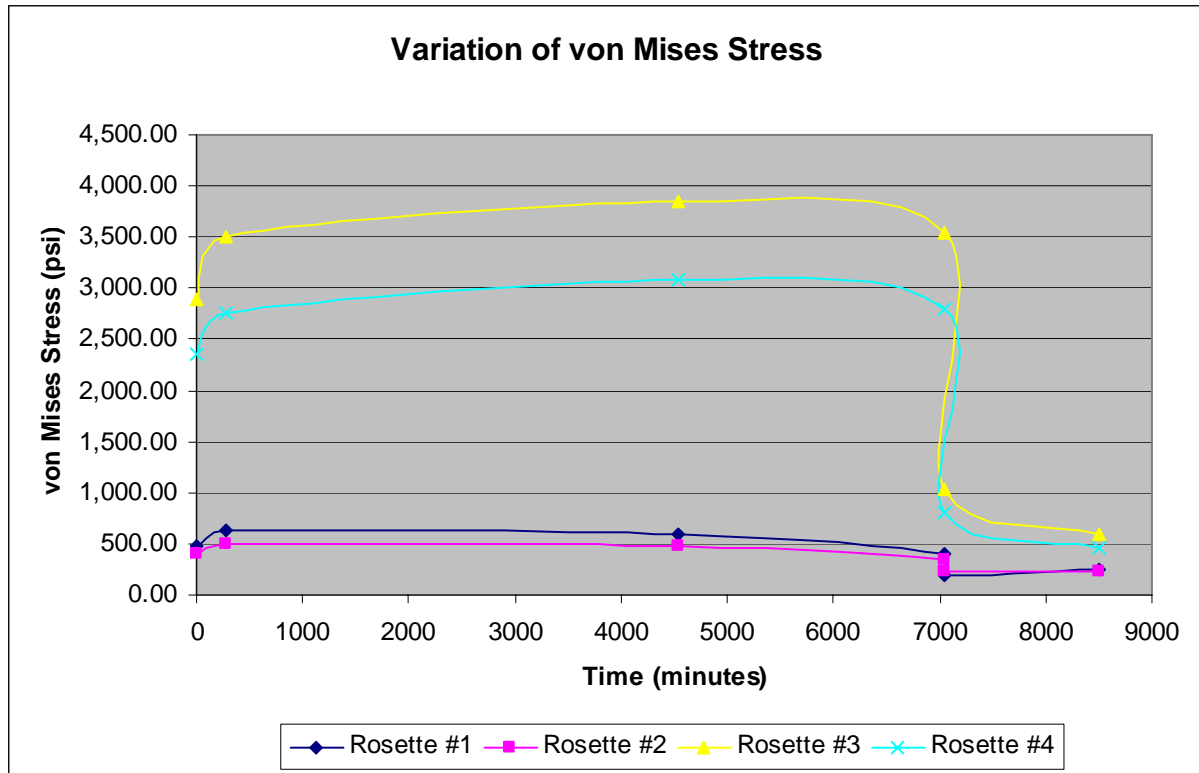


Fig. 17.64: Measured change in von Mises stress with time.

### 17.6.1.3 Evaluation of results

It can be seen in Figure 17.64 that the stresses increase over a short period of time from their initial values. This increase is most likely due to the initial high creep rate that occurs when PVC is stressed. The calculations of the von Mises stress used a constant modulus (550,000 psi) however the initial modulus was most likely higher and then declined over time. It is felt that the initial increase in stress is due to a high level of initial creep strain. The drop in stress at 7000 minutes is most likely due to temperature variation in the building. The temperature dropped about 15° F between these two measurements and we know that the PVC strain is dependent upon temperature.

It is significant however, that the stress did not return to zero after the pressure was released, and remained even after 24 hours later.

The von Mises stress match closely with the calculated stresses for a single extrusion under pressure as seen in Figure 17.65. The initial von Mises stress in the side wall on the scallop averaged 437 psi but then increased to 566 psi over a short period. This matches well with the value of 698 psi calculated in the FEA model. The difference is attributed to the averaging affect of the gage over the area that it covers and variation of the thickness within the extrusion. The strain/stress varies rapidly in this region and the strain gage can only average over the 6mm area that it covers. The stress compares very well for the 66 mm sidewall. The gages measured a von Mises stress of 2628 psi initially and this increased after a short period to 3129 psi, which compares well with the FEA result of 2982 psi. Table 17.16 shows a comparison of initial stresses and strains with the FEA results.

The dial indicator on the third scallop indicated an initial deformation INWARD of the scallop of 0.001 inches which increased to 0.008 inches by the end of the test. A similar type of deformation was found in the FEA model on the order of 0.002 inches as seen in Figure 17.66.

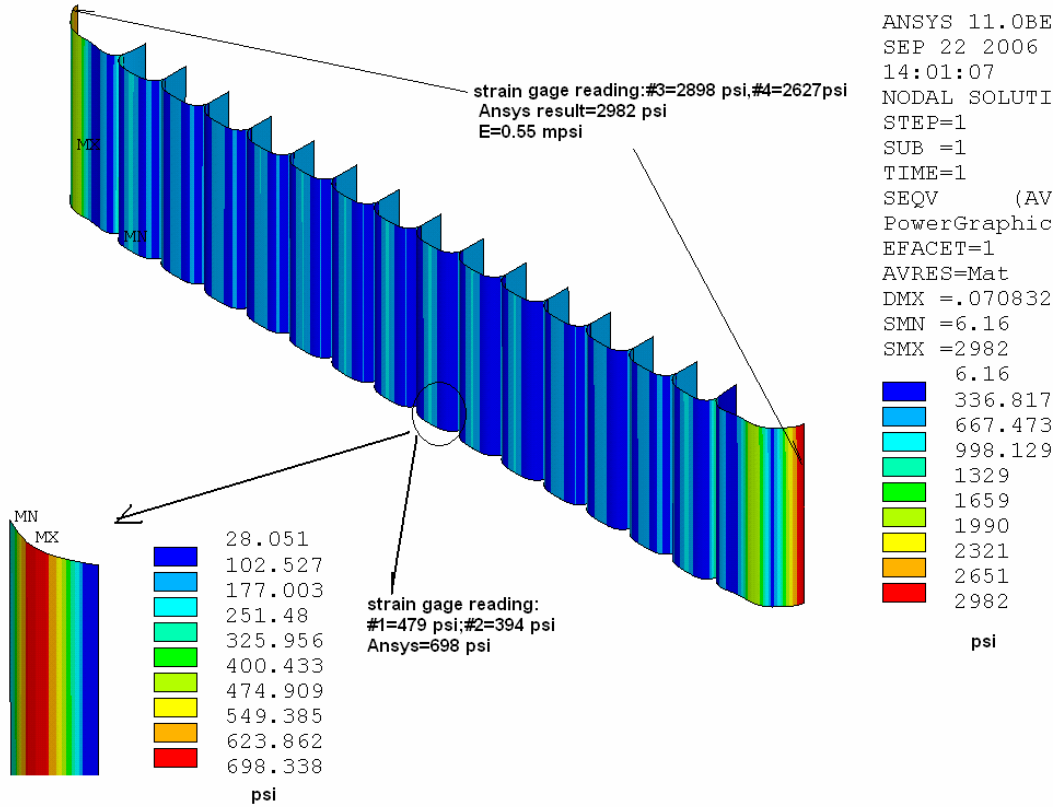


Fig. 17.65: Comparison of strain gage readings with FEA results.

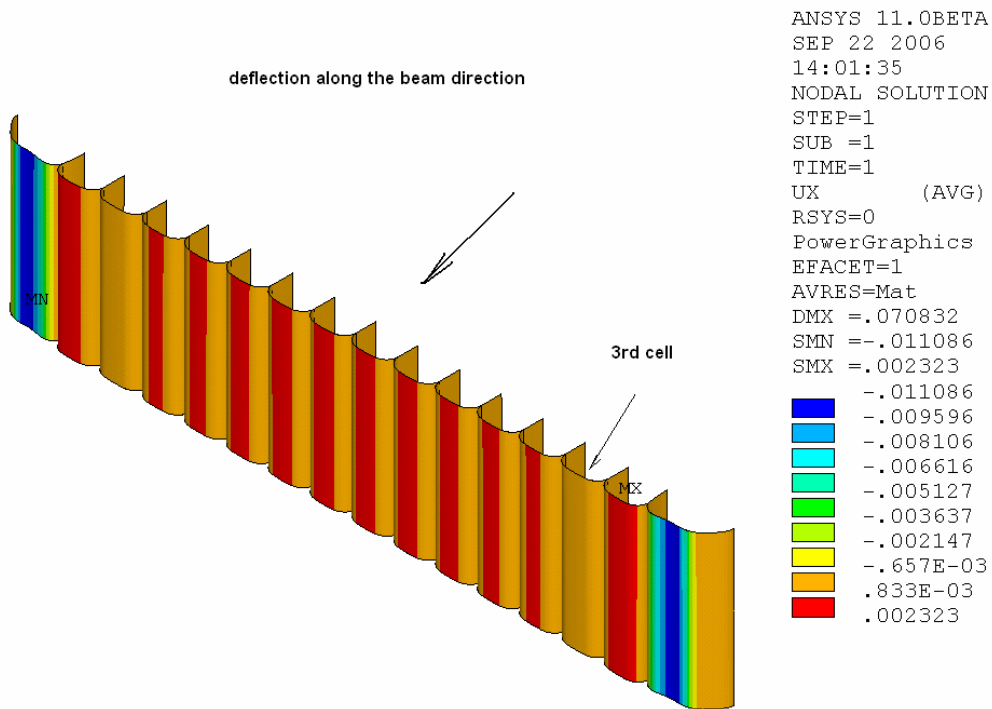


Fig. 17.66: Deformation of scallops predicted by FEA calculation.

	Test Results		FEA Model	
	Stress psi	Strain (Micro)	Stress psi	Strain (Micro)
<b>Scallop side</b>	480	<b>872</b>	694	<b>1270</b>
<b>60 mm side</b>	2900	<b>5270</b>	2982	<b>5422</b>

Table 17.16: Comparison of test results with FEA model for 4-ft extrusion prototype.

#### **17.6.1.4 Conclusions from 4-ft extrusion prototype test**

This initial test demonstrates that the FEA model can predict within reasonable accuracy the strains/stresses in a PVC structure. Variations in the material thickness and modulus, however, will introduce errors. Any future test will need to use the correct modulus from actual material measurements in order to have a valid comparison.

#### **17.6.2 Three-layer/Single-extrusion X-Y Prototype**

The second mechanical prototype constructed was a three layered structure designed to mimic a horizontal extrusion sandwiched between two vertical extrusion. It is described in detail in NOVA-doc-1194. This prototype was constructed using 3M 2216 epoxy with the surfaces of the extrusions roughened using an industrial sander. Figure 17.67 and 17.68 are photographs of this prototype. The extrusions that simulate the vertical extrusions have end caps installed so that these extrusions can be pressurized. The middle extrusion does not have an end cap because the horizontal extrusions are nominally at atmospheric pressure.

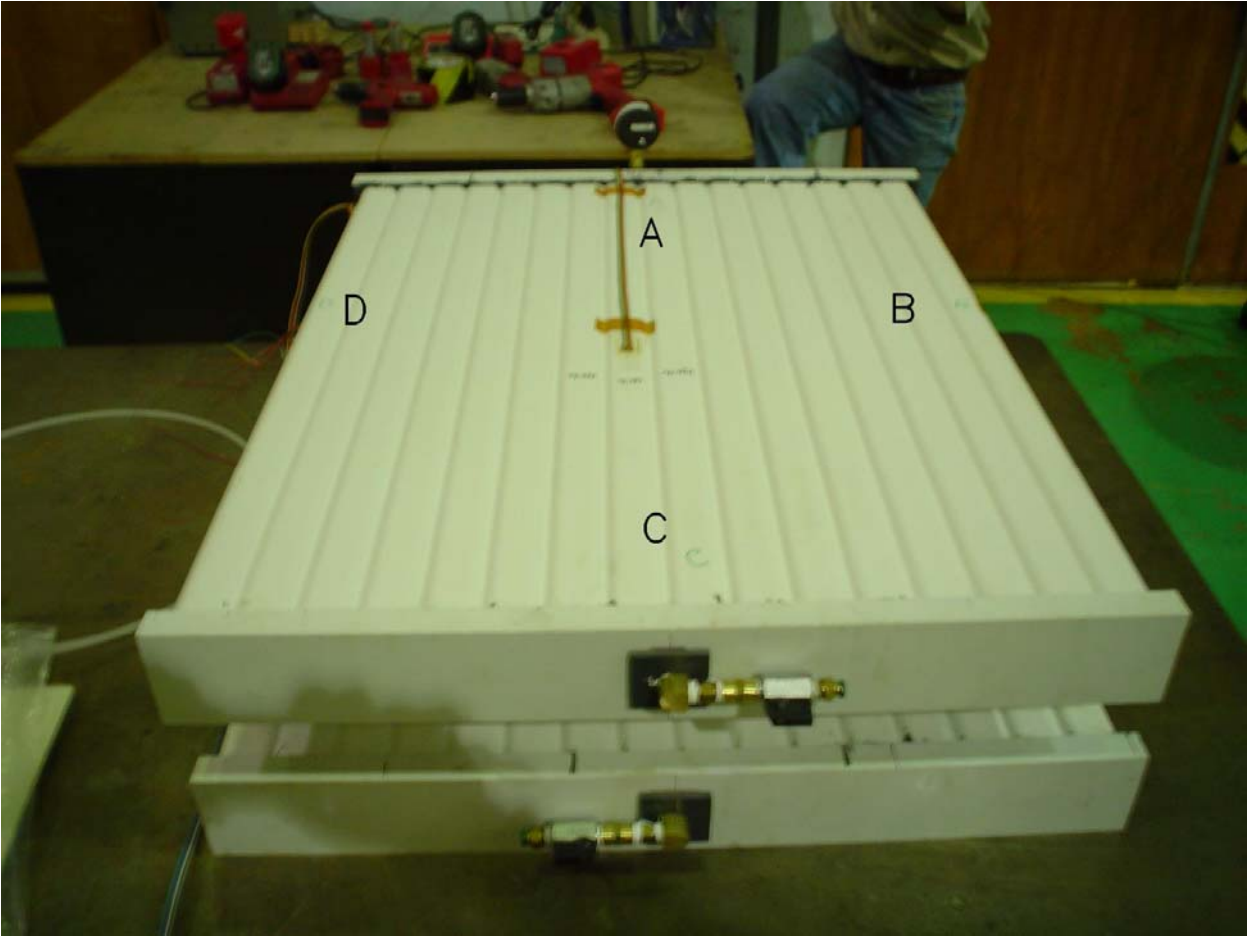


Fig. 17.67: Three-layer X-Y mechanical prototype showing the labeling of the sides. The “vertical” extrusions are on the top and bottom in the photograph.



Fig. 17.68: Three-layer X-Y mechanical prototype showing the top and bottom interfaces. The “vertical” extrusions are on the top and bottom in the photograph.

#### **17.6.2.1 Experimental Setup Description**

Strain gages were placed at the locations shown in Figure 17.69 on the outside extrusions being pressurized. The prototype was placed in a plywood box for protection in the event of catastrophic failure of the extrusion/end-seal while being pressurized. The pressure was increased to 20 psi and held for 1.5 hours. The pressure was then successively increased to 40 psi, 60 psi, and finally 80 psi and held at each of these pressures for 1.5 hours. At each pressure the readings of the strain gages was recorded.

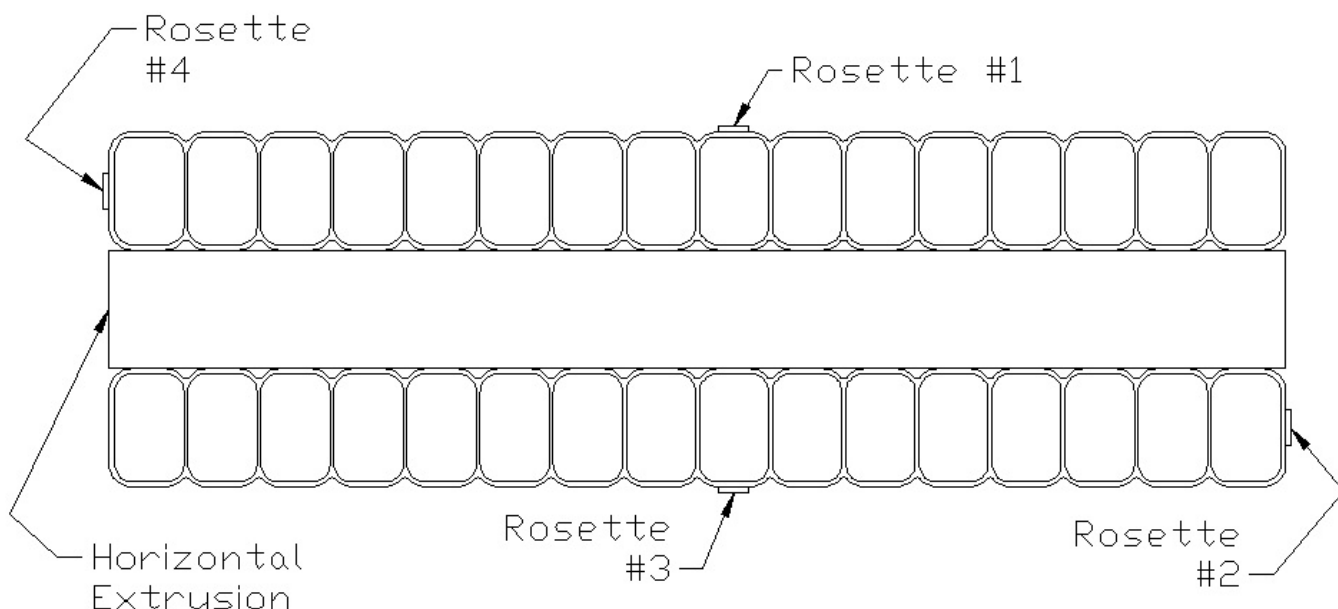


Fig. 17.69: Layout of rosettes on three-layer X-Y mechanical prototype. Figure 17.51 shows the layout and numbering of strain gages in a rosette.

### 17.6.2.2 Experimental Results

The strain gages output strains in the direction of their axis. Groups of three strain gages are called a rosette and are oriented as shown in Figure 17.63. The rosette was oriented so that the X direction was along the direction of extruding. Through geometry the strains in any direction can then be found. The strains from the rosettes were converted to strains in the X and Y direction for comparison to the FEA model. In order to make a valid comparison between the FEA model and the test measurements the thickness of the webs and sidewalls of the extrusion and the modulus of the material must be taken into account. Initial tests on the PVC show that in the short term modulus of the PVC is on the order of 500 ksi. Measurements on the PVC extrusion showed that the wall thickness averaged 1.5 mm for the web and 2.5 mm for the outside wall thickness. These values were used in the FEA model to compare to the experimental measurements.

NOVA-doc-1194 gives the strain gauge readings obtained during the pressure test of the prototype. As the pressure was increased to 40 psi a series of popping noises was heard from the prototype after the pressure passed 35 psi. The popping noise stopped once the pressure stabilized at 40 psi. After 1.5 hours at 40 psi the pressure was increased to 60 psi and immediately the popping noise was heard again until the pressure stabilized again at 60 psi. The same noise was heard again when the pressure was increased from 60 psi to 80 psi. Unfortunately at 80 psi one of the end seals failed and pressure dropped before strain gage readings could be taken.

It is believed that the popping noise that was heard was from failure of the adhesive bonds. Since the prototype was inside the plywood box for protection it was impossible to observe what was happening directly.

A feeler gage 0.0015 inches thick was then used to investigate what bonds had failed. The gage was long enough to be inserted to a depth of 7 cells. Each side of the prototype was labeled as shown in Figure 17.67. At each cell location the feeler gage was inserted in order to measure the depth to which it could be inserted. NOVA-doc-1194 summarizes the measurements and the

number of cells the feeler gage was able to be inserted into the prototype. These are compared with the FEA model of this device in the next section.

**17.6.2.3 FEA Model of Prototype**

A FEA model for the 3-layers X-Y prototype was created as shown in Figures 17.70 and 17.71. The same type of shell element and the mesh size as a real detector model was used so that meaningful comparison can be established. The wall thickness of test piece is 2.5/1.5 mm (side wall/web) for both vertical and horizontal extrusion. The PVC module is 0.55e6 psi which is consistent with t = 90 min of creep predicted by the creep curve. The modulus for the adhesive is 0.5e6 psi with 10 mils thickness assumed. Figures 17.72 and 17.73 show the results for several loading cases which show that the maximum peeling force reaches 20 (lbf/in) for 40 psi loading, where the “popping sound” occurred. The calculation indicates this maximum peel occurs at the edge joint. Compared with the some earlier T-shape and cleavage test results, one will expect that some of adhesive joints will be broken at the peeling force ~20 lbf/in (peeling strength) if 40 psi loading being applied to the test piece. The shear stress is still far below 1,000 psi (average shear strength from the double shear test and technical data sheet for 3M 2216 epoxy). Figures 17.74, 17.75, 17.76 and 17.77 show the model results used for the comparison between the FEA calculations and strain gage measurements. Table 17.17 summarizes the comparisons. The results agree within 11% for the 60 mm side. However, the FEA results give a higher stress/strain for the 38.8 mm side. It could be due to the thickness variation since an average thickness of 2.5/1.5 mm is used for the extrusion. A final cross check with a mini 3-D model for the peeling force shows that the peeling force along the edge reaches its capacity of the 19.2 lbf/in for p = 40 psi with a wall thickness of 2.5 mm/1.5 mm for both vertical and horizontal extrusion as shown in Fig 17.78 and Fig 17.79.

<b>P=18 psi</b>	<b>Von Strain (micro) (FEA)</b>	<b>Von Mises Stress (psi) FEA</b>	<b>Von Mises Strain (micro)(measured)</b>	<b>Von Mises psi (measured)</b>
<b>60 mm</b>	<b>4294</b>	<b>2358</b>	<b>3788</b>	<b>2170</b>
<b>38.8 mm</b>	<b>1145</b>	<b>624</b>	<b>588</b>	<b>323</b>
<b>E</b>	<b>0.55 mpsi is based on the E curve at t = 90 min</b>			

Table 17.17: Comparison for the stress/strain in the 3-layer X-Y prototype.

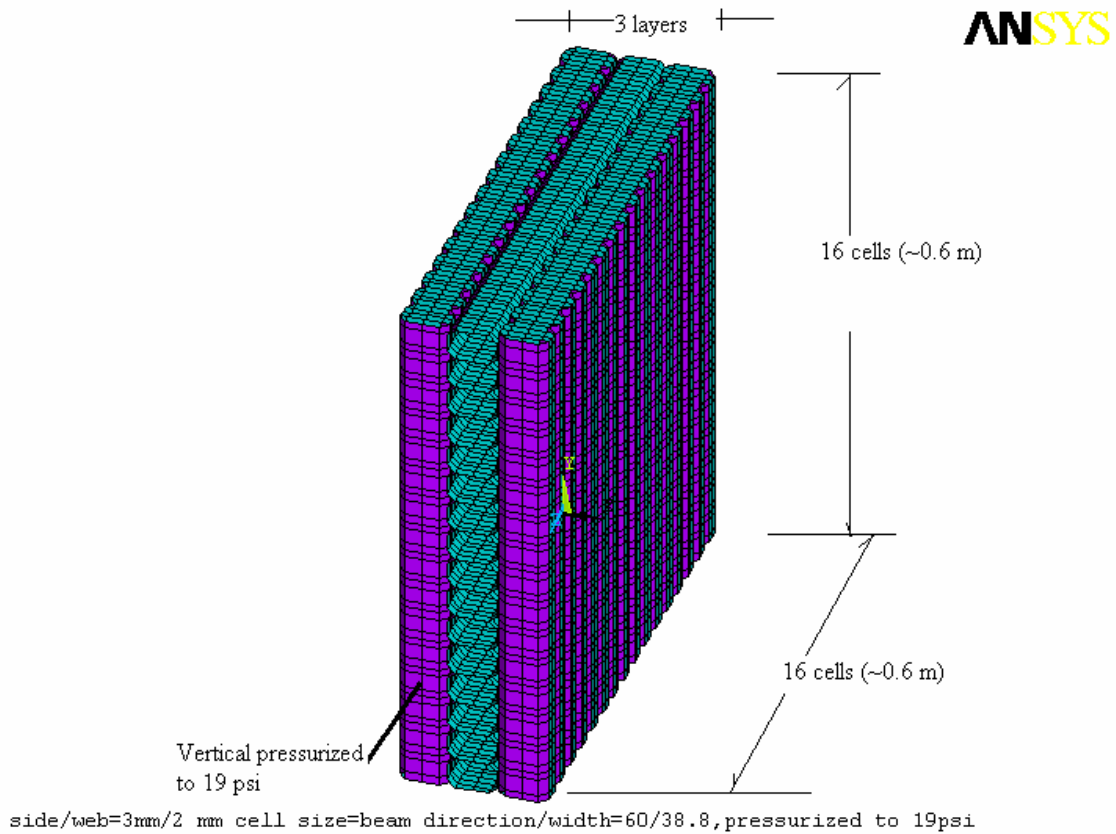


Fig. 17.70: FEA model of 3-layer X-Y prototype structure.

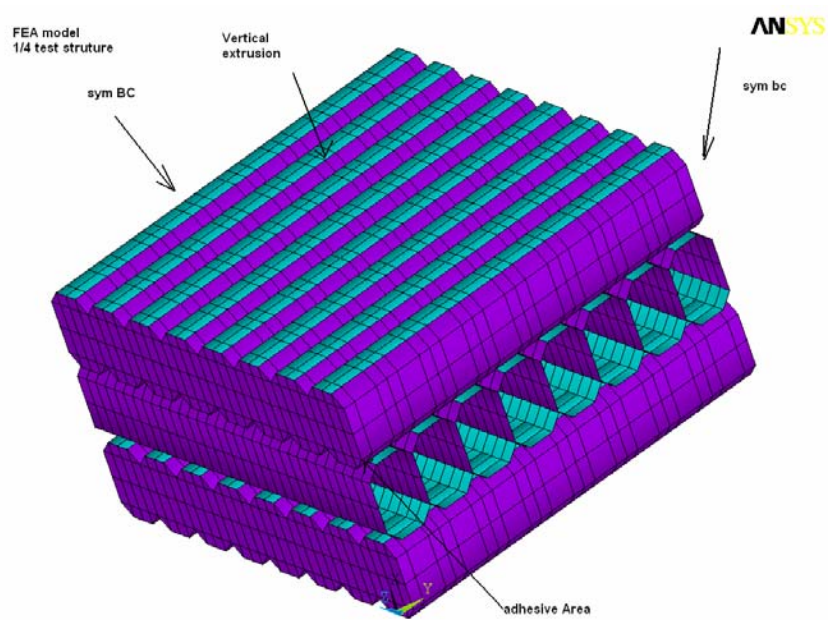


Fig. 17.71: FEA model of one quarter of 3-layer X-Y prototype, using symmetry.

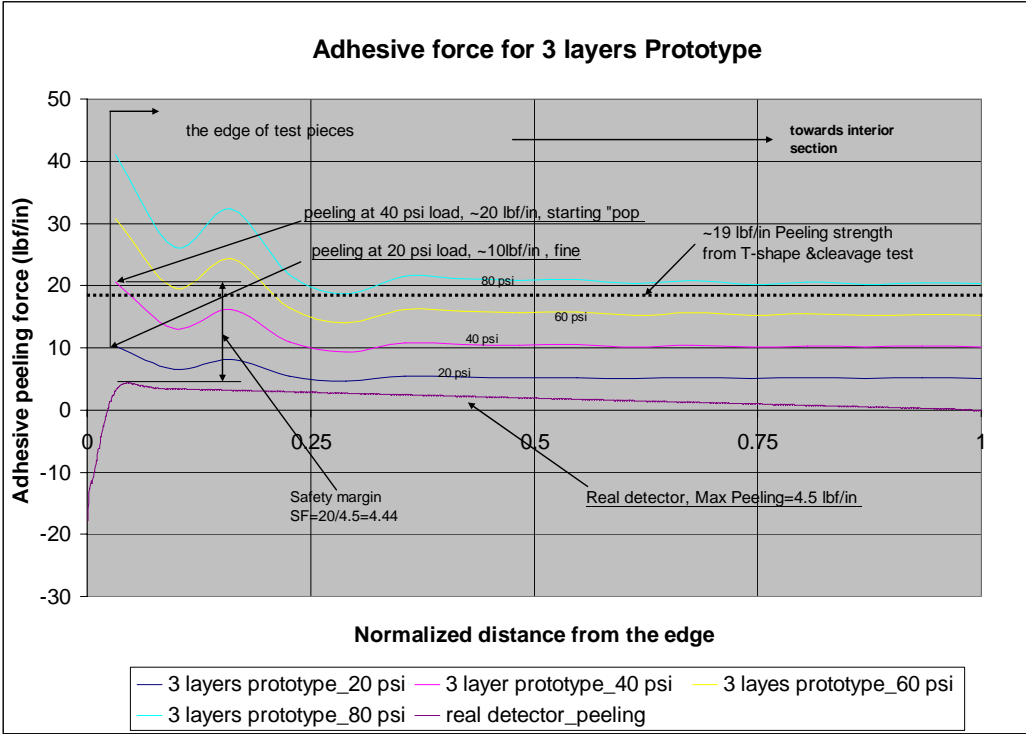


Fig. 17.72: The peeling force comparison. The X axis is a normalized length. The test piece is normalized to its half length, using symmetry, and the real detector is normalized to its full height.

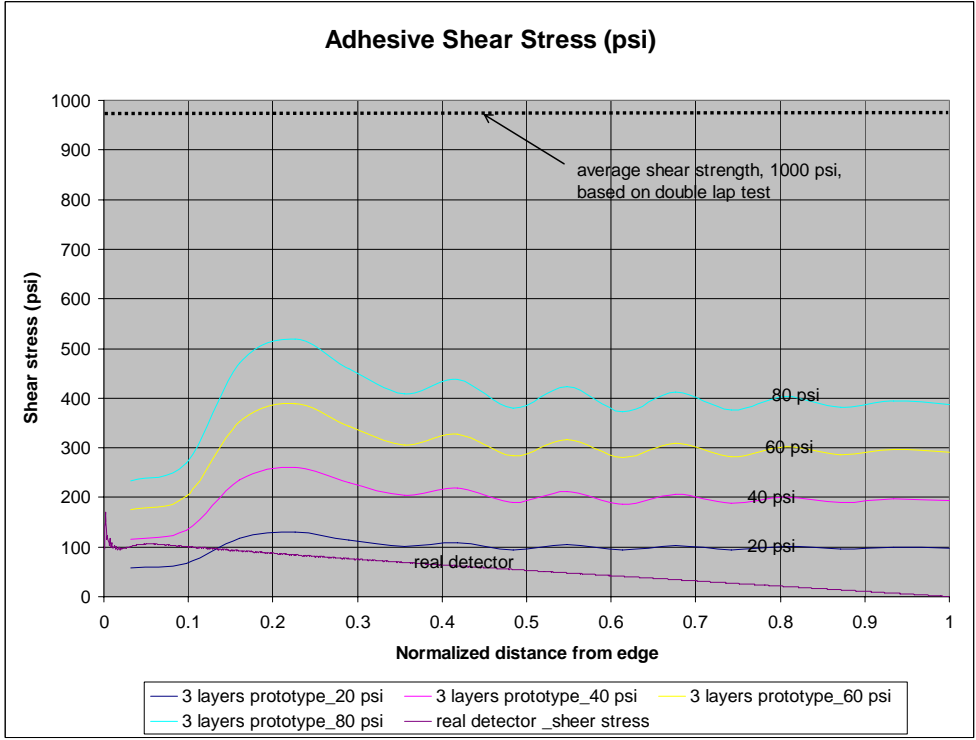


Fig. 17.73: Shear stress comparison. The X axis is a normalized length. The test piece is normalized to its half length, using symmetry, and the real detector is normalized to its full height.

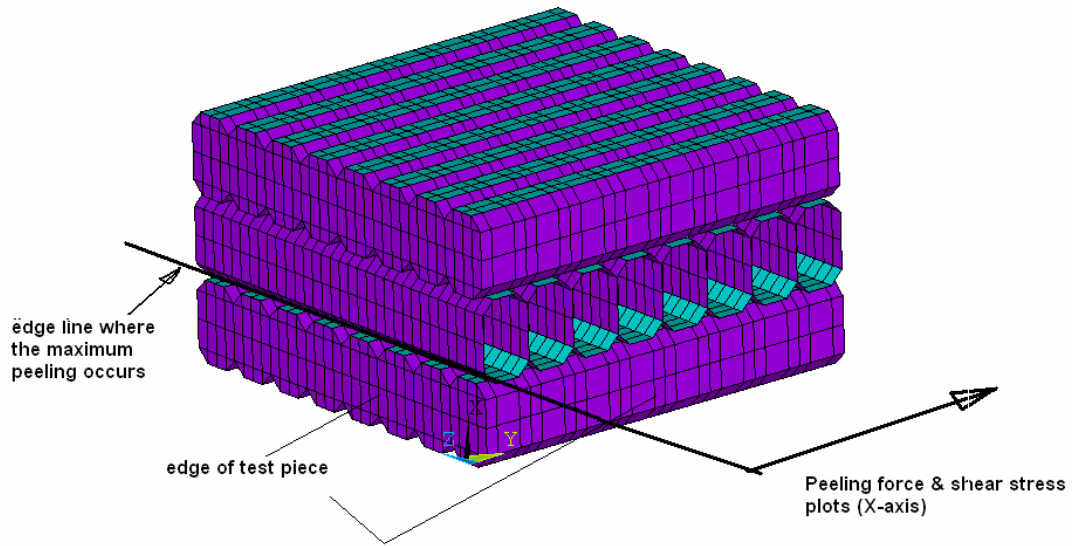


Fig. 17.74: Where the maximum peeling force occurs in 3-layer X-Y prototype.

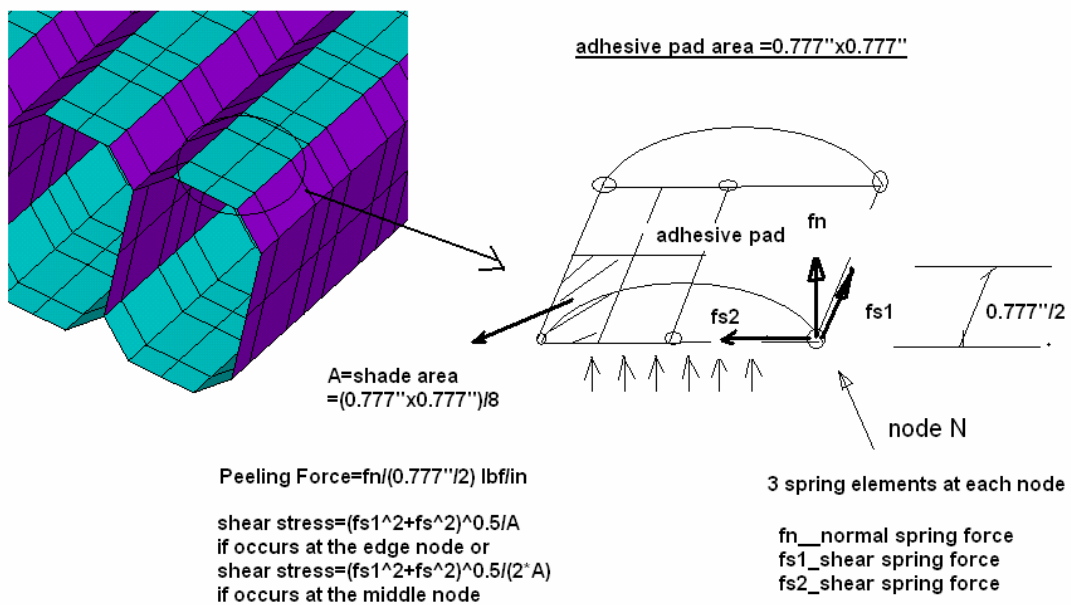


Fig. 17.75: The force extraction from the 3-layer X-Y prototype model.

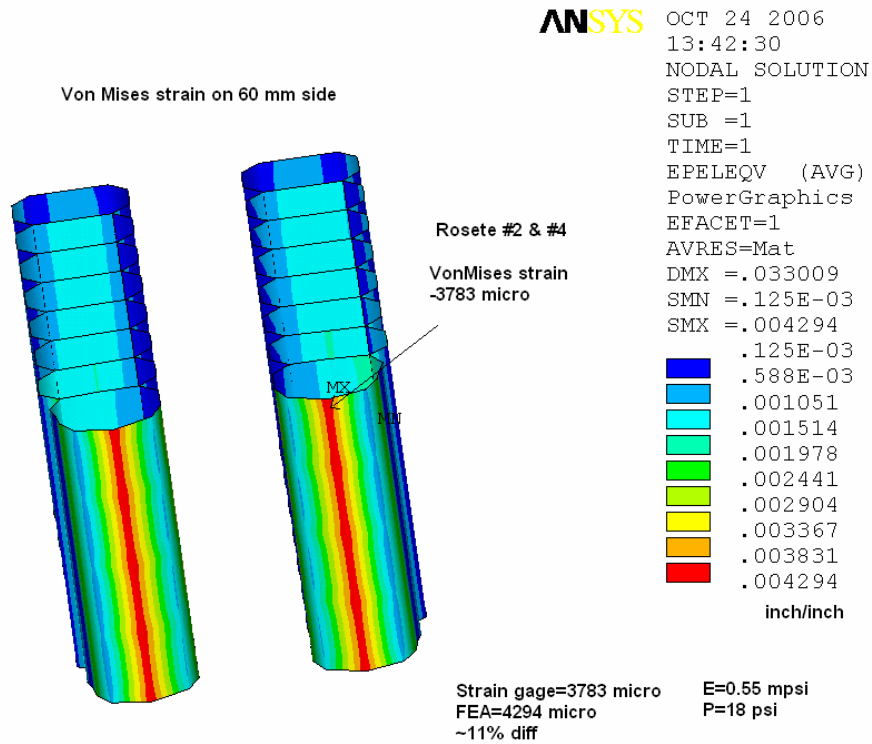


Fig. 17.76: 10 Von Mises strain in the 3-layer X-Y prototype model.

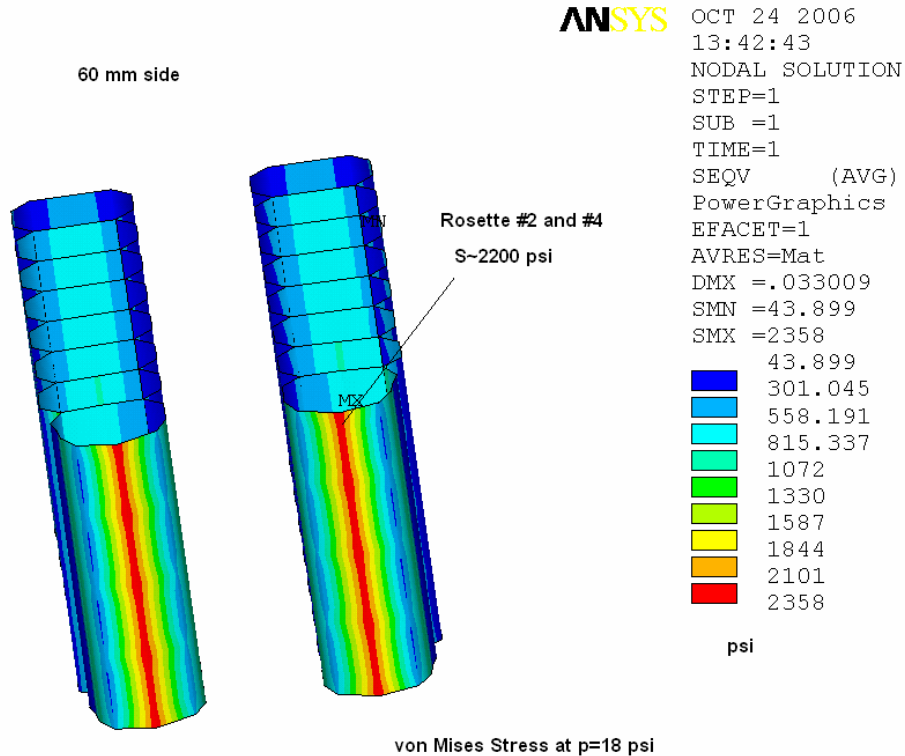


Fig. 17.77: Von Mises stress in the 3-layer X-Y prototype model.

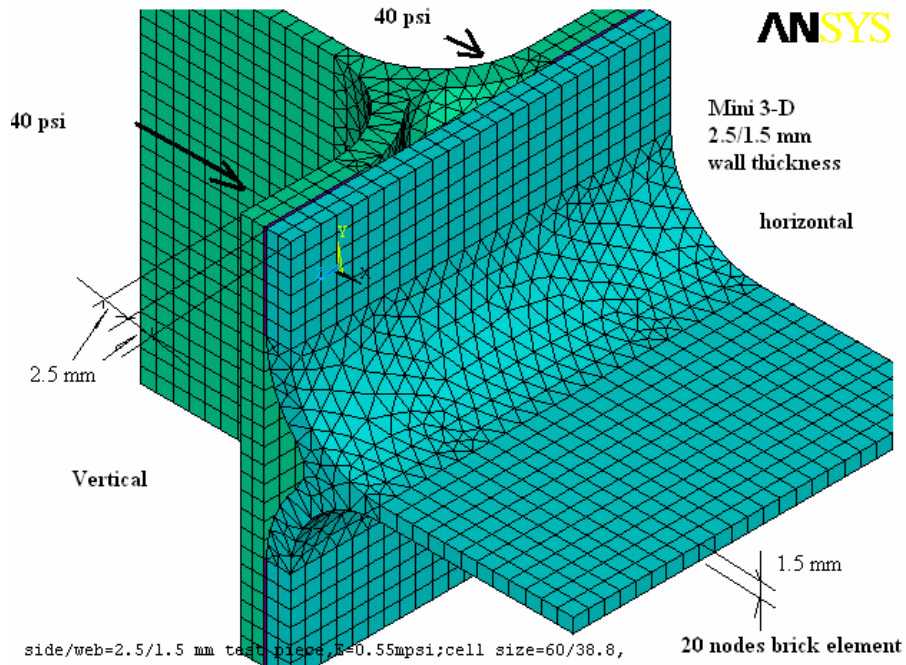


Fig. 17.78: Mini 3-D model for the adhesive peeling force in 3-layer X-Y prototype.

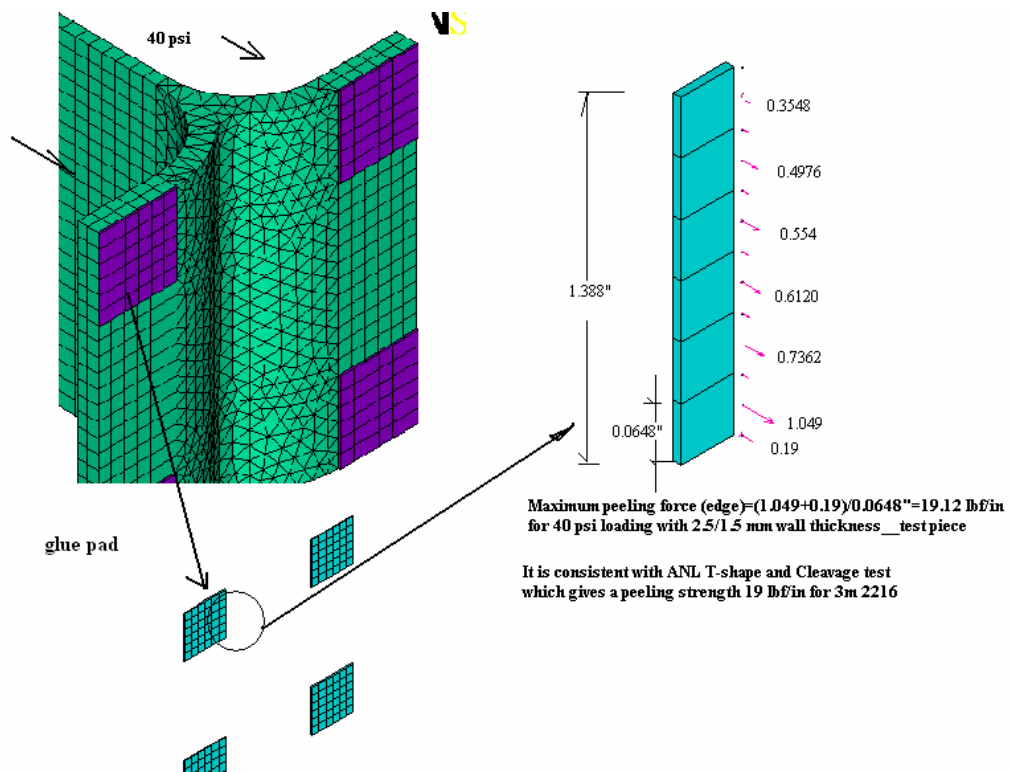


Fig. 17.79+: Maximum peeling for  $p = 40 \text{ psi}$  from mini-3D model of the 3-layer X-Y prototype.

#### **17.6.2.4 Conclusions from the 3-layer X-Y Prototype**

This initial mechanical test of assembled extrusions showed mixed results when compared to the FEA model. The FEA model showed that at 40 psi internal pressure that the peel stresses approached the peel failure strength of the adhesive. However, not all of the bonds failed at this pressure and there were relatively few failed bonds even after the extrusions were pressurized to 80 psi. The FEA model also showed that the shear strength of the adhesive bond was far below the actual strength of the 3M 2216 epoxy. The strain gages showed very good agreement with the gages on outside edges of the extrusion on the 60 mm side. However, there was poor agreement with the strains measured on the scalloped surfaces. Similarly poor comparisons were also seen on the initial 4 ft pressured prototype. The poor comparison with the FEA could be explained by the high strain gradient in this region which could not be measured by the gages which actually only measure the strain averaged over the 0.125 inch individual gages and the 0.5 inch wide rosette.

### ***17.6.3 Seven-layer Hydrostatic Stress Transmission Prototype***

#### **17.6.3.1 Experimental Setup**

The purpose of this prototype was to check the FEA model prediction that the swelling resulting from filling the first cell of a NOvA X-Y structure propagates through the entire block thickness. To test this idea, a series of empirical tests were conducted. Cells were filled with water and deflections measured.

An assembly of early prototype NOvA 3-cell PVC extrusions was constructed with 4 vertical extrusions and 3 horizontal extrusions. The vertical extrusions are ten feet high while the horizontal extrusions are 5 inches long. The hydrostatic pressure at the bottom of the vertical extrusions was 4.32 psi. 3M 2216 epoxy was used to join the extrusions and one half inch thick plastic plugs were inserted and epoxied into the lower ends of the vertical extrusions. Figure 17.80 is a photograph of the setup.

This assembly is shown behind a ladder used when filling the vertical extrusions with water. Two dial indicators were set up to measure the deflections of the center cell of the outer vertical extrusions at a distance of twelve inches above the bottom. The assembly was placed on a steel plate but was not constrained by it other than by friction. The table and aluminum channel was used as a safety restraint; it did not constrain the extrusion assembly but would prevent the extrusion from moving if the extrusion were bumped. This test is described in more detail in NOVA-doc-1198.



Fig. 17.80: Photograph of the 7-layer X-Y prototype used to measure transmission of swelling from hydrostatic pressure.

### 17.6.3.2 Results

The vertical extrusions in the 7-layer structure were filled with water twice. A full water column height provides 3.9 psi on the extrusion at an elevation of 12 inches above the bottom (this corresponds to where the dial indicators were located). Figure 17.81 shows the cell numbering scheme. The order of cell filling changed with each filling, but the cell numbering remains

<b>V11</b>	<b>Horz.</b>	<b>V8</b>	<b>Horz.</b>	<b>V5</b>	<b>Horz.</b>	<b>V2</b>
<b>V10</b>		<b>V7</b>		<b>V4</b>		<b>V1</b>
<b>V12</b>		<b>V9</b>		<b>V6</b>		<b>V3</b>

Fig. 17.81: View looking down on the top of the 7-layer X-Y prototype assembly.

For the first test, cell V1 was filled first, then V2, then V3, etc. until cell V12 was filled last. For the second test, the center cells were filled first, and adjacent cells were filled from the center outwards. The detailed results of these tests are described in NOVA-doc-1198, and are compared with the results of an FEA analysis in the next section.

### 17.6.3.3 Comparison of 7-layer prototype results with FEA model

The seven-layer PVC structure is modeled with a shell element and a spring element was used for the glue layers. Figures 17.82, 17.83 and 17.84 show the details of the FEA model. This

is very similar to the approach used for the NOvA far detector structure, except that the cell geometry and wall thicknesses were modified to reflect the 3-cell extrusions used for this study. A linear distributed pressure is applied on the vertical extrusion with maximum value of 4.32 psi at the bottom. The bottom of extrusion is assumed to be fixed by the plastic end plug. The calculation reflects the the filling sequences used for the measurements. A PVC modulus of E of 0.36 mpsi and 0.4 mpsi, based on a single layer 8-ft high extrusion test, is used in the calculation.

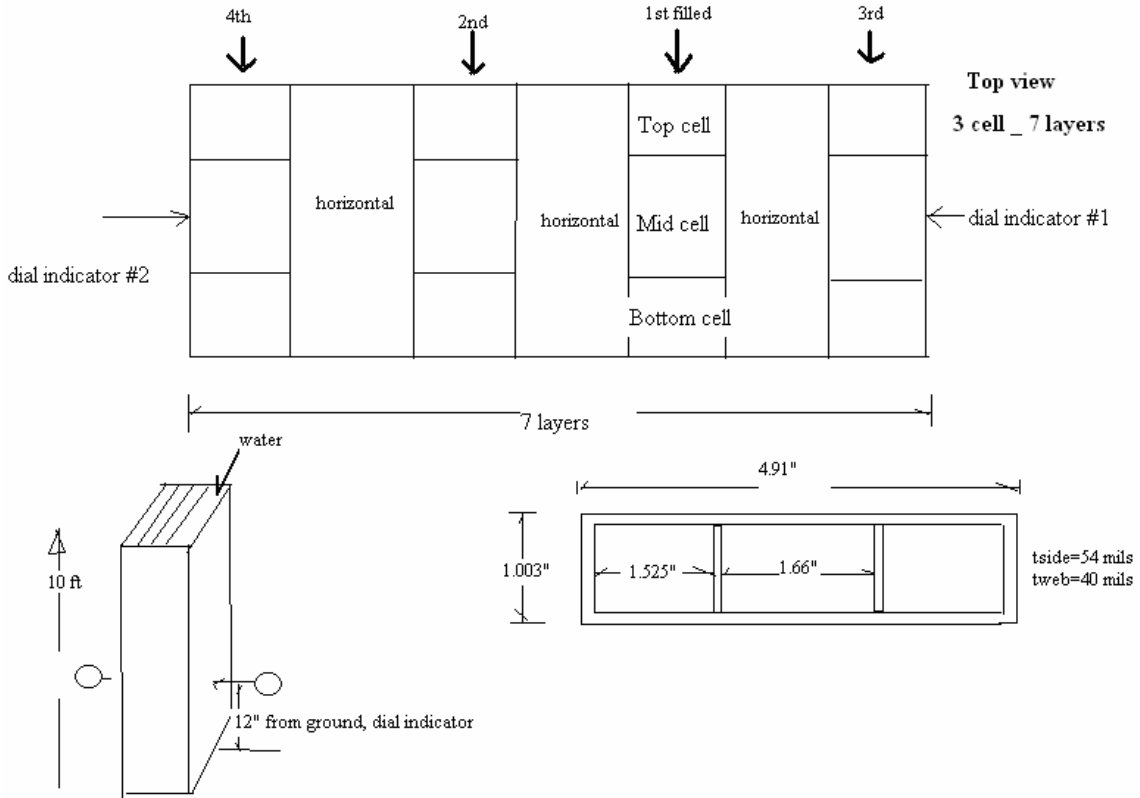


Fig. 17.82: Sketch of the geometry of the 7-layer prototype constructed of 3-cell extrusions.

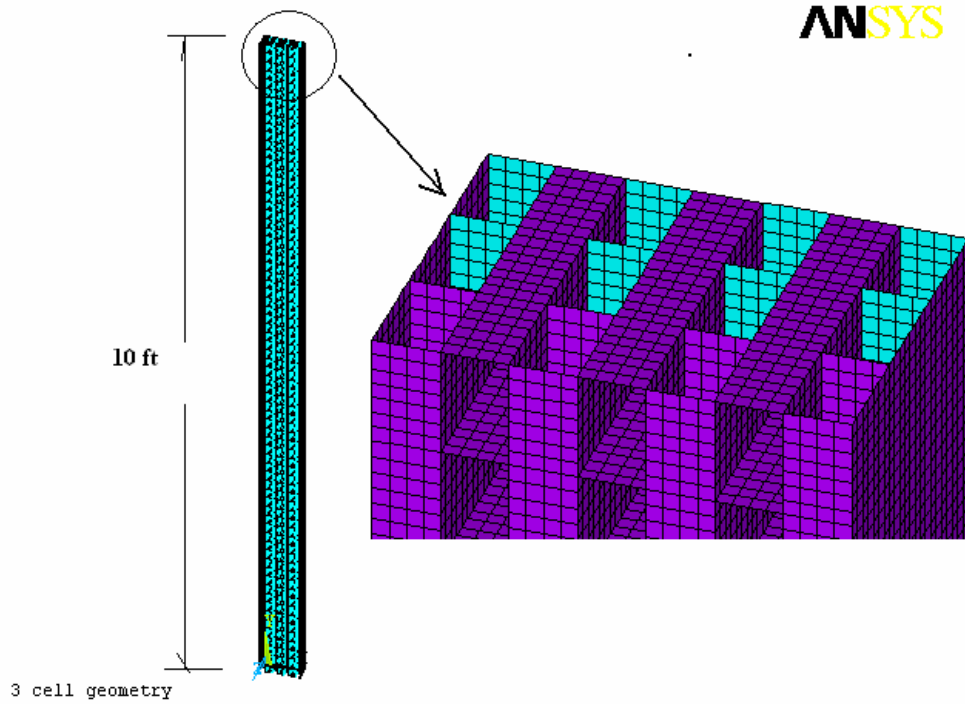


Fig. 17.83: FEA model of 7-layer prototype.

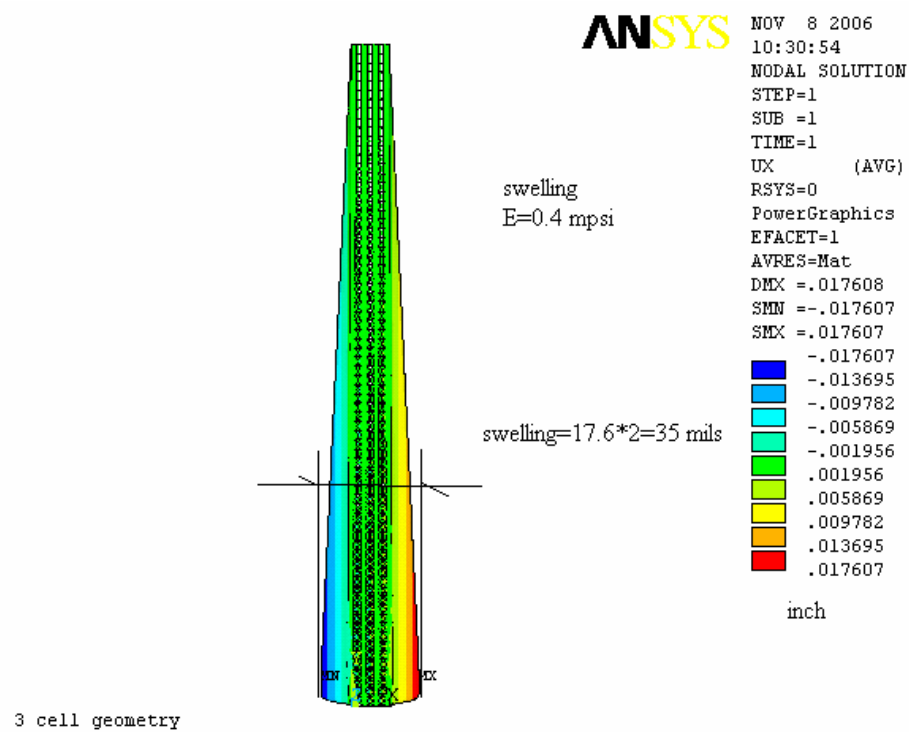


Fig. 17.84: Swelling results from the FEA model of the 7-layer prototype.

The results summarized in Table 17.18 and Figure 17.85 show good agreement between the measurement and FEA calculation. The deflection is relatively small when the first two layers filled since these are internal layers with “double wall” thickness. When third and fourth layers are filled, the deflection is increased noticeably due the single wall for the exterior layers. With four layers completely filled, the FEA result gives a 33 mil deflection for E=0.4 mpsi and 36.6 mils for the E = 0.36 mpsi, respectively, in excellent agreement with the test result of 32.67 mils. It is interesting to note that the total deflection (swelling) can be approximated as

*Total deflection ~ Single-layer deflection ( for two exterior surfaces) + double wall deflection \* number of interior vertical layers.*

The second term represents accumulative nature of the swelling. For example, total swelling is 28.1 mils for a single-layer, 10-ft high extrusion. The double wall reduces its deflection by a factor of ~8, resulting in a 3.5 mil deformation. For a seven layer structure with two interior vertical layers, the total deflection is estimated as  $28.1 + 3.5*2 = 35$  mils. The FEA gives a deflection of 33 mils compared to the test result of 32.67 mils. The deflections in this 7-layer test structure are smaller than those in a structure with more planes glued together, where the second accumulative term would be larger.

Filled Layers		1	2	3	4
Mid cell (mils)		1	-8	21	33.5
Top cell (mils)		2	-10	18.5	33
Bottom cell (mils)		2	-11	20	31.5
<b>Average (mils)</b>		<b>1.67</b>	<b>-9.67</b>	<b>19.83</b>	<b>32.67</b>
FEA (E=0.4 mpsi) (mils)		<b>1.27</b>	<b>2.54</b>	<b>18.86</b>	<b>33.19</b>
FEA (E=0.36 mpsi) (mils)		<b>1.41</b>	<b>2.82</b>	<b>20.96</b>	<b>36.88</b>

Table 17.18: Comparison of 7-layer prototype hydrostatic swelling measurements with FEA model calculations.

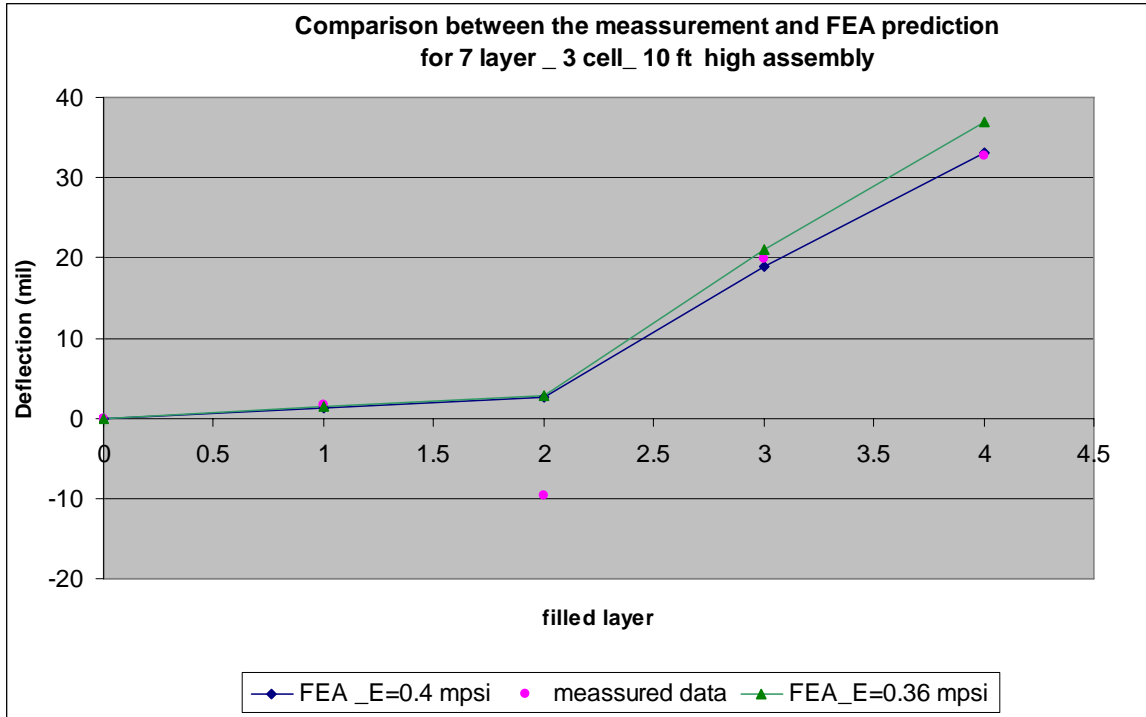


Fig. 17.85: Graphical comparison of the 7-layer test results and the FEA calculation.

#### 17.6.4 Eleven-layer/Single-extrusion X-Y Prototype

The eleven-layer prototype was similar in size and construction to the three-layer prototype described in Section 17.6.2. As in the earlier prototype, the edges and outside surfaces were instrumented with strain gages and dial indicators. Figure 17.86 shows a photograph of the 11-layer prototype and its instrumentation. The initial test conducted on the 11-layer prototype was a progressive pressurization of its layers, progressing from the first to the second to the third, etc. The purpose of this test was to validate FEA calculations that predicted the propagation of hydrostatic swelling of one plane in a detector block to produce stresses and strains in subsequent layers. The strain gages in the prototype did not indicate any strain unless the extrusion on which it was mounted was itself subjected to pressure. The pressurization of one extrusion did not cause strain in adjacent layers. However, the dial indicators showed pressurization of one layer caused was deformation of the extrusions in layers that were not pressurized. When only the first layer was pressurized, the eleventh layer moved 0.002 inch. It moved 0.004 inch when the first and third layers were pressurized and 0.006 inch when the first, third and fifth layers were pressurized, etc. The swelling of the pressurized layers simply expanded the entire assembly, moving adjacent layers as single bodies. These results are in agreement with FEA model predictions. Additional tests are planned in which the pressure will be increased above 19 psi until failure occurs in the adhesive bonds. Strain gage readings will then be compared to FEA model calculations.



Fig. 17.86: Photograph of the 11-layer prototype showing dial indicators (to measure PVC deformation) and strain gauges.

### ***17.6.5 Four-layer IPND-Block Prototype***

A four plane IPND mechanical prototype was constructed using extrusions produced during tuning of the 16-cell prototype extrusion die. This initial mechanical prototype did not have any end seals or manifolds and was intended to provide an initial experience gluing together large extrusions using the new adhesive. NOVA-doc-1369 describes this prototype in detail.

There were two vertical and two horizontal planes. Each vertical plane had four 16 cell extrusions and each horizontal plane had six 16 cell extrusions. Each plane will be glued together using Devcon 60 adhesive. The prototype block will weigh approximately 600 kg.

The goals of this prototype were the following:

- Perform a large scale application of the Devcon adhesive.
- Perform ES&H measurements during the application of the Devcon adhesive in large quantities over a large area.
- To begin to get a feel for difficulty of handling large extrusions and placing them together into a block.
- To evaluate the need for compression on extrusions during gluing.

During the entire construction the air was monitored for volatiles from the adhesive. In addition, the two people applying the adhesive wore personal monitoring devices the entire time.

### 17.6.5.1 IPND Block Fabrication

Four planes of an IPND module will be constructed. The block will be constructed on the floor starting with a layer of horizontal modules. Devcon adhesive will be applied to the next layer of vertical modules from 400-ml cartridges using a pneumatic powered gun. A glue line bead of approximately 0.125 inch diameter was placed down the center of each scallop. The vertical modules were staged on a set of supports so that they are at a convenient height to apply the adhesive. The extrusions will then be flipped over by hand and placed in the appropriate position on the horizontal extrusions.

A series of right angle fixtures were mounted to the floor to be used for alignment of each plane. The fixtures consisted of Unistrut at right angles to the floor. A wire/survey was used to align all of the fixtures in the same plane and perpendicular to each other. The construction of each layer will begin by placing the first extrusion against the two sets of stops and then locating subsequent extrusions with respect to this initial extrusion. This setup is a rough approximation of fixturing and tooling that will be on the block pivoter for locating the modules. Measurements showed that the fixtures were located within 0.040 inches of each other.

As each extrusion is placed in position a 75 lb roller was run over the surface of the extrusion to spread out the glue and obtain compression.

The top layer of the prototype was a vertical layer. The two outside vertical extrusions were placed as before. The center extrusions though were shrink wrapped and placed into the assembly. One of the shrink wrapped extrusions was rolled with the 75 lb weight while the second shrink wrapped extrusion had no compression. The purpose of the shrink wrapping is to allow the extrusions to be removed after the adhesive had cured in order to observe the glue pattern that was achieved.

Figures 17.87 (a), (b) and (c) show schematics of the assembly. Eight planes are shown in these figures because the same fabrication method will be used for the eight plane prototype that will be constructed using modules with end seals.

Figures 17.88, 17.89 and 17.90 are photographs of the assembly process.

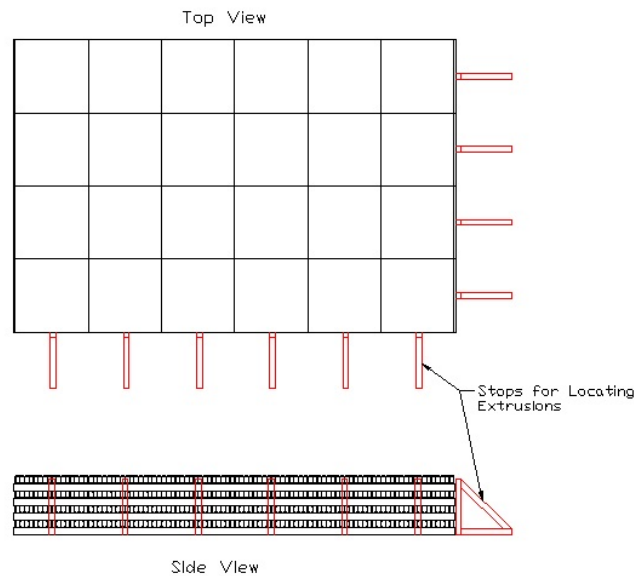


Fig. 17.87(a): View of IPND prototype block in construction orientation.

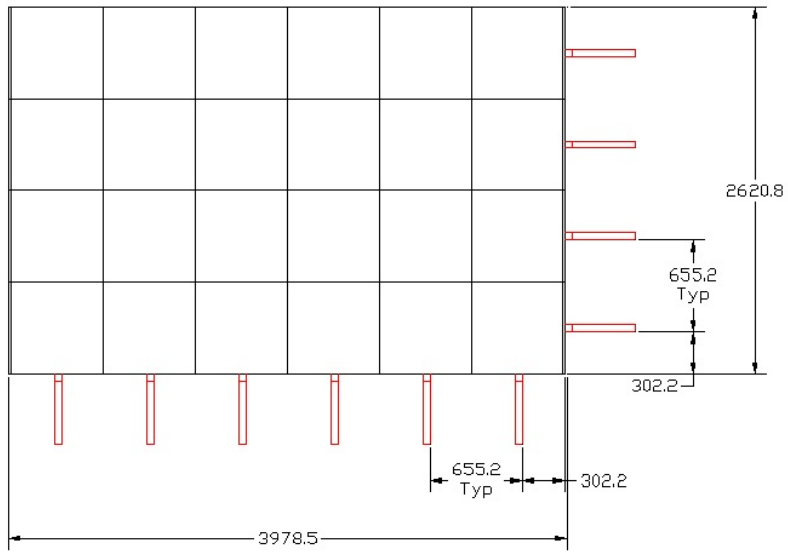


Fig. 17.87(b): Plan view of block during construction with location of fixtures.

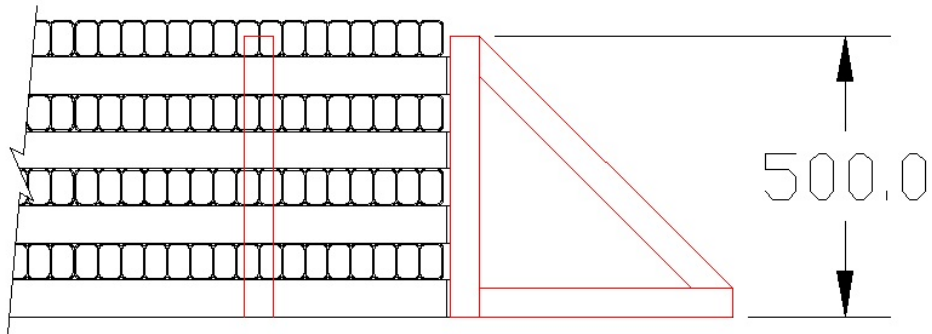


Fig. 17.87(c): Close-up view of block assembled against assembly fixture.



Fig. 17.88: Positioning an extrusion.



Figure 17.89: Applying the adhesive.



Fig. 17.90: Rolling the extrusion and applying pressure to remove the banana shape.

#### 17.6.5.2 Results

During the construction the following was learned.

1. Alignment. It was difficult to get all of the extrusions within a plane to align perfectly parallel to each other and perpendicular to the previous plane. This was caused by non-perpendicular cuts on the bottom of the extrusions. Also, the sides of the extrusions do not appear to be parallel or straight. It was clear that some of the extrusions were straighter than others. On the first layer of verticals it was observed that the second vertical placed down had a banana shape that created a gap of approximately 1mm between extrusions. A force was applied to the extrusion and the banana shape was removed, however, after a few minutes the extrusion relaxed and assumed nearly its previous shape. The glue surface tension is clearly not enough to hold extrusions into place after they had been deformed.

It was also found that it was possible to move extrusions in order to align them after they had been placed. The adhesive surface tension was not so high that it became difficult to move the extrusions after placing them into position.

2. Extrusion thickness. The thickness of the extrusion at each cell was measured for each extrusion. Figure 17.91 shows the dedicated measurement fixture used. Figure 17.92 shows a plot of the variation in extrusion thickness for each cell.

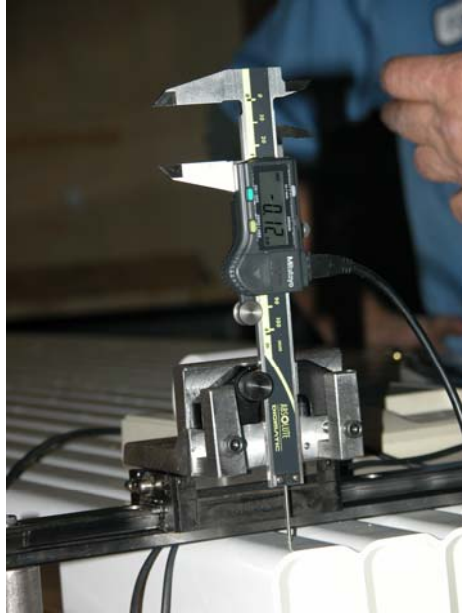


Fig. 17.91: Measuring fixture.

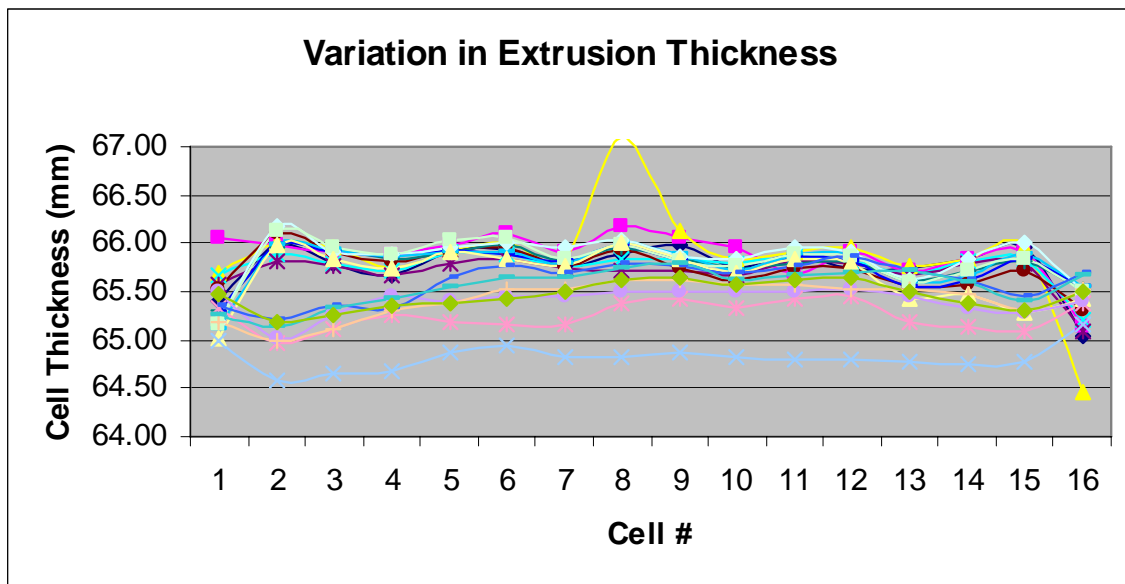


Fig. 17.92: Variation in extrusion thickness.

It can be seen in Figure 17.92 that the extrusions tended to be thinner at the outside cells. Also, whereas the overall thickness is less than the nominal thickness it is still within specification and tolerance variation that has been requested of the extruder.

3. Compression of modules. The 75 lb roller appeared to work well. The ends of the extrusions tended to bow upwards and loose contact. Repeated rolling of these areas tended to eliminate this problem and achieve compression. However, the second vertical extrusion on the second layer continued to bow upward after repeated rolling. After the third layer of horizontals was placed though and rolled the gap in this region closed and appears to made good contact.

After curing the top two vertical extrusions that were shrink-wrapped were removed and the glue line compression observed. It was clear that the adhesive did not spread out at all on the extrusions that had not been compressed. Figure 17.93 and 17.94 are close-up photographs of the compressed and non-compressed extrusions.

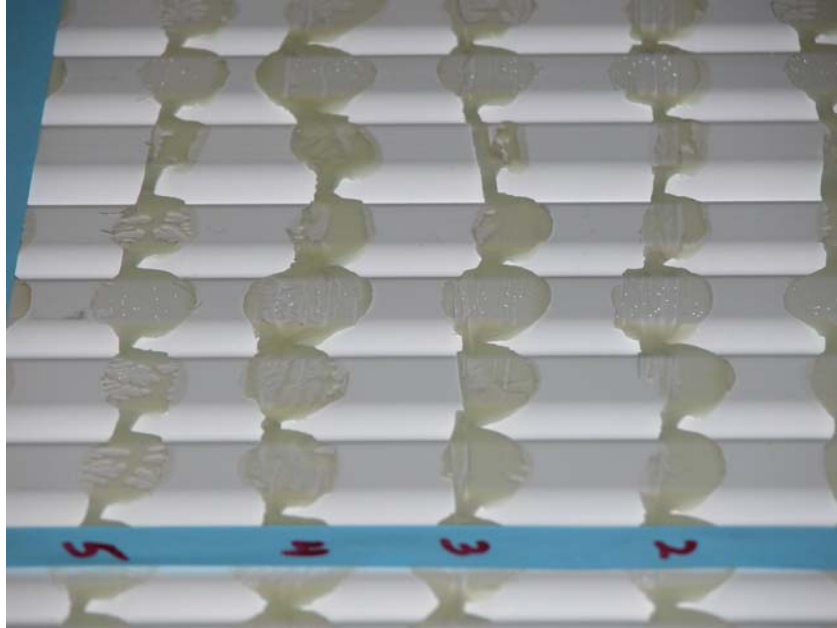


Fig. 17.93: Adhesive pattern under compressed extrusion.

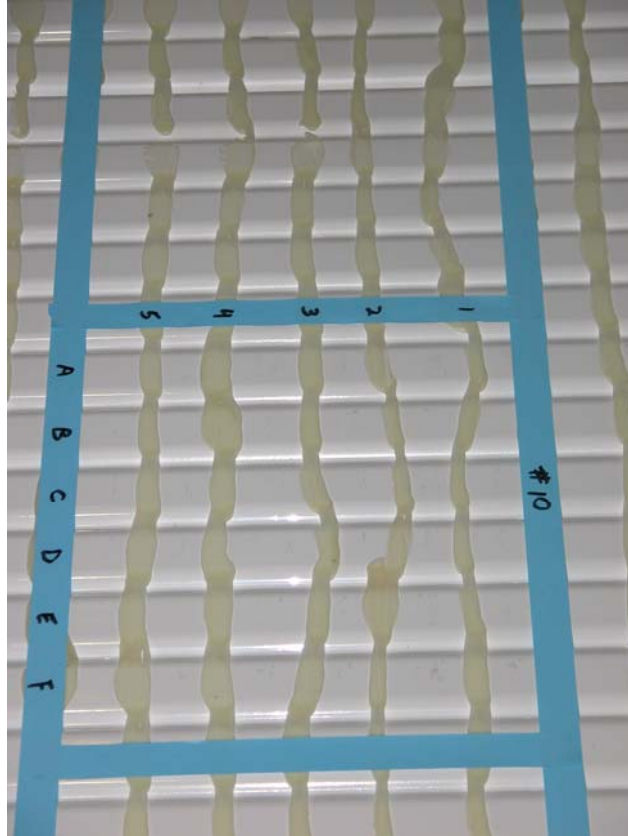


Fig. 17.94: Adhesive pattern under non-compressed extrusion.

Looking at these compression patterns it was clear that along the first and 16<sup>th</sup> cells which were not as wide as the remainder of the extrusions that there adhesive was not as compressed. The thickness of the extrusions played a role in the amount that the adhesive was compressed. Figure 17.95 shows the adhesive pattern in a region of the boundary between two extrusions. It is clear that along the first cell of one extrusion and the 16<sup>th</sup> cell of its neighbor that less compression occurred.

The exposed adhesive was divided into a grid as shown in Figure 17.96 and the glue line thickness was measured. Measurements were only recorded on an inside square that was two cells in from the outer edges of both the vertical and horizontal extrusions. This was done because of the obvious difference in compression along the outer edges of the extrusions and it was desired to obtain an average thickness that was not biased by the lack of compression on the edges due to the thinner extrusions in that area. Within each pad of adhesive there was sometimes significant variation in thickness if the adhesive bead had not been placed on the center of the scallop. In these cases the adhesive would be squeezed out towards the scallop and a radius would be formed in the adhesive. The average thickness of the compressed pads was 0.33 mm which is similar to the 0.010-0.012 inch diameter beads that were in the adhesive with a standard deviation of 0.11 mm which is identical to the standard deviation of the extrusion thickness measurements. The non-compressed patterns had an average thickness of 0.60 mm and also a standard deviation of 0.11 mm.



Fig. 17.95: Compression along boundary between adjoining extrusions.

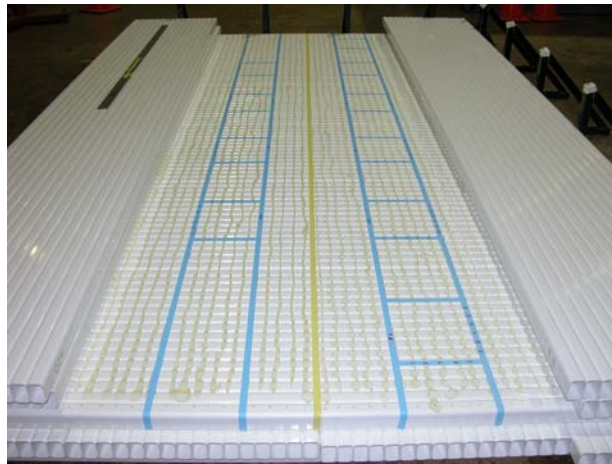


Fig. 17.96: Measurement pattern.

### 17.6.5.3 ES&H

During this test there was no direct air movement in the area of gluing (e.g., by fans) but the actual volume exchange in the building is not known. More important, the gluing occurred in a large high bay area with a very large volume of air over 1.5 hours so there was a very large volume for the methyl methacrylate vapors to dissipate into. Over time the concentration would likely have increased as the methyl methacrylate filled the volume of the building. There was clearly an unpleasant smell in the area, which was most intense in the area where gluing occurred and diminished as further away from the prototype area. A person working in the building 60 ft away could not smell the adhesive until he was within 30 ft of the prototype fabrication area.

Area monitors and personal monitors worn by the two people performing the gluing provided measurements of the integrated methyl methacrylate concentration during this

construction. The ES&H report is included in NOVA-doc-1347. The highest time weighted average concentration of methyl methacrylate was 21.3 ppm for one of the glue applicators but only 3.1 ppm in the area immediately next to the block being constructed. These are below the 100 ppm OSHA permissible exposure limit of 100 ppm and the 50 ppm 8-hr threshold limit value recommended by the American Conference of Governmental Industrial Hygienists. However, extrapolation of these values to the far detector assembly process at Ash River indicates that aggressive ventilation to remove adhesive vapor will be required around the adhesive dispenser and block pivoter assemble table.

#### **17.6.5.4 Conclusions**

The following conclusions were made:

- The use of rollers for compression looks promising.
- Need to do further tests to understand glue compression and coverage.
- It is possible to move modules once they have been placed.
- For assembly it would be best if any gaps due to banana were accepted and no effort was made to take them out.

#### **17.6.6 Eight-layer/Single-extrusion X-Y Prototype**

An eight plane IPND mechanical prototype block was constructed using extrusions produced during a tuning run with the 16-cell prototype extrusion die. This mechanical prototype was constructed with the “vertical” extrusions with end seals on both ends. There were no end seals on the “horizontal” extrusions. Figure 17.97 shows the completed prototype with some of the assembly crew. NOVA-doc-1981 describes the 8-layer prototype study in detail.

There were four vertical and four horizontal planes. Each vertical plane had four 16 cell extrusions and each horizontal plane had six 16 cell extrusions. The modules in each plane were glued into the block with Devcon 60 adhesive.

The prototype block weighs approximately 1200 kg.

The purpose of this prototype was:

- To perform a large scale application of the Devcon adhesive.
- To perform ES&H measurements of methyl methacrylate (MMA) vapor during the application of Devcon 60 adhesive in large quantities over a large area.
- To gain experience with the handling large extrusions and placing them accurately into a block.
- To evaluate the need for compression on extrusions during gluing.
- To construct a prototype that could be filled with liquid and loaded to simulate the stresses and deflections in a full height block.

During the entire construction process, the air in the assembly area was monitored for MMA vapor released by the adhesive. In addition, the two people applying the adhesive wore personal monitoring devices the entire time.



Fig. 17.97: Completed 8-plane prototype with assembly crew.

Eight planes of an IPND module were constructed. A procedure identical to that followed during the construction of the 4 plane IPND mechanical prototype was followed. The block was constructed on the floor starting with a layer of horizontal modules. Devcon adhesive was applied to the next layer of vertical modules from 400-ml cartridges using a pneumatic powered gun. A glue line bead of approximately 0.125-inch diameter was placed down the center of each scallop. The vertical modules were staged on a set of supports so that they are at a convenient height to apply the adhesive. The extrusions will then be flipped over by hand and placed in the appropriate position on the horizontal extrusions.

A series of right angle fixtures were mounted to the floor to be used for alignment of each plane. The fixtures consisted of Unistrut at right angles to the floor. A straight wire was used to align all of the fixtures in the same plane and perpendicular to each other. The construction of each layer will begin by placing the first extrusion against the two sets of stops and then locating subsequent extrusions with respect to this initial extrusion. This setup was a rough approximation of fixturing and tooling that will be on the block pivoter for locating the modules. Measurements showed that the fixtures were located within 0.040 inch of each other.

As each extrusion was placed in position a 75 lb roller was run over the surface of the extrusion to spread out the glue and obtain compression.

During construction the main observation was the alignment of modules and the bottom end seals. The 13-ft long vertical extrusions had a slight banana shape to them which could not be taken out. The edges of the verticals were aligned on two of the stops but the banana shape resulted in a misalignment of the bottom end seal. The bottom of the IPND will be grouted to fill

gaps and ensure uniform support of the load-bearing vertical module end seals before the structure is raised to the vertical position.

Area monitors and personal monitors worn by the two people performing the gluing were used to record any volatiles from the adhesive. There was clearly an unpleasant smell in the area that was most intense in the area where gluing occurred and diminished as further away from the prototype area. Someone working in the building but 60 ft away could not smell the adhesive until he was within 30 ft of the prototype fabrication area.

Monitors were placed in the area of gluing and at the inlet and outlet of the ventilation fan. The ventilation fan had a 0.5-inch thick activated carbon filter on the inlet and approximately 2,000 cfm of air flow. The concentrations of MMA at the locations during gluing are summarized in Table 17.19. The concentrations are significantly lower than recorded during the earlier 4 plane IPND prototype construction where Slabaugh had a concentration of 14.7 ppm and Kephart had a concentration of 21.3 ppm (NOVA-doc-1369).

<b>SAMPLE NO.</b>	<b>DATE</b>	<b>NAME/ BADGE NO.</b>	<b>LOCATION/ OPERATION</b>	<b>METHYL METHACRYLATE CONC. (PPM<sup>1</sup>)</b>
39751	4/23/2007	Area Air Sample	E of panels on floor (4 ft. above floor)	0.8
39752	4/23/2007	Area Air Sample	E end below glue table (12 in. above floor)	0.5
39753	4/23/2007	K. Kephart/ 03119N	Adhesive Application	1.5
39754	4/23/2007	M. Slabaugh/ 14132N	Adhesive Application	4.3
39755	4/23/2007	Area Air Sample	E end of glue table, 5 ft. above floor (16 ft. E of exhaust fan)	0.9
39756	4/23/2007	Area Air Sample	Fan exhaust, 3.5 ft above floor (2.5 ft. W of fan)	0.3
39757	4/23/2007	Area Air Sample	Fan inlet (4 in. from filter)	0.7
39758	4/23 & 24/2007	Area Air Sample (Overnight)	After Panel Assembly, N side on floor (4 in. from panels on floor, 3 in. above floor)	1.5
39759	4/23 & 24/2007	Area Air Sample (Overnight)	After panel Assembly, on top of panels (9 in. above panel)	0.6

Table 17.19: Concentrations of methyl methacrylate vapor measured during assembly of the 8-plane prototype.

The following conclusions were made from this study:

- A small amount of ventilation can reduce the concentration of MMA significantly.
- This test did not determine the effectiveness the filter is in removing MMA vapor.
- The use of rollers for compression looks promising.
- Additional tests are required to understand glue compression and coverage.
- It is possible to move glued modules immediately after placement in a block.
- For assembly it would be best if any gaps due to banana were accepted and no effort was made to take them out.

The next step of this prototype study will be to fill the gaps between extrusions and end seals at the bottom of the block with epoxy grout and then to raise it vertical. Strain gages will be applied to the prototype and the vertical modules will be filled with water. Additional air pressure will be applied to achieve 19 psi at the bottom of the vertical extrusions. Next, large weights will be placed on top of the vertical modules in order to simulate the adhesive and PVC stresses in a full-height far detector block.

### ***17.6.7 Adhesive shear measurements with 3-layer prototype sections***

The ultimate strength of the adhesive bond in shear and the actual peak stresses can only be determined through testing which uses actual extrusions. The strength and peak stresses in any adhesive bond depends upon the thickness of the material used, the surface of the material, and geometry. A test has been developed to evaluate the shear strength of the adhesive using actual extrusions adhered together in the geometry of extrusion in the NOvA detector.

Figure 17.98 shows a schematic of the test pieces that were made. For the preliminary tests enough adhesive was applied to insure that entire area of contact between the horizontal and vertical extrusions was covered and that there was some minimal squeeze out into the scallop area. Figure 17.99 shows schematically how the extrusion setup was restrained and the force applied.

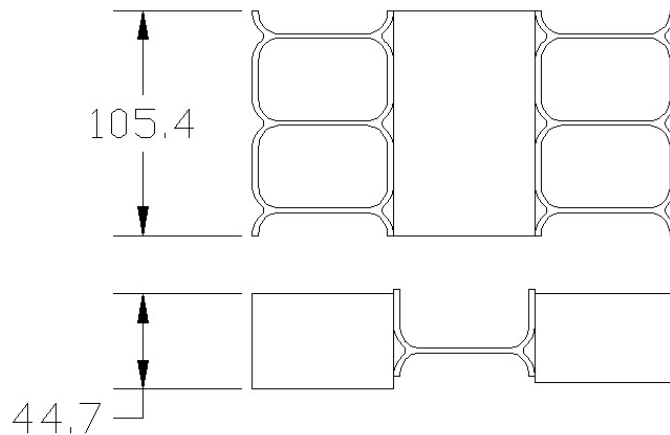


Fig. 17.98: Front and top views of test extrusion assembly. Dimensions shown are in mm.

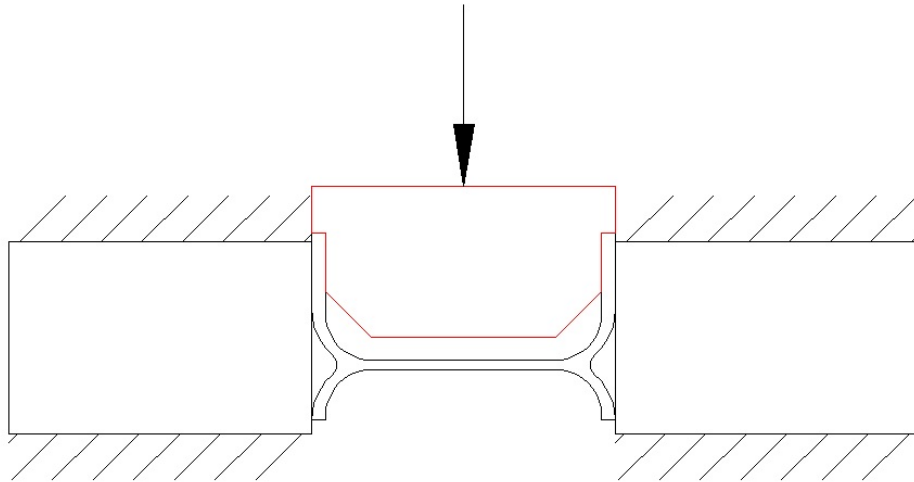


Fig. 17.99: Schematic of test restraint and force application.

In this test it is important that the force be applied direction to the side wall and that the side wall be restrained so that it would not begin to peel due to deformation of the extrusions. The vertical extrusions were restrained to prevent motion and the plug resting in the horizontal extrusion insured that the sidewalls could not move laterally in peel. The plug also insured that the force was applied directly in shear to the side walls. Figures 17.100 and 17.101 show the test setup.



Fig. 17.100: Photograph of 3-layer prototype assembly for adhesive shear strength measurement.

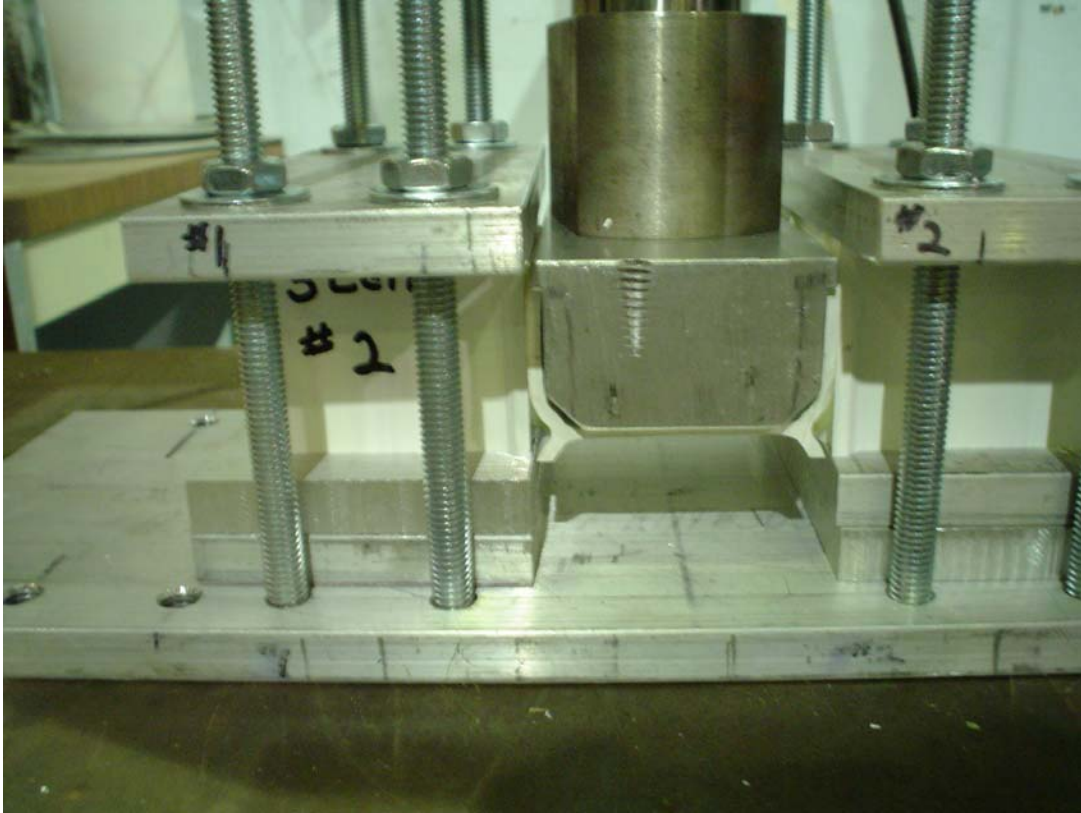


Fig. 17.101: Photograph of 3-layer prototype test setup for adhesive shear strength measurement.

The extrusions used in this test have a nominal 19-mm flat across scallops so that when horizontal extrusions are mated with vertical extrusions the contact area is  $19\text{ mm} \times 19\text{ mm} = 361\text{ mm}^2 = 0.56\text{ in}^2$ . In the extrusion setup used in this test the applied force is resisted by four of these pads for a total theoretical area of  $2.24\text{ in}^2$ .

Using this theoretical area the shear stress in the adhesive was plotted versus deflection and is shown in Figure 17.102.

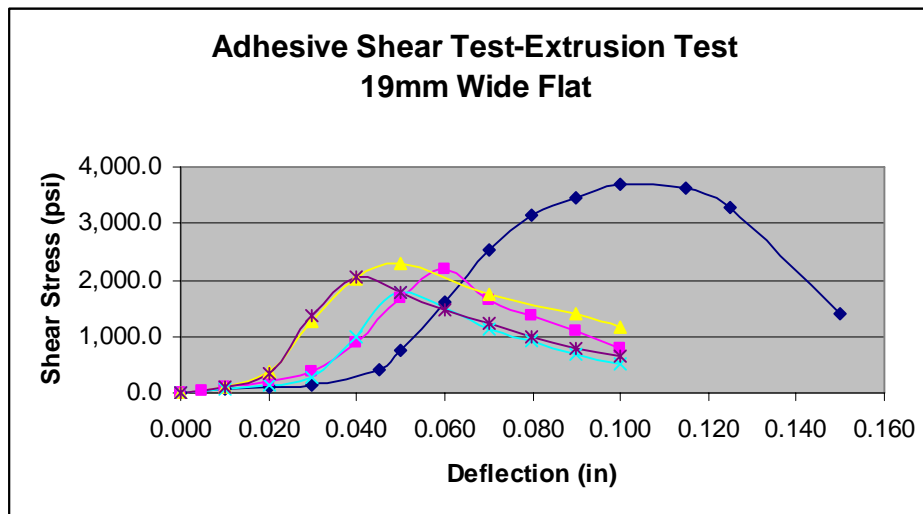


Fig. 17.102: Shear stress in adhesive using theoretical contact area of  $2.24\text{ in}^2$ .

Figure 17.102 shows that the peak shear stress occurred above 2,000 psi, which is well above the shear strength obtained using ASTM standards. This increase in strength could be attributed to the increased adhesive area due to the squeeze out into the scallops. Based on observations made during testing it was felt that the ability of the extrusions to continue to resist an applied force was due to adhesive squeeze out in the scallops and since the adhesive has a significantly lower modulus than the PVC large deformations were occurring.

Observations of the actual adhesive area after failure showed that the contact area was closer to 1.125 inches, which results in a total shear area that is closer to 5.0 in<sup>2</sup>. Figure 17.103 shows the results plotted versus deflection using this value for the shear area. The actual shear stress at failure is closer to that measured using standard ASTM tests.

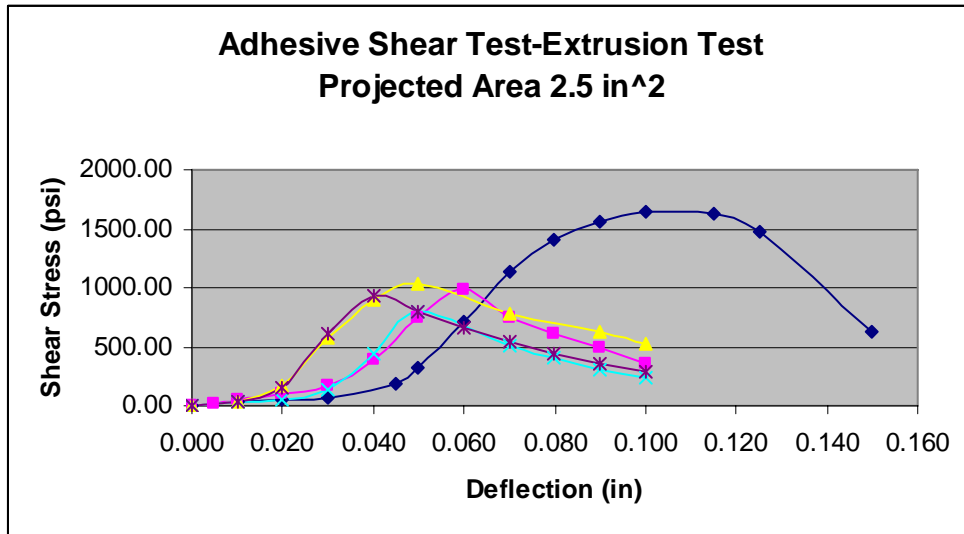


Fig. 17.103: Shear stress calculated using observed bond area of 5.0 in<sup>2</sup>.

This test using actual extrusions demonstrates that the adhesive joint has considerable strength. Also, the strengths found from standard ASTM tests closely match the strength found using actual extrusions and therefore these results are a good predictor of the strength that can be expected.

## 17.7 Far Detector Infrastructure

Far detector installation and operation make use of several large structures and equipment complexes that are specified and designed jointly by the WBS 2.1 and WBS 2.9 tasks. One or the other of these tasks has the primary responsibility for fabricating and installing a given system. The main infrastructure systems are described in the following sections.

### 17.7.1 Environmental Control Systems

#### 17.7.1.1 Temperature and Humidity Specifications

The dimensions of PVC extrusion modules depend on both the temperature and humidity of their environment. The coefficient of thermal expansion of PVC is  $7 \times 10^{-5}/^{\circ}\text{C}$ . At 20°C and 40% relative humidity, a temperature change of 3°C causes about three times the change in PVC dimension as a 1% change in relative humidity, as measured by strain gages on NOvA extrusions in an environmentally controlled chamber (NOVA-doc-1535).

The temperature and humidity in the assembly area where far detector blocks are constructed will be controlled to prevent significant changes in PVC dimensions as modules in a

block are glued together over the course of several weeks. In addition, modules will be installed in blocks only after their dimensions have stabilized in the environment of the assembly area. Extrusion modules reach temperature equilibrium within 24 hours of being subjected to a large temperature change upon delivery to the far detector site, however they will require several days to come to equilibrium after a large humidity change. These considerations, weighed against the cost of controlling temperature and humidity in the assembly and loading dock areas at different seasons, have resulted in the following specifications. The temperature in both the loading dock and assembly areas will be maintained at  $70\pm 5^\circ\text{F}$ , summer and winter. The relative humidity will be maintained at  $50\pm 10\%$  during the summer and  $15\pm 10\%$  during the winter. FEA calculations confirm that these conditions will limit the buildup of internal stresses during block assembly to acceptable levels (NOVA-doc-xxxx).

After a block has been assembled and its adhesive has cured, its modules will expand and contract together as environmental conditions change, so PVC dimensional stability considerations are not the dominant factor in determining environmental specifications in the detector hall. Instead, the change in liquid scintillator volume with temperature sets these specifications. Since the volume coefficient of expansion of liquid scintillator is 3.5 times larger than that of PVC (NOVA-doc-344), a two liter liquid overflow volume is provided for each module to accommodate temperature increases in the detector hall. Similarly, detector modules will be initially overfilled by two liters to prevent liquid levels from dropping unacceptably low during negative temperature excursions. For vertical modules, this  $\pm 2$ -liter volume is provided by the module manifolds plus the length of vertical module extrusion that extends above the top of adjacent horizontal module plane. For horizontal modules, a separate 4-liter “overflow” tank is attached to each module manifold.

The humidity in the detector hall will be kept below a dewpoint of  $50^\circ\text{F}$  to prevent condensation on the chilled water plumbing to the APD thermoelectric coolers. These considerations require that the detector hall temperature be maintained at  $70\pm 5^\circ\text{F}$ , summer and winter. Short-term fluctuations are of little consequence because of the large thermal inertia of the filled detector. The relative humidity will be kept below 45% ( $50^\circ\text{F}$  dewpoint) during the summer and around 15% during the winter.

#### **17.7.1.2 Ventilation Requirements**

Approximately four tons of Devcon Plastic Welder 60 adhesive will be used in the assembly of each detector block. During the adhesive application and curing process, 1 to 3% of the adhesive mass (depending on environmental conditions) is released into the surrounding environment as methyl methacrylate (MMA) vapor (NOVA-doc-1975, 1979, 1984). The block assembly area at the far detector site will include a substantial ventilation system in order to limit the exposure of far detector assembly workers to MMA vapor. NOVA-doc-1520 describes the design criteria for this system.

The American Conference of Governmental Industrial Hygienists Threshold Limit Values in 2006 for methyl methacrylate is an 8-hr time-weighted average concentration (Threshold Limit Value, or TLV) of 50 ppm ( $205\text{ mg}/\text{m}^3$  air). The OSHA Permissible Exposure Limit is 100 ppm. The target concentration for NOvA is set well below these values to protect the health of the assembly crew workers. For NOvA detector assembly, we have adopted the requirement that MMA vapor concentrations will be limited to 5 ppm. This specification is based on our review of literature on the health effects on workers exposed to MMA.

Calculations described in NOVA-doc-1520 lead to separate ventilation specifications for the two areas at the far detector site with the greatest potential for worker exposure to MMA vapor. To meet our 5 ppm limit, MMA-contaminated air will be removed from each of these areas at a rate of 20,000 cfm. These localized ventilation systems operate in parallel with the 13,000 cfm loading dock and assembly area HVAC systems. These MMA removal systems are

expected to limit MMA vapor levels within 100 ft of the far detector building complex to much less than 1 ppm.

Methyl methacrylate vapor levels were recorded during assembly of the 4-layer and 8-layer IPND-block prototypes, as described in Sections 17.6.5 and 17.6.6 (NOVA-doc-1369 and 1981). Additional, more detailed measurements of MMA vapor levels will be made during future large-scale gluing exercises, as IPND blocks and the far detector full-scale assembly prototype are constructed. These will provide experimental verification of the effectiveness of our ventilation requirements for controlling worker MMA exposure levels during far detector assembly. In addition, the adhesive dispenser design incorporates ventilation ductwork to remove MMA-contaminated air as close to the source as possible. Measurements made with the adhesive dispensers for the IPND and the full-scale assembly prototype will provide early opportunities to test this system and optimize its design for the more challenging environment of the far detector assembly areas.

### ***17.7.2 The South Bookend***

The first (south) bookend provides a strong, flat surface to which the first detector block is attached. The bookend is a reinforced concrete wall, spanning the full height and width of the detector building, with doorway apertures for each of the east and west side walkways. It is supported by the building walls. The bookend is designed to resist the hydrostatic pressure of the first plane of vertical extrusions (19.2 psi at the bottom) and to withstand the forces exerted by a buckling failure of the completed, filled detector. These forces were calculated using a PVC modulus weakened by 25 years of creep and allowing the detector blocks to deform into the expansion gaps between superblocks as described in Section 17.5.5. In this Section, the worst case scenario is calculated where the blocks all buckle in the same direction, make contact with each other, and are prevented from collapsing because they are restrained by the bookend. The forces acting on the bookend are shown in Figures 17.53 and 17.54. Calculations have found that the middle force on the bookend of 255 tons is distributed over a distance of 108 inches starting at approximately 110 inches from the bottom of the detector. The top force of 67 tons is distributed over a distance of approximately 60 inches at the top of the detector.

The block which is located adjacent to the bookend will have a spacer that is 20-mm thick located in this in the calculated regions of contact. A survey will be made of the south bookend wall before installing the first block. Based on this survey the thickness of the nominal 20-mm thick spacer will be increased to account for the bookends out of flatness in order to insure contact. The spacer has to be a minimum of 20-mm thick to insure that the manifolds which overlap the extrusions do not make contact with the wall. The spacer thickness will be increased as needed based on the survey to insure contact. The first block will be placed into contact along the spacers with the south bookend wall when it is rotated vertical. It should be noted that the location of contact is significantly higher than the location where the swelling in the block occurs due to hydrostatic pressure. The 20-mm thick spacers will insure that the location where swelling occurs does not make contact with the bookend. This is important so that the stresses in the PVC and adhesive due to swelling are not increased.

The concrete bookend structure is constructed by WBS 2.1. WBS 2.9 is responsible for surveying the surface of the bookend, and for attaching PVC sheet material to it as necessary to make it smooth, flat and plumb to a tolerance of about 2 mm.

### ***17.7.3 The North Bookend***

The second (north) bookend provides a strong, flat surface against which the final detector block rests. Its mechanical strength requirements are the same as those for the south bookend.

After the detector assembly has been completed, the block pivot table will be converted to a stationary object serving as the north bookend. The majority of the block pivoter structure will

remain intact, with only the hydraulic cylinders disconnected and replaced with rigid structural members and the vertical loads transferred from the rolling elements to permanent cribbing.

Since the vertical side supports (Section 17.13) are not sufficient to transfer the entire horizontal load from the north bookend to the floor, additional structural steel column sections will be attached to the back side of the block pivot table and anchored to the building floor (Figure 17.104).

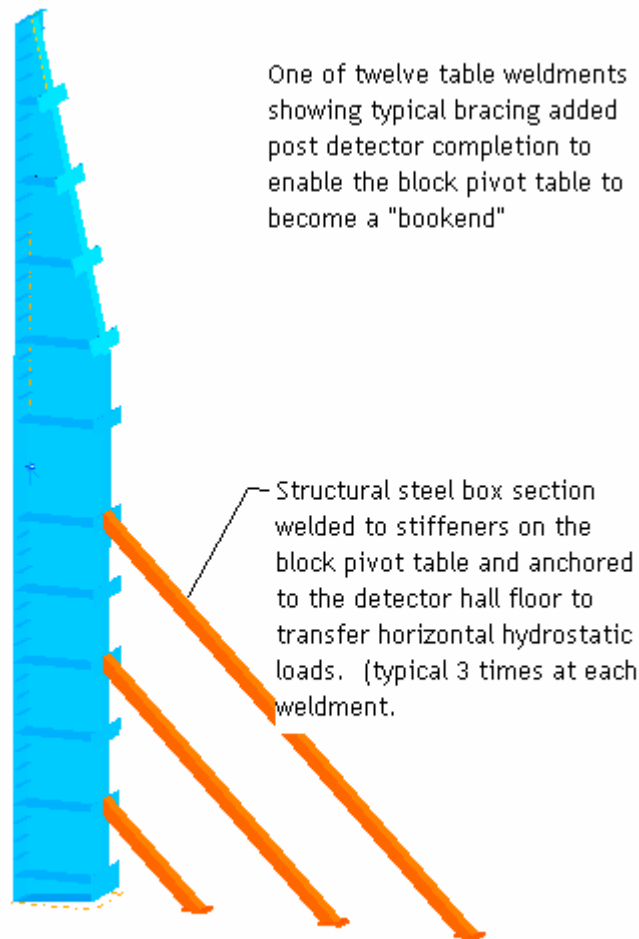


Fig. 17.104: Section through a portion of the block pivoter table showing the additional bracing needed to achieve the requirements of the bookend.

The north bookend consists of the block pivoter, which is permanently installed and braced with additional structures to support it against the floor and walls of the detector building. The north bookend is installed by the WBS 2.9 assembly crew. WBS 2.9 is responsible for the design and fabrication of the additional bracing structures. WBS 2.1 provides the anchor points for these structures.

#### ***17.7.4 Cosmic-Ray Shield Wall***

A 1-m thick concrete-block cosmic-ray shield wall is constructed across the south end of the loading dock after the north bookend is installed. This wall completes the cosmic-ray

shielding of the detector, most of which is provided by the concrete roof, barite overburden and building walls that surround the rest of the detector hall. The shield wall consists of pre-cast concrete blocks that are stacked by the bridge crane up to its hook-height limit. The top few feet of the wall consists of smaller blocks that are hand stacked up to the ceiling. The east and west sides of the wall are penetrated by personnel passageways to allow easy access to the detector hall from the loading dock and office areas during routine experiment operation.

NOvA engineers have worked with manufacturers of pre-cast concrete structures to design an optimum block for the cosmic-ray shield wall. These blocks can be easily handled, stacked, and locked together to form a continuous wall. The concrete blocks are interlocking for structural stability and to eliminate gaps that cosmic rays could pass through. A preliminary design of the basic block is shown in Figure 17.105 below. Figure 17.106 shows a conceptual design of the assembled wall, including the provision for personnel access doors through the wall.

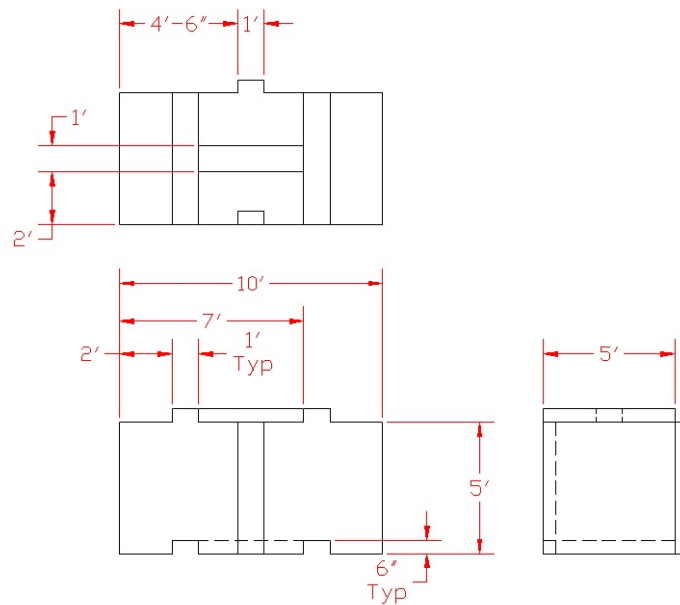


Fig. 17.105: Design of pre-cast concrete blocks for the cosmic-ray shield wall.

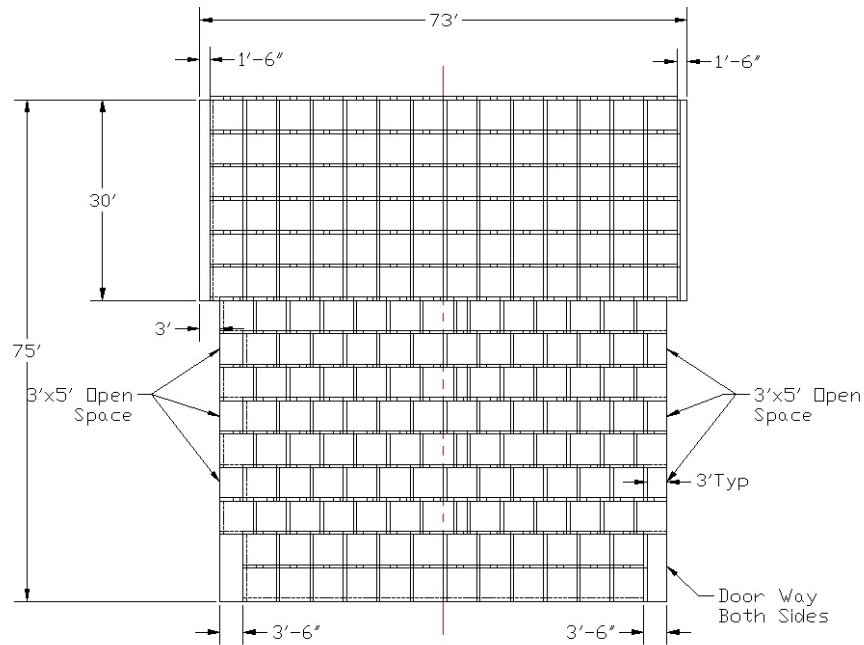


Fig. 17.106: Conceptual design of the cosmic-ray shield wall assembly.

### 17.7.5 Access to the Installed Detector Blocks

The detector assembly crew must have good access to the top and side surfaces of the 52-ft high by 52-ft wide detector blocks in order to fill the blocks with liquid scintillator and to outfit them with electronics and DAQ hardware. Scintillator filling involves the manipulation of heavy transfer lines, through which large volumes of potentially hazardous liquid flow, near the top and side surfaces of the detector. Subsequent installation of photodetectors, front-end electronics, plumbing for the APD water cooling system and data acquisition cabling and hardware, involves careful alignment of delicate hardware in awkward locations, as well as manipulation of cable trays and pipes that could damage the detector modules. Cooling hardware, racks containing electronics hardware, and building utilities (mounted on the building walls) are also located close to the detector surfaces. Even after detector installation is completed, readout hardware maintenance requires occasional access to the top and sides of the detector. These diverse requirements have motivated a substantial design effort aimed at providing safe and convenient access to the top and sides of detector blocks.

Access to the sides of the detector is provided by two sets of six walkways, one along each side of the detector, extending the full length of detector area, with east and west walkways at the same level joining together behind the south bookend. These are shown in Figure 17.107. The 5-ft wide walkways are separated by approximately 8.5 ft in elevation. Each walkway accommodates a 3-ft wide egress path and an 8-inch wide space along the building wall that is allocated for building utilities and ventilation ducts.

The building floor and the bottom five walkways each give access to two levels of horizontal module manifolds, with movable stepladder platforms used to reach the upper manifolds. The top walkway is located 20 inches above the top surface of the detector and is 7 ft wide, so that it extends out over the detector. The top walkway gives access to the rolling access platforms and also supports electronics power-supply racks and cooling-water chillers.

Two rolling access platforms, like the one shown in Figure 17.108, are supported by three rails attached to the concrete ceiling, like light-weight overhead crane bridges. Each platform gives access to the full width of the detector. The platforms are designed for both scintillator filling and to provide access for electronics outfitting. Each platform is suspended 14 inches above the top surface of the detector, 6-inches below the top walkway level, and can carry three workers.

Stairs provide safety egress from the building and allow personnel movement between walkways at three locations: behind the south bookend and both sides of the detector hall at the north (loading dock) end of the building. Heavy equipment can be moved from the loading dock area through the shop to the personnel elevator/materials hoist on the west side as described in Section 17.9.

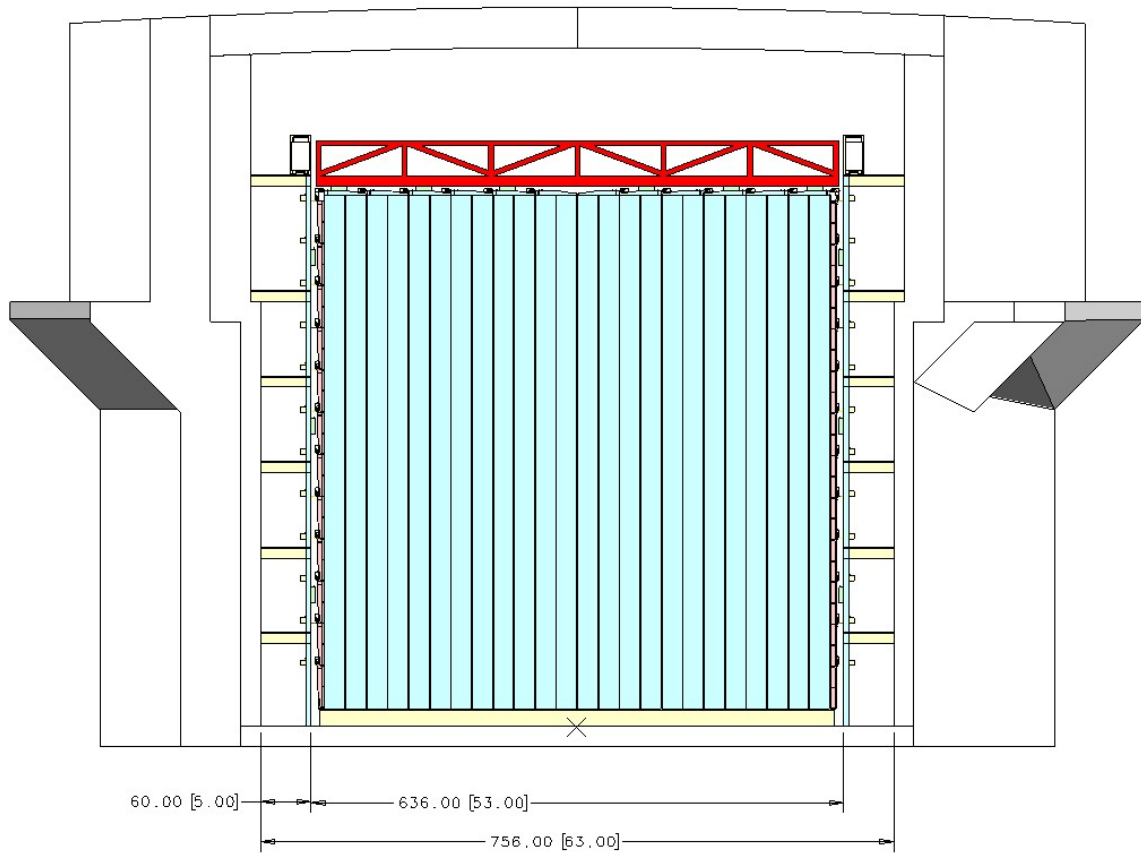


Fig. 17.107: Elevation view of the NOvA far detector, showing the six detector-access walkways on each side.

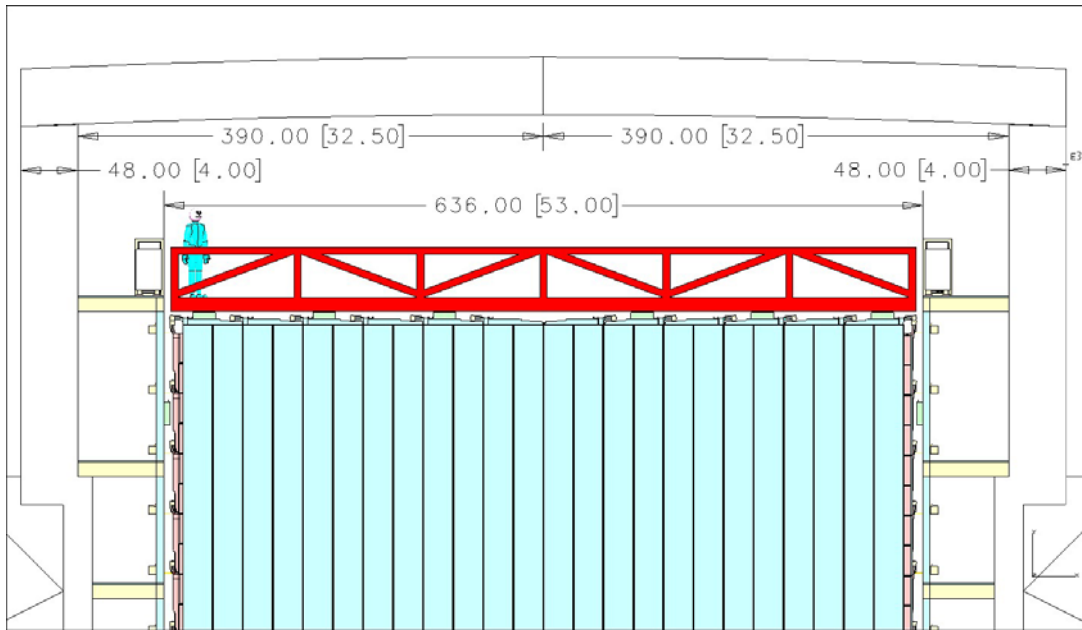


Fig. 17.108: Elevation view of the NOvA far detector, showing one of two rolling access platforms that are used for filling vertical modules with liquid scintillator and outfitting them with electronics.

### ***17.7.6 Detector Control Room***

The detector control room is located on the west side of the detector hall near the elevator and the north end of the detector, as shown in Figures 17.109 and 17.110. The elevation of this facility is at the same (1245' 6") level as the upper level walkway on the west side of the detector. The labyrinth, at the (1226' 10") level of the loading dock, provides access from the outside of the building to the control-computer room facility. Cable trays connect the computer room to the top walkways and to the top and sides of the detector where the front-end electronics are located.

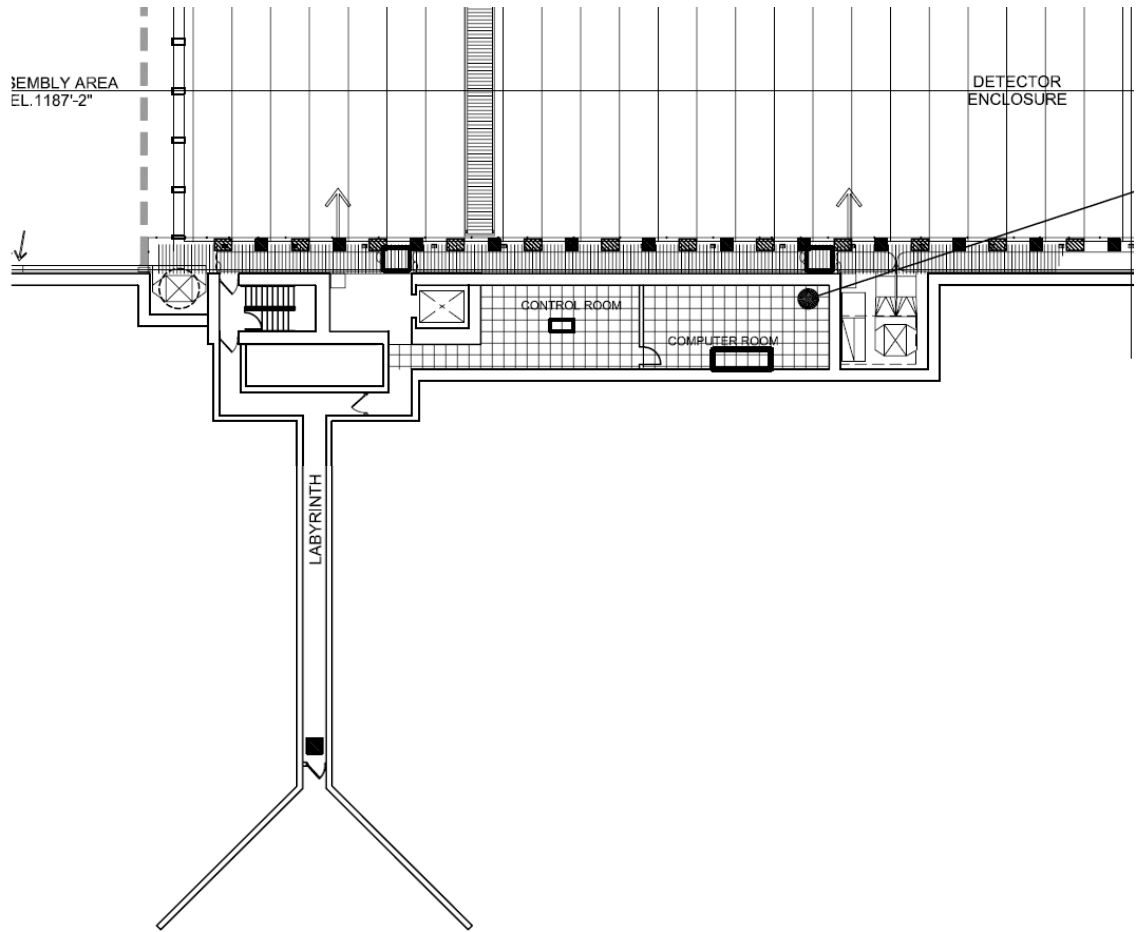


Figure 17.109: Plan view of the control room and computer room.

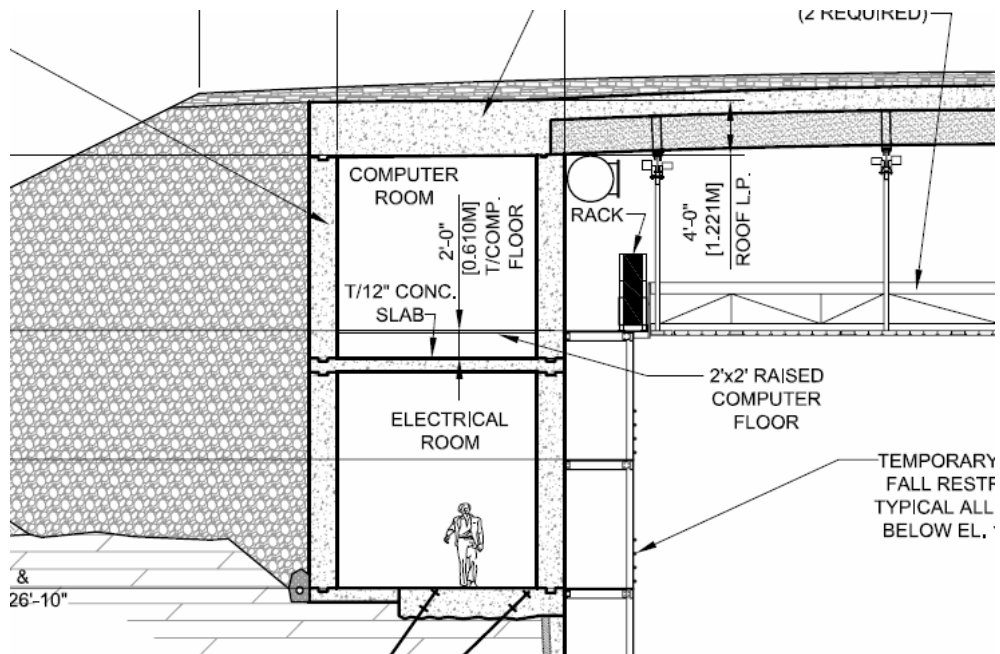


Figure 17.110: Side view of the control room and computer room.

## **17.8 Liquid Scintillator Distribution and Supply System**

### ***17.8.1 Scintillator Distribution System***

The scintillator distribution system is designed to accept scintillator from delivery tankers at a rate of roughly one tanker per day at the far site, and to deliver this oil to the modules being filled in a safe and reliable manner. The sustained flow rates of roughly 24 gpm required to fill the detector at the same rate that blocks are lifted into position imposes a number of requirements on the distribution system, which we describe below. During the period of full-rate installation, blocks are installed at the rate of one every 2.6 weeks. Filling will occur during one 40-hour shift per week about 85% of the time. The scintillator delivery system includes components that ensure that the scintillator is delivered to the module at a precisely controlled temperature and flow rate. Thermal control is necessary to minimize post-filling changes to the scintillator volume as it comes to the ambient hall temperature.

The delivery system is designed to eliminate all possible hazards associated with static generation and charge accumulation resulting from the flow of a non-conductive fluid. As described in NOVA-doc-1118, an anti-static agent (Stadis 425) is added to the scintillator at a concentration that reduces the discharge time, and therefore, the steady state fluid charge, by orders of magnitude. The distribution system itself uses conductive plumbing fixtures at all points, bonded and discharged to ground. Finally, a vapor return system is included in the scope of the scintillator distribution system. During filling, this system returns the displaced gas volume to the tanker being discharged. During normal operation, this system maintains nominal pressure in the trapped gas volume in the detector modules as the scintillator volume changes due to temperature changes in the detector hall. For the horizontal modules, the vent system includes a 4 liter overflow tank that provides a 2 liter reservoir of scintillator at nominal hall temperature, allowing the full active volume to be maintained over decreases in hall temperature of as much as 5° F. In addition, the overflow tank provides a take-up volume sufficient to accommodate increases in hall temperature of as much as 5° F.

This section presents a detailed description of the scintillator distribution and filling system, starting from the tanker and working towards the module filling hardware, and ending with a description of the vent system design.

### ***17.8.2 Distribution Control System***

Figure 17.111 shows a schematic representation of the scintillator distribution control system. It includes connections to the delivery tanker, pump, filter, thermal control system, as well as temperature, flow rate, and pressure monitoring. Figure 17.112 shows the connections between the distribution system and the scintillator delivery tanker yard. The scintillator in each tanker will be tested for light output, attenuation length and conductivity before the transfer line is attached to the tanker. The scintillator control system then ensures that the scintillator is filtered, temperature corrected, and at the correct pressure and flow rate for delivery to the detector.

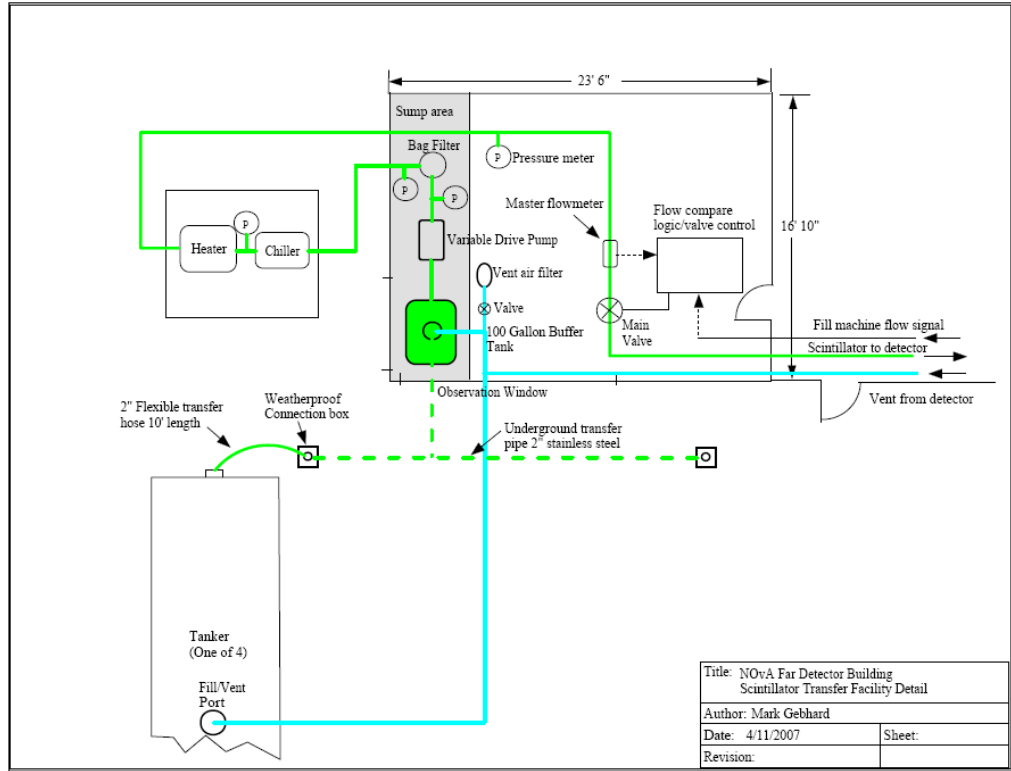


Figure 17.111: Scintillator distribution control system.

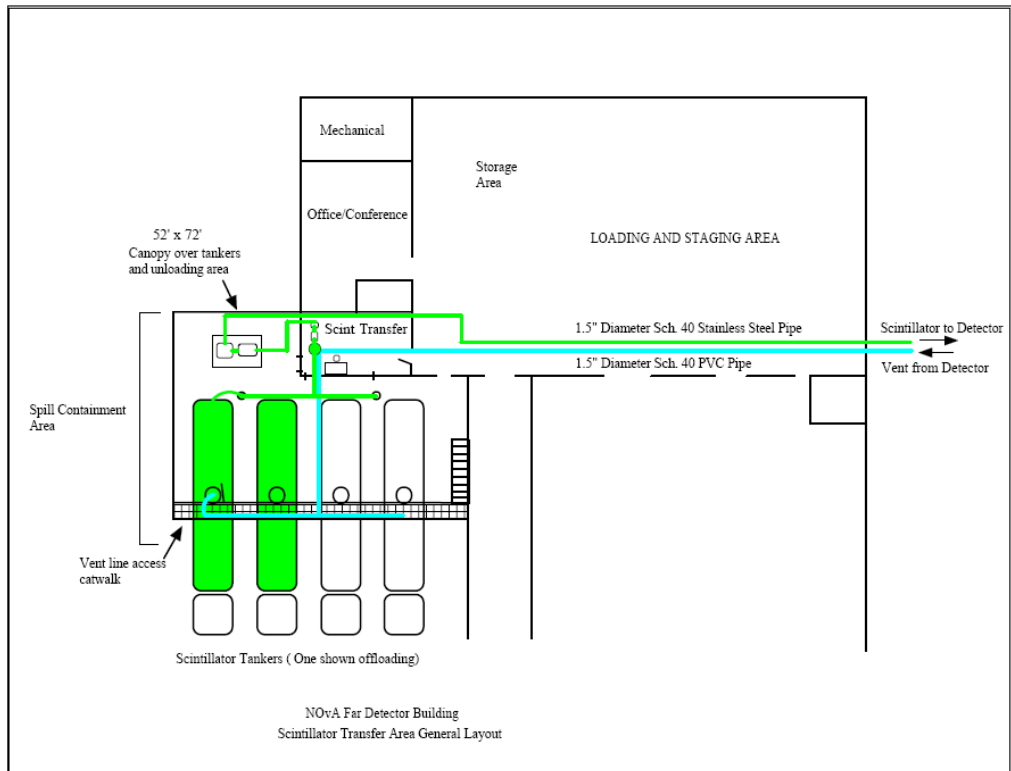


Figure 17.112: Scintillator transfer area layout.

The tanker location is elevated to a height that permits gravity feed of the scintillator out of the tanker, through a flexible 2-inch transfer hose and pipe leading to a 100 gallon buffer tank. This buffer tank is equipped with level sensors that close valves at the module fill stations when the delivery tanker is fully drained, and before air is allowed into the distribution plumbing. The tank is equipped with a valved vent line to allow venting of trapped air back into the tanker.

The distribution system pump is designed to provide 24 gpm of oil through a system flow impedance that includes the effects of the filter, heater, chiller, valves, piping, and hoses to the module manifolds. A variable frequency drive is used to control the motor speed driving the centrifugal pump. This drive is controlled by the fill machine operator, who soft starts the fill system and brings the pump up to the speed required to deliver 2.3 gpm to the eight manifolds being filled.

Following the pump, the scintillator makes one pass through a 10 micron filter, which is a standard size for oil filtration. A trade size 8 holder and bag are appropriate for the nominal flow rate of 24 gpm, assuming that the scintillator is relatively free of particulate matter. The pressure drop across the filter is measured and used to determine when replacement of the filter bag is necessary.

The tankers are preheated prior to shipment to ensure that they arrive at the far site at a known temperature. The thermal control system described below is designed to accommodate scintillator at the tanker that is within a  $\pm 10^{\circ}\text{C}$  range about room temperature, and to deliver oil to the detector within  $1^{\circ}\text{C}$  of ambient hall temperature. The  $\pm 10^{\circ}\text{C}$  temperature range of scintillator in the tanker is maintained by setting the temperature at the point of origin to compensate for the expected environment during transit. Under extreme conditions in which this input temperature range is exceeded, the scintillator flow rate (and consequently, detector fill rate), will be adjusted to compensate, allowing the distribution system thermal system to bring the scintillator to ambient hall temperature at the module.

From the filter, the scintillator passes to the heater, where the temperature of the scintillator is corrected as needed. The heater is designed to provide control to  $\pm 1^{\circ}\text{C}$  of the output temperature at 24 gpm. The heater is followed by a chiller which again is designed to provide thermal control to  $\pm 1^{\circ}\text{C}$ . A flow meter following the chiller serves as a master supply reference. If the supply flow in this meter does not equal the supply total flow of the 8 meters in the fill machine running at the extrusions, the flow master control in the fill machine will issue a halt command to the pump and terminate all filling to the 8 output lines. This avoids spills due to a catastrophic failure of the plumbing between the scintillator transfer facility and the fill machine.

### ***17.8.3 Distribution Plumbing***

Figure 17.113 shows a schematic for the distribution system plumbing. Liquid scintillator enters the detector hall plumbing filtered and temperature corrected and at a known pressure and flow rate. The scintillator is then delivered to the fill site through a combination of fixed and flexible stainless steel pipe (Figure 17.113). The mainline pipes for the distribution system in the detector hall are 1.5-inch diameter stainless steel. O-ring unions are used on all serviceable equipment to ease removal and replacement when required. Valves are used to isolate sections of the system for service and to ensure leak free hookups at the hydraulic quick disconnects in the system.

The top of the detector is serviced through a pipe located on the west wall of the detector hall at the sixth catwalk level, with ports at six locations along the length of the detector, each having a valve and quick disconnect. A 30-ft long, 1-inch diameter flexible, conductive delivery hose is used to couple a quick-disconnect at this level to the rolling access platform, which provides access to the top of the detector. A 1-inch stainless steel pipe runs along the platform, with quick disconnects every 8 ft. A fill machine is located on this bridge at all times and connected to one of six outlet ports with a conductive flexible hose.

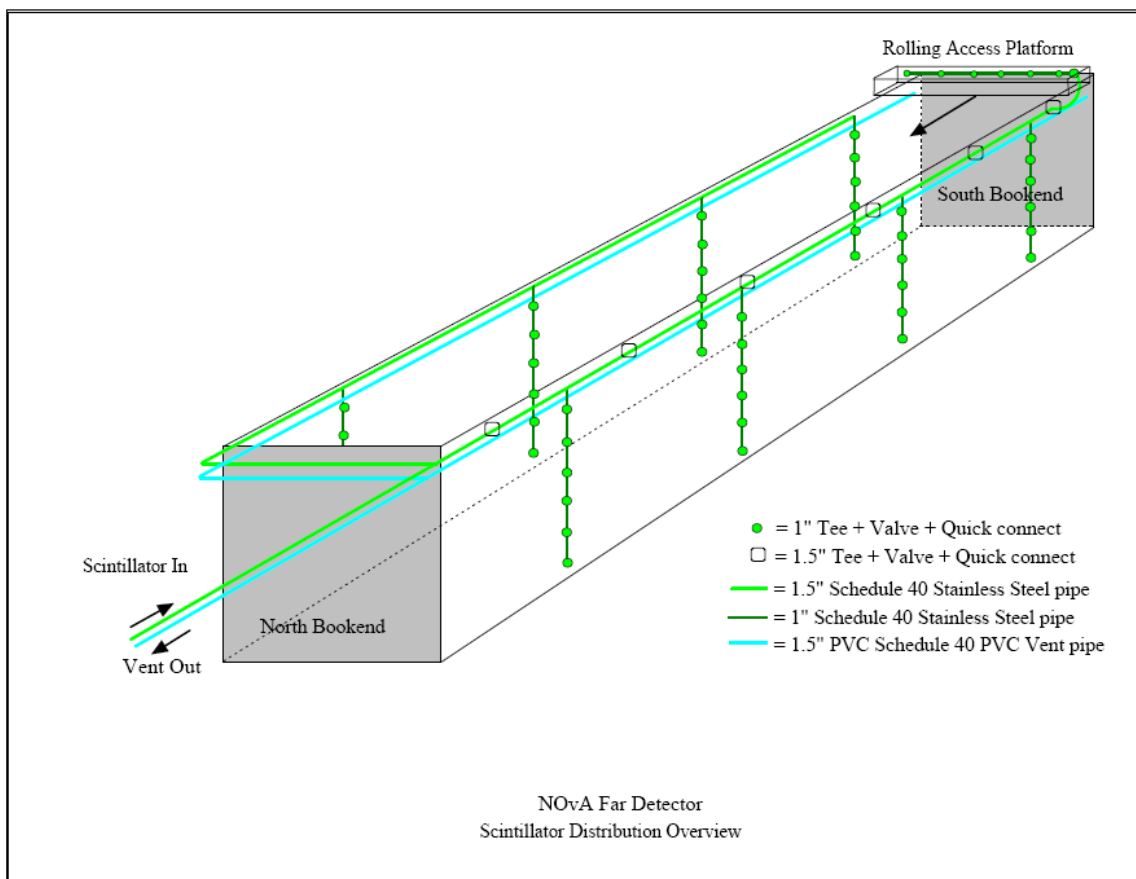


Figure 17.113: Scintillator distribution system plumbing.

The sides of the detector are serviced by four down going fixed pipe runs on each side. Each down-going pipe consists of a 1-inch diameter stainless steel pipe teed off from the 1.5-inch diameter mainline (on the sixth catwalk level) and running to the ground floor level, with a quick disconnect installed at each catwalk level. A 1-inch diameter conductive flexible hose connects the wall mounted quick disconnect to an extension pipe, which in turn connects to a fill machine through a length of 1-inch diameter flexible conductive hose.

#### 17.8.4 Scintillator Filling Machines

The fill machines, one for each side and one for the top, are the final components of the delivery system. Figure 17.114 shows a schematic diagram of one fill machine. Each is mounted on a two-wheel hand truck, and consists of nine positive displacement oval gear GPI flow meters that control solenoid valves and provide a display of the total scintillator delivered to each extrusion. The ninth flow meter measures the total flow into the machine.

The NOvA extrusions must be filled to  $\pm 1$  liter without visible feedback on a volume of 1,031 liters (horizontal) and 1,116 liters (vertical). The initial fill will be terminated well before the extrusion is completely filled, and the scintillator and extrusion allowed to come to thermal equilibrium. The final top-off of the extrusions is controlled by ultrasonic level sensors mounted on the exterior of the extrusion or horizontal expansion tanks. The final fill level will be accurate to  $\pm 1$  cm. When the proper level is reached and detected, a signal will be issued to close a solenoid valve on the output line and terminate fill. The fill machine output lines are 4-ft flexible conductive 0.5-inch diameter hose ending in a custom fill nozzle, shown in Figure 17.115. The

nozzle design is described in more detail in NOVA-doc-1525. While filling, precautions are taken to terminate a fill if a nozzle should detach or begin to leak. Spill trays, also shown in Figure 17.115, are located directly under all active fill ports, and are equipped with optical liquid level detectors that terminate flow in response to the detector of standing oil in the tray.

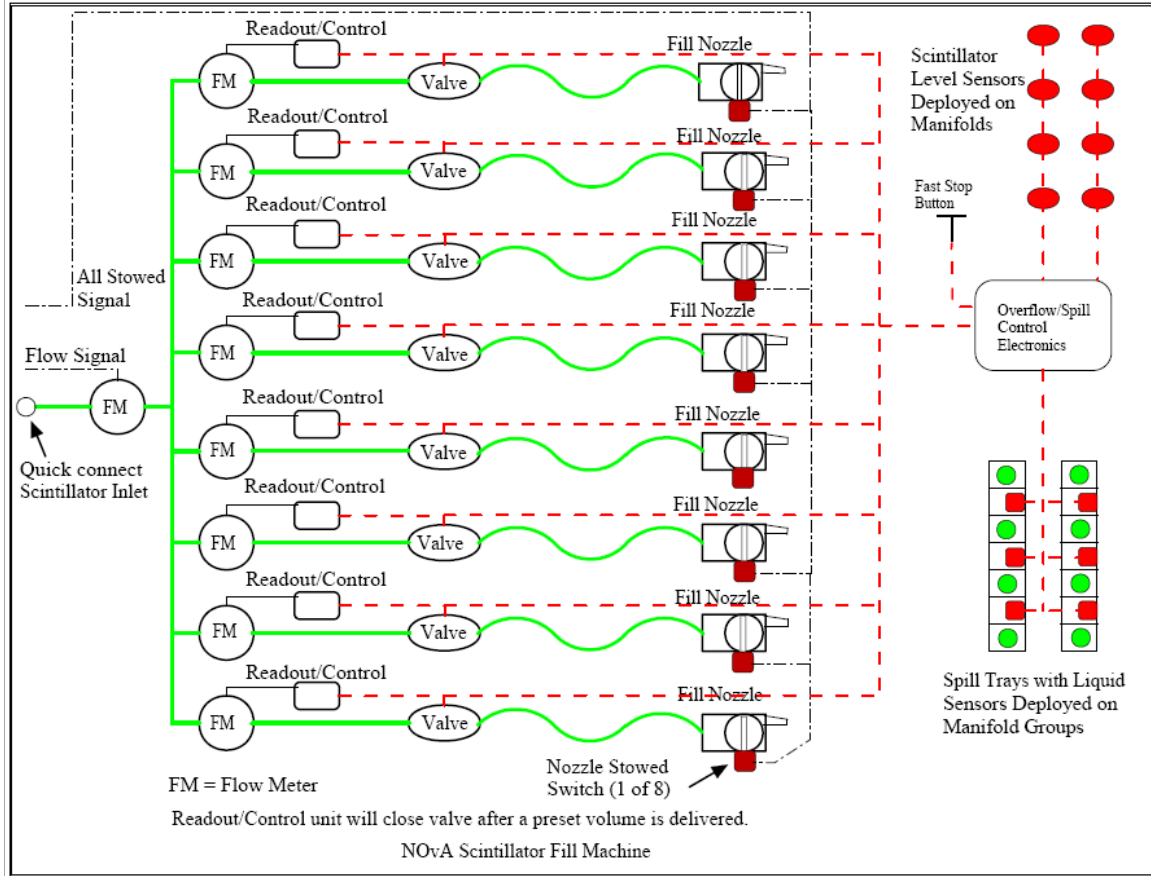


Figure 17.114: Schematic drawing of the fill machine.

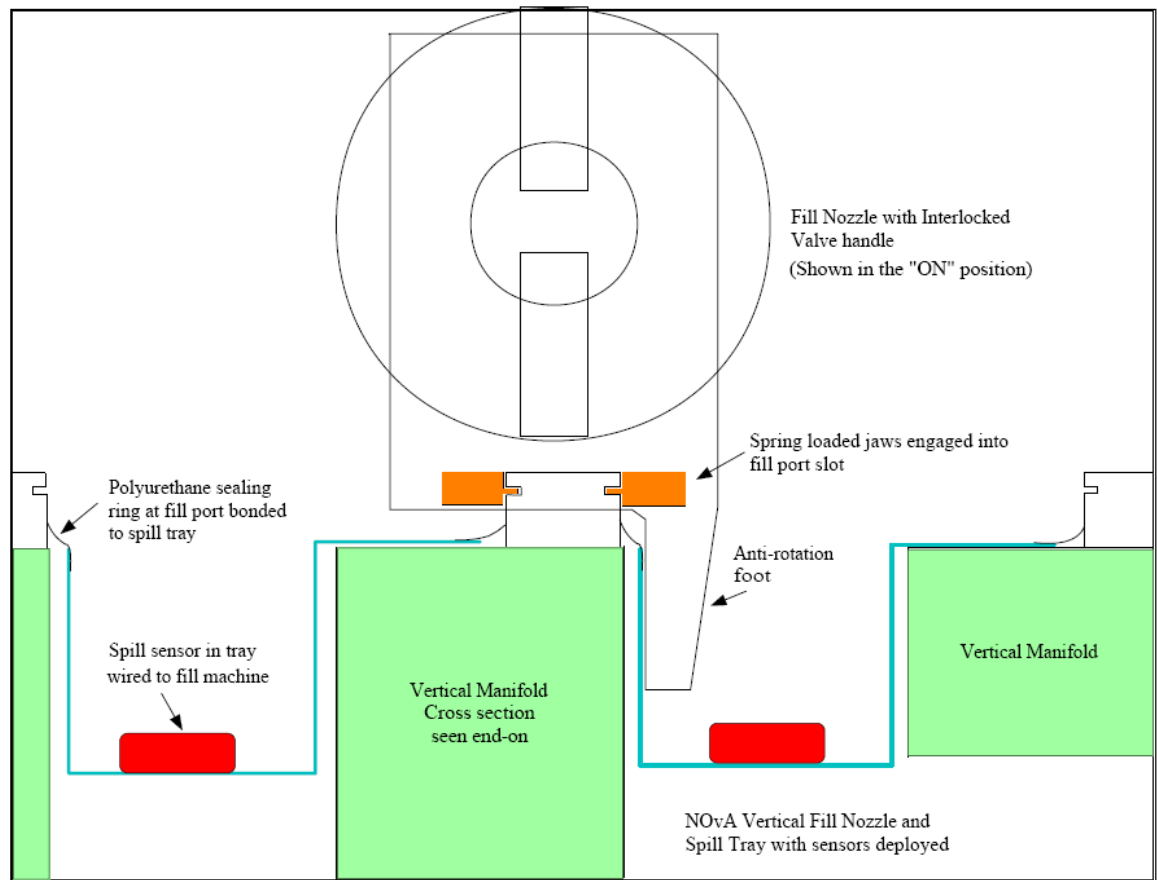


Figure 17.115: Schematic drawing of the fill nozzle and spill tray.

### 17.8.5 Vapor Recovery System

During filling, a large volume of scintillator-laden vapor is displaced from the extrusions, which must be vented from the hall and filtered before exhausting to the local environment. To accomplish this, a vapor transfer system is installed on the detector and plumbed out of the hall and to the off-loading delivery tanker. The vapor transfer lines consist of a black PVC tubing plenum servicing one plane. Connections to the plenum from tubing running from the module vent port are made by black nylon barbs with steel compression bands sealing each joint. Figure 17.116 shows the vent line layout for horizontal planes, where connections are made to both the manifold and expansion tank. Each plenum terminates at a manifold of 1.5-inch diameter black schedule-80 PVC pipe running along the length of each module, which in turn is connected to fixed pipe runs to the scintillator transfer room. During filling, the displaced vapor is returned to the unloading tanker. During normal operation, the vapor is exhausted to the air through a charcoal filter.

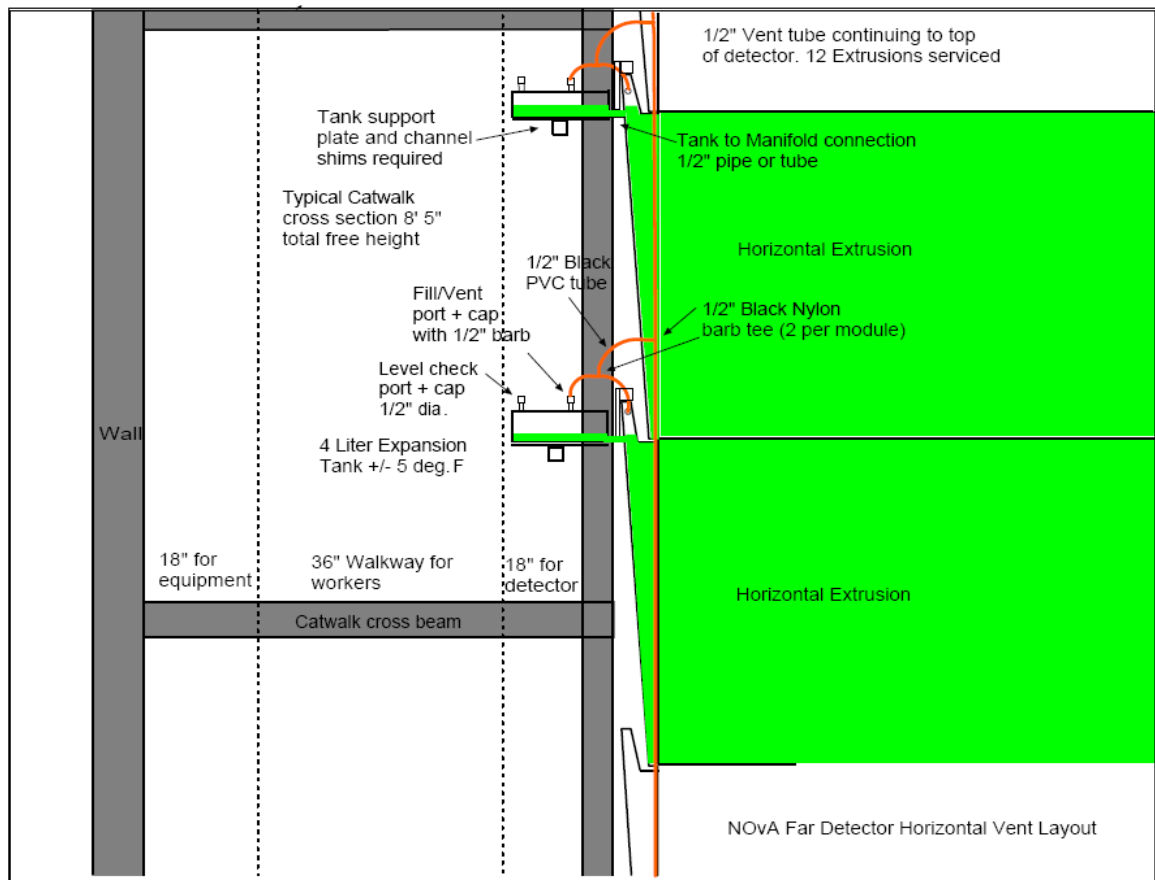


Fig. 17.116: Horizontal module vent layout.

### 17.8.6 Scintillator Distribution System Installation

The scintillator distribution and supply system is installed in three major pieces. This work is performed during the ~10 months between beneficial occupancy and the time when the first block is ready to be filled. All non-block installation work is expected to take approximately 4-6 FTE months to complete for the scintillator technicians. Figure 17.112 shows the scintillator transfer facility, which is located in a room next to the truck canopy where tankers deliver the premixed scintillator. This system is installed and tested by scintillator experts with help from the scintillator technicians so that they become familiar with the equipment. Installation may begin any time after beneficial occupancy of the building.

Installation of the rigid stainless steel distribution pipe begins immediately after beneficial occupancy of the far detector enclosure, as filler work for the scintillator technicians. This piping connects from the scintillator transfer facility to the distribution points needed around the detector. The 2-inch stainless steel mainline is located on the top walkway and is installed by the scintillator technicians and tested by the scintillator experts. There are three permanent 1-inch stainless steel pipes on each side of the detector that feed the lower catwalk levels, as described in Section 17.8.3. The rolling access platform is also installed with a rigid stainless steel pipe to feed the top of the detector. All pipes are fitted with shutoff valves and quick disconnects as needed. The exact location of these pipes in relationship to the building infrastructure has not yet been determined but they would be somewhere on the outside detector hall walls.

The third part of the system is the vapor recovery. Two schedule-40 1.5-inch black PCV pipes run down both sides of the detector hall back to the scintillator transfer facility. These mainline vapor pipes have fittings to connect to each of the completed blocks. These mainline

pipes should be located just under the top walkway to eliminate tripping hazards on the walkways. The smaller flexible schedule-80 PVC pipes that connect each module and the 0.75-inch plane manifold are installed during the block outfitting stage of construction by the module technicians while each block is still in the horizontal position.

## 17.9 Far Detector Assembly Equipment

During the 10-week setup period, which begins immediately after beneficial occupancy of the far detector building, the first members of the assembly crew begin the setup of equipment needed to assemble and install detector blocks. The assembly crew increases from 5 to 12 workers during this period. The setup work schedule includes time for the training of new crew members as they are hired, and for management safety reviews of equipment and procedures. The equipment is shipped to the site both from commercial suppliers and from NOvA institutions where it has been fabricated and tested prior to shipment. In the latter case, engineers and technicians who designed and built the equipment will travel to the far detector site to supervise and assist the assembly crew, and to provide training in operating it. The setup period is followed by a 15-week startup period, when the equipment is used to build and install the first three detector blocks while the installation crew ramps up to its full size of 29 workers. The following sections give detailed descriptions of the major items of equipment. Figures 17.117, 17.118 and 17.119 show the layouts of the loading dock and assembly areas at the north end of the detector hall, where most of this equipment is installed.

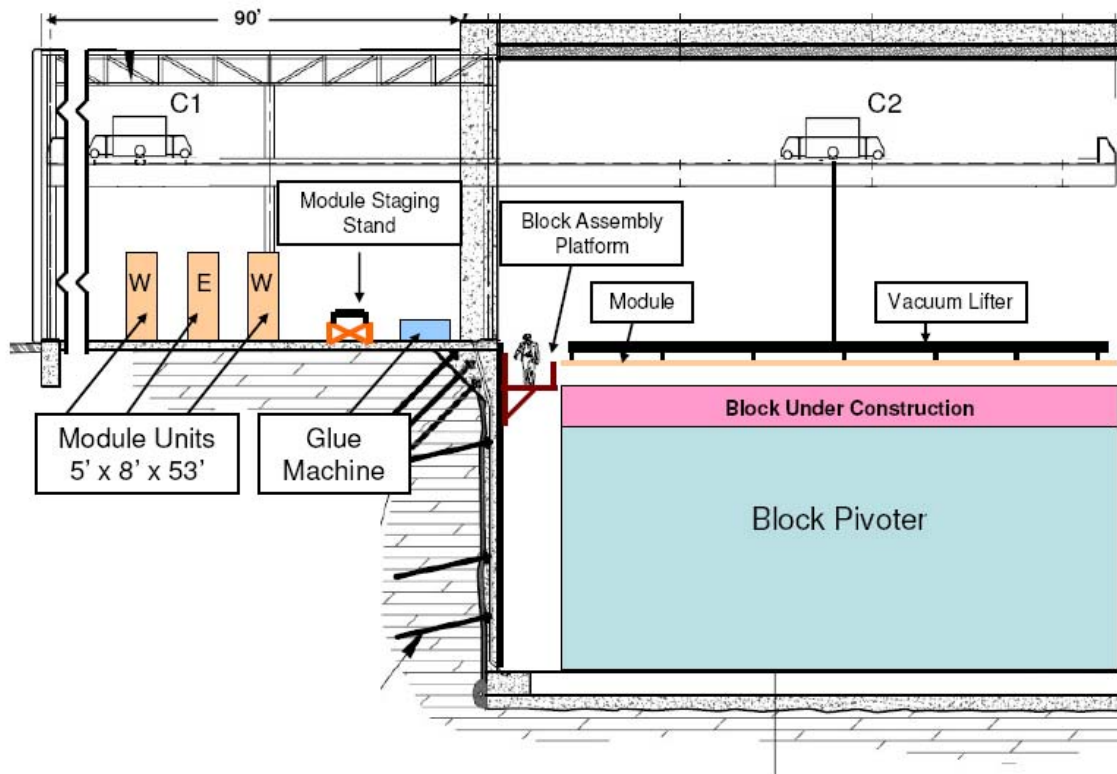


Fig. 17.117: Side view of the loading dock and assembly areas. The drawing shows a module being placed into the block under construction by the 25-ton bridge crane (C2). The 10-ton bridge crane (C1) is picking up a module that is ready for the adhesive dispenser. The elevation of the work surface of the block pivoter is ~9 feet below the loading dock. Access to all elevations below the loading dock level is provided by the block assembly platforms, which move vertically on rails mounted to the walls. Only the south block-assembly platform is shown in this view; the east and west platforms are not shown.

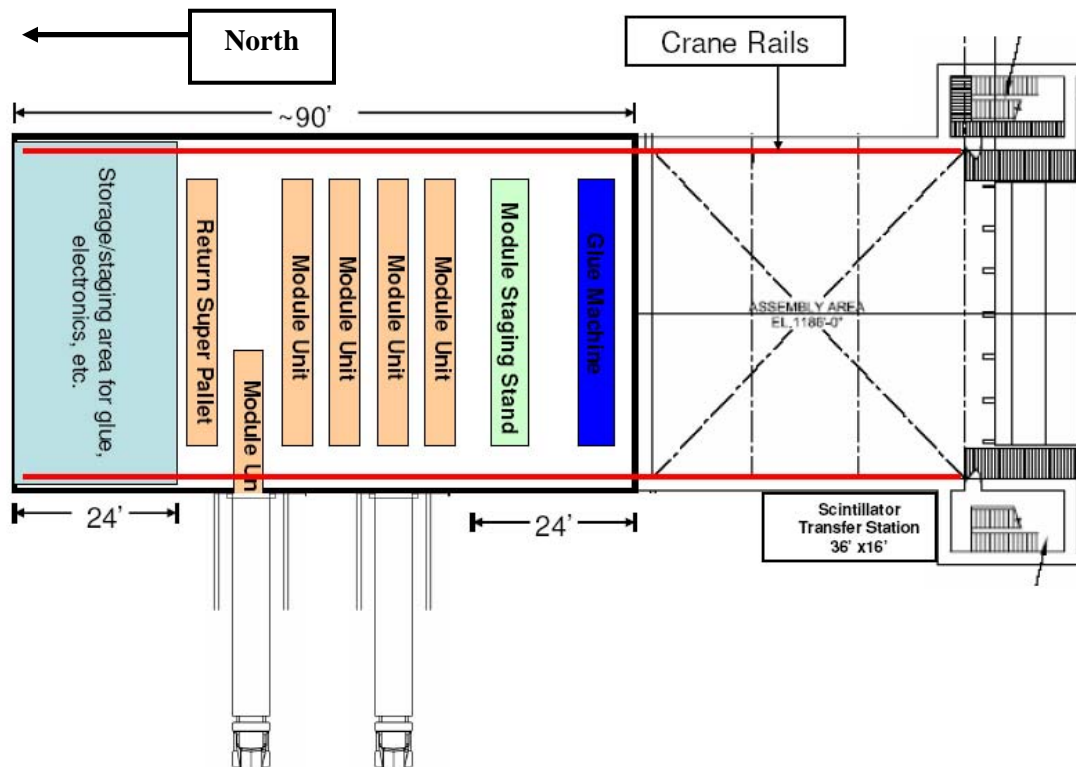


Fig. 17.118: Plan view of the loading dock area. Four module units are shown in the loading dock area and one (lower right) is being moved from an arriving delivery truck. Module units are prepared for testing after they have come to thermal equilibrium. A module unit weighs about 14 tons, including the custom pallet system, and is moved with a motorized pallet jack (NOVA-doc-1030 and 1038). The area at the left is used for temporary storage of pallets of glue, electronics and other items. It is shown in detail in Figure 17.119.

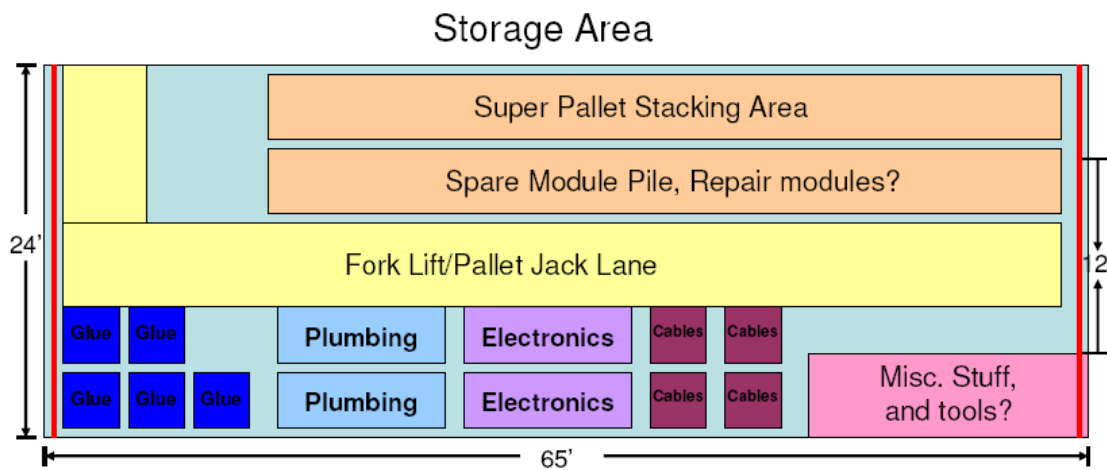


Fig. 17.119: Typical usage of the loading dock storage area for detector installation materials.

The list below gives an overview of the far detector assembly equipment. Most of this will be installed during the setup period.

- **Primary bridge crane**  
A 25-ton overhead bridge crane runs over the assembly area (block pivoter) and the loading dock. It is used to place modules onto the block pivoter and lower equipment to the main floor. It is operated by a remote control unit and also provides electrical power for the module vacuum lifter suspended from its hook. This crane is purchased by WBS 2.1 and installed before the setup period begins.
- **Secondary bridge crane**  
A 10-ton crane bridge runs on the same rails as the 10-ton bridge and is used to move single modules to the adhesive dispenser. It is operated by a remote control unit and provides electrical power for the module vacuum lifter suspended from its hook. This crane is purchased by WBS 2.1 and installed before the setup period begins.
- **Vacuum lifting fixture (NOVA-doc-1112)**  
The vacuum lifter (described in Section 17.10) is a 52-ft long vacuum spreader bar for moving single modules. It attaches to a module with long rectangular suction cups that line up with the flat cell surfaces of the extrusions.
- **Adhesive dispenser (NOVA-doc-1357)**  
The adhesive dispenser (described in Section 17.11) is located in the loading dock area adjacent to the block pivoter. A module is placed on the adhesive dispenser by the 10-ton bridge crane with a vacuum lifting fixture. The module remains stationary as the glue head with 16 nozzles lays beads of Devcon 60 adhesive along the top of each cell. The adhesive dispenser incorporates a module flipping device to orient each module glue-side-down before it is picked up by the 25-ton bridge crane and moved to the block pivoter.
- **Module staging stand**  
This device is a platform located near the adhesive dispenser in the loading dock area. It allows the vacuum lifter to be moved from one crane to the other, while giving easy access to the crane hook and power feed.
- **Block pivoter (NOVA-doc-989)**  
The block pivoter (described in Section 17.12) is at the center of block assembly and installation. Its top surface is the block assembly table and it rotates completed blocks (Far Detector Parameter Sheet NOVA-doc-2066) from the horizontal to the vertical. It provides alignment fixtures for modules within a block, and ensures that blocks are plumb, level and square. NOVA-doc-1396 describes module and block survey and alignment requirements.
- **Block pivoter work platforms (NOVA-doc-1946)**  
These commercial platforms provide access to the east, west and north sides of the block assembly surface of the pivoter. The platform elevation is adjustable to accommodate the changing elevation of the work surface as new planes are installed.
- **Scintillator handling equipment (NOVA-doc-1118)**  
The tanker truck hardstand and canopy, with room for four tankers and the liquid transfer conduit to the detector, is constructed by WBS 2.1. As described in Section 17.8, WBS 2.9 is responsible for installing the grounded metal supply pipes, the supply system plumbing, the vapor return system and the three filling machines. WBS 2.2 provides the scintillator test equipment used by the WBS 2.9 assembly crew.
- **Module unit mover (NOVA-doc-1030 and 1038)**  
Module units are stacks of 24 modules that are prepared and shipped from module factories to the detector site. A module unit is pulled out of the delivery truck on a set of

long narrow air casters by a motorized pallet jack. The air casters are narrow enough to be placed on each side of the module pallets while still in the truck.

- **Module test equipment (NOVA-doc-1031)**  
WBS 2.5, 2.6 and 2.7 provide equipment used for quality assurance testing of arriving modules and electronics. These tasks also provide experts to train the assembly crew in the routine use of the equipment.

## 17.10 Module Vacuum Lifter

Figure 17.120 shows the vacuum lifting fixture (NOVA-doc-1320), which is a 52-ft long vacuum spreader bar for moving single modules. It has six cross bars, evenly spaced along its length, each with four rectangular vacuum cups that easily aligned with the flat surfaces of a module's extrusion cells. The vacuum lifter is carried by an overhead crane that provides electrical power to operate the vacuum pump. It is a commercial lifting fixture that has been slightly modified for attaching to the NOvA modules. The simple modifications involve a change in the suction cups, lengthening of the main spreader beam, and the addition of guides to help locate the suction cups. These changes were incorporated into an existing fixture that was used in the MINOS experiment. Subsequent tests with prototype modules have verified the feasibility of this design. Figure 17.120 shows the full span of the lifting fixture with the vacuum pump and lifting point located in the center of the spreader beam and six cross supports containing the suction cups. The vacuum pump is operated by 120 VAC and is valve connected in a failsafe manner such that, in the event of electrical power loss, the vacuum is maintained long enough to allow a module to be lowered safely to the ground.

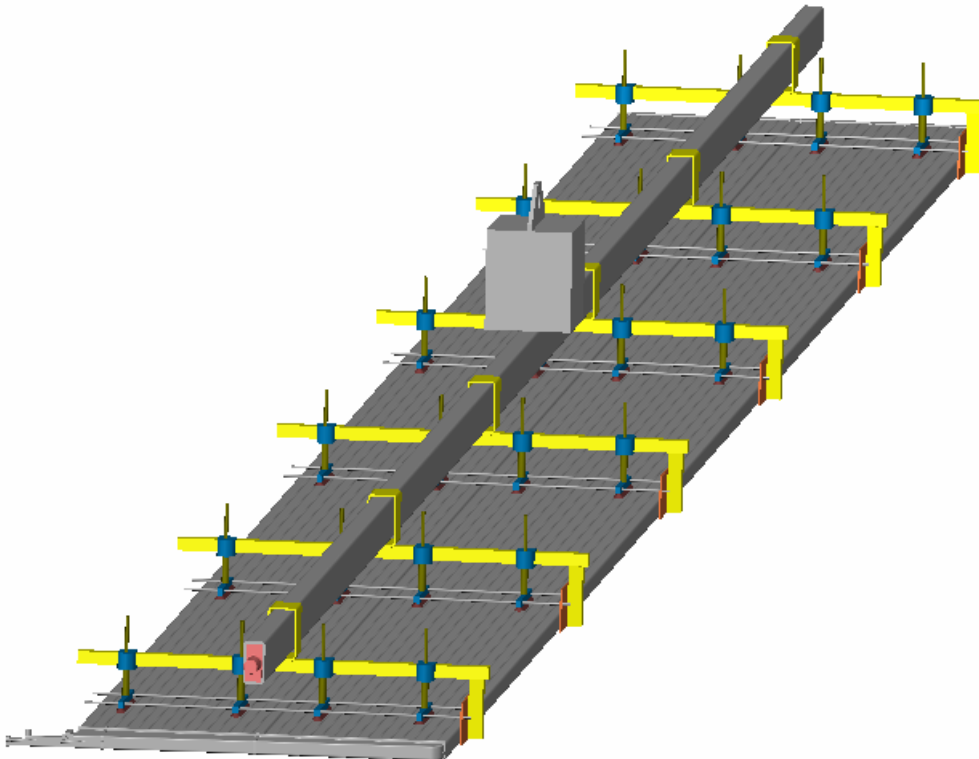


Fig. 17.120: Lifting fixture with module attached.

Figure 17.121 shows some important features in greater detail. Because of the scalloped surface of the extrusion, narrow rectangular suction cups are needed to provide a reasonable area for the

lift points without crossing into the troughs between extrusion cells. To ensure that the suction cups are located properly with respect to the troughs, a guide is built into the cross piece to properly locate the suction cups upon making contact with the side of the extrusion. (This guide piece has an additional structural function that is described in Section 17.11.) The suction cups are prevented from rotating into the troughs by connecting rods that pass through the suction cup mounts and are connected to the side guide. Finally shown in Figure 17.121 is a pivot shaft that projects out of the spreader beam near the center of gravity of the combined lifting fixture and module. This feature is also used by the adhesive dispenser, as described in Section 17.11.

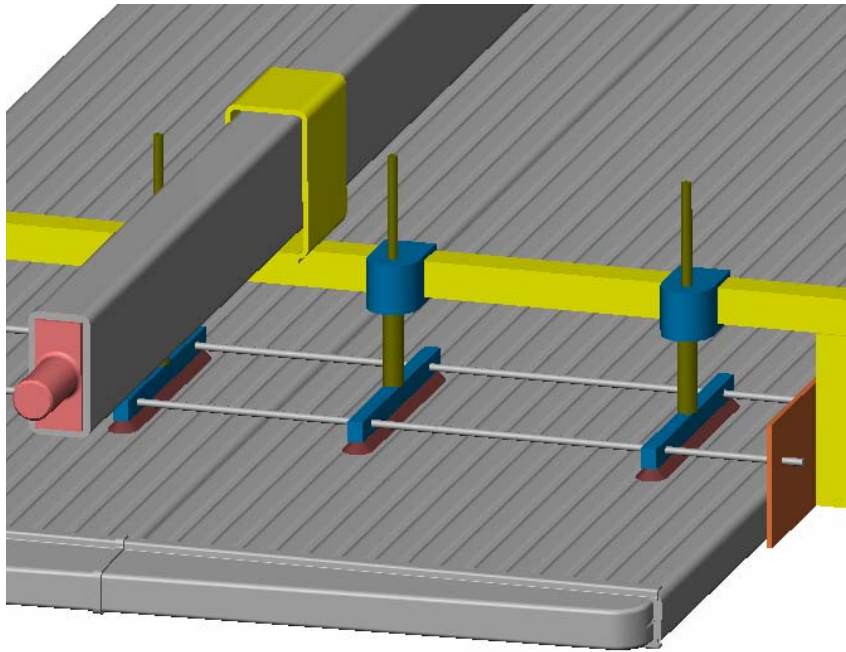


Figure 17.121: Close-up view of the lifting fixture suction cups and alignment guide.

## 17.11 The Adhesive Dispenser

Module adhesive dispenser (NOVA-doc-2067) applies the adhesive to one surface of each extrusion module before it is installed in a block. The module is supported by the vacuum lifting fixture, allowing direct movement from the adhesive dispenser to the block pivoter. Figure 17.122 shows the glue table and its sequence of operations, starting with an extrusion attached to the fixture being lowered onto the adhesive dispenser by the 10-ton bridge crane (not shown). The fixture is lowered until the two support pivot shafts (one on each side of main spreader beam, as described in Section 17.10) are set into the compliant bearing supports on the adhesive dispenser table. A drive mechanism is then connected to the pivot shaft and the fixture is rotated 180° to expose the unobstructed bottom surface of the module. As the fixture is rotated, the suction cups are still active and additional side support is provided by alignment guides described in Section 17.10. After this rotation is complete and the module is secured, the glue carriage (formerly parked out of the way at the base end of the table) travels across the table. The carriage contains the glue dispenser for the two part adhesive as well as two 55 gallon drums containing the adhesive components. The carriage includes 16 dispensing nozzles mounted to a bearing rail and a lead screw assembly that allows the nozzle position to traverse the module width. With 16 nozzles, the carriage makes two trips along the length of the module and returns to the park position upon completion. The module is then rotated by 180° so that the lifting hook is on top.

The glued module is ready to be rigged to the block pivoter with adhesive applied to its bottom surface.

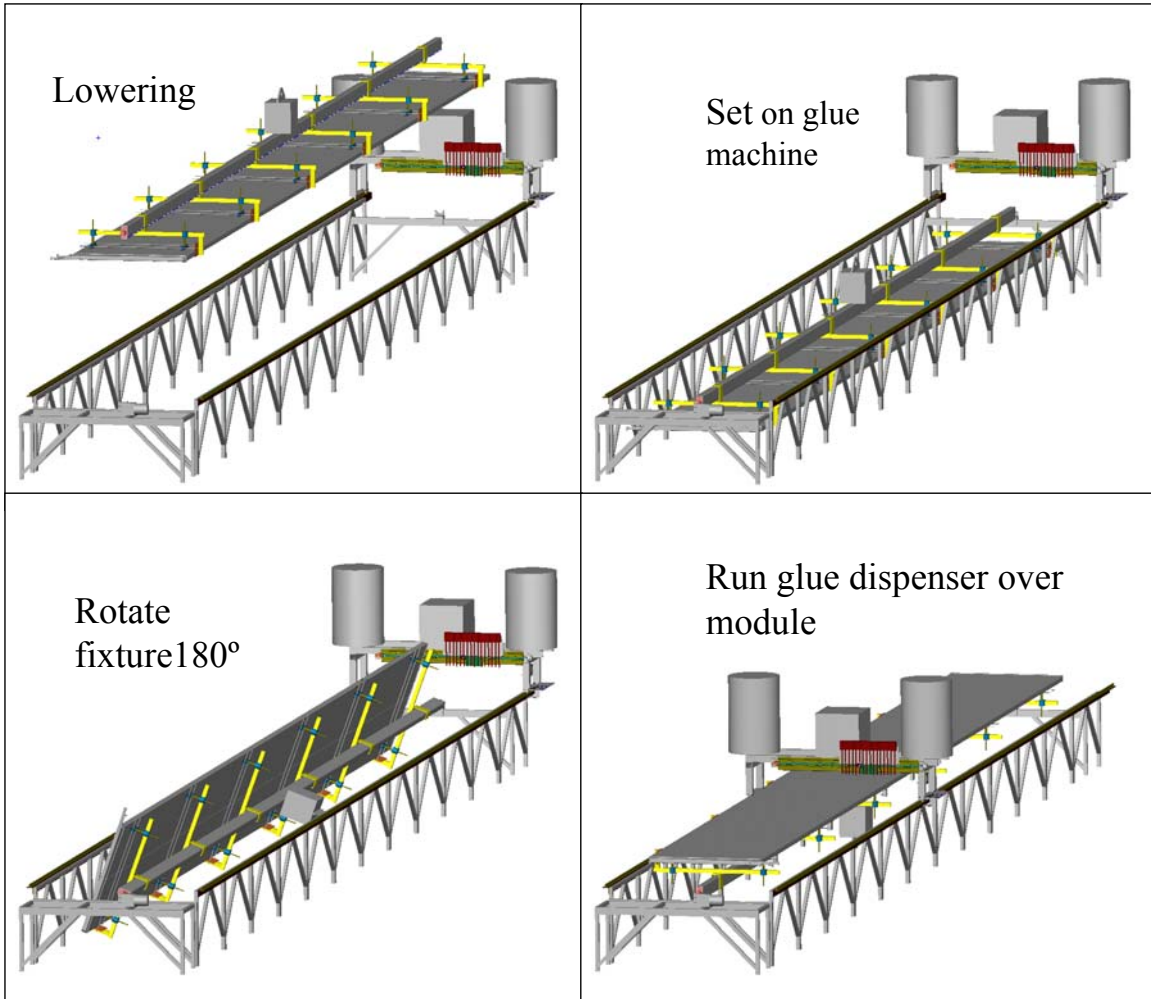


Fig. 17.122: Adhesive dispenser sequence of operations.

Figure 17.123 shows the adhesive dispenser in more detail. The carriage travels the length of the module supported by bearing rails that are mounted to the glue table. It is driven by servo motors using a rack and pinion system. The carriage and dispenser are specified to dispense adhesive and travel at 0.5 m/s. The adhesive dispenser uses a PLC for supervisory control of the carriage motion, dispenser actuation, fixture rotation, and safety monitoring. The operator is responsible for engaging the rotation mechanism and for initiating the various automatic sequences. Depending on the stiffness of the lifting fixture, intermediate supports for the modules may be needed to reduce module deflection while on the fixture. There are several possible methods for quickly attaching the rotation device to the fixture but further analysis is needed to select the optimal mechanism. The pivot points of the fixture are located very near the center of gravity of the combined module/lifting fixture. The thick-walled vertical modules weigh 36% more than the horizontals, resulting in locations for the centers of gravity that are 0.75 inch apart.

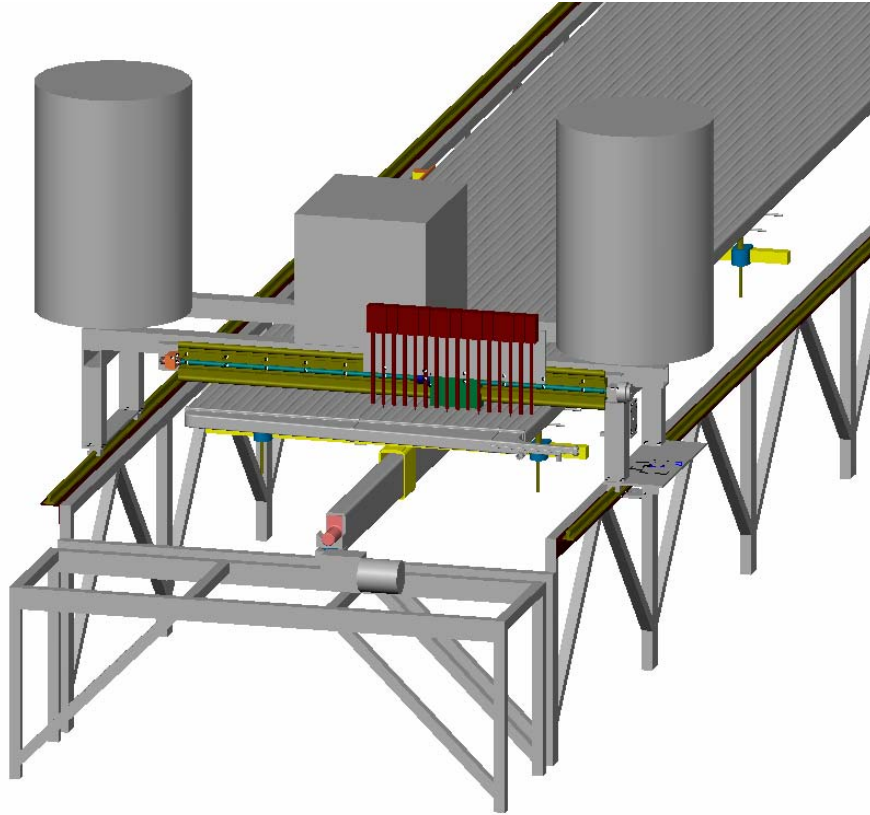


Fig. 17.123: Close-up view of adhesive dispenser and rotating support point.

## 17.12 Block Pivoter

The block pivoter (NOVA-doc-989) performs several functions during the installation process. First, the pivoter provides a flat surface for block assembly, including alignment fixtures and tooling to ensure that each block meets dimensional requirements. Second, it moves each completed block from the assembly area to the detector face. Third, the pivoter rotates the assembled block from the horizontal to a near vertical orientation and moves it approximately 9 meters to place it in the correct location in the detector. Finally, the pivoter rotates the block the last few degrees into a vertical orientation and then lowers the block and pallet approximately 2 to 3 centimeters onto the floor.

When the detector installation is complete, the block pivoter is permanently installed against the last block to serve as the north bookend.

The requirements for the block pivoter are described in NOVA-doc-113.

### 17.12.1 Block Pivoter – General Configuration

In Figure 17.124, the block is shown in violet, the block pivoter table is in blue and the structure that supports the pivoter table is shown in orange and purple. The pink structural steel shown above the drive wheels is provided to limit the table deflection when the table is in the horizontal position.

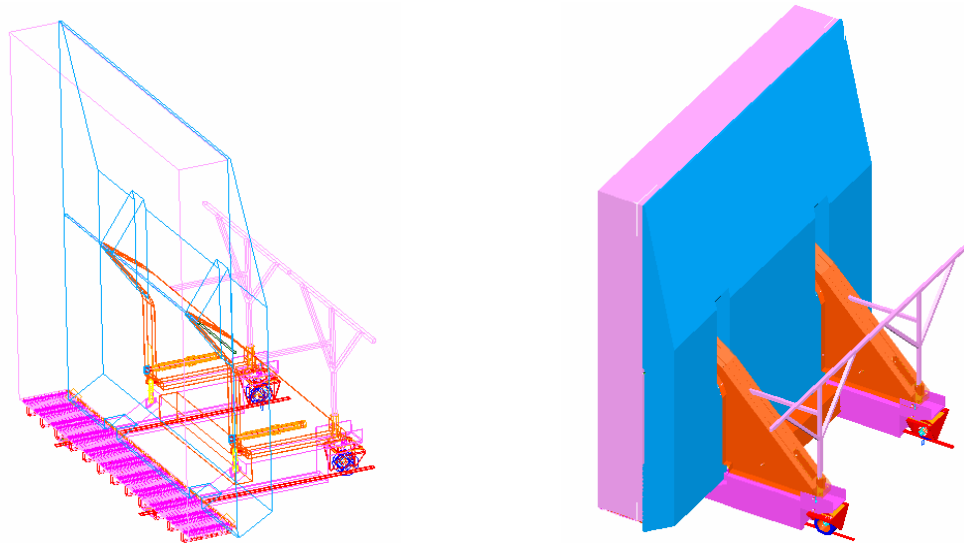


Fig. 17.124: Two isometric views of the block pivoter table shown in the vertical position.

### 17.12.2 Block Pivoter – Detector Assembly Table

Figure 17.125 shows the detector assembly table as a solid object for the simplicity of rendering the images. However, the detector assembly table will be fabricated from steel plate to provide a flat, relatively rigid surface for assembling the detector on, and at a minimum expense. Figure 17.126 shows an image of the block pivot table as viewed from below to show the plate structure. The upper surface and each of the webs are made from 0.25-inch thick carbon steel plate. A structural grade material, ASTM A36 low alloy carbon steel, is suitable for this application because the deflections dominate the design criteria and not the overall strength. Higher strength steels will have the same deflection as A36, but will cost more to procure. The lower cord of the weldment is 0.75-inch thick, 12 inch wide A36 bar stock. The open structure allows access to the bottom of the top surface and the webs for welding.

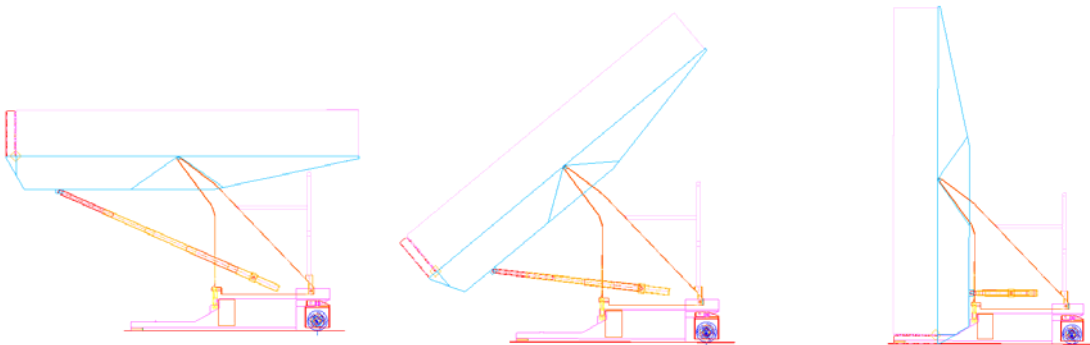


Fig. 17.125: Three side views of the block pivoter showing the block in the horizontal, intermediate, and vertical positions.

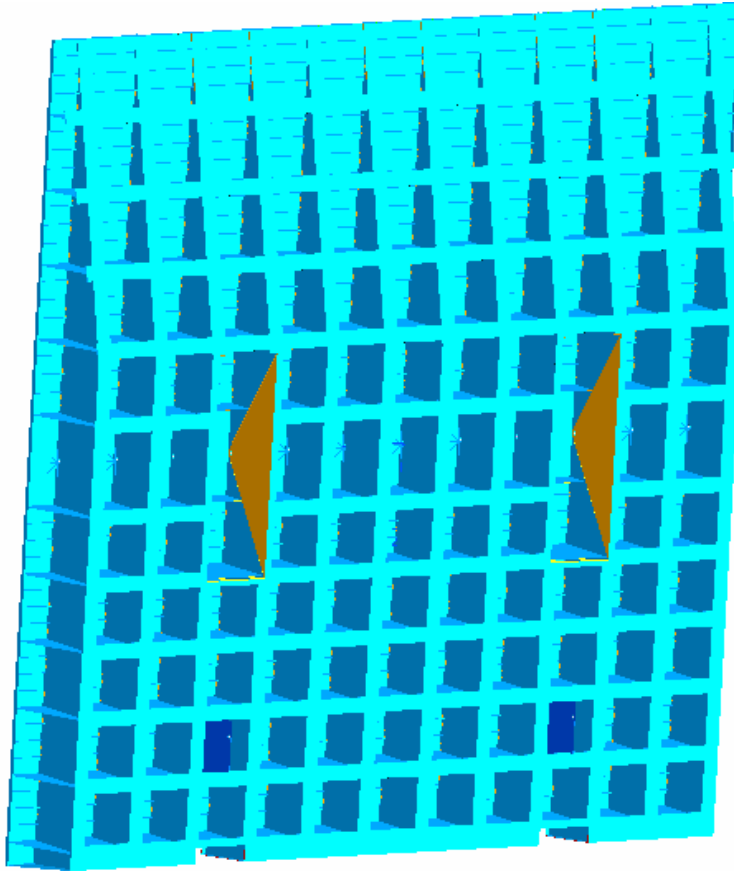


Fig. 17.126: View of the block pivoter table bottom surface when table is near vertical, showing the weldment structure.

In Figure 17.126, the two rectangular areas shown with the orange triangles are the locations where the arms of the upper vertical side supports fit into the table to allow the pivot location to be near to the top (when table is horizontal) surface. The two small cut-outs near the bottom edge are provided to allow clearance for the lower table support arms that allow rolling elements to be positioned under the assembled block for stability.

The top surface of the assembly table, when the table is horizontal, is 620 inches wide. When the table is vertical, it is 640 inches tall. Clearly, this exceeds the normal shipping dimensions, so the table will be made from 12 sections. Figure 17.127 depicts the table in an exploded view to show these sections. Two sections will be joined in the shop into an assembly approximately 104 inches wide, 60 inches tall, and 53.3 feet long. Weight of each two section assembly will be less than 20,000 pounds. Six truck loads will be required to transport the table sections to the far detector site.

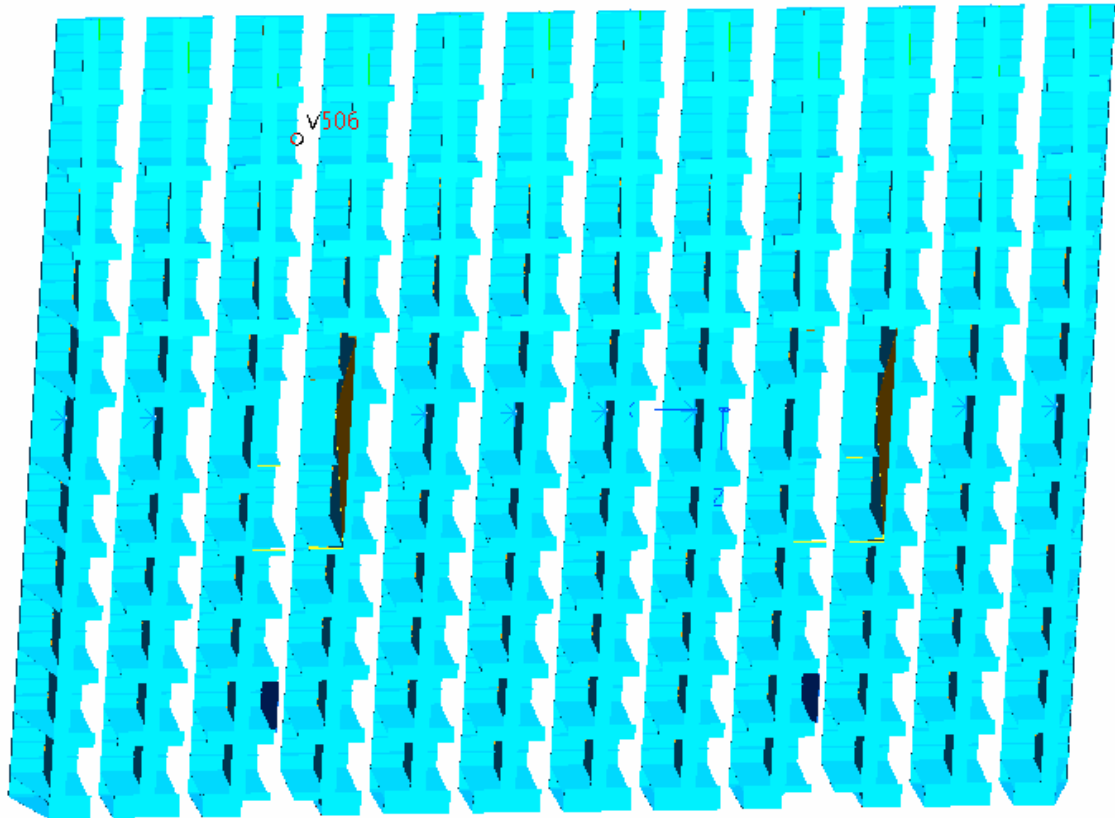


Fig. 17.127: Exploded view of the block pivoter table, showing the individual weldments.

Each of the weldment sections shown in Figure 17.127 is shop fabricated using the same techniques used to fabricate bridge girders used in highway overpass construction. This is a mature technology using standard welding practices and common low alloy carbon steel. The cost estimate for this table includes line item costs for the welding fixtures needed to achieve the required flatness of each weldment. FEA modeling of one weldment has been performed and the deflections are shown in Figure 17.128. This analysis was performed using symmetric boundary conditions and a uniform pressure applied to the top surface of the detector of 0.82 psi. This pressure is the pressure that would be uniformly applied to the top surface of the table by the fully assemble detector block assuming that the PVC block has no stiffness. As such, this is a very conservative loading condition and over predicts the deflection and stresses on the table.

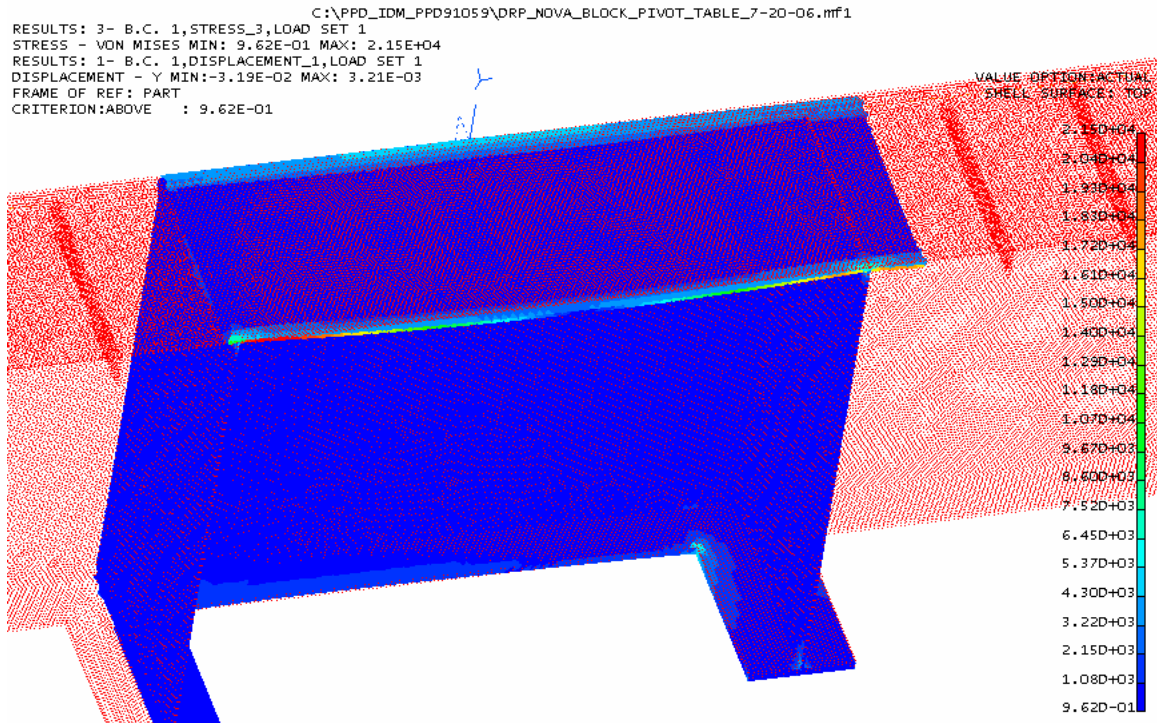


Fig. 17.128: FEA deflection results for loading on one weldment of the block pivoter table.

### 17.12.3 Block Pivoter – Pivoting Hydraulics

Figures 17.125 and 17.129 show the hydraulic cylinders used to push the pivoter table into the horizontal position. These cylinders retract to allow the table to pivot into the vertical position. Figure 17.129 shows that the pivot bearing is positioned very close to the top (when horizontal) of the assembly table.

There are several important considerations in the overall layout of the block pivoter:

- To provide a moving structure that is inherently stable and not prone to tipping.
- To place the pivot location as close as is possible to the center of gravity of the assembled block and table to reduce the loading during rotation.
- To shop fabricate the block pivoter components, preassemble and test the pivoter, partially disassemble the device and ship the components to the far detector location using commercial trucking. All components are designed to break down into parts that are easily shipped and are within the lifting capacity of the crane at the far detector.

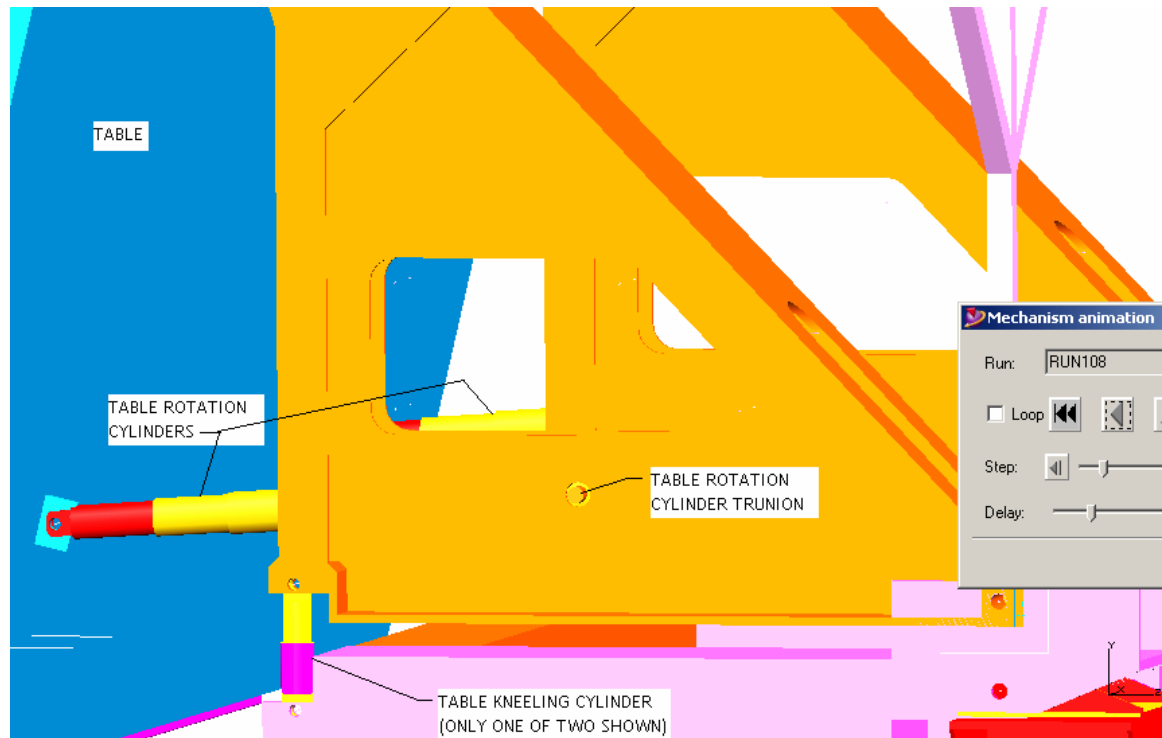


Fig. 17.129: Detail of the block pivoter showing the table approaching vertical, highlighting the table rotation cylinders and one table kneeling cylinder.

Stability of the block pivoter structure is maximized in several ways. First, the structural support (shown in purple in the Figures 17.124 and 17.125) is extended forward to the front side of the block (when the block is vertical) to maximize the wheel base and therefore the stability. Second, the maximum velocity of the pivoter is limited so that even if the loaded table were to stop immediately while moving at maximum velocity, the pivoter would not tip.

Two multistage, double acting, hydraulic cylinders control the rotation of the block pivoter table. These cylinders are commercially produced by several manufactures and are available in strokes and capacities in excess of those needed for this application. The compressive load is shown as a function of cylinder extension in Figure 17.130.

When the block is fully assembled on the table and the table is horizontal, the cylinders exert a combined axial force of 25 tons. As hydraulic fluid is allowed to exit the cylinders and the table rotates, the axial force peaks at about 31 tons (15.5 tons per cylinder), returning to a combined value of 25 tons when the table is fully vertical. This is shown as the purple line at the top of Figure 17.130.

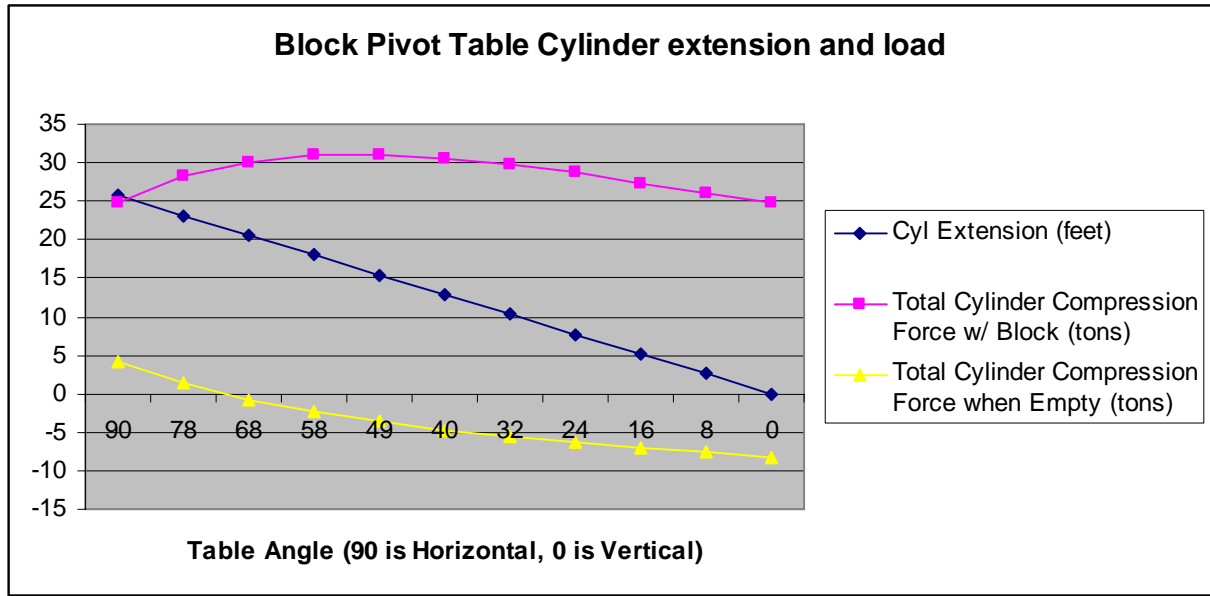


Fig. 17.130: Hydraulic cylinder extension (feet) and compressive load (tons) for the pivoter design using two cylinders and a pivot location near the block center of gravity.

As the block is lowered onto the concrete detector hall floor, the load on the hydraulic cylinders changes sign to become a tensile load. When the table is vertical and unloaded, the combined axial load on the cylinders is 8.3 tons in tension. This is why double acting cylinders are necessary. As fluid is pumped into the cylinders to allow the table to rotate to the horizontal position, the load steadily increases until reaching a maximum value of about 5 tons compression. As each module is positioned during block assembly, the load on the pivoter table rotation cylinders increases until it reaches 25 tons with the block fully assembled.

Figure 17.129 shows a detail of block pivoter table hydraulics with the key components labeled. The table is shown in the near vertical orientation and both of the table rotation cylinders can be seen, although the second cylinder is partially obscured by the orange table support structure. Also visible is one of the two kneeling cylinders that lowers the entire table and block as the block is set down on the detector hall floor.

When the block is rotated to the vertical position, its weight is supported by the block base pallet, which is cantilevered from the block pivoter table surface. The pallet is shown in Figure 17.131. Each block has its own dedicated pallet that remains with the block until detector decommissioning. The gaps below the pallet surface provide space for the pivoter's front support legs (Figure 17.124). They also serve as witness spaces so that any scintillator leaks from the modules can be observed and perhaps located. Irregularities in the detector hall floor are accommodated by setting each pallet in place on a grout bed and leveling it before attaching it to the pivoter and beginning block assembly.

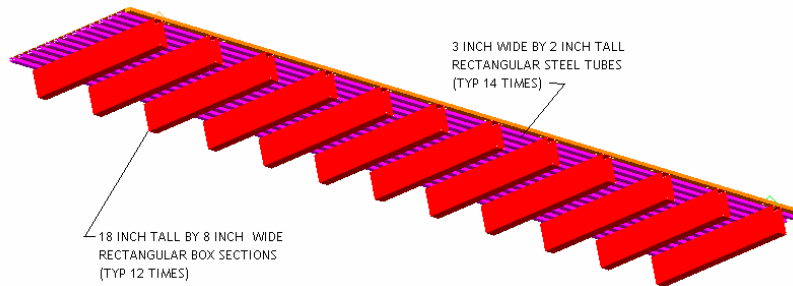


Fig. 17.131: Bottom view of a pallet with twelve 18-inch deep by 8-inch wide box beam cantilever members and fourteen 3-inch by 2-inch transverse stringers.

#### 17.12.4 Block Pivoter – Propulsion Drive

Figure 17.132 shows the mechanism used to move the pivoter along the hall from the assembly area to the detector face. Hydraulic motors driving a planetary gear drive, directly attached to a solid urethane wheel, provide the traction effort to move the loaded block pivoter down the length of the detector hall. These commercially produced drive units are similar to those used on large earth moving equipment. The chief advantage of these units is that they can propel very heavy loads at steady but slow speeds. The disadvantage of these units is that the lead time to procure them is on the order of twelve months. Spare parts are available off the shelf because of the demands of the construction industry. Two units are used, one driving each side of the pivoter.

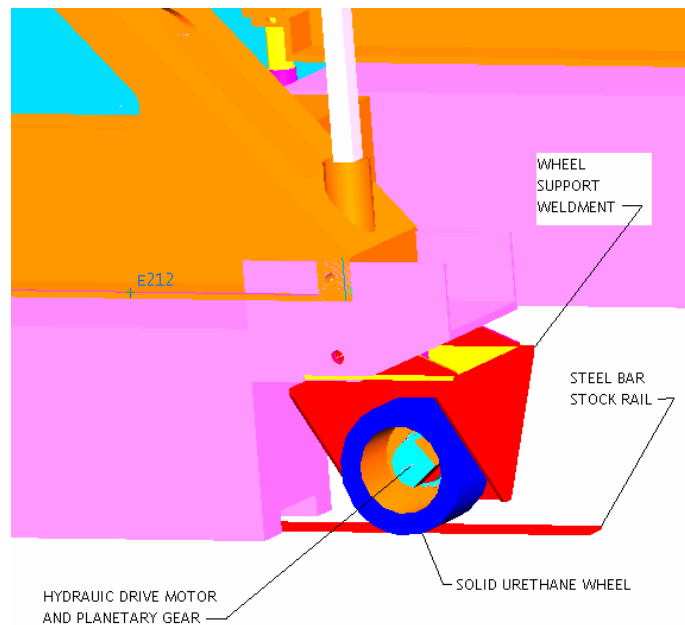


Fig: 17.132: Detail of block pivoter drive wheel mounting and hydraulic drive motor.

The pivoter moves on Hilman rollers for the non-driven rolling elements. These rollers include cam followers to allow the pivoter to follow the flat bar-stock rails. Hilman rollers are available in capacities above 300 tons, although 100-ton capacity units are used here. On each

lower side support, one roller is located at the tip of the extension of the lower side support. For stability reasons a second roller is located directly below the kneeling cylinder.

#### ***17.12.5 Block Pivoter – Block Base Pallet***

Each detector block will rest on a detector support pallet (Figure 17.131) when installed in its final location in the detector hall. Prior to stacking the extrusions for each block, the pallet will be located in its final position on the detector hall floor, grouted to accommodate irregularities between the detector hall floor and the steel pallet weldment. Once the grout has cured, the pallet will be lifted off the grout with the block pivot table, the table rotated to the horizontal position, taking the pallet to the vertical position, and moved to the detector assembly area.

Cantilevering the pallet from the block pivoter table introduces a moment into the table, causing a rotation. This rotation over the width of the pallet and the deflection of the pallet (cantilevered beam deflection) have been quantified and shown to induce an acceptable level of stress into the PVC extrusions in a block (NOVA-doc-1953). Figure 17.133 shows the result of a finite element analysis of the combined table and cantilevered pallet. Beam elements were used to model a 72-inch deep table and twelve 18-inch deep pallet members. Since twelve pallet members were used, the load applied to each member was 313,000 / 12 pounds (26,100 pounds). The calculation applies this load at a point in the center of the cantilevered pallet and assumes that the block has no stiffness. This conservative assumption gives an upper limit on the tip deflection.

In Figure 17.133, the dashed purple line represents the deformed shape of the table and cantilevered pallet. The green lines indicate the original shape while the orange line segments indicate the beam elements. (The red dimension lines are artifacts remaining from the geometry creation.) Note that the deflection of the vertical purple line representing the table is nearly indistinguishable from the original geometry.

This result indicates that the block pivoter design, with very deep members for the table and a pallet supported by 18-inch deep tubes, meets the block deflection criteria established to prevent damage to the vertical module end seals during block rotation (NOVA-doc-1860).

The 3 inch by 2 inch box sections between the 18-inch deep members also deflect when loaded by the detector weight. Figure 17.134 shows the deflection for the empty-block case under the assumption that the detector has no stiffness. The deflection is calculated to be 0.028 inches by the FEA and 0.024 inches using hand methods. While this deflection may be acceptable for the empty condition, the estimated maximum weight of a filled block is 1.2 million pounds. This gives a linear loading of 137 pounds per inch. Resulting stresses would be about 13 ksi and deflections would approach 0.1 inch. *This deflection may not be acceptable and may require the box section depth to be increased an inch or two. This analysis remains a work in progress.*

C:\PPD\_IDM\_PPD91059\NOVA\_BOX\_BLOCK\_RAISER.mf1  
DEFORMATION: 1- B.C. 1,DISPLACEMENT\_1,LOAD SET 1  
DISPLACEMENT - MAG MIN: 0.00E+00 MAX: 1.30E-01  
FRAME OF REF: PART

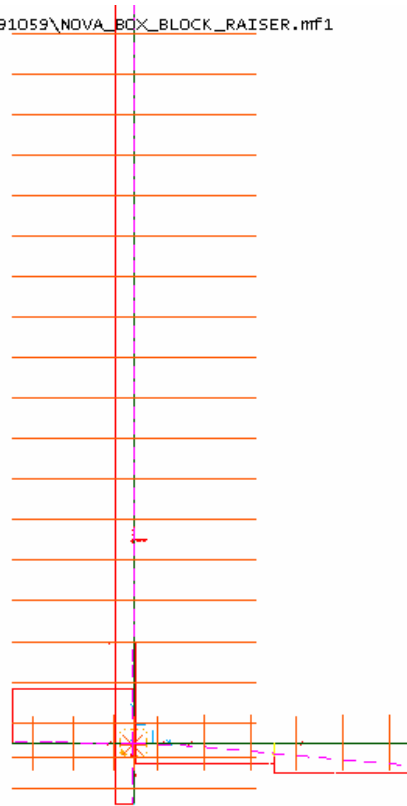


Fig. 17.133: Results of the FEA calculation of the deflection of a plate structure block pivoter table and cantilevered pallet. The deflection at the edge of the pallet is 0.13 inches.

C:\PPD\_IDM\_PPD91059\NOVA\_BOX\_BLOCK\_RAISER.mf1  
DEFORMATION: 1- B.C. 1,DISPLACEMENT\_1,LOAD SET 1  
DISPLACEMENT - MAG MIN: 0.00E+00 MAX: 2.85E-02  
FRAME OF REF: PART

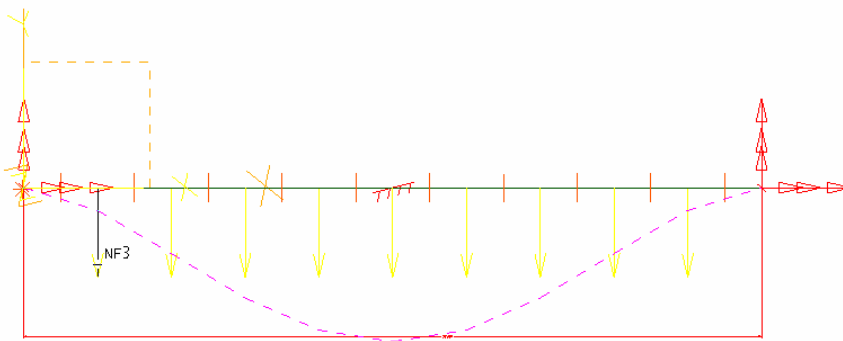


Fig. 17.134: Deflection of the transverse 3 inch by 2 inch stringer between each 18 by 8 box beam on the pallet due to a uniform 36 pounds per linear inch load. The total deflection is 0.028 inches.

### ***17.12.6 Block Pivoter – Upper Table Support Weldment***

The upper structural support (Figure 17.135) has been analyzed using Ideas and the results are shown as a screen-capture image in Figure 17.136. There are two upper side support members which transfer the weight of the table and the assembled block to the lower side support members. A 300,000 pound vertical load was applied to the table pivot bearing and vertical restraints were applied at the kneeling cylinder and rear cylindrical bearing. This 300,000 pound load is a conservative estimate of the combined table (150,000 pounds) and block weight (313,000 pounds) shared between two upper side supports. Stresses in the side support are less than 10,000 psi and the deflection at the bearing is approximately 0.2 inches. This weldment weighs about 32,000 pounds, so it must be moved by the 25-ton bridge crane in the far detector hall. The stresses and the deflections for a conservatively estimated load are acceptable.



Fig. 17.135: Block pivoter upper side support weldment as viewed from the rear quarter.

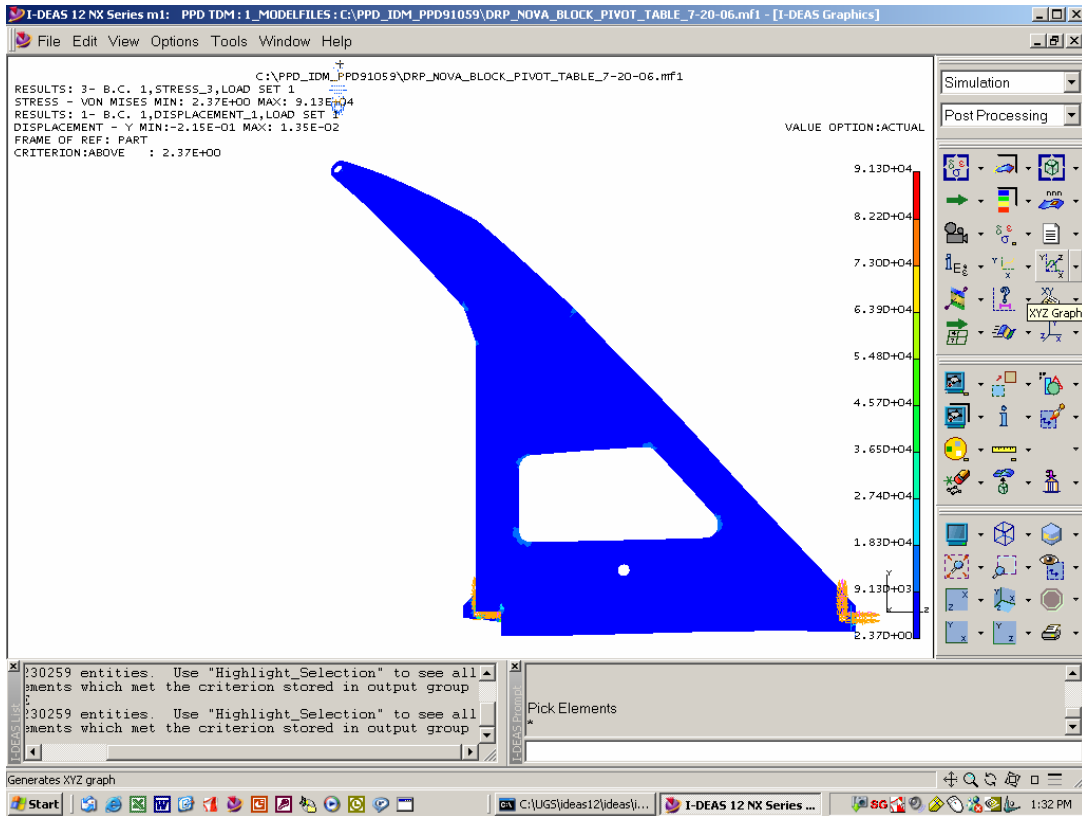


Fig. 17.136: Analysis image of the upper side support stresses and deflection.

### 17.12.7 Block Pivoter – Lower Table Support Weldment

The lower structural support is shown in Figure 17.137. This part transfers load from the upper structural support to the Hilman rollers and the hydraulic drive unit. The narrow portion shown in the lower left corner of Figure 17.134 extends below the table and pallet to ensure the stability of the entire loaded block pivoter.

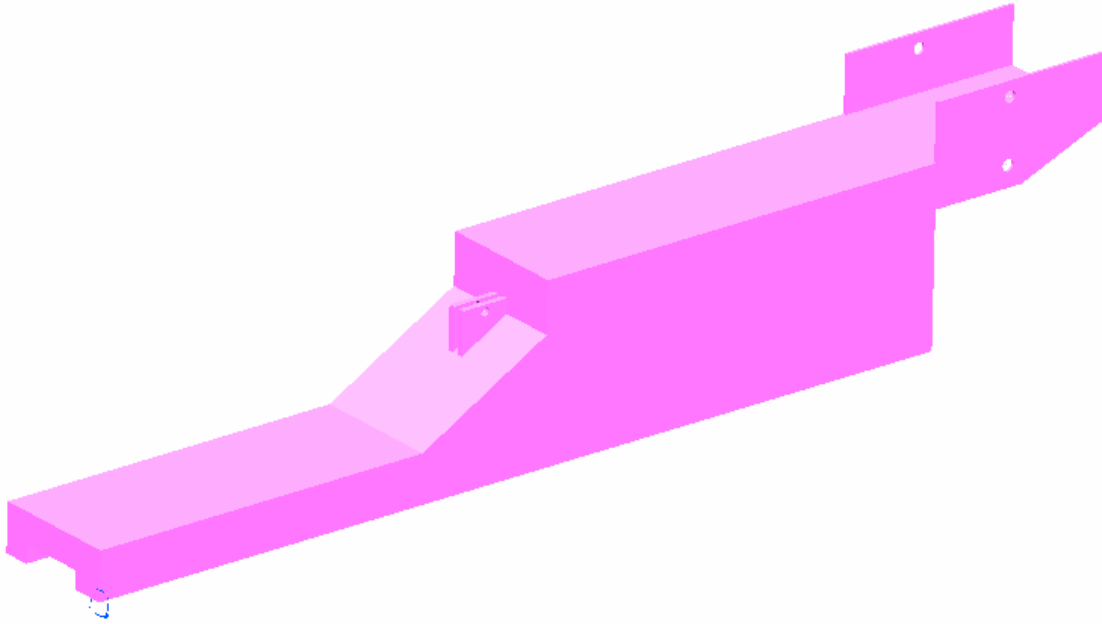


Fig. 17.137: Block pivoter lower structural support.

Figure 17.138 show the results of an FEA analysis of the lower structural support. This analysis was performed using a half section of the part and applying symmetric boundary conditions. The results indicate that the high stress region corresponds to where the kneeling jack applies it load while the bulk of the structure is very lightly stresses and the deflections are minimal. Each of the two lower structural supports currently weighs about 16,000 pounds (8 tons). Results of the analysis indicate that some of this weight can be removed by making the sections thinner, saving cost. However, optimizing the lower structural support is not an urgent design task as the design presented here works satisfactory and meets the shipping and installation requirements.

C:\PPD\_IDM\_PPD91059\DRP\_NOVA\_BLOCK\_PIVOT\_TABLE\_7-20-06.mrf1  
 RESULTS: 3- B.C. 1, STRESS\_3, LOAD SET 1  
 STRESS - VON MISES MIN: 5.46E-03 MAX: 2.99E+04  
 RESULTS: 1- B.C. 1, DISPLACEMENT\_1, LOAD SET 1  
 DISPLACEMENT - Y MIN:-6.18E-03 MAX: 3.62E-04  
 FRAME OF REF: PART  
 CRITERION: ABOVE : 5.46E-03

VALUE OPTION: ACTUAL

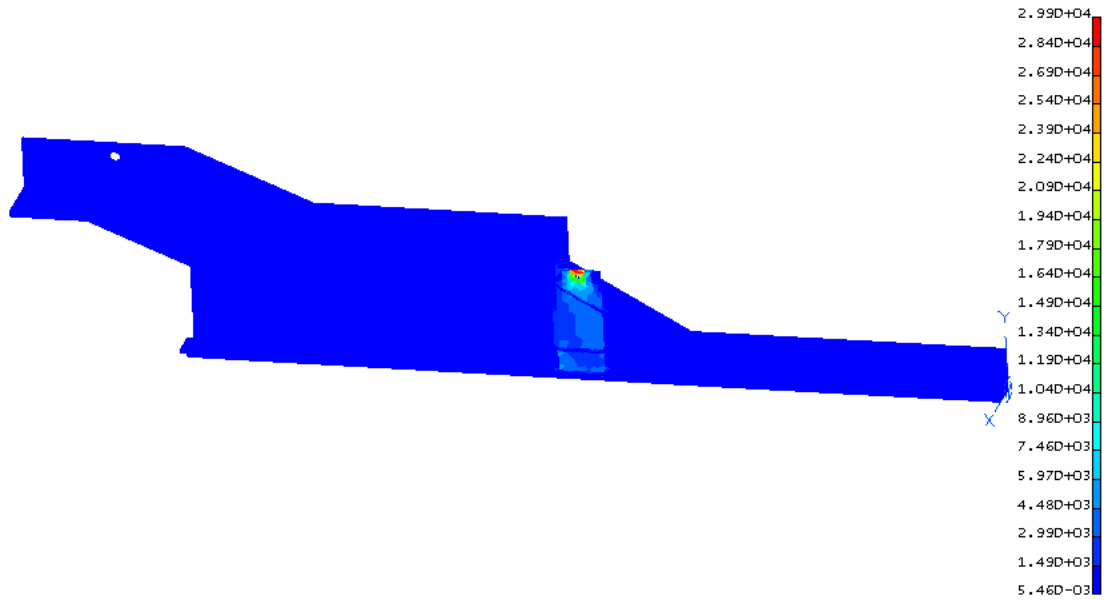


Fig. 17.138: Analysis image of the lower side support stresses and deflection.

### 17.12.8 Block Pivoter – Rear Table Support

The deflection of the detector assembly table can be minimized during the detector assembly by supporting the back end of the table when it is in the horizontal position. A simple structure provides this support and is shown in Figures 17.124, 17.125 and 17.139. This structure is fabricated from ordinary steel box sections ASTM A500 material and serves to limit the table bulk deflection changes while a block is being fabricated.



Fig. 17.139: Image of the rear table support.

### 17.12.9 Block Pivoter – Parameter Summary

Table 17.20 summarizes the most important parameters of the block pivoter.

PVC Extrusion Block Weight (estimated based on nominal extrusion)	313,000 pounds
Pivot Table Weight (estimated)	150,000 pounds
Depth of Pivot Table	6 feet
Distance from Table Surface to Pivot centerline	4 inches
Vertical Distance from Pivot to Cylinder Centerline (table vertical)	216 inches
Vertical Distance from Assembly Table top to Floor (table horizontal)	317 inches
Maximum Vertical Distance from Floor to top corner of 31 plane block (at nominal dimensions) when pivoting	651 inches
Lower Structural Support Weight (per unit – two units used), estimated	30,000 pounds
Upper Structural Support Weight (per unit – two units used), initial design, not final.	32,000 pounds
Pivot Bearing Size and Type	4” Plain Spherical
Pivot Bearing Capacities (static and dynamic), pounds, each	533,000 static, 173,000 dynamic
Number of Pivot Bearings Used	4
Forward Roller Capacity, metric tons	100 metric tons
Forward Roller Load, tons (estimated)	96 short tons
Pallet Weight (estimated)	10,000 pounds
Depth of Pallet	20 inches
Deflection of Pallet between 18” by 8” members with empty block	0.028 inches
Deflection of Pallet between 18” by 8” members with full block	0.1 inches
Deflection of Pallet Cantilever with empty block	0.13 inches
Hydraulic Cylinder closed Length	76 inches
Hydraulic Cylinder Length when Table is Horizontal	309.02 inches
Kneeling Cylinder Load (with block on table), estimated	180 tons
Kneeling Cylinder Load (without block), estimated	70 tons

Table 17.20: Summary of block pivoter parameters.

## 17.13 Detector Assembly Sequence

### 17.13.1 Overview of the Detector Assembly Process

The installation task (NOVA-doc-1141) begins with a 12-week “Setup” period, which starts with beneficial occupancy of the far detector building. The setup period is devoted to installing and commissioning installation equipment, including the block pivoter, the adhesive dispenser and the south bookend. The on-site assembly crew size increases from three to twelve people during this period, during which the crew leaders and other workers are trained. The setup period is followed by a 15-week “Startup” period, during which the first three blocks are built and installed. The startup period also includes safety tests of installation equipment and the review and approval of materials handling and block assembly procedures. During this period many of the expert physicists and engineers from WBS 2.2, 2.5, 2.6 and 2.7 assist in training the local

assembly crew technicians. The crew size ramps up to 29 during this period and work schedule changes from five 8-hour shifts per week to eight overlapping 10-hour shifts per week. Shift 1 runs Monday through Thursday and Shift 2 runs Wednesday through Saturday and shown in Table 17.21. The offset in shift start times provides 68 hours per week for block assembly work. The startup period is followed by 87 weeks of full-rate installation, with a full crew of 29 workers. During the full-rate period, all but the last two blocks are installed, with a new block completed every 2.6 weeks.

### Shift Schedule

Monday	Tuesday	Wednesday	Thursday	Friday	Saturday	Sunday
Installation Team 1						
		Installation Team 2				
Outfitting Team 1				Outfitting Team 1		
Administration-Team 1						
		Administration-Team 2				

Table 17.21: Schedule for two assembly crews working eight overlapping 10-hour shifts per week. Team 2 begins work 4 hours later than Team 1 each day, giving 14 hours for block assembly work on each of the two overlap days (Wednesday and Thursday).

Two types of 31-plane blocks are used to construct a superblock. A blocks start and end with vertical module planes and B blocks start and end with horizontal module planes. There are no gaps between blocks within a superblock, but there is a 2-cm expansion gap between superblocks to prevent superblocks from touching after filling with liquid scintillator.

Filling with liquid scintillator (NOVA-doc-1118) begins after the second superblock is completed. Filling always lags one completed superblock behind block installation. Electronics installation begins after the first two blocks are installed. With the exception of the electronics boxes, all electronics, chilled water and vapor return systems are installed before filling begins. Electronics boxes are installed only after a block has been completely filled.

The full-rate period is followed by a 10-week ramp-down period, during which the last two blocks are installed and crew size is reduced to 18 people. During a final 14-week period, the north bookend is installed and the remaining blocks are filled and outfitted with electronics. By the end of this period, the crew size has been reduced to the seven people who will operate and maintain the detector during data taking.

The assembly crew installs blocks and readout hardware but WBS 2.6/2.7 engineers and collaboration physicists perform the initial turn-on and commissioning of the electronics and DAQ systems. Data taking with cosmic-ray and neutrino beam events begins as soon as the first block is commissioned. An operations crew (not part of WBS 2.9) operates the completed sections of the detector and is also responsible for building and site maintenance during detector installation. The first five kilotons will be reading out approximately 16 months after the start of the installation setup period. A new five kiloton segment is completed every 6.5 months. The total detector installation time is 138 weeks or about 2.8 years.

During the full-rate detector assembly period the local assembly crew consists of:

- 3 administrators: lab manager, assistant lab manager (safety officer), administrative assistant
- 4 crew bosses: supervise work crews and fill in for absent crew members
- 4 heavy equipment operators: operate the two bridge cranes and block pivoter
- 2 glue technicians: operate the adhesive dispenser

- 4 module technicians: feed modules to adhesive dispenser, move them to the block pivoter
- 8 block pivoter technicians: assemble modules into blocks
- 4 scintillator/outfitting technicians: install front-end electronics infrastructure, DAQ hardware; receive and test liquid scintillator, fill modules

In addition to the assembly crew, an operations crew consisting of two to five workers is responsible for building and site maintenance and (eventually) routine detector operations. The operations crew is not included in the WBS 2.9 task.

Section 17.16 describes the tasks performed by assembly crew members in detail.

### ***17.13.2 Quality Control and Assurance***

Quality control and assurance activities for the far detector include the checkout of detector components as they are delivered, block assembly, block erection, scintillator filling, installation of readout hardware and the commissioning of the detector.

Experts from other Level 2 tasks develop and document procedures to verify that delivered components, e.g., modules and readout hardware, have not been damaged in transit. They also train assembly crewmembers to perform these tests, which eventually become routine. WBS 2.9 engineers develop and document procedures for testing critical commercial products, for example the block assembly adhesive, to verify that it meets specifications. In addition, they develop and document procedures for applying and testing adhesive properties during the block assembly process itself to ensure that the expected structural properties and overall mechanical stability of the detector are achieved.

The far detector assembly crew performs routine testing and maintenance of critical equipment, e.g., the block pivoter, adhesive dispenser and moving equipment, to ensure that they are operating properly. This includes testing each shipment of 55 gallon drums of Devcon 60 adhesive immediately after arrival. The crew administrative staff develops and documents operating procedures for this equipment and ensures that operators are properly trained in its use.

PVC modules are assembled and fully tested at remote module factories before the completed modules are shipped to the far detector hall. The modules are inspected at the far detector site to ensure that they have not been damaged in transport. The leak test described in Chapter 13 is repeated at the far detector site, before modules are assembled into planes, to ensure that there are no leaks. Filling the extrusion modules with liquid scintillator and verifying that they do not leak during filling is also a WBS 2.9 responsibility. The crew ensures that the liquid scintillator passes tests for attenuation length and light output before it is put into the detector, and also maintains a database that records the origin and history of the scintillator in every module. In the unlikely event that a module is found to leak while it is being filled, the filling will immediately stop. The module will be examined and a decision will be made to repair the module in-situ or to leave the module unfilled.

Alignment fixtures attached to the block pivoter assembly table ensure the accurate positioning of extrusion modules within each block during assembly (NOVA-doc-1396). This ensures that the weight of each block is uniformly supported on the bottom end seals of the vertical modules and also that the block is properly aligned to its neighbors and will fit within the available space. A positioning accuracy of about 1 cm is expected to be adequate to meet both of these requirements. Transverse alignment of cells is not critical for the physics performance of the far detector, which is essentially a tracking calorimeter. The transverse cell size is  $\sim 4$  cm, so the required accuracy is about  $4 \text{ cm} / \sqrt{12}$ , or again about 1 cm. Multiple scattering arguments and the transverse size of the electron showers that propagate through the detector lead to similar conclusions. The plane assembly process works to achieve this accuracy over the full 15.7 m length. Tooling, fixtures and procedures are developed to achieve this goal. The same scale of accuracy is required between adjacent 31-plane blocks. The block pivoter is designed to satisfy

this requirement. Care is also taken to ensure that each 31-plane block is erected square and plumb, and that it maintains a vertical detector face. Spacers between 31-plane blocks may be required to accomplish this.

Readout system cables, power distribution and water lines for cooling the far detector electronics are installed by the far detector installation team, which is responsible for ensuring that they operate properly and that water lines do not leak. The installation team is also responsible for making the detector light tight and for initial checkout of module readout hardware after being trained by WBS 2.6 and 2.7 experts.

### ***17.13.3 Detector Component Delivery and Storage***

As a rule, delivery is on a just-in-time basis because on-site storage is limited. Stores of all of the critical detector components are located within one day's travel of the Ash River site and larger stores are readily available from more distant suppliers. Scintillator oil is delivered in 6500 gallon tanker trucks to a canopy-covered area. There is room for as many as four tankers under the canopy which has been equipped with cooling and heating capabilities to maintain scintillator oil close to 70° F. The scintillator in each arriving tanker undergoes quality assurance testing and is then pumped through the scintillator supply system into the detector modules. The loading dock area (NOVA-doc-1159) is large enough to hold six module units (stacks of 24 modules that are delivered from the module factories) and the adhesive dispenser. Figures 17.117 through 17.119 show the layouts of the loading dock and assembly areas. Modules are tested for leaks and fiber continuity before they are installed in blocks. Before leak testing, arriving module units are set aside for at least 16 hours to come to thermal equilibrium. Supplies of Devcon 60 plane adhesive and other detector components required for installation are also stored in the loading dock area.

### ***17.13.4 Block Assembly on the Block Pivoter***

Module installation in a block is described in detail in NOVA-doc-1141. This process requires the coordination of three independent teams of technicians, one at the adhesive dispenser, one to move modules and a third to install modules at the block pivoter. The two crew bosses direct the work of the three teams and stand in for workers who are sick or on vacation. Since the working lifetime of the Devcon 60 adhesive is approximately 20 minutes, the process cannot be stopped once the module has been processed by the adhesive dispenser. The main block assembly tasks are described in the list below. Both cranes run simultaneously during plane construction. Table 17.22 shows the crane moving sequence during the 10 minutes per module movement. Figure 17.140 shows a snapshot of the position of the cranes during this sequence.

## Crane Moving Sequence

<b>Minutes</b>	1	2	3	4	5	6	7	8	9	10	11	12	13	14	15	16	17	18	19	20	
<b>Crane 1</b>	Move module to adhesive dispenser				Move empty crane to North			Pick up empty fixture		Move module to adhesive dispenser				Move empty crane to North			Pick up empty fixture				
<b>Adhesive Dispenser</b>				Unhook crane, glue module, hook-up crane										Unhook crane, glue module, hook-up crane							
<b>Crane 2</b>		Align module on block pivoter			Move Vacuum Fixture back			Move module to block pivoter			Align module on block pivoter			Move Vacuum Fixture back				Move Module			

Table 17.22: Crane moving sequence during module installation.

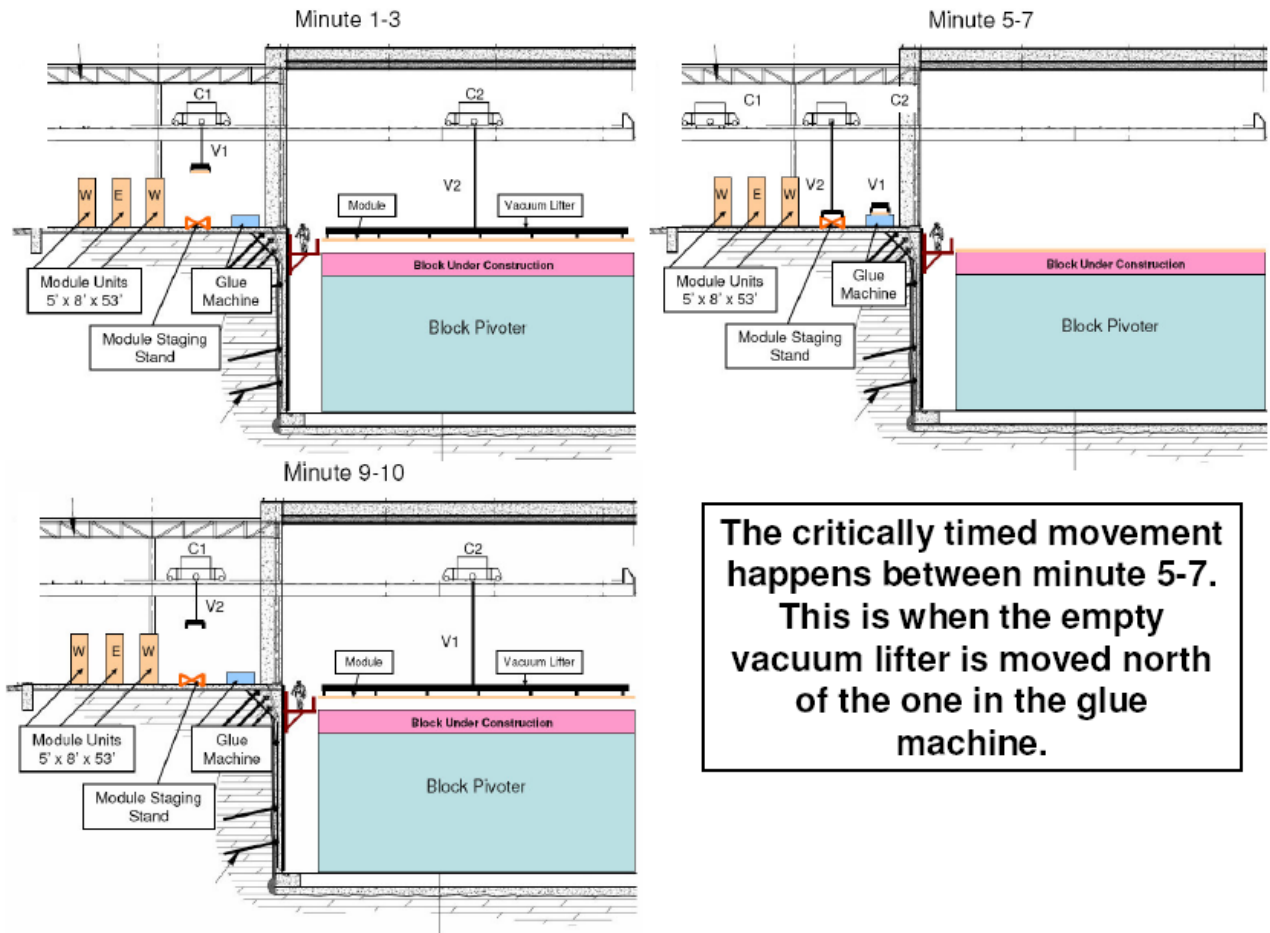


Fig. 17.140: Snapshot of crane and vacuum lifting fixture locations during the 10 minute module moving sequence.

- **Receive and check out arriving modules (3 FTE for 2 hours)**  
A module unit (stack of 24 modules) is pulled out of a truck and moved into the loading dock area (Figure 17.118). Each module unit contains 12 vertical modules and 12 horizontal modules. The protective coverings are removed and the module unit is set aside overnight to come to thermal equilibrium. Two fully-automated quality assurance tests are run on every module prior to its installation, a leak test and a fiber-continuity check. It takes about 15 minutes to attach the leak test equipment and the leak rate measurement takes about two hours. The LED fiber test is performed at the same time as the leak test after attaching the fiber test fixture to each module manifold. Module stacks are 2.4-m high so an adjustable work platform is used to reach the top modules. When the tests are completed the straps are removed from the module unit so that single modules can be moved. Block assembly requires an average of 30 modules per day.
- **Return module packing materials (3 FTE for 2 hours)**  
Packing material between modules is stacked on a “Return Super Pallet” for return to the module factory. A “Return Super Pallet” consists of a pallet and extrusion base, 23 inches of foam and a top extrusion to hold it in place. It uses the same straps to tie it in a neat stackable package ~35 inches high. Three Return Super Pallets will be shipped back to the module factory in one truck load. Assembly of these three units takes the same floor space as two module units. Two return truck loads are shipped each week. Crane work for this process is done while module installation is not taking place, usually while plane survey is taking place.
- **Prepare block pivoter (6 FTE for 9 hours)**  
Before the first plane of modules can be laid, the block base pallets must be installed to match the floor where the completed block will lie.
  - **Block base pallets**  
At the start of block assembly, a 5-ton block base pallet is lowered to the detector floor by the overhead crane and attached to the block pivoter. It is moved to the location where the new block will be installed and placed on the detector hall floor. Irregularities in the floor are accommodated by setting each pallet on a grout bed and leveling it before reattaching it to the pivoter. The pivoter and base pallet are then moved back to the assembly area to begin plane installation.
  - **Module alignment fixtures (2 FTE for 15 min)**  
The first plane in an “A” block consists of vertical modules. The alignment fixture is installed before plane assembly, as shown in Figure 17.141. B blocks are started with a horizontal module plane. The horizontal modules are marked with a center survey line that is aligned to a mark on the block base pallet.

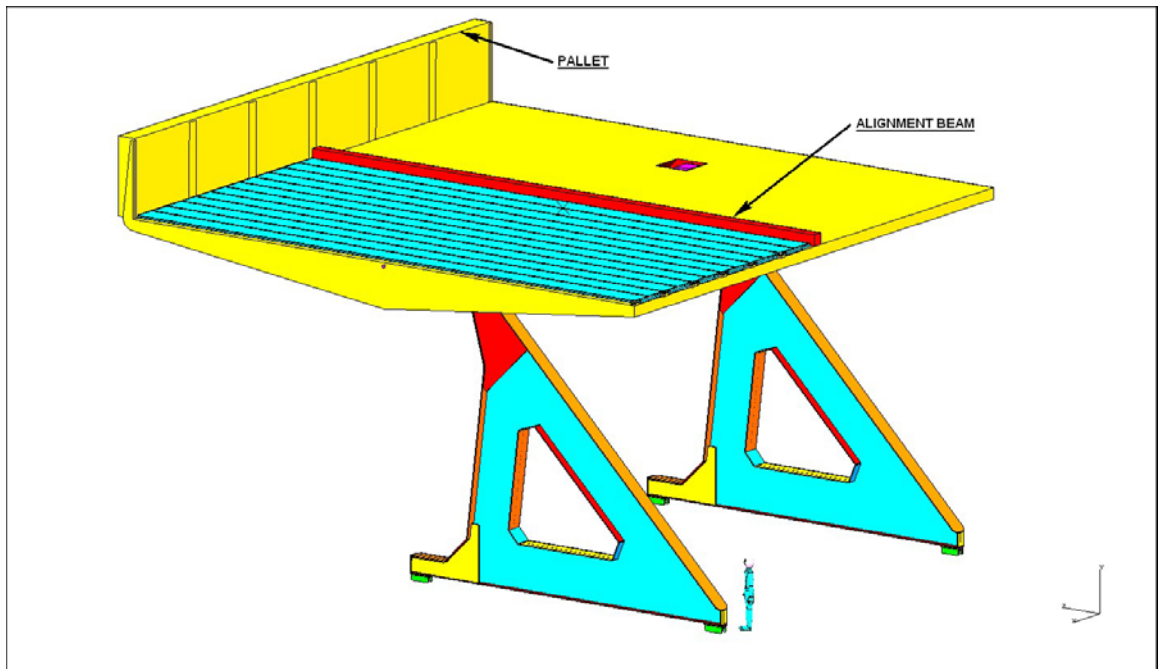


Fig. 17.141: Block pivoter with the alignment beam used for locating the first vertical module in a plane.

- **Assemble the first plane (9 FTE for 2 hours)**

The first plane of each block is not glued, but some of its modules will need to be flipped to the correct orientation in the module staging stand. If it is a vertical plane, the alignment beam is put in place and the six modules on one side are put in place. The outside edges of the two outside vertical modules have edge stiffeners, which are attached at the module factory, to control swelling under hydrostatic pressure. Module alignment fixtures are installed to hold the plane in place after the last vertical module is positioned. If the first plane is horizontal, spacers are installed against the block base pallet and the modules are centered on the block pivoter. Module handling tasks are shown in Table 17.23.

	1 Adhesive Dispenser Technician 1 Crane Operator 1 Module Technicians			1 Crane Operator, 1 Module Technician			4 Block Pivoter Technicians		
Time-Min.	Load Glue Table	Flip & Glue Process	Get Next Module	Move Module	Locate Module	Get Next Module	Position Modules	Roll Modules	
1	3 min.			1 min.					
2					3 min.				
3									
4		5 min.							
5									
6				6 min.			3 min.		
7									
8									
9				3 min.					
10									
11	3 min.								
12					3 min.				
13									
14		5 min.							
15									
16				6 min.			3 min.		
17									
18									
19				2 min.					
20									

Table 17.23: Module handling schedule for three assembly crews, for full rate assembly at ten minutes per module, ~ 2.5 planes per day. Each installation team as shown in Table 17.21 consists of the same 9 workers plus a crew boss.

- **Assemble planes 2-32 (9 FTE complete 1 plane every ~2.5 hours)**  
 After the first plane is completed, installation alternates between horizontal and vertical planes. Two to three new planes are added to the block under construction every day.
  - **Glue modules (3 FTE glue one module every 10 minutes)**  
 It takes three workers to move modules, run the adhesive dispenser and move modules to glue table with the 10-ton bridge crane and vacuum lifter. Modules are flipped as required in the module staging stand to the proper orientation before the adhesive dispenser applies the adhesive.
  - **Move glued modules onto block (2 FTE move one module every 10 minutes)**  
 Each module is picked up off the adhesive dispenser table by the overhead crane and vacuum lifting fixture. This is the only location that is wide enough to rotate modules. Modules are rotated end-for-end if necessary before they are lowered to the block pivoter assembly table. Since the elevation of the block pivoter work platform is ~9 feet below the loading dock both the crane operator and module technician remain on the loading dock level. Once the module is released, this team then moves the crane and vacuum lifter back for the next module.
  - **Locate modules on block pivoter (2 FTE position one module every 10 minutes)**

- Two block pivoter technicians position the modules. It is important that the bottom end cap on the vertical modules is placed against the block base pallet.
- **Set final module position (2 FTE for 10 minutes per module)**  
They then move a 75-pound steel roller over the length of the module to ensure a good bond between planes.
  - **Fill gaps in planes, install module alignment fixture (4 FTE block pivoter technicians for 60 minutes)**  
Epoxy grout is used to fill any gaps between modules in the bottom 6 meters of each plane, including the spaces between the bottom module and the block base pallet. The epoxy level extends to the upper surface of the plane. While the gaps are being filled by two of the technicians, the module alignment stops are installed for the next plane by the other two. After each vertical plane is installed a spacer is added to set the position of the first horizontal plane module, to separate it from the adjacent vertical-module end seal and to provide a positive alignment stop.
  - **Survey module position (2 FTE module/glue technicians 1 hour)**  
Modules locations are measured to  $\pm 5\text{mm}$  and survey data are entered into the database. NOVA-doc-1396 describes module and block survey and alignment requirements. For the vertical modules the module alignment fixtures located on the east/west side of the block pivoter have steel measuring tape holders that securely hold the tape to the “0” reference point. The center line of the first cell in each module (Cell 1 is the closest to the module snout) has been marked with a target at the module factory. Because of the long length of the modules they are marked at the top manifold, bottom end cap and the middle. A laptop computer is used to enter the numbers into a form which automatically checks for errors. This information is then downloaded into the main database. A similar technique is used for the horizontal modules, which are referenced off the block base pallets and horizontally centered about the detector axis. Horizontal modules are tilted at an angle of 2.5 mrad, with the manifold end raised about the end-seal end, to prevent air entrapment in extrusion irregularities. A powered magnetic base is used to hold the tape in position.
  - **Service adhesive dispenser, perform other maintenance (3 FTE for 1 hour)**  
During this 60 minute period there are two equipment operators and one module/glue technician available for additional work on the completed plane. One or two workers perform cleaning and other maintenance on the adhesive dispenser as needed. Additional tasks include testing and moving module units in preparation for assembly of the next plane.

### ***17.13.5 Raising and Securing a Block***

After the last vertical plane has been installed, the adhesive is allowed to cure for a minimum of 48 hours before the block is moved. During this time period, the module and block pivoter technicians spend two shifts cleaning and maintaining the adhesive dispenser and performing the following tasks on the assembled block:

- **Glue block spacer to the first block in a superblock (2 FTE for 2 hours)**  
A PVC spacer board (2 cm x 30 cm x 15.7 m) sets the width of the expansion gap between superblocks and ensures adequate clearance between the manifolds on planes of vertical modules in adjacent superblocks. The adhesive dispenser is used to apply the adhesive to one side of the spacer board.
- **Remove module alignment stops (2 FTE for 2 hours)**  
Remove module alignment stops as needed.

- **Install brackets to support the top cable trays (4 FTE for 2 hours)**  
Brackets that support the cable trays and electronics distribution systems are glued in place before the light-proofing paint is applied.
- **Apply light-proofing paint (4 FTE for 11 hours)**  
Measurements show (NOVA-doc-378) that the 4.5-mm side walls of the vertical modules are sufficient to block most of the light to which APDs are sensitive but this is not the case for the 3.0-mm thick walls of horizontal modules. NOVA-doc-140 describes the application of light-proofing paint to NOvA modules. PVC paint primer is applied by brush to exposed surfaces of horizontal modules and allowed to dry overnight. This is followed by a topcoat of black PVC paint that is also applied by brush.
- **Block pivoter moving sequence (~ 8 hours)**
  - **Secure block for movement (1 hour)**  
The block and pivoter top and side clearances are checked and the rails and floor area are checked for obstructions.
  - **Move block pivoter (1 hour)**  
The block pivoter moves from the assembly area to about 30 ft away from the detector face at a maximum speed of 20 feet per minute.
  - **Rotate pivoter (2 hour)**  
The pivoter rotates the block to within a few degrees of a vertical orientation. Most of the 2-hour time allocation is for setup and safety checks. The actual rotation takes 10-15 minutes.
  - **Move into final position (1 hour)**  
The pivoter moves the block the last 30 ft to within a few inches of the detector face. It then rotates the block last few degrees to a vertical orientation. After the location is checked, the pivoter moves the block against the detector face and sets in down on the floor of the detector hall.
  - **Move block pivoter back to assembly area (1 hour)**  
The assembly crew detaches the block base pallet from the pivoter and moves the pivoter back until it is clear of the detector. They then rotate the pivoter to the horizontal orientation and move it to the assembly area where the process of installing the next block base pallet begins.
  - **Install block safety restraint beam (2 hour)**  
After the block pivoter is clear of the detector face, the block safety restraint beam is moved against the last block (Figure 17.142). This device is supported by the same rails as the top-of-detector moving access platform. A hydraulic system presses the beam against block. The beam is removed just before the next block is installed.
  - **Survey newly installed block (2 hour)**  
The location of each block will be surveyed with the V-STARS Industrial Photogrammetry System [6], similar to that used on other Fermilab experiments.

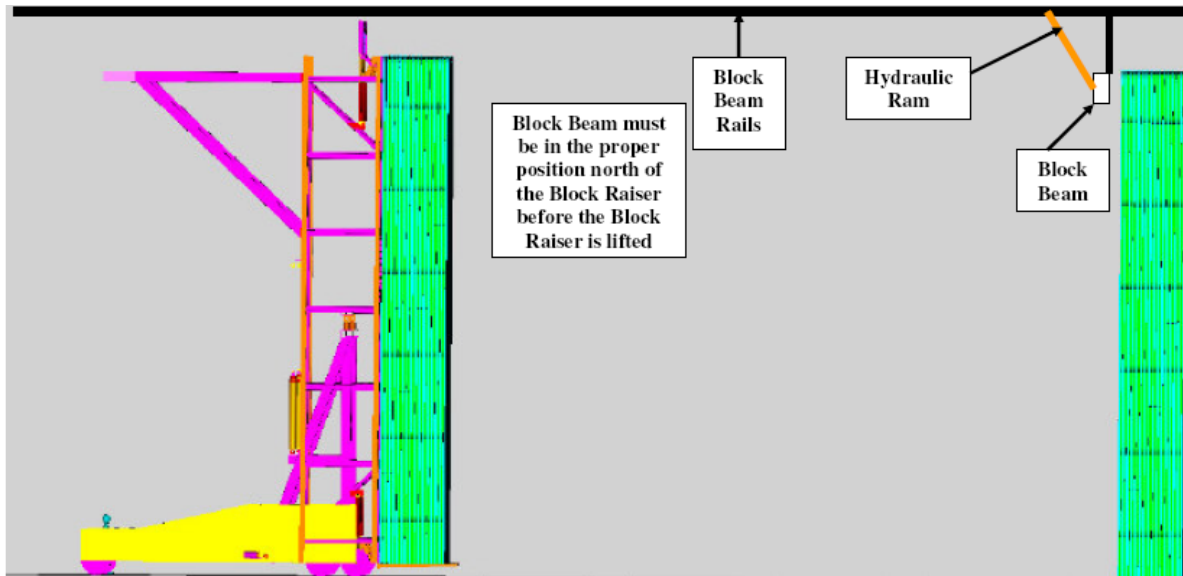


Fig. 17.142: Locations of block safety restraint beam and access bridge rails.

### ***17.13.6 Construction of a Superblock***

A superblock consists of five blocks with no gaps between them. An A-type block, with vertical module planes on its outside faces, is the first to be installed. It is the only block with a spacer board attached, to set the expansion gap between superblocks.

The first block in the sequence has 31 planes, starting and ending with a vertical plane. This block is the only one that gets the 20-mm thick spacers added to it. The remaining four blocks alternate between A and B types. A superblock contains a total of 1860 modules in 155 planes, 78 vertical planes and 77 horizontal planes. The 18 kton detector consists of 7 five-block superblocks and one three-block superblock. Figure 17.143 shows a side view of a completed superblock.

The steel block base pallets provide support for the vertical module planes, so the pallets for A-type blocks are wider than those for B blocks (with horizontal modules on their outside faces). The steel pallet widths must accommodate blocks that have the widest extrusions and thickest glue bonds between planes, so A-block pallets will generally extend a few inches beyond the south faces of these blocks. Within a superblock, this excess pallet width fits under the horizontal module plane of the adjacent B block. However, the pallet for the first block in each superblock is custom made, taking into account the thicknesses of modules in the block (which are known many weeks in advance of block assembly). The pallet in this first block of each superblock is not allowed to extend beyond the 2-cm width of the expansion gap to the adjacent superblock.

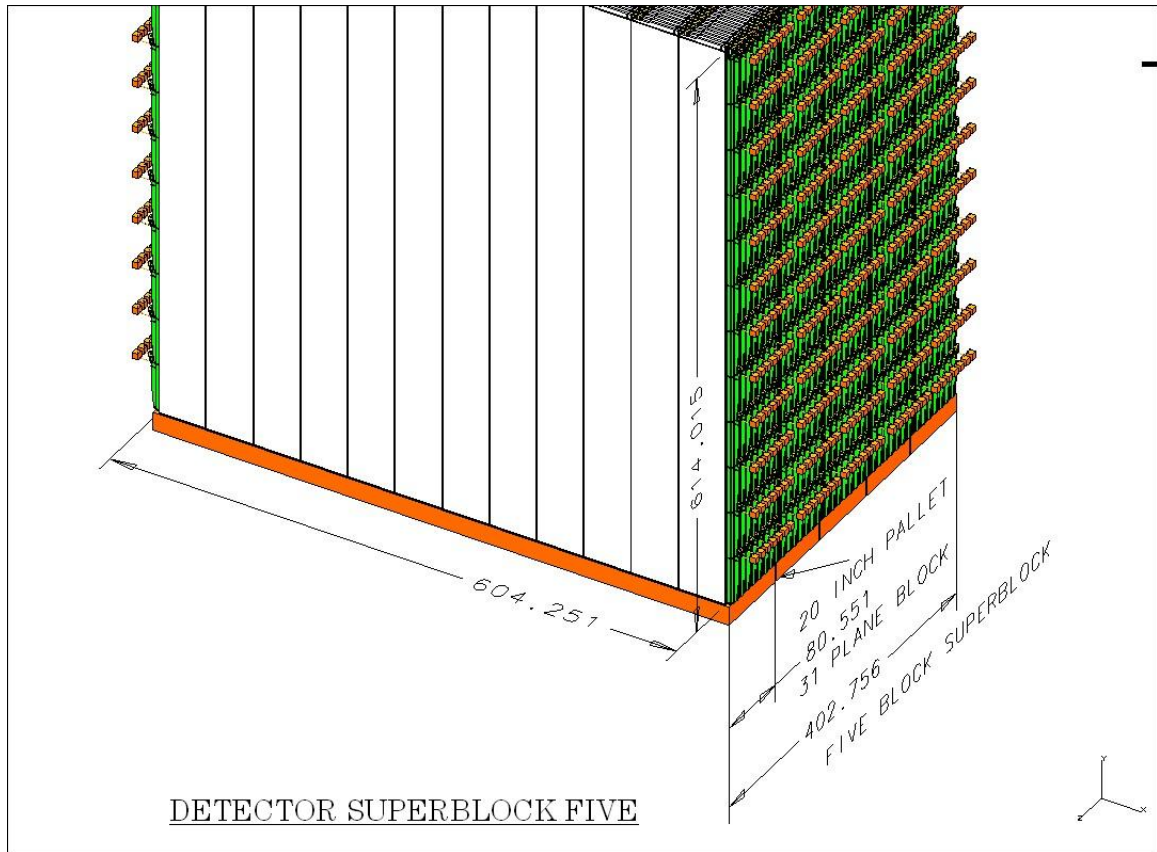


Fig. 17.143: CAD drawing of a superblock, showing nominal dimensions.

## 17.14 Filling the Detector With Liquid Scintillator

Section 17.8 describes the liquid scintillator distribution and filling system in detail. The present section provides only a short summary.

The 38-block detector holds 12,590 tons (3.9 million gallons) of liquid scintillator. During the full-rate assembly period at the far site, one block (102,600 gallons) will be filled every 2.6 weeks (about 100 hours of working time), giving an average flow rate of about 24 gal/minute. Allowing time for the liquid level to equalize between the 32 cells in a module, this corresponds to filling 8 modules in parallel at an average flow rate of 3 gal/min. About one 6,500 gallon delivery tanker per day will be needed during this full-rate period. The scintillator receiving station can accommodate up to four tanker trucks under a gas-station-type canopy, so there is always a few-day buffer on hand. Empty tankers are sent back to the scintillator blending facility to be refilled.

The modules in each superblock are filled with liquid scintillator as soon as the last block in a superblock is installed. Blocks within a superblock are filled one at a time, beginning with the south-most block. Planes of horizontal modules within a block are completely filled before the filling of vertical modules begins (NOVA-doc-1298).

Chapter 10 describes the liquid scintillator composition and properties, including the potential hazards resulting from electrostatic charge buildup during transfer operations. The scintillator handling procedures at the far detector site are designed to mitigate the risks associated with such charge buildup and possible sparking during the movement of scintillator in supply pipes and especially during the filling of vertical extrusion modules. Such sparking has the

potential for causing personal injury, damaging equipment and igniting scintillator vapors or aerosols. NOVA-doc-1118 gives the detailed requirements for safely filling the detector.

NOVA-doc-1521 reports the results of a Minimum Ignition Energy (MIE) test of an aerosol of NOvA scintillator in air. The MIE was higher than standard test equipment could measure, so the buildup of static charge during vertical module filling poses no risk of fire or explosion. However, it is still important to reduce the risk of static electricity discharges that could damage equipment or injure workers, as described below.

Delivery tankers are grounded to earth and electrically bonded to the distribution system prior to the transfer of scintillator to the detector. The scintillator tanker area is equipped with a sump and spill-control berm that is sufficient to contain 100% of the liquid from a single tanker. The transfer process is controlled from the small scintillator control building located between the truck bays at the scintillator receiving station. Samples of scintillator from arriving tanker trucks are hand carried in small containers to the scintillator transfer facility located along the main detector building. They are used for quality assurance measurements of attenuation length and light yield. These samples are saved and sent to Fermilab for archiving and possible additional testing.

After evaluating test results, the scintillator filling technicians connect an arriving tanker to the scintillator supply system through conductive hoses. Scintillator from a tanker is pumped directly into the detector modules through a 7.6-cm diameter electrically conductive pipe, permanently mounted and electrically bonded to the earth, with a resistance to ground less than 10 ohms. The temperature of the arriving liquid is raised or lowered by the heater or chiller unit at the scintillator receiving station, so that it is within 2° C of the 20° C temperature of the detector. It is pumped to the detector hall through an underground pipe and delivered to the detector through a flexible, conductive hose. The total flow rate from a tanker is limited to 40 gal/min.

At the detector, the fill system includes metering, level sensing and automatic safety shutoff valves. Fill system hoses are conductive and electrically bonded to the distribution system. Flow velocities in any given line are kept below 2 m/s in order to limit electrostatic charge buildup. Filling at the detector end makes use of 1.27-cm diameter or larger connections to vertical module manifolds or horizontal module expansion tanks.

All horizontal modules in a block are filled before vertical modules are filled. (Horizontal modules are installed at an angle of 2.5 mrad to the horizontal, with the manifold end raised about the end-seal end, to prevent air entrapment in extrusion irregularities.) Flow rates into each extrusion are metered, totalized and logged. A preset total is used as the primary means of determining when a module is full. Once this preset is reached, a “top-off” phase is initiated, in which ultrasonic sensors mounted on either side of the manifold/extrusion joint are monitored to determine when the final desired fluid level is obtained. Connections between the fill system and detector are made with hydraulic quick-disconnect fittings.

The flow of scintillator in the vertical extrusions is controlled to eliminate the formation of mist or aerosols by restricting flow to occur only along the walls of the extrusion, and with minimal free-fall and consequent breakup of the fluid stream. This is accomplished by distributing the flow to individual cells in the extrusion with a plenum interior to the manifold, with orifices on the plenum positioned and sized to ensure that the flow rate per cell is uniform, directed to the cell walls, and sufficiently low to avoid breakup and freefall of the fluid stream.

The gas volume displaced during the fill process is returned to the delivery tanker through a vapor recovery system. A vapor-tight connection to each manifold vent is made using 1.27-cm diameter flexible hose, connecting to a rigid plenum pipe servicing one plane. Each plane's plenum is connected with flexible hose to a primary plenum running the length of the detector. During transfer of scintillator from a tanker, the vapor recovery hose connects to the tanker, replacing the volume of scintillator delivered with an equivalent volume of vapor. In the steady state detector operation, changes in the detector volume due to temperature fluctuations can result in vapor flow rates of up to 1 liter/s from the entire detector, containing up to 0.5 ml/s of

pseudocumene. For the outflow, volatiles are removed from the vapor prior to venting to the atmosphere using a filter attached to the primary vent return. Intake air is also filtered.

During filling, flow rates on the liquid intake and vapor outlet sides of the distribution loop are monitored, in addition to the total fill rate, to detect an out-of-balance condition that would indicate a leak in the distribution loop. A solenoid valve at the distribution loop intake is closed if an out-of-balance condition is detected. This safety system is intended primarily to address catastrophic leaks in the distribution system. Two ultrasonic sensors mounted on the side of each manifold are used to detect “full” and “over full” conditions. The full condition is used to terminate filling on this extrusion. An overfull condition halts all filling operations. A spill pan is placed in position to catch spillage due to leakage of fittings, breaking of fittings, etc. An optical sensor mounted to the bottom of this pan senses liquid level, and shuts down all fill operations if a spill is detected.

Liquid scintillator similar to NOvA’s is commonly used in laboratory settings and can be handled safely by following a few precautions. Chemically impervious gloves must be worn at all times when working with the scintillator. No smoking is allowed in or around the detector site. No welding should occur in close proximity to filling operations. All oil-soaked rags and absorbent materials will be stored in fire-proof, covered steel containers. Chapter 9 and NOVA-doc-1021 describe the spill containment provided by the far detector hall itself.

The scintillator filling task requires two full-time scintillator technicians and a half-time crew boss (who is shared with the electronics outfitting task). The crew boss directs the work and also fills in for sick or vacationing technicians.

## **17.15 Installation of Electronics**

Each extrusion module has a front-end electronics box, which includes the APD and its TE cooler (TEC), attached to the module manifold snout. Each front-end electronics box requires chilled water, low voltage, high voltage and a connection to the data acquisition system. These services are distributed throughout the far detector hall and are connected to individual front-end electronics boxes through different distribution systems. The vertical extrusion modules are all read out on the top of the detector but the readouts for sequential planes of horizontal modules alternate between the east and west sides of the detector. The electronics boxes are installed on vertical modules only after their blocks have been filled with scintillator, in order to reduce the risk of damage to the boxes. All of the cable trays, cable harnesses, chilled water pipes and scintillator-vent plumbing are installed prior to filling the modules.

A crew of two technicians, supervised half-time by a crew boss, installs electronics, cabling and plumbing at a rate of one block every three weeks during the full-rate period. Collaboration physicists and graduate students assist the outfitting crew. WBS 2.6 and 2.7 engineers install and commission the relay racks and main power supplies.

The distribution systems (except for the chilled water) originate in the relay racks that contain the power supplies and data crates. Each rack requires two 20-A quiet power receptacles, one at 120 V and one at 208 V, and one 20 A, 120 V convenience power receptacle, with a total power load of 3.4 kW per rack. The quiet power circuits have shunt/trip circuit breakers triggered by smoke and heat detection devices. Each rack feeds one side and half of the top of two adjacent blocks. Racks are located on both sides of the detector on the top-level side walkways. The average weight of DAQ and power cables is 2.3 lbs/ft. The estimated weight of the chilled water plumbing is 2 lb/ft on the sides and 3.4 lb/ft on the top. Cable trays on the top of the detector are supported by PVC spacers that rest on the flat sections of the vertical module manifolds. The cable trays on the sides are mounted to the walkway support columns. All cable and plumbing harnesses are made and tested offsite and shipped to the far detector site by the WBS 2.6 task.

### 17.15.1 Detector Readout Infrastructure

WBS 2.9 is responsible for installing the cable trays and distribution systems listed below.

- **Chilled water**

Each electronics box requires chilled water for its TECs, as described in NOVA-doc-1293. The 21-zone chilled water distribution system is installed by WBS 2.9 and is based on a two-block layout. Each zone has two air-cooled 3-kW chiller units that serve ~756 APDs. The chiller units exhaust their heat into the building air, which the building HVAC system maintains at constant temperature. The system is installed in 2-block increments with manifold feed lines running parallel to the detector planes and service manifold lines running perpendicular to the planes. Chilled water lines are located at a slightly higher elevation than the fittings supplying chilled water to the electronics boxes. Figure 17.144 shows a schematic of the plumbing layout.

The service manifolds (Figure 17.145) and feed manifolds are made off-site and delivered to Ash River in two-block lengths. All service manifolds are made of 1-inch PVC schedule-80 pipe. The feed manifolds are all schedule-80 1-inch PVC pipe on the top of the detector and 1.25-inch PVC pipe on the sides. Service and feed manifolds are also pre-insulated in standard foam jackets. Inexpensive supports hold the pipes in place above the electronics cable trays.

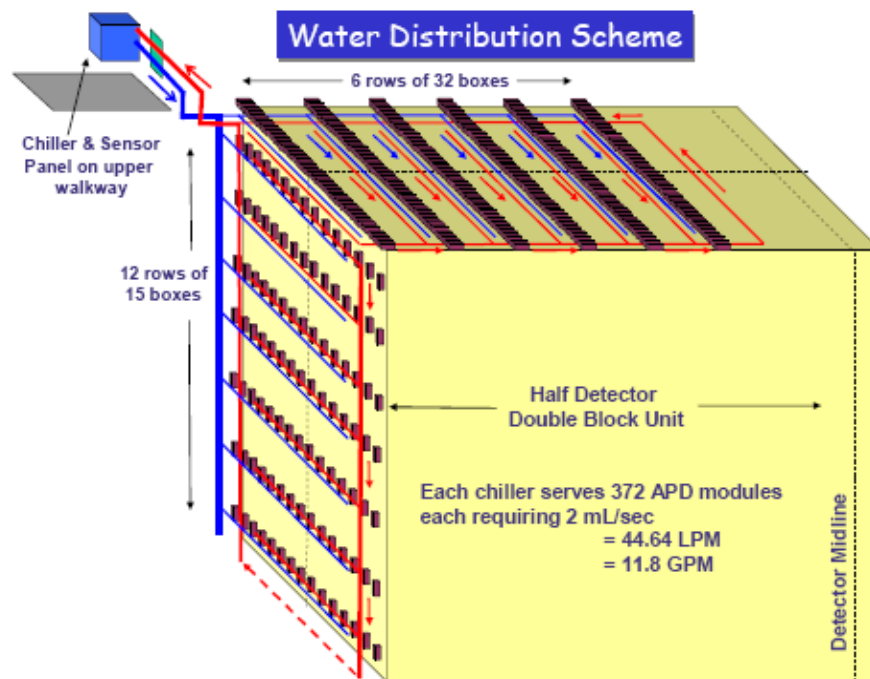


Fig. 17.144: Layout of chilled water manifolds and feeder lines.

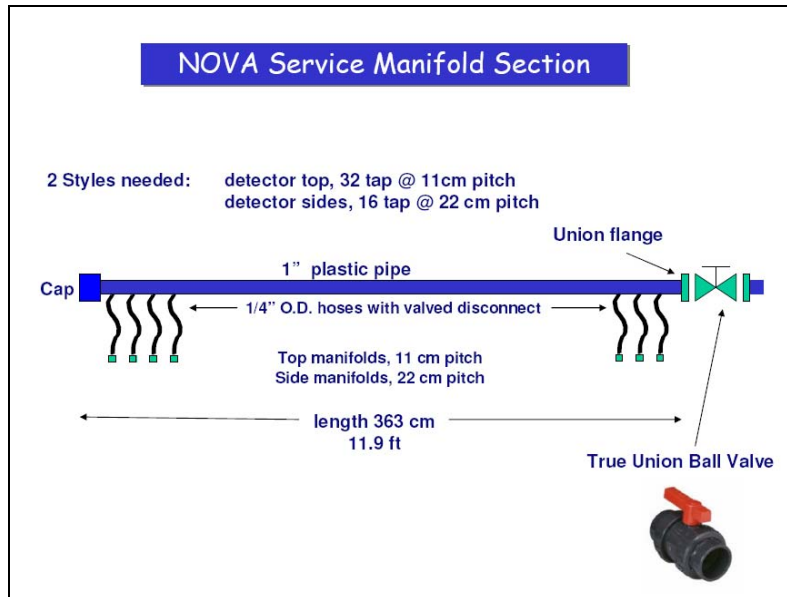


Fig. 17.145: TE-cooler chilled-water distribution service manifold section.

- **Low voltage to the front-end board**  
Each front-end board requires 1 A at 3.3 V.
- **Low voltage to TE cooler**  
Each TEC requires 0.25 A at 12 V, which is fed through the front-end board.
- **High voltage to APDs**  
Each APD requires 450 V, which is connected through the electronics box.
- **Data connection to the front-end board**  
Each front-end board is connected to a data cable, which connects to a data concentrator.
- **Monitoring system**  
The slow control system is installed by WBS 2.7 engineers and students. It monitors power supplies, chilled water, distribution boxes and environmental conditions. It will shut down TEC power in the event of cooling loss. The total installation effort is estimated to be 6 FTE-months.
- **Electronics readout box**  
The electronics readout box, shown in Figure 17.146, is mounted to a support bracket on the module manifold. The box is 22.5 cm by 10 cm by about 6 cm wide. The electronics box, containing the APD module, the TEC and the front-end board, is installed after the mechanical connections are completed. There are a total of eight connections to the electronics readout box: two for the chilled water and six electrical connections. All connections are simple plug-ins from pre-made harnesses. Plumbing connections have valves and drip-less connectors, making TECs relatively easy to replace. The electronics box is the last piece of readout hardware installed on detector blocks.

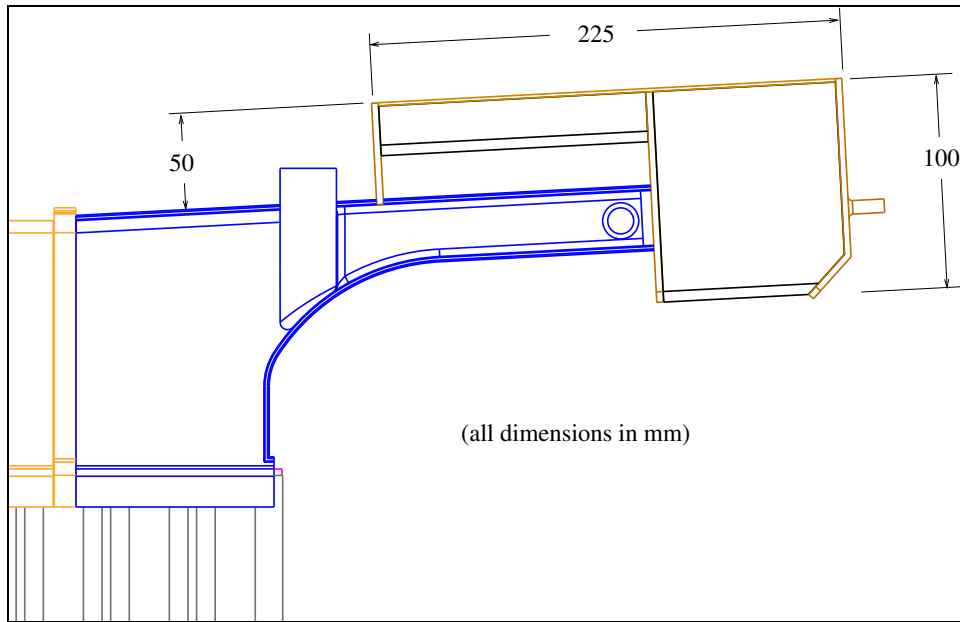


Fig. 17.146: Schematic representation of an electronics box mounted on a module. The module manifold “snout” is the blue object that extends across the middle of the sketch. The electronics box is in the upper right corner, with the TEC chilled water line connections on its right end. The vertical cylinder near the middle of the manifold snout is the liquid scintillator fill port. The circular object at the right end of the snout is the vapor vent port.

### 17.15.2 Detector Outfitting Integration

The installation of readout hardware, or detector outfitting, is performed on pairs of adjacent blocks to take advantage of the natural lengths of cable trays and chilled water pipes. There are three major systems to be installed: electronics cable trays, chilled water piping and vapor return plumbing. Most of this equipment is installed as soon as each new pair of blocks is erected. Outfitting of the east and west sides of the detector is straightforward because of the easy access afforded by the side walkways. A Unistrut frame supports the cable trays and plumbing. Filling of horizontal modules with liquid scintillator is done by way of the overflow tanks, which are located well away from the vertical sides of the detector. There is little or no interference between outfitting and filling, so the sides of the detector can be fully outfitted, including electronics box installation, before modules are filled.

Outfitting the top surface of the detector is more difficult. The rolling access platforms (Section 17.7.5) allow workers to reach the top detector surface and the vertical module manifolds by lying flat on the platform. All outfitting hardware except for the delicate electronics boxes is installed before the vertical modules are filled. The vertical module electronics boxes are installed only after filling is completed.

The sequence for installing equipment on both the top and the sides of the detector is important because cable trays and pipes have interleaved segments that are routed both across and along the length of the detector. The chilled water manifolds must be at or above the level of the electronics boxes to prevent air entrapment, so this is the last system to be installed (except for the electronics boxes themselves). On the top of the detector, most cable trays and pipes are supported by the flat sections of the vertical module manifolds. The next few paragraphs describe the installation sequence for the top of the detector.

The vapor return plumbing and the 2-inch x 2-inch lateral cable trays that feed the power distribution boxes are installed first, as shown in Figure 17.147. Trays are supported and leveled by custom built spacers on top of the horizontal modules. Wiring harnesses are placed in the trays

as soon as they are installed. The pre-made 0.75-inch black PVC vapor-return manifolds are supported by clips that hang from the flat sections of vertical module manifolds. The level of the vent pipe is kept at or above the level of the manifold vent port. The 0.5-inch flexible vent pipe must be connected to the vent port before the electronics box is installed because of the restricted access.

The next stage in the sequence is to lay the 4-inch x 2-inch cable trays that feed the cables from the Power Distribution Boxes (PDBs) to the electronics boxes, as shown in Figure 17.148. These are placed directly behind the electronics boxes to minimize cable lengths. They rest on top of the flat sections of the vertical module manifolds, shimmed level as needed. The PDBs and Data Concentrator Modules (DCMs) are installed next. These also rest on the flat sections of the manifolds, supported by thin insulating boards to protect the manifold from heat and to spread their weight. All cable harnesses are installed in cable trays at this time.

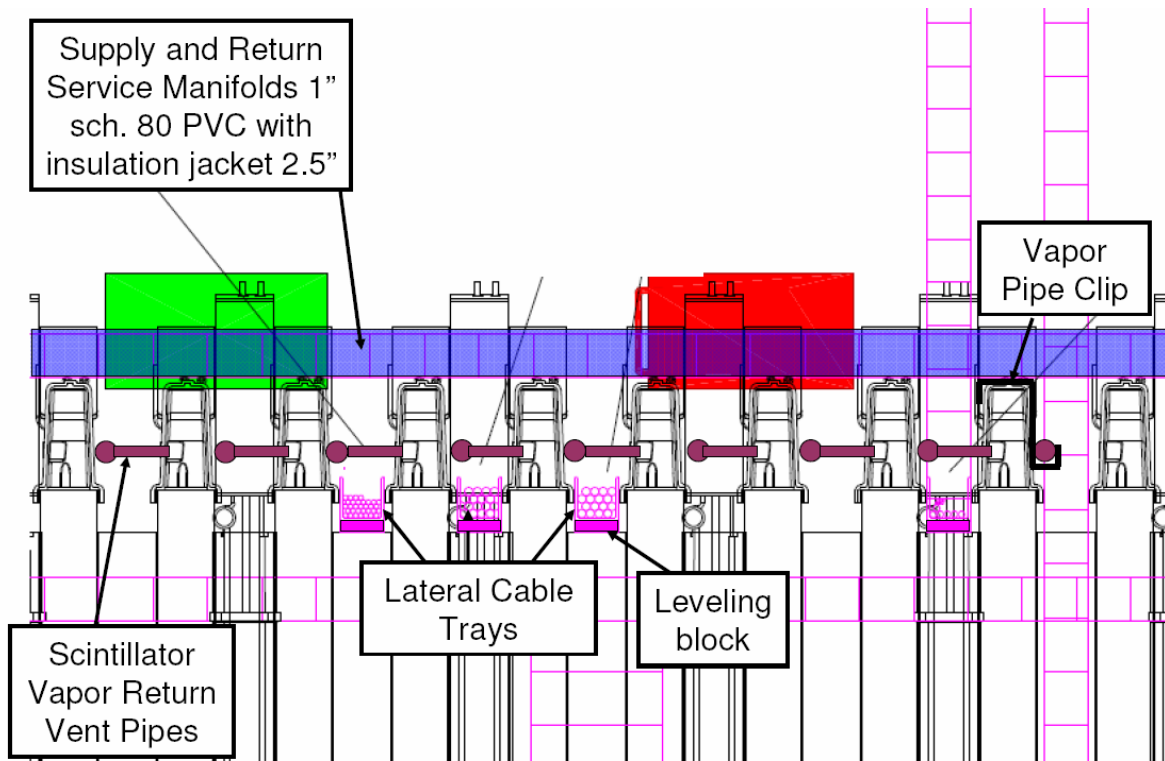


Fig. 17.147: Layout of cable trays, chilled-water and vapor-return plumbing shown from the side of the detector.

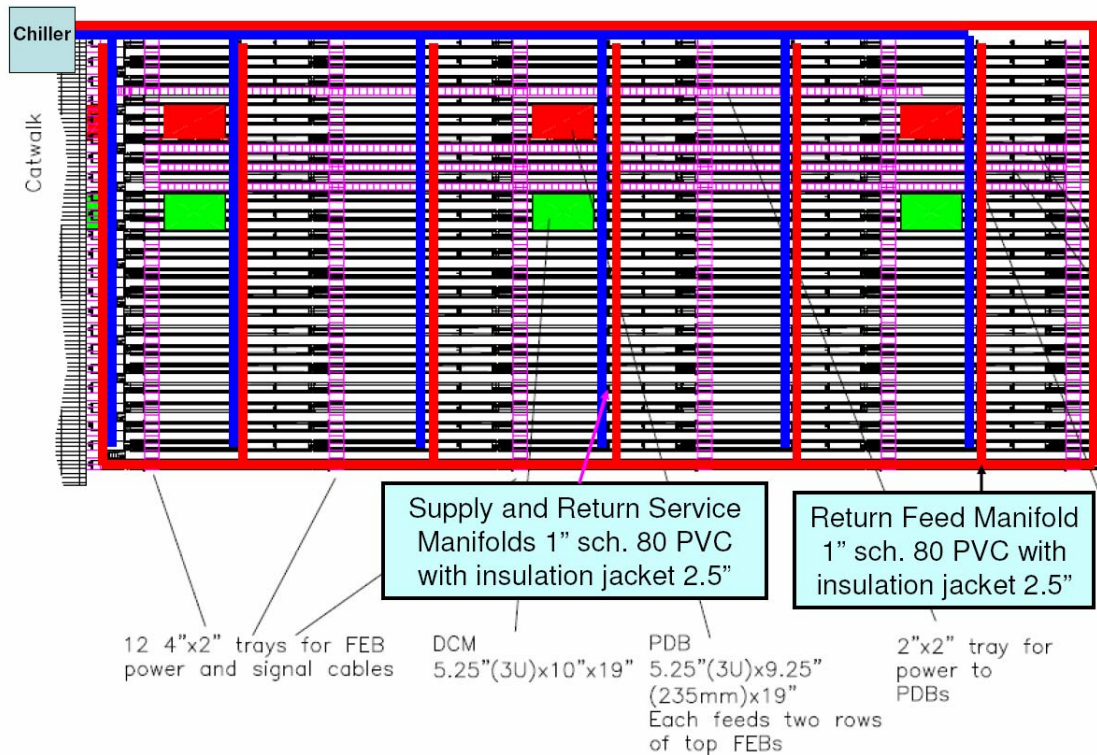


Fig. 17.148: Plan view of electronics infrastructure on the top of the detector.

The chilled water system is installed next. The supply and return service manifolds are supported by shims to keep them at the same height. A light weight structure, supported by the vertical modules, holds the water manifolds in place. The estimated weight load is ~3.4 lbs per foot for each manifold. The feed manifolds (Figure 17.148) run above the cable trays and service manifolds. The bottom of the rolling access platform is only 8 inches above the flat surfaces of the vertical module manifolds, so infrastructure hardware cannot extend above this level.

The most congested areas for detector outfitting hardware are the top corners along the east and west sides. These areas contain the vertical and horizontal module snouts and electronics boxes as well as the chilled water lines and the PDB cables. Figures 17.149 and 17.150 show close-up views of this area.

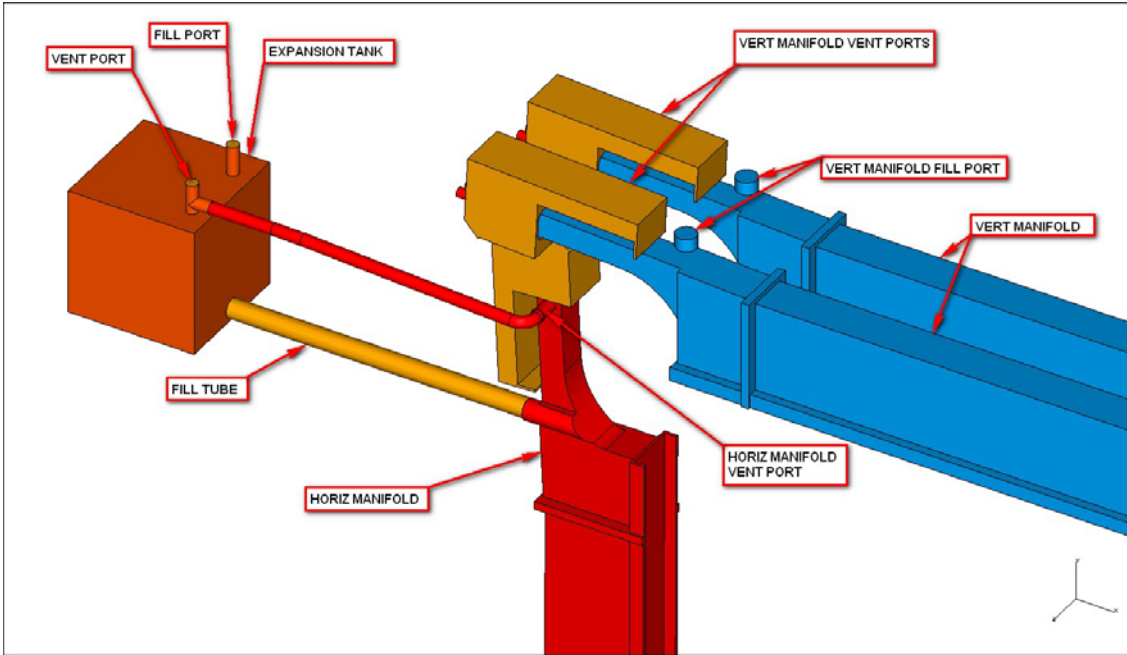


Fig. 17.149: End view of how horizontal and vertical module manifolds, electronics boxes and overflow tanks fit together at the top corner of the detector. The module extrusions are not shown.

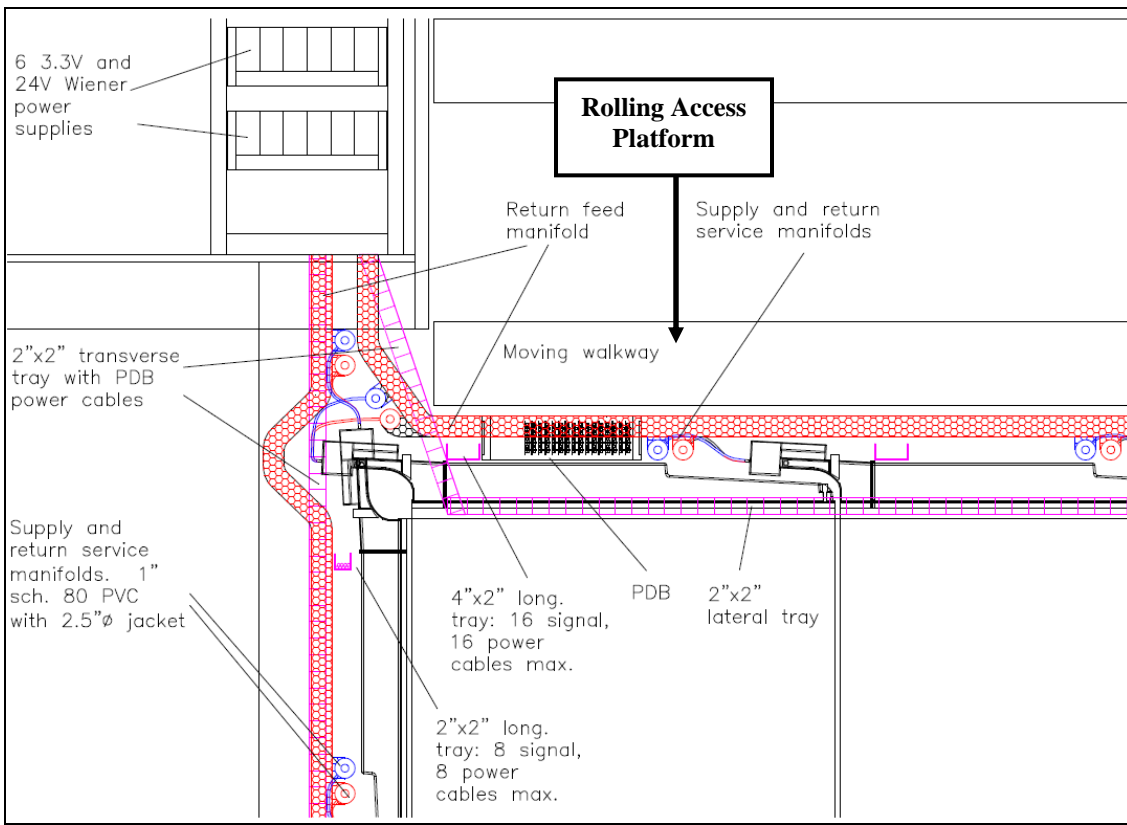


Fig. 17.150: Detailed end view of readout system infrastructure locations near a top corner of the detector.

## 17.16 Assembly Crew and Rate of Detector Assembly

Section 17.13.1 provides an overview of the detector assembly process and the tasks performed by assembly crew workers. The present section describes these tasks and the assembly schedule in more detail. Table 17.24 summarizes the activities, schedules and effort levels during the different stages of the installation task.

### 17.16.1 Job Classifications

The effort levels shown below are for the full-rate installation period.

- **Crane operator (4 FTE)**  
The two bridge cranes are operated by four certified heavy equipment operators. One crane carries modules to the adhesive dispenser the other moves glued modules to the block under construction.
- **Glue technicians (2 FTE)**  
The glue technicians are responsible for operating the adhesive dispenser. They also disconnect and reconnect the crane hook and vacuum lifter AC power for every module.
- **Module technicians (4 FTE)**  
Because the modules are so large and must be placed accurately, one module technician assists each crane operator during module movement, both into and out of the adhesive dispenser. They are also responsible for moving the packing material from the module units to the return super pallet as time permits.
- **Block pivoter technicians (8 FTE)**  
Modules are rolled with a 75-pound steel roller to ensure good compression of the glue bond. The technicians who perform this work are also responsible for installing module alignment fixtures and for filling the gaps between modules with epoxy grout.
- **Outfitting/Scintillator technicians (2 FTE)**  
The two outfitting/scintillator technicians share several tasks. They are responsible for installing electronics and cooling hardware, including cabling and plumbing for the outfitting task. They are also responsible for receiving and testing arriving shipments of scintillator, and for filling scintillator modules.
- **Crew bosses (4 FTE)**  
One of the two crew bosses in each team supervises the block construction work and other supervises the outfitting and scintillator tasks. They also serve as replacement workers when someone is sick or on vacation, or a position is temporarily vacant.
- **Administration (3 FTE)**  
The administrative staff consists of a lab manager, assistant lab manager and an administrative assistant. These people are the first assembly crew members hired and are responsible for hiring the rest of the crew. The assembly crew administrative staff is augmented by the Laboratory Safety Officer, hired by the University of Minnesota, who is a member of the operations staff and not paid for by WBS 2.9.
- **Operations staff (3 FTE)**  
During the installation period, additional staff is needed to operate the completed sections of the detector, maintain computer networks, and perform building maintenance and grounds keeping tasks. These operations crew members are not included in WBS 2.9, and most will continue after installation is complete as members of the experiment operations staff.

Installation stage	# of Blocks	Starting # of FTEs	Ending # of FTEs	Job Class at end of period
60 days – Setup		4*	14	3-Admin, 2 Crane, 2 Crew Boss, 6 Tech
75 days– Startup	3	14	29	3-Admin,4 Crane,4 Crew Boss, 18 Tech
437 days – Full rate	33	29	29	3-Admin,4 Crane,4 Crew Boss, 18 Tech
50 days – Ramp down	2	29	18	3-Admin,2 Crane,2 Crew Boss, 10 Tech
50 days – Install bookend, complete filling	0	18	10	2-Admin, 1 Crane, 2 Crew, 4 Tech
20 days – Complete outfitting		10	5	2 Admin, 1 Crew, 2 Tech
<b>Total: 692 days (138 wks)</b>	<b>38 blocks</b>			<b>29 FTE in full-rate stage</b>

Table 17.24: Far detector installation stages and effort levels. (\* Two administrators and two crew bosses are hired before the setup phase begins.)

### 17.16.2 Crew Size, Shift Schedule and Training

Schedules are based on overlapping 10-hour shifts 4 days/week (Table 17.21). Team 1 works from 6 am to 4:30 pm (0.5 hour for lunch) and Team 2 works from 10 am to 8:30 pm. Two hours of each day are scheduled for lunch, coffee breaks and work inefficiencies. Workers are paid for 10 hours per day. Installation rates are based of 8.5 hours of productive work each day. Table 17.24 shows the numbers of workers during the different stages of the installation process. Table 17.25 illustrates the breakdown into the different job classifications.

- **Training**

Training falls into two major categories: task-related and safety. While standard industrial safety training is included for all tasks and procedures, additional first aid safety training is provided because of the remoteness of the site. All training is documented to provide a record of compliance. It is 45 miles to the closest hospital, so a one-hour travel time to expert medical assistance is assumed. The parking area on the north-west side of the building complex is large enough to land a life-flight helicopter.

- **Procedures and tasks**

The crew bosses and experts (physicists and engineers) for each of the systems conduct the training classes. A safety committee comprised of experts from Fermilab, the University of Minnesota and the assembly crew staff approves all procedures. Outside experts in specific fields like materials handling, adhesive usage and scintillator spill cleanup are brought to the site as needed. Most procedures are developed, documented and approved during full-scale prototype work at Fermilab or Argonne before far detector installation begins.

- **Safety training**

Due to the remoteness of the site, it is important to have several trained first responders or EMTs as members of the assembly crew. Personnel with such training will be given preference during the hiring process. Equipment required

for emergency medical treatment is kept on site. All personnel are trained in first aid, CPR, defibrillators and high-flow oxygen techniques. Specific safety training for dealing with scintillator spills, vapor control and other detector-related safety issues is provided, with refresher classes given each year. Monthly safety meetings with specific training topics are mandatory for all workers.

### **Summary of Labor Breakdown**

Task assignment	Team 1	Team 2
<b>Crane Operators</b>	<b>2 FTE</b>	<b>2 FTE</b>
<b>Module Technicians</b>	<b>2 FTE</b>	<b>2 FTE</b>
<b>Glue Technicians</b>	<b>1 FTE</b>	<b>1 FTE</b>
<b>Block Pivoter Technicians</b>	<b>4 FTE</b>	<b>4 FTE</b>
<b>Outfitting/Scintillator Technicians</b>	<b>2 FTE</b>	<b>2 FTE</b>
<b>Crew Bosses</b>	<b>2 FTE</b>	<b>2 FTE</b>
<b>Administration</b>	<b>2 FTE</b>	<b>1 FTE</b>
<b>Total</b>	<b>15 FTE</b>	<b>14 FTE</b>
<b>Grand Total 29 FTEs</b>		

Table 17.25: Job classifications and effort levels during full-rate installation period.

#### ***17.16.3 Block Installation Schedule***

The total assembly and installation time for each block is 2.6 weeks (including 16 hours of float time) during the full-rate installation period. Some modifications to the crew size may be made after time-and-motion studies have been completed with the full-scale block assembly prototype. Tables 17.26 to 17.28 show the 2.6 week full-rate schedule. Tasks like moving and testing modules are not shown, but will be performed as background work, as time permits, by some of the 9 crew members working on block construction. An average of one module unit per day is delivered to the loading dock area. Since the scintillator filling and electronics installation teams work independently of the block construction teams, the former can be made available to help with module shipment unloading as needed.

## Week 1

	Mon.	Tues.	Wed.	Thurs.	Fri.	Sat.
7:30	Start	Start	Start	Start	Start	Start
8:00	Pivoter Prep	Pivoter Prep	2:HM 7-9	5:VM 1-3	Survey & Stops	10:HM 7-9
8:30			2:HM 10-12	5:VM 4-6		10:HM 10-12
9:00			Survey & Stops	5:VM 7-9	8:HM 1-3	Survey & Stops
9:30			5:VM 10-12	8:HM 4-6		
10:00	Break	Break	Break	Break	Break	Break
10:30	Pivoter Prep	Pivoter Prep	3:VM 1-3	Survey & Stops	8:HM 7-9	11:VM 1-3
11:00			3:VM 4-6	8:HM 10-12	11:VM 4-6	
11:30			3:VM 7-9	6:HM 1-3	Survey & Stops	11:VM 7-9
12:00			3:VM 10-12	6:HM 4-6		11:VM 10-12
12:30	Lunch	Lunch	Lunch	Lunch	Lunch	Lunch
13:00	Pivoter Prep	1:VM 1-3	Survey & Stops	6:HM 7-9	9:VM 1-3	Survey & Stops
13:30		1:VM 4-6		6:HM 10-12	9:VM 4-6	
14:00		1:VM 7-9	4:HM 1-3	Survey & Stops	9:VM 7-9	12:HM 1-3
14:30		1:VM 10-12	4:HM 4-6	9:VM 10-12	12:HM 4-6	
15:00	Break	Break	Break	Break	Break	Break
15:30	Pivoter Prep	Survey & Stops	4:HM 7-9	7:VM 1-3	Survey & Stops	12:HM 7-9
16:00			4:HM 10-12	7:VM 4-6		12:HM 10-12
16:30		2:HM 1-3	Survey & Stops	7:VM 7-9	10:HM 1-3	Survey & Stops
17:00		2:HM 4-6	7:VM 10-12	10:HM 4-6		
17:30		Clean	Clean	Clean	Clean	Clean

Table 17.26: Full-rate block installation schedule for week 1 of the 3-week period. It takes ~15 ten-hour shifts to complete a 31-plane block. One superblock is completed in approximately 13 weeks.

## Week 2

	Mon.	Tues.	Wed.	Thurs.	Fri.	Sat.
7:30	Start	Start	Start	Start	Start	Start
8:00	13:VM 1-3	Survey & Stops	18:HM 7-9	21:VM 1-3	Survey & Stops	26:HM 7-9
8:30	13:VM 4-6		18:HM 10-12	21:VM 4-6		26:HM 10-12
9:00	13:VM 7-9	16:HM 1-3	Survey & Stops	21:VM 7-9	24:HM 1-3	Survey & Stops
9:30	13:VM 10-12	16:HM 4-6		21:VM 10-12	24:HM 4-6	
10:00	Break	Break	Break	Break	Break	Break
10:30	Survey & Stops	16:HM 7-9	19:VM 1-3	Survey & Stops	24:HM 7-9	27:VM 1-3
11:00		16:HM 10-12	19:VM 4-6		24:HM 10-12	27:VM 4-6
11:30	14:HM 1-3	Survey & Stops	19:VM 7-9	22:HM 1-3	Survey & Stops	27:VM 7-9
12:00	14:HM 4-6		19:VM 10-12	22:HM 4-6		27:VM 10-12
12:30	Lunch	Lunch	Lunch	Lunch	Lunch	Lunch
13:00	14:HM 7-9	17:VM 1-3	Survey & Stops	22:HM 7-9	25:VM 1-3	Survey & Stops
13:30	14:HM 10-12	17:VM 4-6		22:HM 10-12	25:VM 4-6	
14:00	Survey & Stops	17:VM 7-9	20:HM 1-3	Survey & Stops	25:VM 7-9	28:HM 1-3
14:30		17:VM 10-12	20:HM 4-6		25:VM 10-12	28:HM 4-6
15:00	Break	Break	Break	Break	Break	Break
15:30	15:VM 1-3	Survey & Stops	20:HM 7-9	23:VM 1-3	Survey & Stops	28:HM 7-9
16:00	15:VM 4-6		20:HM 10-12	23:VM 4-6		28:HM 10-12
16:30	15:VM 7-9	18:HM 1-3	Survey & Stops	23:VM 7-9	26:HM 1-3	Survey & Stops
17:00	15:VM 10-12	18:HM 4-6		23:VM 10-12	26:HM 4-6	
17:30	Clean	Clean	Clean	Clean	Clean	Clean

Table 17.27: Full-rate block installation schedule for week 2 of the 3-week period.

## Week 3

	Mon.	Tues.	Wed.	Thurs.	Fri.	Sat.				
7:30	Start	Start	Start	Start	Start	Start				
8:00	29:VM 1-3	Survey & Stops	Light Tighten	Final Position and Move Back	Pivoter Prep	1:HM 1-3				
8:30	29:VM 4-6					1:HM 4-6				
9:00	29:VM 7-9	Light Tighten				1:HM 7-9				
9:30	29:VM 10-12					1:HM 10-12				
10:00	Break	Break	Break	Break	Break	Break				
10:30	Survey & Stops	Light Tighten	Light Tighten	Place Block Beam	Pivoter Prep	Survey & Stops				
11:00						2:VM 1-3				
11:30	30:HM 1-3					2:VM 4-6				
12:00	30:HM 4-6					2:VM 7-9				
12:30	Lunch	Lunch	Lunch	Lunch	Lunch	Lunch				
13:00	30:HM 7-9	Light Tighten	Move Block Pivoter	Pivoter Prep	Pivoter Prep	2:VM 10-12				
13:30	30:HM 10-12					Survey & Stops				
14:00	Survey & Stops					Break	Break	Break	Break	Break
14:30						Break	Break	Break	Break	Break
15:00	Break	Break	Break	Break	Break	Break				
15:30	31:VM 1-3	Light Tighten	Rotate and Position	Pivoter Prep	Pivoter Prep	3:HM 1-3				
16:00	31:VM 4-6					3:HM 4-6				
16:30	31:VM 7-9					3:HM 7-9				
17:00	31:VM 10-12					3:HM 10-12				
17:30	Clean	Clean	Clean	Clean	Clean	Clean				

Table 17.28: Full-rate block installation schedule for week 3 of the 3-week period.

### 17.17 Changes in the Far Detector Assembly Since the CDR

1. Detector mass: decreased from 25 kton (64 blocks) to 18 kton (38 blocks).
2. Detector structure: 1-cm expansion gaps between all blocks changed to 2-cm gaps only between 5-block superblocs.
3. Block structure: All A-type blocks changed to alternating A-type and B-type blocks within superblocs.
4. Building size: decreased from 30 kton to 20 kton (42 blocks).
5. Building/detector orientation: rotated 180 deg so detector assembly starts at south end.
6. Top of detector access: roof support truss walkways changed to rolling access platforms.
7. Maximum assembly rate: one block/80 crew hours changed to one block/150 crew-hours.
8. Shifts/day: changed from ten 8-hour shifts/week to eight 10-hour shifts/week.
9. Maximum assembly crew size: decreased from 39 to 29.
10. Block raiser design: block raiser changed to block pivoter.
11. Block assembly location: moved from detector face to loading dock.
12. Detector component inventory: 30-day on-site buffer changed to just-in-time delivery.
13. Plane adhesive: changed from 3M 2216 epoxy to Devcon 60 acrylic adhesive.
14. Plane adhesive application: applied by machine to each module before installation.
15. Liquid scintillator charge buildup mitigation: antistatic additive, grounded metal supply pipes, elimination of splash filling, slower fill rate.

16. Scintillator supply system: design simplified to match slower fill rate.
17. APD condensation control: dry nitrogen system replaced by local desiccant system.
18. Additional WPS 2.9 responsibilities: Scintillator supply system, block pivoter access platforms, horizontal module overflow tanks, block safety restraint beam, north-end cosmic-ray shield wall, electrical installation from main building panels to all equipment and electronics.
19. Design improvements: structural design validation with 16-cell NOvA extrusion prototypes, adhesive application to modules, block pivoter design, block base pallet design, detector access platforms and walkways.

### **17.18 Work Remaining to Complete the Far Detector Assembly Design**

1. Completion of studies needed to determine requirements for methyl methacrylate vapor control at adhesive dispenser and block pivoter.
2. Completion of detailed designs of methyl methacrylate ventilation systems.
3. Completion of calculations to determine block pivoter and base pallet design requirements to keep block stresses at acceptable levels during block raising.
4. Further optimization of module bonding and block assembly procedures.
5. Development of detailed module and block alignment and survey procedures.
6. Development of QC procedures for plane adhesive, block gap filling grout, block base pallets and block base pallet grout.
7. Procedure validation, time-and-motion studies with full-scale block assembly prototype.
8. Structural design validation with full-height structural engineering prototype.
9. Long-term structural stability validation with ongoing creep and aging measurements of module and block materials.
10. Prototyping of the liquid scintillator supply and filling equipment.
11. Initial system integration and commissioning studies with IPND.

### **Chapter 17 References**

- [1] Engineered Materials Handbook - Adhesives and Sealants Volume 3, ASM International.
- [2] E. Ray Harrell, Jr., "Modeling of the Creep Modulus of PVC 1111-BB for Predicting Creep at 20°C for 20 Years," NOVA-doc-667, March 3, 2006.
- [3] E. Ray Harrell, Jr., "Modeling of the Creep Modulus of NOvA 2P for Predicting Creep at 20°C for 20 Years," NOVA-doc-667, July 25, 2006.
- [4] F. Tahmasebi, PhD, "Finite Element Modeling of an Adhesive in a Bonded joint", FEMCI, NASA Goddard Space Flight Center, July, 1999.
- [5] Y. Zhu and K. Keyword, "Method of Analysis and Failure Predictions for Adhesively Bonded Joints of Uniform and Variable Bond Line Thickness", DOT/FAA/AR-05/12, Final Report, May, 2005.
- [6] V-STARS Industrial Photogrammetry Systems, Geodetic Systems, Inc., 3D Industrial Measurement Systems, <http://www.geodetic.com>.